# Late Quaternary planktic foraminifera assemblages in the South Atlantic Ocean: Quantitative determination and preservational aspects

Dissertation
zur Erlangung des
Doktorgrades der Naturwissenschaften

am Fachbereich 5 - Geowissenschaften
der Universität Bremen

vorgelegt von

Nicolas Dittert
Bremen 1998

*'You think that I am just amusing myself with side issues? And it annoys you? But it is not that. Once I went professionally to an archæological expedition - and I learnt something there. In the course of an excavation, when something comes up out of the ground, everything is cleared away very carefully all around it. You take away the loose earth, and you scrape here and there with a knife until finally your object is there, all alone, ready to be drawn and photographed with no extraneous matter confusing it. That is what I have been seeking to do - clear away the extraneous matter so that we can see the truth - the naked shining truth.'*

Hercule Poirot

## Preface

$CO_2$ records from the South Pole and Mauna Loa, Hawaii, show a 15 ppm $CO_2$ increase since 1958 (Keeling et al. 1996) which can be attributed - at least partially - to fossil fuel emissions and other human activities. Besides short term variations there are long term atmospheric $CO_2$ variations as recorded by readings of gas bubbles trapped in polar ice (e.g., Delmas et al. 1980; Neftel et al. 1988; Barnola et al. 1995). As we need to predict the consequences of future climate change both due to natural as well as to anthropogenic causes we have to understand the Earth's systems that control atmospheric $CO_2$. On this matter, a rich source of information is the view into the past. Drillings into the polar ice, analyses of deep-sea sediments, the distribution of pollens of trees and grasses, annual rings of tropic coralls, etc. draw attention on basic mechanisms of global climate changes. One further essential topic - dealt with in this thesis - are planktic foraminifera from open ocean sediments which were in their lifetime the inhibitants of the upper few hundred meters of the oceans water column. Much is known about today's preferences of various species (e.g., Hemleben et al. 1989; Wefer et al. 1996) and hence planktic foraminifera have evolved as a particularly sensitive tool to decipher and to evaluate surface water mass properties and to estimate their control of past and future climate.

In order to contribute to the growing information within the climate research community, the Special Research Project (Sonderforschungsbereich; SFB) 261 *The South Atlantic in the late Quaternary: Reconstruction of material budget and current systems* provides relevant knowledge to that topic. The publication on hand is submitted as a PhD thesis and has been supervised by Prof. Dr. Rüdiger Henrich within the frame of the subproject B3 *Calcareous plankton and carbonate budget*. This study was conducted as part of the SFB 261 at the University of Bremen and was funded by the German Research Foundation (Deutsche Forschungsgemeinschaft).

This PhD thesis consists of four main chapters. *Part I Introduction* gives the thematic context on the different studies carried out. *Part II Publications* presents a collection of articles related to the general subject. All papers have been submitted to international journals. *Part III* gives the main *Conclusions* and *Contemplations*. Last but not least, *Part IV Appendix* deals with the taxonomy of planktic foraminifera investigated in this study and the presentations at international conferences.

For reasons of consistent presentation English is used in every part. All data presented here are archived in the PANGAEA database at the Alfred Wegener Institute for Polar and Marine Research (http://www.pangaea.de).

## Table of contents

## Abstract

In order to determine a calibration of the modern to the fossil situation in the South Atlantic Ocean four surface sediment depth-transects into the Brazil-, the Guinea-, the western and the eastern Cape Basin were investigated. Late Quaternary paleoceanographic and paleoclimatic aspects were focussed on the central equatorial Atlantic and the time frame of 300 kyrs.

*The modern South Atlantic situation.* In surface sediments of the central equatorial Atlantic the planktic foraminiferal assemblages are dominated by tropical (*G. sacculifer* ) and subtropical (*G. ruber* ) index species. In the northern Cape Basin (Walvis Ridge) transitional species (*G. inflata* ) are of major importance. At the Namibia Continental Margin species showing also a certain preference to nutrient enriched water masses are abundant (*G. bulloides, N. pachyderma* ). Sea surface temperatures (SST's) estimated by factor analysis reveal excellent correspondence to the data measured by Levitus and Boyer (1994).

*The Late Quaternary central equatorial Atlantic situation (Site GeoB 1117-2/3).* The planktic foraminiferal and coccolithophorid assemblages are dominated by variations in the periods of orbital eccentricity and precession. The transfer function technique (five factors) applied on the orbital-to-suborbital alternating planktic foraminiferal assemblages displays two significant factors: (1) the subtropical-tropical factor with maxima during interglacials and the Holocene; and (2) the warm-transitional factor with maxima during glacials. Highest estimated SST's are attained during interglacials, and lowest SST's occur during glacials. Glacial maxima are supposed to become warmer from oxygen isotope event 8.2 to 2.2 by about 2.5 °C. The difference between the modern and the Last Glacial Maximum SST amounts to about 6 °C for this area. During glacials advection of cold and nutrient enriched water masses via the eastern boundary currents is the most important feature in the surface water circulation at the site. The equatorial upwelling is controlled by trade-wind and monsoonal wind stress. During interglacials the thermocline is deep, and equatorial upwelling is only moderate; cool water advection is weak or absent. Minima in the upwelling intensity are monitored by the increase in *F. profunda* and the tropical planktic foraminiferal assemblage; both are positively correlated to the insolation at 15°N. The site is located at the southern rim of the modern equatorial upwelling area. Presumably, this domain was not extended or moved significantly during

glacial times.

*Carbonate dissolution in the modern South Atlantic. Globigerina bulloides'* ultrastructural breakdown during increasing carbonate dissolution is converted into the *Globigerina bulloides* Dissolution Index (BDX). BDX indicates the calcite lysocline as the boundary between NADW and AABW; either it distinguishes the Calcite Compensation Depth (CCD). During increasing dissolution *G. bulloides'* stable isotope composition ($\delta^{13}C$, $\delta^{18}O$) becomes isotopically heavier. The results show an increase of 0.4 ‰ and 0.76 ‰ per 1,000 m water depth for $\delta^{13}C$ and $\delta^{18}O$, respectively. Sea-water carbonate ion content, bulk sediment parameters, and calcareous micro- and nannoplankton parameters are capable of distinguishing the area above from the area below the calcite lysocline. BDX, the *Calcidiscus leptoporus - Emiliania huxleyi* Dissolution Index (CEX) and the rain ratio are suited to distinguish the upper open ocean and the deep ocean (sublysoclinal dissolution) as well as the upwelling influenced coastal ocean (supralysoclinal dissolution). Each dissolution index investigated yields an excellent calibration datum of the modern to the fossil situation.

*Carbonate dissolution in the Late Quaternary central equatorial Atlantic (Site GeoB 1117-2/3).* Indices commonly used as dissolution proxies were applied to one sediment core. BDX shows better preservation during glacials; the $CaCO_3$ content and the Foraminiferal Dissolution Index (FDX) imply better preservation during interglacials; the rain ratio and the composition of assemblages >150 µm give no indication to enhanced dissolution at all. Cross spectral analysis shows no signal at the period of orbital tilt (41 kyrs) of the warm-transitional factor which would indicate dissolution in this region. Hence, there is no evidence for strong dissolution increase during the last 300 kyrs which would fake the paleo-reconstructions. Moreover, this site presumably was dominated by NADW influence and AABW never reached that location. Thus, under carbonate (super-) saturated conditions BDX is supposed to serve as deep-water circulation index rather than as dissolution proxy.

# Part I *Introduction*

## 1. Modern and past surface water environment in the South Atlantic Ocean

### *1.1 Modern surface water circulation*

In the South Atlantic, the surface water current system is dominated by a subtropical anticyclonic gyre (Fig. I-1). The gyre is the result of general atmospheric circulations in low to temperate latitudes dominated by trade winds and westerlies. During the southern winter, the subtropical high-pressure area moves north-west which results in an intensification of the SE trades. In opposite seasons and hemispheres trade winds alternate in strength; that is, strong SE trades co-occur with weak NE trades and vice versa.

The surface water oceanography of the equatorial Atlantic is characterized by the westward flowing South Equatorial Current (SEC) and the eastward flowing South Equatorial Counter Current (SECC), the North Equatorial Current (NECC), and the Equatorial Undercurrent (EUC). Variations in the surface water oceanography are driven by the interaction of low-latitude trade- and monsoonal winds. Warm surface waters from the subtropical gyre, reinforced by the Benguela Current (BC), move as SEC through the South Atlantic much of it crossing the equator into the North Atlantic (Gordon and Bosley, 1991; Peterson and Stramma, 1991). Moreover, the seasonally changing wind system reflects a combination of cool eastern-boundary waters advected westwards and a wave-like movement of the thermocline (Moore et al., 1978; Cane, 1979; Philander, 1979; Philander and Pacanowski, 1986).

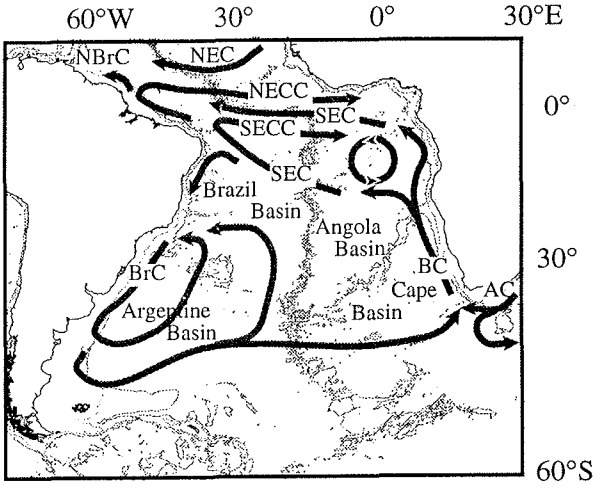


**Fig. I-1:** Sketch of the recent main surface water distribution paths in the equatorial South Atlantic Ocean (modified after Peterson and Stramma 1991). AC...Aghulas Current; BC...Benguela Current; BrC...Brazil Current; NEC...North Equatorial Current; NECC...North Equatorial Counter Current; NBrC...North Brazil Current; SEC...South Equatorial Current; SECC...South Equatorial Counter Current

The SEC consists of two branches of different velocity separated by the SECC

(Richardson and Reverdin, 1987). At about 10°S off the coast of Brazil, the SEC splits into the southwards flowing Brazil Current (BrC) and the northwards moving North Brazil Current (NBrC). The NBrC as the stronger one contributes water to the NECC which seasonally interacts with the northern branch of the SEC. In the mixing area of NECC and SEC the convergence of water masses results in (1) downwelling of surface waters and (2) depression of the thermocline (Philander and Pacanowski, 1986). Within the thermocline the equatorwards transported water supports the EUC. The contact between EUC and the southern branch of the SEC forms the equatorial divergence zone where cold water from thermocline depths is upwelled. However, nutrient content and depth of the thermocline seasonally change.

### *1.2 Modern latitudinal and vertical distribution of planktic foraminifera in the South Atlantic Ocean and their use as (pale-) oceanographic proxies*

Many plankton investigators have noted a close relationship between the faunistic and hydrographic features of the major oceanic water masses (e.g., Ravelo et al., 1990; Sautter and Thunell, 1991a). Actually, planktic foraminifera are one of the most common groups of pelagic organisms in the open ocean. Their distribution through passive transport, coupled with their sensitivity to environmental variations emphasize their importance for interpreting marine sediments regarding climate variations and other (pale)

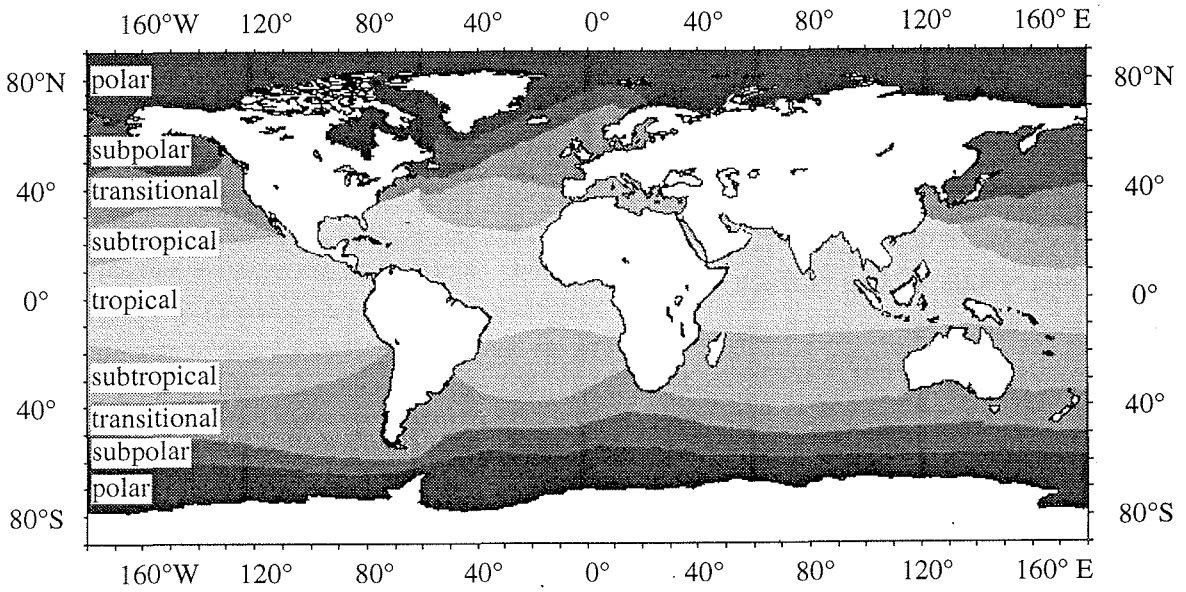


**Fig. I-2:** Five major world distributional zones of planktic foraminifera in rather distinct latitudinal belts primarily influenced by ecologic and hydrographic features of the surface water masses (modified after Bé and Tolderlund, 1977).

oceanographic applications. Depending on the reference there are some 30 living species

which can be grouped into five major zoogeographic provinces (e.g., Bé and Hutson, 1977; Hemleben et al., 1989, Fig. I-2). The majority of the planktic foraminiferal species live in tropical and subtropical waters. The regions in the northern and southern hemisphere where cold- and warm-water species overlap in distribution and where the greatest faunistic contrasts occur are designated "transition zones". Actually, subtropical and subpolar species occur together in transitional waters, and only *G. inflata* and *G. truncatulinoides* sin. appear to be indigenous to the transition zone (Kemle-von Mücke, 1994; Niebler and Gersonde, 1998). The cold-water fauna can be divided into some subpolar species and a single polar species (*N. pachyderma* sin.). However, rare are the eurythermal, cosmopolitan species that have a world-wide distribution in all water types (e.g., *G. glutinata*).

Each species distribution can be looked at from a certain point of view including latitudinal, bathymetric, environmental, preservational aspects etc. (Fig. I-3). From plankton net investigations, Bé and Tolderlund (1971) found that each zoogeographic province is represented by at least one principal species which actually is not necessarily limited to that area:

| | |
|---|---|
| Northern and southern cold-water regions: | *Neogloboquadrina pachyderma* sin. (polar) |
| | *Neogloboquadrina pachyderma* dex. (subpolar) |
| | *Turborotalita quinqueloba* (subpolar) |
| Northern and southern transition zones: | *Globorotalia inflata* |
| Northern and southern subtropical regions: | *Globigerinoides ruber* pink variety |
| | *Globigerinita glutinata* |
| Tropical zone: | *Globigerinoides sacculifer* |
| | *Pulleniatina obliquiloculata* |

Additionally, most living species can be attributed to distinct water depths (Ravelo et al., 1990; Oberhänsli et al., 1992; Ottens, 1992). Due to the access of light and food, the majority of the spinose species are surface dwellers, or at least prefer to live in the upper part of the euphotic zone (e.g., *Globigerinoides* spp.). Non-spinose species preferentially live at sub-surface depths below 50 m (e.g., some *Globorotalia* spp.), and a few species inhibit depths below 100 m and even below 200 m (e.g., *G. theyeri* ). However, some species prefer thermocline conditions (e.g., *N. dutertrei* ) and consequently follow the seasonally changing thermocline depth within the water column; other species (e.g., *G. bulloides* ) also correlate with high nutrient supply or low temperature (*N. pachyderma* sin.). Consequently, each species is assigned to discrete hydrographic characteristics and, vice versa, reflects discrete hydrographic characteristics

which are used to reconstruct past oceanic environments (Ravelo et al., 1990). Regarding carbonate dissolution susceptibility, Berger (1968) classifies thick-shelled (e.g., *G. tumida* ) and thin-shelled (e.g., *G. ruber* ) species.

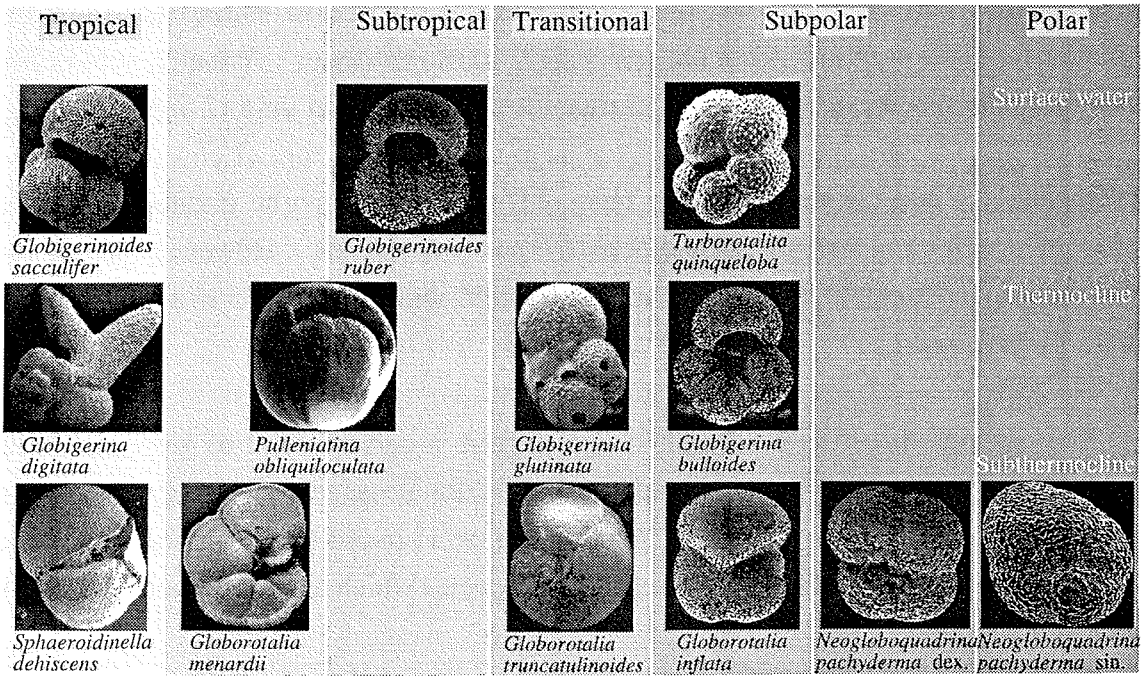


**Fig. I-3:** Exemplary sketch on some planktic foraminiferal species with respect to their habitat: *Globigerinoides sacculifer* belongs to the highly carbonate dissolution susceptible, thin-shelled surface dwellers of the tropics whereas *N. pachyderma* sin. is part of the dissolution resistant subthermocline denizens of the polar region (GeoB 1117-2; shell size is about 350 µm).

Since environmental conditions lastly depend on the predominant water mass distribution, Mix and Morey (1996) divide sedimentary planktic foraminiferal assemblages of the Atlantic South Equatorial Current into three major groups: (1) the tropical-subtropical warm pool group (e.g., *G. ruber*), (2) the equatorial and coastal upwelling group (e.g., *N. dutertrei*), and (3) the eastern boundary current advection group (e.g., *G. inflata*).

*1.3 Modern distribution of planktic foraminifera in the equatorial Atlantic Ocean and in the northern Cape Basin* (referring to own results; see Part II - chapters 1, 2, 3, 4)

Each sediment surface transect investigated (Table I-1; Fig. I-4) belongs to a distinct surface water environment; that is, each investigated surface sample of one transect should consequently reflect more or less the same surface water parameters. The method of transfer technique provides two data sets, namely (1) the composition of planktic foraminiferal assemblages and (2) the seasonal and annual mean sea surface temperatures

(SST's) of the upper 30 m of the water column. However, where either the species composition, the recalculated SST, or the communality show strong alteration, carbonate dissolution is supposed to become important, and the inferred surface water parameters are biased.

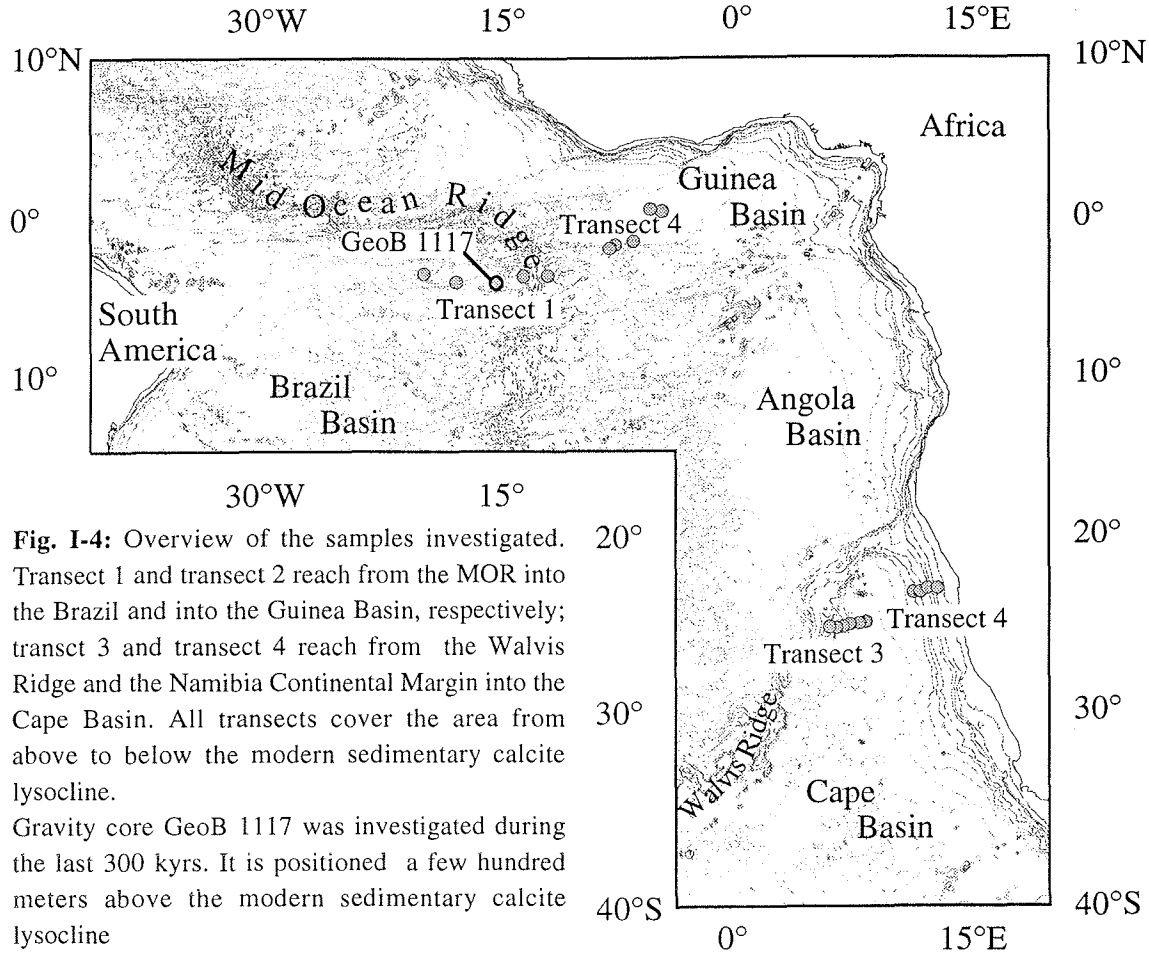


**Fig. I-4:** Overview of the samples investigated. Transect 1 and transect 2 reach from the MOR into the Brazil and into the Guinea Basin, respectively; transct 3 and transect 4 reach from the Walvis Ridge and the Namibia Continental Margin into the Cape Basin. All transects cover the area from above to below the modern sedimentary calcite lysocline.
Gravity core GeoB 1117 was investigated during the last 300 kyrs. It is positioned a few hundred meters above the modern sedimentary calcite lysocline

In both the equatorial Brazil Basin (Transect 1) and in the equatorial Guinea Basin (Transect 2), the modern sedimentary planktic foraminiferal assemblages mainly consist of species of the subtropical-tropical group, and species of the warm-transitional group are of subordinate importance. SST's recalculated via transfer function technique range from 25.7 °C ($T_{cold\ season}$) to 27.4 °C ($T_{warm}$); the annual mean temperature is 26.6 °C.

The two transects of the northern Cape Basin belong to different ecosystems. Whereas the Walvis Ridge transect shows normal open ocean conditions, the Namibia Continental Margin transect is affiliated to the Benguela upwelling system which is indicated by both the species composition and the recalculated SST. Sediment surface samples of the Walvis Ridge are dominated by the warm-transitional fauna, and species of the subtropical-tropical group are of subordinate importance. However, the Namibia Continental Margin transect only consists of species of the warm-transitional fauna; the

subtropical-tropical fauna is quasi-absent. SST's range from 18.4 °C ($T_{cold\ season}$) to 23.2 °C ($T_{warm\ season}$) regarding the Walvis Ridge surface water ($T_{annual\ mean}$ = 21.2 °C) and range from 15.3 °C ($T_{cold\ season}$) to 17.6 °C ($T_{warm\ season}$) regarding the Namibia Continental Margin surface water ($T_{annual\ mean}$ = 17.4 °C).

All recalculated SST's are close to the measured SST's ($\sigma_n$ <1 °C) as published by Levitus and Boyer (1994).

At water depths of 4,100 m (eastern Cape Basin), 4,350 m (Brazil Basin), and 4,400 m (western Cape Basin) carbonate dissolution turns out to be significant. All reconstructed SST's lower by several degrees ($\sigma_n$ >>1 °C), the species composition becomes statistically insignificant (factor loadings<<0.5), and communalities switch to the "no-analogue" situation (-999.999).

| Location | Device | Latitude | Longitude | Water depth | Sample interval |
|---|---|---|---|---|---|
| **Transect 1: MOR - Brazil Basin** | | | | | |
| GeoB 1115-4 | Giant box corer | 3°33.5'S | 12°34.8'W | 2,921 m | 0 cm - 1 cm |
| GeoB 1116-1 | Giant box corer | 3°37.4'S | 13°11.2'W | 3,471 m | 0 cm - 1 cm |
| GeoB 1117-3 | Giant box corer | 3°49.0'S | 14°54.2'W | 3,977 m | 0 cm - 1 cm |
| GeoB 1117-2 | Gravity corer | 3°49.0'S | 14°54.2'W | 3,977 m | 0 cm - 1,038 cm |
| GeoB 1118-2 | Giant box corer | 3°33.6'S | 16°25.9'W | 4,675 m | 0 cm - 1 cm |
| GeoB 1119-2 | Giant box corer | 2°59.9'S | 18°22.7'W | 5,213 m | 0 cm - 1 cm |
| **Transect 2: MOR - Guinea Basin** | | | | | |
| GeoB 1106-5 | Giant box corer | 1°45.6'S | 12°33.1'W | 2,471 m | 0 cm - 1 cm |
| GeoB 1105-3 | Giant box corer | 1°39.9'S | 12°25.7'W | 3,231 m | 0 cm - 1 cm |
| GeoB 1105-4 | Gravity corer | 1°39.9'S | 12°25.7'W | 3,225 m | 0 cm - 668 cm |
| GeoB 1104-5 | Giant box corer | 1°01.0'S | 10°42.3'W | 3,724 m | 0 cm - 1 cm |
| GeoB 1103-3 | Giant box corer | 0°36.1'N | 9°15.8'W | 4,321 m | 0 cm - 1 cm |
| GeoB 1102-3 | Giant box corer | 0°30.9'N | 8°35.3'W | 4,779 m | 0 cm - 1 cm |
| **Transect 3: Walvis Ridge - Cape Basin** | | | | | |
| GeoB 1217-1 | Giant box corer | 24°56.7'S | 6°43.5'E | 2,007 m | 0 cm - 1 cm |
| GeoB 1207-2 | Giant box corer | 24°35.9'S | 6°51.3'E | 2,593 m | 0 cm - 1 cm |
| GeoB 1208-1 | Giant box corer | 24°29.5'S | 7°06.8'E | 2,971 m | 0 cm - 1 cm |
| GeoB 1209-1 | Giant box corer | 24°30.7'S | 7°17.0'E | 3,303 m | 0 cm - 1 cm |
| GeoB 1211-1 | Giant box corer | 24°28.4'S | 7°32.2'E | 4,089 m | 0 cm - 1 cm |
| GeoB 1212-2 | Giant box corer | 24°19.9'S | 8°15.0'E | 4,669 m | 0 cm - 1 cm |
| **Transect 4: Cape Basin - Namibia Continental Margin** | | | | | |
| GeoB 1709-3 | Giant box corer | 23°35.3'S | 10°45.5'E | 3,837 m | 0 cm - 1 cm |
| GeoB 1710-2 | Giant box corer | 23°25.8'S | 11°42.2'E | 2,987 m | 0 cm - 1 cm |
| GeoB 1711-5 | Giant box corer | 23°19.0'S | 12°22.7'E | 1,964 m | 0 cm - 1 cm |
| GeoB 1712-2 | Giant box corer | 23°15.3'S | 12°48.2'E | 1,007 m | 0 cm - 1 cm |

**Table I-1:** Table of the box corer and the gravity core samples investigated.

*1.4 Late Quaternary surface water circulation*

A vast range of different opinions exists about the processes driving Late Quaternary variations of the SEC in the South Atlantic Ocean (e.g., Cane, 1979; Philander and Pacanowski, 1980; Philander and Pacanowski, 1981), and at present there is non consensus.

However, Mix and Morey (1996) propose a sequence of events during a "generic" ice age cycle in the South Atlantic (near-) surface circulation which is based on planktic foraminifera investigations and down-core Q-mode factor analysis. This scenario supports and expands on the views of several other authors (e.g., Gardner and Hays, 1976; McIntyre et al., 1989). They speculate on a central equatorial system driven by thermal gradients in the southern hemisphere (1) first by meridional gradients associated with cooling in high southern latitudes which modulate the zonal component of the southern trades; and (2) by a feedback process associated with land-sea contrast, which modulate meridional winds in the SE Atlantic and draw water offshore from the BC towards the equator.

Prior to the transition into an ice age, reduction of atmospheric $CO_2$ and initial greenhouse cooling in the southern oceans strengthen hemispheric thermal gradients. The resulting compression of atmospheric pressure gradients drive stronger zonal trade winds and equatorial upwelling which begin to cool the equatorial region. Oceanic cooling relative to a warm African land mass shifts the thermal equator northwards and intensifies the land-sea atmospheric pressure gradients along the southern hemisphere eastern boundary. Stronger southerly winds enhance the BC drawing these cool waters off the eastern boundary to reach the SEC in the central Atlantic amplifying further cooling. The cyclonic gyre in the Guinea Basin continues to be active during the glacial maximum. During the ice melting phase in high latitudes, warmth in the southern ocean reduces thermal gradients, and trade winds and equatorial upwelling diminish. The advection of Benguela water lessens, and the central equatorial Atlantic returns to full interglacial conditions.

*1.5 Late Quaternary distribution of planktic foraminifera in the equatorial Atlantic Ocean* (referring to own results; see Part II - chapters 1, 2)

Planktic foraminifera and coccolitophores are the major sediment components during the last 300 kyrs in the investigated core GeoB 1117-2/3. Although carbonate sedimentation seems to be dominated by tropical planktic foraminifera, coccolithophores contribute largely to the carbonate sedimentation in times of higher surface water

productivity; however, siliceous microfossils are of minor importance. During glacials, low carbonate contents correlate with higher percentages of terrigeneous material which is attributed to stronger eolian dust input (deMenocal et al., 1993; Verardo and Ruddiman, 1996; Wagner and Dupont, in press).

Regarding the relative abundances and the absolute numbers of planktic foraminifera there is a distinct glacial-to-interglacial modification. Using a five-factor model, the transfer function technique displays two highly significant factors: (1) The subtropical-tropical factor which attains maximum loadings during all interglacials and the Holocene; (2) the warm-transitional factor which occurs with maximum loadings during glacial events; during the Holocene this factor almost expires. As already discovered by Ericson and Wollin (Ericson and Wollin, 1968), the *G. menardii* group is missing completely from 80 ka to 12 ka in the equatorial Atlantic Ocean.

Late Quaternary transfer technique temperatures of the last 300 kyrs range from 19.1 °C to 27.5 °C ($T_{warm\ season}$), from 15.5 °C to 26.5 °C ($T_{cold\ season}$), and from 17.7 °C to 27.2 °C ($T_{annual\ mean}$). Maximum temperatures are attained in the Holocene, and minimum temperatures are attained during oxygen isotope event (OIE) 8.2 (249 ka). In general, highest estimated sea surface temperatures (SST's) are attained during interglacials corresponding to maximum insolation at 15°N, and lowest SST's occur during glacials. Moreover, regarding the last 300 kyrs, there is a certain trend that glacial maxima are supposed to become warmer by about 2.7 °C; annual mean temperatures range from 17.7 °C (substage 8.2) over 19.3 °C (substage 6.2) and 20.3 °C (substage 4.2) to 20.4 °C (substage 2.2). The difference between the modern and the Last Glacial Maximum (LGM) SST amounts to about 6 °C for the central tropical South Atlantic. With huge data sets and improved transfer functions the present marine temperature signals and that by other authors (Mix et al., 1986a; Mix et al., 1986b; McIntyre et al., 1989; Wolff et al., subm.), terrestrial temperature records (Rind and Peteet, 1985; Stute et al., 1995) and SST reconstructions by coral records (Guilderson et al., 1994) all are of comparable magnitudes between the modern and the LGM tropical Atlantic Ocean.

The paleo-environmental reconstruction distinguishes two oceanic situations for the tropical Atlantic Ocean during the last 300 kyrs. Both are of 23 kyrs and 100 kyrs cyclicity and coherent with the global ice volume record in the $\delta^{18}O$ of the benthic foraminifer *Cibicides wuellerstorfi.*: (1) Cool water temperature, lower salinities and a somewhat higher nutrient supply corresponding to high loadings of the warm-transitional factor *G. bulloides* and *N. pachyderma* dex.; and (2) warm and salty surface water masses with a deep thermocline indicated by high loadings of the subtropical-tropical factor as demonstrated by enhanced relative abundances and absolute numbers of *G. ruber, G. sacculifer* and *G. menardii*. That is, during glacials cool and nutrient-rich

waters are advected off the eastern boundary, reach the equatorial Atlantic Ocean, and amplify cooling. Equatorial upwelling may be enhanced somewhat; however, the upwelling factor does not reach loadings that explain any significance. During interglacials, the thermocline is deep and equatorial upwelling is only moderate. Cool water advection is weak or absent in the equatorial Atlantic Ocean. Mix and Morey (1996) who reconstructed Pleistocene variations in the Atlantic south equatorial current distinguished three significant factors. However, factor loadings indicate that upwelling and eastern boundary assemblages covary, and both upwelling and advection drive glacial cooling of the equatorial Atlantic Ocean.

## 2. Modern and past deep-water environment in the South Atlantic Ocean

### *2.1 Modern deep-water circulation*

The thermohaline circulation (global conveyor belt, Broecker, 1991) may be even more important to the climate system than the wind-driven circulation as it couples the full volume of the oceans to the atmosphere and contributes substantially to the global transport of heat and water (e.g., Schmitz, 1995; Gordon, 1996). Regarding present-day thermohaline circulation (Figs. I-5, 6), the South Atlantic receives mid-depth waters from the North Atlantic, namely the North Atlantic Deep Water (NADW). These water mass remains stratified as it circulates within the Atlantic Ocean, and produces a deep, thick and southwards directed layer of warm, saline water of high $CO_3^{2-}$ and low $CO_2$ content at mid depths between about 2,000 m and 4,000 m. The effect of this warm and saline layer is to contribute salinity to the other oceans, and to set up the formation of the Weddell Sea Bottom Water (WSDW) (Reid, 1996).

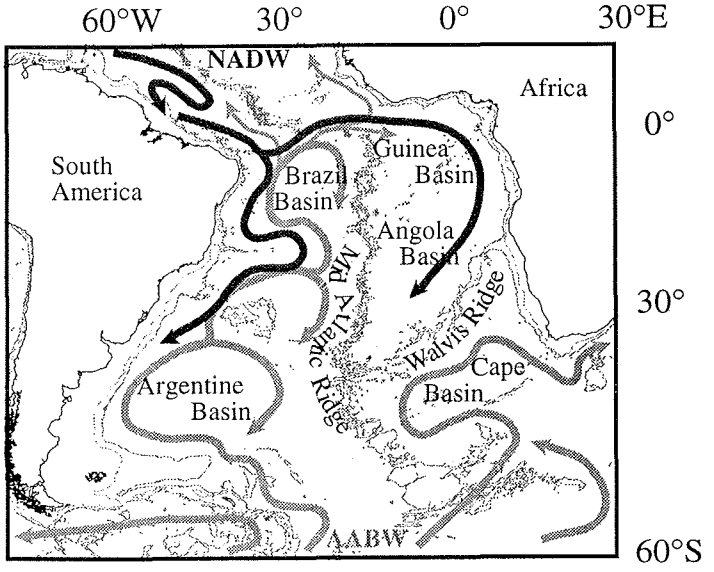


**Fig. I-5:** Sketch of the recent main deep-water distribution paths in the South Atlantic Ocean (light gray - Antarctic Bottom Water (AABW); dark gray - North Atlantic Deep Water (NADW); modified after Faugères et al. (1993) and Sarnthein et al. (1994).

From the Southern Ocean the South Atlantic gathers its densest waters, (1) the WSDW, (2) the

Circumpolar Deep Water (CDW) at all depths from the circumpolar flow through the Drake Passage, and (3) shallow Antarctic Intermediate Water (AAIW) from near the surface along about 50°S to 55°S (Talley, 1996). The density characteristics make the NADW divide the CDW in an upper (UCDW) and a lower branch (LCDW), whereas WSDW and LCDW unify into Antarctic Bottom Water (AABW; Figs. I-5, 6). AABW can be distinguished as an extremely cold water mass of low $CO_3^{2-}$ and high $CO_2$ content (Kroopnick, 1985; Boyle, 1988). Regarding temperature, a rather impressive depiction basing on the *Wissenschaftliche Ergebnisse der Deutschen Atlantik Expedition Meteor 1925-1927* already is given by Dacqué (1930, see half-title).

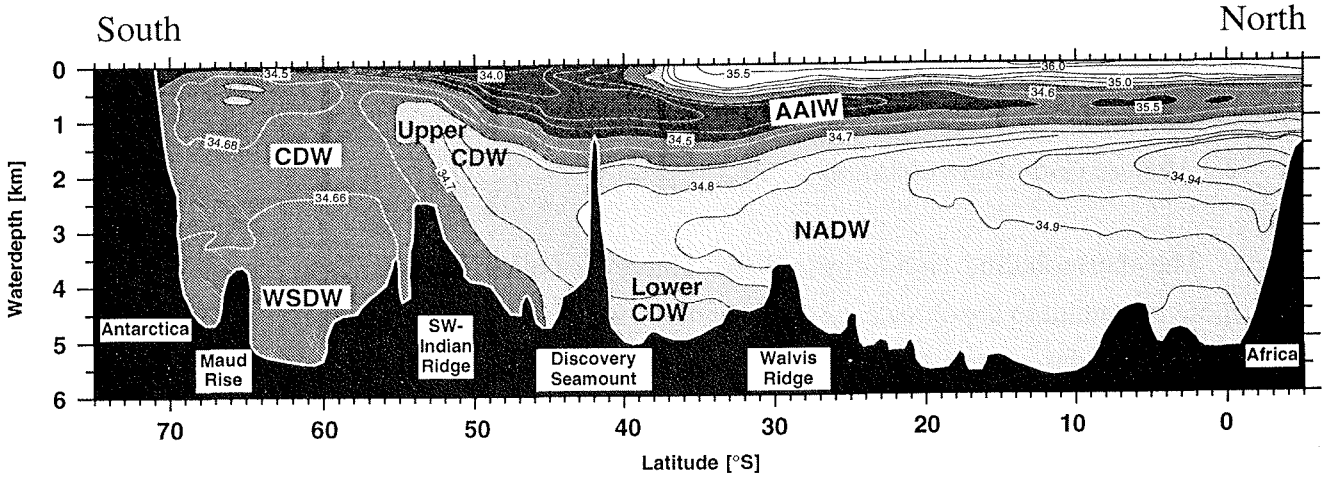


**Fig. I-6:** Present-day stratification of main ocean water masses in the South Atlantic as displayed by salinity contour lines [‰] at a north-south transect along the Greenwich Meridian; modified after Reid (1989).

CDW...Circumpolar Deep Water; AAIW...Antarctic Intermediate Water; NADW...North Atlantic Deep Water; WSDW...Weddell Sea Deep Water; AABW...Antarctic Bottom Water (WSDW + Lower CDW)

While AABW is moving more or less unhampered northwards within the Brazil Basin, it is orographically detained within the Cape- and the Guinea Basins by the Mid Atlantic Ridge and the Walvis Ridge (Fig. I-5). The inflow of AABW into the Guinea Basin is restricted to only small quantities passing the sills through the Romanche-, the Chain Fracture Zone and the Walvis Passage (Van Bennekom and Berger, 1984; Shannon and Chapman, 1991; Warren and Speer, 1991; Mercier et al., 1994). Consequently, the deepest parts of the Guinea Basin are filled almost exclusively by NADW (Kroopnick, 1985). The Cape Basin, although located eastwards of the Mid Atlantic Ridge, is dominated by AABW below 4,000 m due to a bottom water passage, which allows AABW to enter the basin from the south (Reid, 1989).

*2.2 Modern carbonate dissolution and its use as oceanographic proxy*

From the surface water as the place of life-history down to the sedimentological archive planktic foraminiferal assemblages sometimes are changed qualitatively and quantitatively due to carbonate dissolution. Actually, each type of planktic foraminiferal test architecture yields different crash behavior with *G. ruber* rapidly dismantling into single chambers along the sutures and *N. pachyderma* undergoing long lasting ultrastructural breakdown before the final smash. That is, calcite dissolution is a process which affects individual species in a different extent (Berger, 1970; Parker and Berger, 1971; Berger, 1979; Malmgren, 1983; Baumann and Meggers, 1996). Where carbonate dissolution suddenly increases both the hydrographic lysocline (in the water column) and the sedimentary lysocline (at the sediment pore water interface) are attained. Regarding the modern South Atlantic Ocean the lysocline marks the boundary between the carbonate ion undersaturated and highly corrosive AABW and the carbonate ion saturated NADW (Broecker and Takahashi, 1978) which is close to the 90 µmol/kg $CO_3^{2-}$ isoline (GEOSECS, Bainbridge, 1981). Consequently, the disintegration of planktic foraminifera due to carbonate dissolution is a valuable tool to run deep- and bottom water reconstructions, respectively. However, where carbonate dissolution becomes evident, the relationship planktic foraminifera - hydrography expires. Ergo, surface water reconstructions will fail (e.g., Hemleben et al., 1989; Boltovskoy and Totah, 1992; Le and Shackleton, 1992).

In order to assess the validity of planktic foraminifera for surface and deep-water reconstructions some method is required to determine the degree of carbonate dissolution. There are micropaleontological and sedimentological parameters considered to be linked to carbonate dissolution. These methods include (1) percent fragmented planktic foraminiferal tests (e.g., Keigwin, 1976; Le and Shackleton, 1992); (2) proportions of solution susceptible and solution resistant planktic foraminiferal species (e.g., Schott, 1935; Berger, 1979; Boltovskoy and Totah, 1992); (3) the ratio of one organism group to another (e.g., Kennett, 1966; Hay, 1970; Parker, 1971; Berner, 1977; Peterson and Prell, 1985); the ultrastructural breakdown of planktic foraminiferal tests (Henrich, 1989; Baumann and Meggers, 1996; Van Kreveld, 1996; Dittert and Henrich, subm.) etc.

*2.3 Modern carbonate dissolution* (referring to own results; see Part II - chapters 3, 4)

For the carbonate dissolution investigations the "depth-transect approach" was applied (e.g., Farrell and Prell, 1989; Curry and Lohmann, 1990; Bickert et al., 1997) which gives a calibration of the modern to the fossil situation.

In general, all parameters applied to the carbonate dissolution in the deep ocean are capable of distinguishing the area above from the area below the top of the calcite lysocline. Beyond that, some parameters are suited to distinguish the upper continental margin of the coastal ocean within an upwelling area controlled by enormous productivity, high export and rapid sedimentation. In detail, these are the carbonate ion content of the water column and the weight percentage of sediment $CaCO_3$-content (Archer, 1996), the rain ratio (Berger and Keir, 1984), the *Globigerina bulloides* Dissolution Index (BDX, Dittert and Henrich, subm.), and the *Calcidiscus leptoporus - Emiliania huxleyi* Dissolution Index (CEX, Dittert et al., subm.-a).

Regarding the three different oceanographic regimes, only the carbonate ion content and the percentage of sediment carbonate content put us in the position to determine top, bottom, and thickness of the lysocline. If these parameters are not available, a combination of BDX, CEX and rain ratio gives the best approach to the authentic conditions.

According to the investigated transects, the top of the calcite lysocline can be set to about 4,300 m in the open ocean realm of the Brazil- and the western Cape Basin. The thickness of the lysoclines amount to about 800 m. With respect to the continental margin of the eastern Cape Basin, the lysocline is situated at about 4,100 m water depth; the lysocline thickness becomes >900 m.

Regarding the top and the bottom of the sedimentary calcite lysocline, all reconstructions show a consistent picture which we attribute to the bottom water distribution. That is, lysocline depth and sublysoclinal carbonate dissolution pattern in the open ocean seem to depend on both the influence of the corrosive AABW and the asymmetry of its oceanographic distribution.

### *2.4 Late Quaternary deep-water circulation*

Oeschger et al. (1984) were the first who suggested that the climate events measured in Greenland ice-cores jump between two modes of operation. This proposal was enhanced by Broecker et al. (1985) who postulated that this climate system oscillations can be applied on the whole Atlantic conveyor circulation system which was regularly switched on/off. Simulations of a simple coupled atmosphere-ocean model (Stocker and Schmittner, 1997) support these suggestions showing that there are (1) a final atmospheric concentration of 750 ppm $CO_2$ which was able to shut down the thermohaline circulation permanently and (2) a rate of greenhouse-gas increase of about 1 % $yr^{-1}$ that would yield the same results. However, the final shut-down never was recorded in sediments of the Atlantic Ocean. Rather, there are indications for short-term

climate oscillations of one or more millennia duration showing a broad spectrum of amplifying and weakening the intermediate and deep-water circulation (Keigwin et al., 1994; Keigwin and Jones, 1994; Sarnthein et al., 1994; Curry, 1996).

On the basis of observed phase relationships between ice volume and several deep-water circulation proxies, the SPECMAP group proposed a four stage model of the glacial-to-interglacial-cycle (Imbrie et al., 1992; Imbrie et al., 1993). During a preglacial phase, reduced production of LNADW results in (1) a decrease in the heat flux to the southern ocean which (2) causes an early cooling at high latitudes of the southern hemisphere, (3) early sea-ice growth, (4) northward migration of oceanic fronts, and (5) drawdown of atmospheric $p\ CO_2$ (the so-called *Nordic heat pump*). During the glacial phase, production of the UNADW increases whereas the LNADW production remains suppressed (the so-called *Boreal heat pump*). During the deglacial phase, early warming at high latitudes of the northern hemisphere pushes the production of LNADW which culminates in the operation of both the upper and the lower heat pump. Nearly simultaneous warming occurs in the southern hemisphere, sea-ice melts, oceanic fronts migrate southwards, and atmospheric $p\ CO_2$ increases.

This model is supported by investigations of $\delta^{13}C$ and the Cd/Ca ratio of benthic foraminifera which show that the production of LNADW (below 2,000 m water depth) was reduced whereas the production of UNADW (above 2,000 m water depth) was enhanced during glacials (e.g., Boyle and Keigwin, 1987; Curry et al., 1988; Duplessy et al., 1988; Oppo and Lehman, 1993). The restricted production of LNADW was compensated for by intensified extension of the AABW farther north than it does today (e.g., Broecker et al., 1985; Corliss et al., 1986; Broecker et al., 1988). Consequently, AABW went higher in the water column over the critical sill depths of the Romanche Fracture Zone (~ 3,850 m), and the Guinea- and the Angola Basins were filled with AABW. That is, today's asymmetry of deep-water circulation in the South Atlantic Ocean was not present during glacial times (Bickert and Wefer, 1996). Using a zonally averaged three-basin ocean model, Duplessy et al. (1996) support these results suggesting that the glacial AABW production was slightly higher than the modern one, whereas that of the NADW was reduced by about 40 %. Moreover, there are indications for ice-free regions in the nordic seas during the last glacial maximum - at least during summer months (e.g., Henrich et al., 1989; Henrich et al., 1995; Sarnthein et al., 1995; Pflaumann et al., 1996) and Atlantic water masses passing far northwards into the Fram Strait (Hebbeln et al., 1994; Dokken and Hald, 1996). That is, wintry convection and deep-water production in the nordic seas could have taken place also during glacials due to moisture supply and salt advection (Weinelt et al., 1996) - which would strongly contradict the on/off conveyor circulation system mentioned above.

### *2.5 Late Quaternary carbonate dissolution cycles as integral part of the carbon cycle*

Since sedimentary calcite cycles were first identified in cores recovered during the Swedish Deep Sea Expedition 1947-1948 (Arrhenius, 1952) implications for temporal changes in marine chemistry are still under discussion. The preservation state of calcareous deep-sea sediments is linked to the carbonate chemistry in the water column and at the sediment pore water interface. This carbonate chemistry mainly is driven by (1) the rain rate and accumulation rate of carbonate and non-carbonate particles; (2) the extent to which seawater is saturated with $CaCO_3$; (3) the amount of organic matter that is buried by $CaCO_3$; (4) whether the carbonate particles have an organic coating retarding dissolution; (5) whether there are currents to stir the layer of dissolution around the $CaCO_3$ particles; and (6) the benthic mixing process that continually acquires new calcite into the sediment removing the necessity for a long diffusion path (Broecker and Takahashi, 1977; Broecker and Takahashi, 1978; Emerson and Bender, 1981; Broecker and Peng, 1982; Le and Shackleton, 1992; Martin and Sayles, 1996).

Deep ocean carbonate chemistry is, in turn, one of several influences on the partial pressure of $CO_2$ in the atmosphere. More detailed, the pH equilibrium reaction $CO_2 + CO_3^{2-} + H_2O \leftrightarrow 2HCO_3^-$ maintains an inverse relationship between $[CO_3^{2-}]$ and $p\,CO_2$. Thus, the preservation and dissolution history of calcareous deep-sea sediments carries information on (1) the transition from super- to undersaturation (*lysocline*, Broecker and Takahashi, 1978) regarding carbonate ion content which (2) subsequently would drive variations in $p\,CO_2$ (Broecker and Peng, 1993; Archer and Maier-Reimer, 1994). As revealed from sediment core investigations, changes in carbonate dissolution over time can be attributed both to changes in the rain rates of organic carbon and calcium carbonate that reach the floor (Archer, 1991) and/or to changes in the bottom water and pore water activity at that depth (Farrell and Prell, 1989; Farrell and Prell, 1991). Both may result in deepening the top and/or the bottom of the lysocline (Archer, 1996) and in turn change $p\,CO_2$.

### *2.6 Late Quaternary carbonate dissolution* (referring to own results; see Part II - chapter 1)

The modern sedimentary calcite lysocline in the northern Brazil Basin is located at about 4,300 m (Dittert and Henrich, subm.), and the hydrographic calcite lysocline is not far above at about 4,150 m water depth (Bainbridge, 1981). How can one assess whether the lysocline did raise during the last 300 kyrs and affect the samples investigated by

calcite dissolution?

In the *South Atlantic Dissolution Experiment* Dittert et al. (subm.-a) investigated some commonly used dissolution indices in a depth-transect of sediment surface samples to determine the qualitative and quantitative modification of these indices during increasing carbonate dissolution. More detailed, these are the *Globigerina bulloides* Dissolution Index (BDX, Dittert and Henrich, subm.), the rain ratio (Berger and Keir, 1984), the composition of assemblages >150 µm (modified after Diester-Haass and Rothe, 1987), and the Foraminiferal Dissolution Index (Berger, 1979). Where the depth-transect crosses the calcite lysocline the corresponding value of each dissolution index yields an excellent calibration datum of the modern to the fossil situation. Applied to down-core investigations, these indices reveal at which time the dissolution of sedimentary calcite increases.

Regarding the investigated sediment core GeoB 1117-2/3, these indices are not consistent. BDX shows better preservation during glacials, whereas FDX and the $CaCO_3$ content imply better preservation during interglacials. Last not least, the rain ratio and the composition of assemblages >150 µm give no indication to enhanced dissolution at all.

Enhanced calcite dissolution could be attributed to the productivity of marine organic carbon in surface waters (Berger et al., 1994) which is supposed to be increased during glacials leading to intensified metabolic respiration (Emerson and Bender, 1981). Actually, the input of eolian terrigenous carbon contributes to the total organic carbon content (Verardo and Ruddiman, 1996; Wagner and Dupont, in press). Since it is inert, it is not available to calcite dissolution. On the other hand, enhanced calcite dissolution during interglacials could be attributed to maximum NADW production leading to enforced deep-water circulation (Gamboa et al., 1983). That is, the enhanced interchange between deep-water and sediment pore water might yield some calcite dissolution (Santschi et al., 1983; Le and Shackleton, 1992) which is monitored by the highly sensitive BDX. Regarding cross spectral analysis of the planktic foraminiferal assemblages, it can be ascertained that there is a lack of coherent variations at the period of orbital tilt (41 kyrs) of the warm-transitional factor. As this period is clearly present in the oxygen isotope record, we infer that carbonate dissolution is not strongly affecting the samples investigated, because dissolution imparts a 41 kyrs rhythmic signal in calcite preservation indices similar to that of $\delta^{18}O$ in this region (Verardo and McIntyre, 1994; Mix and Morey, 1996).

However, no index investigated gives clear evidence for such strong dissolution increase which would be induced by the rise of the lysocline. That is, the site (3,984 m) was dominated by the NADW influence during the last 300 kyrs, and the AABW never reached that location. Consequently, the critical sill depth of the Romanche Fracture Zone

(~ 3,850 m) supposedly was not activated, and the Guinea- and the Angola Basins were not filled with AABW. This would contradict the statement of Bickert and Wefer (1996) that today's asymmetry of deep-water circulation in the South Atlantic Ocean was not present during glacial times (cf. Part I - chapter 2.4).

## 3. Some additional subtleties

Each methodical procedure is divided into several steps starting from the source sample and resulting in proxy data (Fig. I-7). Following routines are of major importance: (1) measuring of organic and inorganic carbon in order to determine the sediment $CaCO_3$ and total organic carbon (TOC) content; (2) qualitative and quantitative faunal analysis in order (a) to estimate production and distribution modifications of planktic foraminifera and (b) to estimate calcium carbonate preservation and dissolution modifications in the modern open ocean as well as over the last 300 kyrs; (3) SEM ultrastructure investigations on *Globigerina bulloides*' in order to estimate calcium carbonate preservation and dissolution modifications in the modern open ocean as well as over the last 140 kyrs.

This chapter refers to own results and serves as an anthology of additional delicacies which yet had no chance to be published - at least partly.

### *3.1 Meaningfulness of the* Globigerina bulloides *Dissolution Index* (cf. Part II - chapters 1, 3, 4)

When the *Globigerina bulloides* Dissolution Index was investigated on sediment surface samples (Part I - chapter 2.3), this marvelous tool was applied on down-core samples from the sediment core GeoB 1117-2/3 during the last 140 kyrs as mentioned above (Part I - chapter 2.6). Actually, the results cause serious obstacles as BDX is supposed to indicate better calcite preservation during glacials and worse calcite preservation during interglacials in the central equatorial Atlantic - which contradicts the common scientific view (e.g., Berger, 1973). So what?

The core site is located at 3,984 m water depth which corresponds to an saturation state $\Delta CO_3^{2-}$ ~ 15 µmol/kg (GEOSECS, Bainbridge, 1981) whereas $\Delta CO_3^{2-}$ is the difference between the concentration of carbonate *in situ* and the concentration of saturated carbonate ion for the mineral phase calcite (Broecker and Takahashi, 1978). However, an saturation state of $\Delta CO_3^{2-}$ ~ 10 µmol/kg is enough to dissolve almost all the calcite descending to the sea-floor (Broecker and Peng, 1982). That is, only small

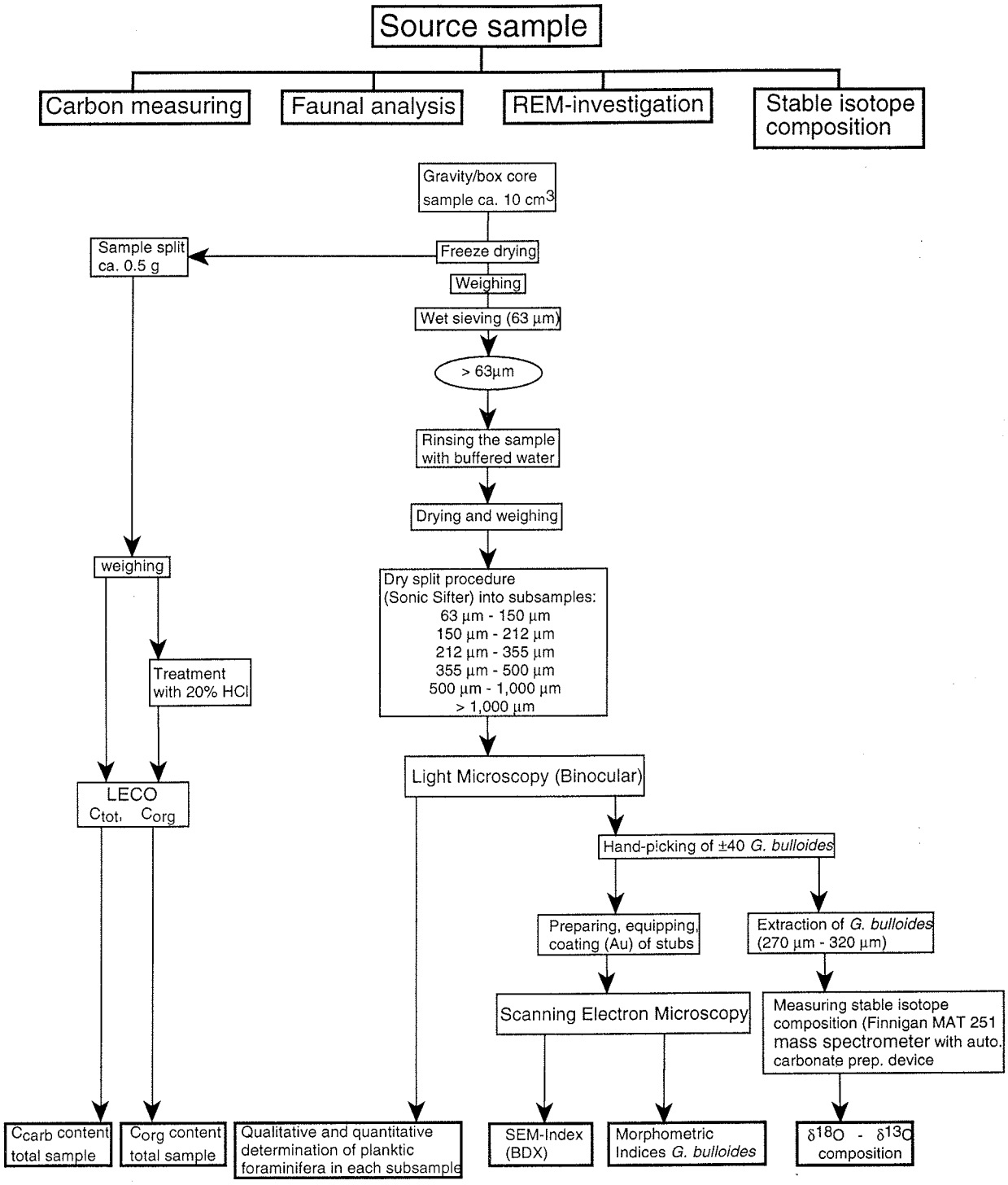


**Fig. I-7:** Flow-chart of all routines carried out, namely investigation of (1) organic and anorganic carbon; (2) planktic foraminiferal assemblages; (3) scanning electron microscopy (SEM); (4) stable isotope composition

variations in the (super-) saturation state are necessary to induce some dissolution.

The precise correlation between deep-water circulation and glacial-interglacial cycles is not known in detail although there is growing evidence that during glacial maxima the production of cold deep-water may lessen and hence dampen bottom water circulation (Gamboa et al., 1983; Faugères et al., 1993). Since the production of NADW is thought to be reduced during glacial periods (Curry and Oppo, 1997), the northwards directed AABW would expand in latitudinal and vertical distribution in the Brazil Basin. Consequently, the southwards directed NADW velocity at the core-site would lessen. During interglacials the onset of NADW production accelerates the southwards directed bottom water; the currents to stir the layer of dissolution around the $CaCO_3$ particles are stimulated, and even under (super-) saturated conditions the preservation of calcite would worsen somewhat. Since there is evidence that the core site never was influenced directly by AABW (Dittert et al., subm.-b) BDX is supposed to serve as deep-water circulation index under carbonate (super-) saturated conditions.

### *3.2 Modification in* Globigerina bulloides' *isotope composition due to carbonate dissolution*

*Globigerina bulloides* stable isotope composition ($\delta^{13}C$, $\delta^{18}O$) was investigated in samples of four sediment surface depth transects into the Brazil-, the Guinea-, and into the Cape Basin (covering areas above and below the calcite lysocline) to find out whether there are patterns which are correlated to carbonate dissolution. In order to minimize statistical errors, 20 right-coiled specimens were hand-picked. They average 250 µm to 500 µm in test size (270 µm - 320 µm mean). The samples were analyzed using a Finnigan MAT 251 micromass-spectrometer coupled with a Finnigan automated carbonate device (KIEL type) at the Alfred Wegener Institute for Polar and Marine Research (group Prof. Mackensen). The carbonate was reacted with orthophosphoric acid at 75°C. The reproducibility of the measurements, as referred to an internal carbonate standard (Solnhofen limestone), is ±0.07 ‰ and ± 0.05 ‰ (1σ over a one year period) for oxygen and carbon isotope, respectively. The conversion to the Pee-Dee Belemnite (PDB) scale was performed using the international standards NBS 18, 19, and 20.

Regarding carbon isotope composition, $\delta^{13}C$ values generally raise with increasing water depth (Fig. I-9A). In detail, carbon isotope values increase regarding the Brazil Basin (-0.7 ‰ to -0.1 ‰), the Guinea Basin (-0.2 ‰ to 0.6 ‰), the western Cape Basin (-0.6 ‰ to 0.4 ‰), and the continental margin (-0.7 ‰ to -0.5 ‰). Regarding oxygen isotope composition (Fig. I-9B) $\delta^{18}O$ values increase with respect to the Brazil Basin (-1.1 ‰ to 0.0 ‰), the Guinea Basin (0.5 ‰ to 1.5 ‰), the western Cape Basin (0.6 ‰

to 2.2 ‰), and decrease with respect to the continental margin (0.3 ‰ to -0.4 ‰). However, the ratio of carbon versus oxygen isotopes (Fig. I-9C) displays rather strong correlation between Brazil- and Guinea Basin ($r^2$=0.704) and between Western Cape Basin and Namibia Continental Margin ($r^2$=0.871), respectively, which can be attributed to different surface water temperatures in the equatorial and the southeast Atlantic surface waters.

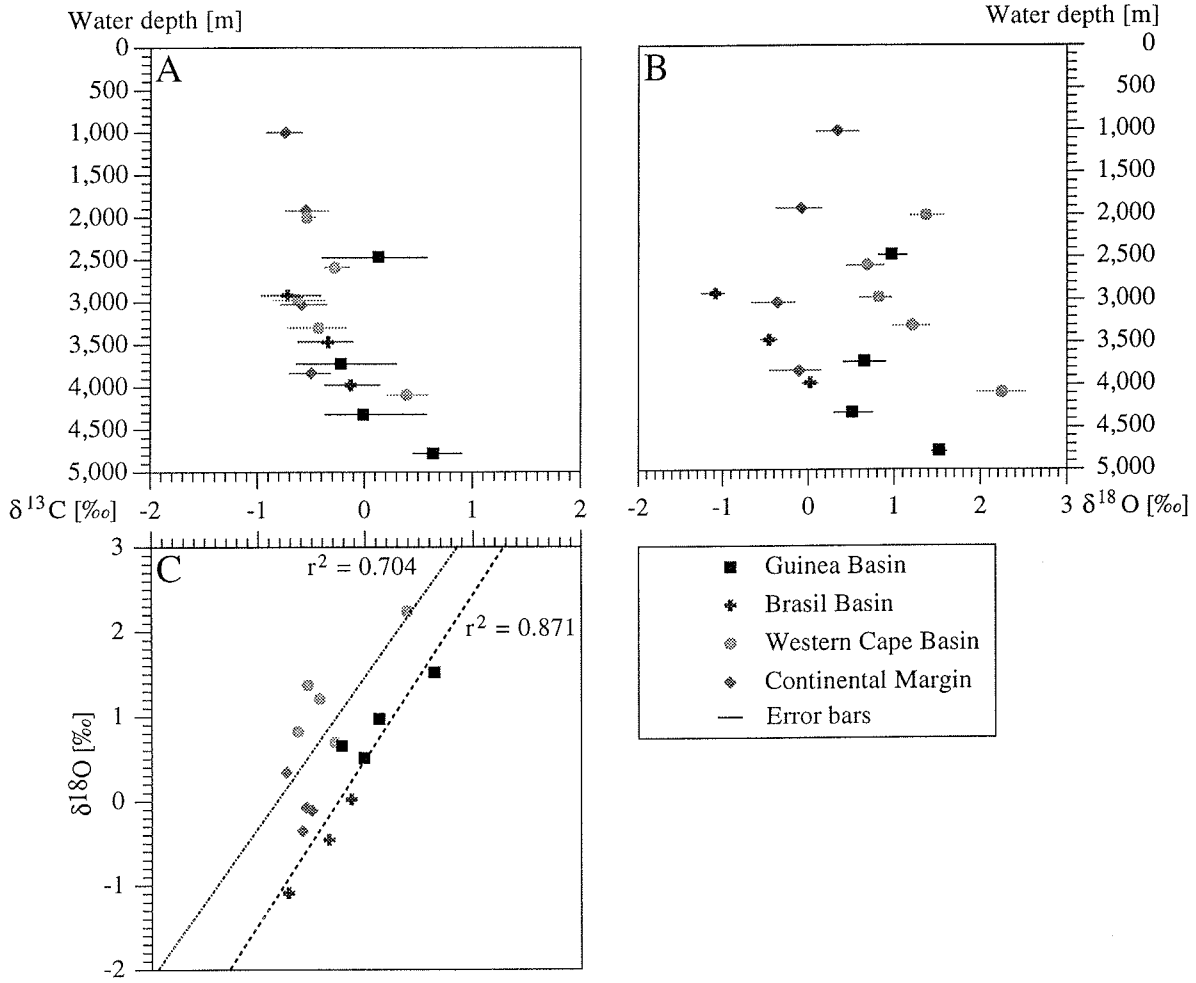


**Fig. I-8**: Stable isotope composition ($\delta^{13}C$ and $\delta^{18}O$) in surface samples of the Brazil-, the Guinea- and the Cape Basin versus water depth (A, B) and $\delta^{13}C$ vs. $\delta^{18}O$ (C).

Since on the exact operation mode of calcite dissolution in planktic foraminiferal tests very little is known (Bonneau et al., 1980), the following model of calcification was adapted, and its task was turned over. Bé (1980) distinguished ontogenetic calcification which involves shell growth through regularly repeated chamber-by-chamber formation, resulting in the lamellar deposition of calcite over each previous chamber and in formation, repair and resorption of elongated spines. As such, it differs from gametogenetic calcification which is the process of calcite deposition restricted to its outer

shell surface during gametogenesis, secreting a secondary calcite crust consisting of an idiomorphous calcite skalenoedra texture at the surface (Fig. I-10). Additional calcite secreted during *in vivo* sinking takes place below the euphotic zone down to a few hundred meters as shown by isotopic shifts (Spero, 1992; Billups and Spero, 1995). *Globigerina bulloides* contains both normalform individuals in which the final chamber is larger than the penultimate chamber, and kummerform individuals with the final chamber reduced or equal in size relative to its predecessor. Since kummerform individuals may be attributed to environmental stress preventing normal growth of the individual (Berger, 1969), present investigations were restricted to normalform individuals.

Likewise, if we know about the life cycle of *G. bulloides* we are able to interpret the stable isotope modifications: *G. bulloides* is enriched in $^{13}C$ in upwelling zones, and it even thrives during the final stage of upwelling when the fixation of $^{12}C$ in the phytoplankton exceeds the amount of $^{12}C$ brought into the surface waters. Incorporation of Mg, Sr, and Na into the shell of *G. bulloides* displays fluctuations along a vertical water column profile (Puechmaille, 1994).

When the upper water column is almost isothermal, *G. bulloides* seems to prefer the upper 50 m of the water column (Deuser and Ross, 1989; Hemleben et al., 1989). As soon as a very weak thermocline starts to form, it may favor the interval below the thermocline. In order to sink to deeper intervals, *G. bulloides* has to adapt for increased seawater density. This problem may be solved by a rapid increase in the calcite:protoplasm ratio (Marszalek et al., 1969). Consequently, *G. bulloides* secretes its shell out of equilibrium with respect to carbon isotopes (Curry and Matthews, 1981; Deuser and Ross, 1989; Hubberten and Meyer, 1989; Sautter and Thunell, 1991b). This is thought to be mainly a function of the incorporation of respired $CO_2$ into shell calcite due to a provable constant fractionation throughout the ontogeny of this species (Spero and Lea, 1996). Because a major part of the $^{12}C$ enriched phytoplankton is respired and remineralized within the first 200 m of the water column (Kroopnick, 1985) each new secreted chamber of *G. bulloides* becomes

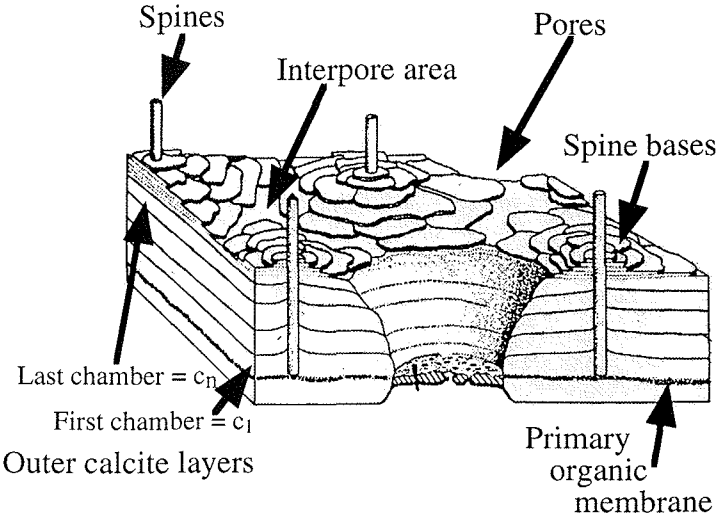


**Fig. I-9**: Schematic structure of planktic foraminiferal shells (Modified after Hemleben et al. 1989).

isotopically lighter. Consequently, if a test undergoes dissolution (either supralysoclinal or below the lysocline) through a layer-by-layer removal of shell material (Berger, 1967) the remaining test will become isotopically heavier with respect to $^{13}C$. Error bars increase (Fig. I-9) if shell calcite is "contaminated" with other elements on its way descending the water column. Isotopic values will become faster heavy because dissolution affects the most "impure" calcite most vigorous. Additionally, since *G. bulloides* lacks symbiont algae (Hemleben and Spindler, 1983), the carbon and oxygen ratios can't be disturbed by their activities. Since dissolution removes the most "impure" calcite parts first and faster than pure calcite (Brown and Elderfield, 1996), one expects that genetic dissolution patterns are somewhat influenced by ecological patterns.

Moreover, if tests undergo dissolution either supralysoclinal or below the lysocline through a layer-by-layer removal of shell material as proposed above (Berger, 1967) there is evidence that the remaining test will become systematically heavier in stable isotope composition with increasing carbonate dissolution. The present results show an increase of 0.4 ‰ and 0.76 ‰ per 1,000 m water depth for carbon and oxygen isotopes, respectively. Comparable results were attained by Bonneau et al. (1980) investigating six different planktic foraminiferal species from surface sediments at 1,598 m to 4,441 m water depth. For all species they observed a similar trend towards increasing $\delta^{18}O$ values with increasing water depths and increasing dissolution. This effect was as high as 0.6 ‰ per thousand meters. However, carbonate dissolution lastly does not affect the known relationship between carbon and oxygen stable isotopes regarding surface water temperature reconstruction (e.g., Spero and Lea, 1996)

### *3.3 Some reflections on sample splitting*

Depending on the size each source sample was split until a fraction containing up to 1,000 specimens was attained. After measuring the source weight and the split weight, the n-th split (as proposed by Pflaumann et al., 1996) of the source sample was found to be not equal to the n-th weight proportion to the source sample. Depending both on the size fraction to be investigated and on the split number, the split proportion and the weight proportion deviate about ±73 %. As can be derived immediately from figure I-11, small size fractions mostly overestimate the source sample whereas large size fractions rather underestimate the source sample if they are regarded as split proportions.

In order to assess the deviation between split and weight proportions, it first was tried to quantify possible errors that might occur. Thus, standard spheres of identical weight, shape and grain size were repeatedly split in order to test the precision of the microsplitter. This calibration attained a reproducible precision >99 % providing that the

work was performed in a thermo- and humidity constant laboratory.

Consequently, the device error of the precision scales which strongly depends on mass and density of the sample and on the density of the air can be neglected. For example, Sarnthein (1971) describes non-linear analytical errors if samples mainly consist of rod-shaped particles or too large grain-size ranges. Likewise, if meaningful comparisons are to be made between modern assemblages and those from the fossil record, Murray (1995) points out that it is essential to use similar size fractions. Samples mainly consisting of spheres or lightweighted shell types result in too low specific weight. The more sorted a sample is, that is, the more a sample is homogen the larger the analytic error will be (Chayes, 1956). Assuming that a given random sample is neither totally homogenized nor entirely un-sorted a deviation of $\pm 2\ \sigma$ is valid for the 95 % confidence limit (Sarnthein, 1971).

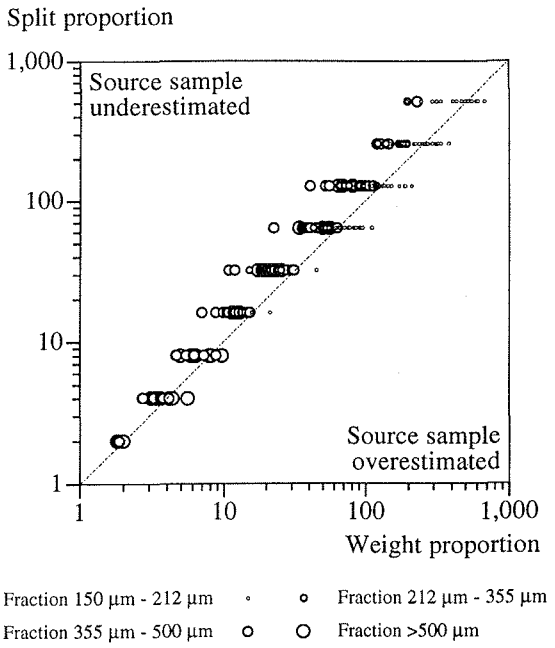


**Fig. 10:** Split proportions vs. weight proportions of different grain size fractions. Small fractions mostly overestimate whereas large fractions rather underestimate the source sample if they are regarded as split proportions.

Thus, it is proposed that the split to be investigated is *not* projected by $2^n$. In contrary, to recalculate split values onto the source sample the ratio between the weight of the source sample and the weight of the split to be investigated should be applied for further examinations (number of specimens per gram sediment, accumulation rate of specimens per area and time, etc.).

### *3.4 Foraminiferal assemblages made anonymous - a reflection on quantitative research*

(see Part II - chapter 5)

Until today, there is still considerable confusion in the micropaleontological community regarding the statistical significance of rarer species, and whether variation in the total number of species between given samples has any bearing on the number of counts required. The relation between number of species and number of individuals occuring in a random sample of any organism assemblage is of major importance within many fields of micropaleontology: e.g., (1) the mapping of surface water assemblages in order to infer general and latitudinal biogeographic zonations (e.g. Baumann and

Mathiessen, 1992); (2) climatic reconstructions through Transfer Function and Modern Analog Technique in order to estimate past sea-surface conditions (e.g. Kipp, 1976; Pflaumann et al., 1996); (3) the constructing of bio- and chronostratigraphies (e.g. Castradori, 1993); (4) the determination of extinction events (e.g. Thierstein, 1982) and dominance changes of related species (e.g. Thierstein et al., 1977) etc.

Determining the exact species diversity of a random sample requires the determination of (1) *all* species and (2) *all* individuals per species. However, the basic problem regarding quantitative research is that a random sample not necessarily consists of all species representing the sample area - which mostly is attributed to the accuracy of sampling method and sample size. Since in real conditions the number of species is limited, and we can presuppose a certain knowledge or expectation on the number of species occuring in an area, we are able to determine the maximum diversity increment.

We introduce a method showing how to minimize labour and how to maximize statistic meaningfulness regarding specimen counts. Depending on the number of species expected to occur maximum within a sample the number of individuals to be determined ranges from tens to several hundreds. However, for belongings of extinction events, dominance changes etc. we propose the approach by Patterson and Fishbein (1989). They refer to Buzas et al. (1982) who found that most species tallied in paleontological analyses are rare and many of these rarer species are important regarding paleoceanographic interpretations as mentioned above. They recommend that researchers count at least 50 individuals regarding indicator species having an abundance of approximately 50 % or greater and counts of several thousands for defining species that comprise 1 % of a sample.

## 4. References

Archer, D.E., 1991. Equatorial Pacific calcite preservation cycles: Production or dissolution? Paleoceanography 6: 561-571.

Archer, D.E., 1996. An Atlas of the distribution of calcium carbonate in sediments of the deep sea. Global Biogeochem. Cycles 10: 159-174.

Archer, D.E., Maier-Reimer, E., 1994. Effect of deep-sea sedimentary calcite preservation on atmospheric $CO_2$ concentration. Nature 367: 260-264.

Arrhenius, G.O.S., 1952. Sediment Cores from the East Pacific - Fasc. 1. Rep. Swed. Deep-Sea Exped. 1947-1948 5: 1-227.

Bainbridge, A.E., 1981. GEOSECS Atlantic Expedition, Hydrographic Data, 1972-1973. National Science Foundation, Superintendent of Documents, US Government Printing Office, Washington, DC, pp. 121.

Barnola, J.M., Anklin, M., Porcheron, J., Raynaud, D., Schwander, J., Stauffer, B., 1995. $CO_2$

evolution during the last millennium as recorded in Antarctic and Greenland ice. Tellus 47: 264-272.

Barnola, J.M., Raynaud, D., Korotkevich, Y.S., Lorius, C., 1987. Vostok ice core provides 160,000-year record of atmospheric $CO_2$. Nature 329: 408-414.

Baumann, K.-H., Mathiessen, J., 1992. Variations in surface water mass conditions in the Norwegian Sea: evidence from Holocene coccolith and dinoflagellate cyst assemblage. Mar. Micropal. 20: 129-146.

Baumann, K.-H., Meggers, H., 1996. Paleoceanographical change in the Labrador Sea during the last 3.1 MY: Evidence from calcareous plankton records. In: Moguilevsky, A., Whatley, R. (Eds.), Microfossils and Oceanic Environments. Aberystwyth-Press, Aberystwyth, pp. 131-154.

Bé, A.W.H., 1967. Foraminifera families: Globigerinidae and Globorotalidae. Fiches d'identification du zooplancton, Cons Perm Intern Explor de la Mer, Charlottenlund Slot, Danemark 108: 9.

Bé, A.W.H., 1977. An ecological, zoogeographic and taxonomic review of recent planktonic foraminifera. In: Ramsay, A.T.S. (Ed.) Oceanic Micropaleontology. Academic Press, London, 1, pp. 1-100.

Bé, A.W.H., 1980. Gametogenic calcification in a spinose planktonic foraminifer, *Globigerinoides sacculifer* (BRADY). Mar. Micropal. 5: 283-310.

Bé, A.W.H., Hutson, W.H., 1977. Ecology of planktonic foraminifera and biogeographic patterns of life and fossil assemblages in the Indian Ocean. Micropaleontology 23: 369-414.

Bé, A.W.H., McIntyre, A., Breger, D., 1966. The shell microstructure of a planktonic foraminifer, *Globorotalia menardii* (d'Orbigny). Eclogae geol Helv 59: 885-896.

Bé, A.W.H., Tolderlund, D.S., 1971. Distribution and ecology of living planktonic foraminifera in surface waters of the Atlantic and Indian Oceans. In: Funnell, B.M., Riedel, W.R. (Eds.), The micropaleontology of oceans. Cambridge University Press, Cambridge, pp. 105-149.

Berger, W.H., 1967. Foraminiferal ooze: Solution at depths. Science 156: 383-385.

Berger, W.H., 1968. Planktonic foraminifera: Selective solution and paleoclimatic interpretation. Deep-Sea Res. 15: 31-43.

Berger, W.H., 1969. Kummerform foraminifera as clues to oceanic environments. Am. Assoc. Petrol. Geol. Bull. 53: 706.

Berger, W.H., 1970. Planktonic foraminifera: Selective solution and the lysocline. Mar. Geol. 8: 111-138.

Berger, W.H., 1973. Deep-sea carbonates: Pleistocene dissolution cycles. J. Foram. Res. 3: 187-195.

Berger, W.H., 1979. Preservation of foraminifera. In: Lipps, J.H., Berger, W.H., Buzas, M.A., Douglas, R.G., Ross, C.A. (Eds.), Foraminiferal ecology and palecology. Society of Economic Paleontologists and Mineralogists, Houston, 6, pp. 105-155.

Berger, W.H., Herguera, J.C., Lange, C.B., Schneider, R., 1994. Paleoproductivity: Flux

proxies versus nutrient proxies and other problems concerning the quaternary productivity record. In: R. Zahn, e.a. (Ed.) Carbon cycling in the glacial ocean: Constains on the ocean's role in global change. (NATO ASI Series) Springer-Verlag, Berlin Heidelberg, 117, pp. 385-412.

Berger, W.H., Keir, R.S., 1984. Glacial-Holocene changes in atmospheric $CO_2$ and the deep-sea record. In: Hansen, J.E., Takahashi, T. (Eds.), Climate processes and climate sensitivity. Geophys. Monogr. 29, Maurice Ewing Series, Washington, DC, 5, pp. 337-351.

Berner, R.A., 1977. Sedimentation and dissolution of pteropods in the ocean. In: Andersen, N.R., Malahoff, A. (Eds.), The Fate of Fossil Fuel $CO_2$ in the Oceans. Plenum Press, New York, NY, pp. 243-260.

Berner, W., Oeschger, H., Stauffer, B., 1980. Information on the $CO_2$ cycle from ice core studies. Radiocarbon 22: 227-235.

Bickert, T., Cordes, R., Wefer, G., 1997. Late Pliocene to Mid-Pleistocene (2.6-1.0 M.Y.) carbonate dissolution in the western equatorial Atlantic: Results of Leg 154, Ceara Rise. Proc. ODP, Sci. Results 154: 229-237.

Bickert, T., Wefer, G., 1996. Late Quaternary deep water circulation in the South Atlantic: Reconstruction from carbonate dissolution and benthic stable isotopes. In: Wefer, G., Berger, W.H., Siedler, G., Webb, D.J. (Eds.), The South Atlantic: Present and past circulation. Springer-Verlag, Berlin Heidelberg, pp. 599-620.

Billups, K., Spero, H.J., 1995. Relationship between shell size, thickness and stable isotopes in individual planktonic foraminifera from two equatorial Atlantic cores. J. Foram. Res. 25: 24-37.

Boltovskoy, E., Totah, V.I., 1992. Preservation index and preservation potential of some foraminiferal species. J. Foram. Res. 22: 267-273.

Bonneau, M.-C., Vergnaud-Grazzini, C., Berger, W.H., 1980. Stable isotope fractionation and differential dissolution in recent planktonic foraminifera from Pacific box-cores. Oceanol. Acta 3: 377-382.

Boyle, E.A., 1988. Vertical oceanic nutrient fractionation and glacial/interglacial $CO_2$ cycles. Nature 331: 55-56.

Boyle, E.A., Keigwin, L.D., 1987. North Atlantic thermohaline circulation during the past 20,000 years linked to high-latitude surface temperature. Nature 30: 35-40.

Broecker, W.S., 1991. The great ocean conveyor. Oceanogr. 4: 79-89.

Broecker, W.S., 1997. Thermohaline circulation, the Achilles heel of our climate system: Will man made $CO_2$ upset the current balance? Science 278: 1582-1588.

Broecker, W.S., Andree, M., Wölfli, W., Oeschger, H., Bonani, G., Kennett, J., Peteet, D.M., 1988. The chronology of the last deglaciation: implications to the cause of the Younger Dryas event. Paleoceanography 3: 1-19.

Broecker, W.S., Peng, T.-H., 1993. What caused the glacial to interglacial $CO_2$ change? In: Heimann, M. (Ed.) The global carbon cycle. Springer-Verlag, New York, NY, pp. 95-116.

Broecker, W.S., Peng, T.H., 1982. Tracers in the Sea. Eldigio Press, New York, NY, pp. 689.

Broecker, W.S., Peteet, D.M., Rind, D., 1985. Does the ocean-atmosphere system have more than one stable mode of operation? Nature 315: 21-26.

Broecker, W.S., Takahashi, T., 1977. The solubility of calcite in sea water. In: Fraser, D.G. (Ed.) Thermodynamics in Geology. D. Reidel, Norwell, MA, pp. 365-379.

Broecker, W.S., Takahashi, T., 1978. The relationship between lysocline depth and in situ carbonate ion concentration. Deep-Sea Res. 25F: 65-95.

Brown, S.J., Elderfield, H., 1996. Variations in Mg/Ca and Sr/Ca ratios of planktonic foraminifera caused by postdepositional dissolution: Evidence of shallow Mg-dependent dissolution. Paleoceanography 11: 543-551.

Buzas, M.A., Koch, S.J., Culver, S.J., Sohl, N.F., 1982. On the distribution of species occurrence. Paleobiology 8: 142-150.

Cane, M.E., 1979. The response of an equatorial ocean to simple wind stress patterns: II. Numerical results. J. Mar. Res. 37: 253-299.

Castradori, D., 1993. Calcareous nannofossil biostratigraphy and biochronology in eastern Mediterranean deep-sea cores. Rivista Italiana Di Paleontologia E Stratigrafia 99: 107-126.

Chayes, F., 1956. Petrographic modal analysis. John Wiley & Sons, New York, NY, pp. 113.

Corliss, B.H., Martinson, D.G., Keffer, T., 1986. Late Quaternary deep-ocean circulation. Geol. Soc. Am. Bull. 97: 1106-1121.

Curry, W.B., 1996. Late Quaternary deep circulation in the western Equatorial Atantic. In: Wefer, G., Berger, W.H., Siedler, G., Webb, D.J. (Eds.), The South Atlantic: Present and past circulation. Springer-Verlag, Berlin Heidelberg, pp. 577-598.

Curry, W.B., Duplessy, J.C., Labeyrie, L.D., Shackleton, N.J., 1988. Changes in the distribution of $\delta^{13}C$ of deep water $\Sigma CO_2$ between the last glaciation and the Holocene. Paleoceanography 3: 317-342.

Curry, W.B., Lohmann, G.P., 1990. Reconstructing past particle fluxes in the tropical Atlantic Ocean. Paleoceanography 5: 487-506.

Curry, W.B., Matthews, R.K., 1981. Equilibrium $^{18}O$ fractionation in small size fraction planktonic foraminifera: Evidence from recent Indian Ocean sediments. Mar. Micropal. 6: 327-337.

Curry, W.B., Oppo, D.W., 1997. Synchronous, high frequency oscillations in tropical sea surface temperatures and North-Atlantic Deep Water production during the last glacial cycle. Paleoceanography 12: 1-14.

Dacqué, E., 1930. Die Erdzeitalter. R. Oldenbourg, München und Berlin, pp. 565.

Delmas, R.J., Ascencio, J.-M., Legrand, M., 1980. Polar ice evidence that atmospheric $CO_2$ 20,000 years BP was 50 % of present. Nature 284: 155-157.

deMenocal, P.B., Ruddiman, W.F., Pokras, E.M., 1993. Influences of high- and low-latitude processes on African terrestrial climate: Pleistocene eolian records from equatorial Atlantic Ocean Drilling Program Site 663. Paleoceanography 8: 209-242.

Deuser, W.G., Ross, E.H., 1989. Seasonally abundant planktonic foraminifera of the

Sargasso Sea: Succession, deep-water fluxes, isotopic compositions, and paleoceanographic implications. J. Foram. Res. 19: 268-293.

Diester-Haass, L., Rothe, P., 1987. Plio-Pleistocene sedimentation on the Walvis Ridge, Southeast Atlantic (DSDP Leg 75, Site 532) - Influence of surface currents, carbonate dissolution and climate. Mar. Geol. 77: 53-85.

Dittert, N., Baumann, K.-H., Bickert, T., Henrich, R., Huber, R., Kinkel, H., Meggers, H., subm.-a. Carbonate dissolution in the deep sea: Methods, quantification and paleoceanographic application. In: Fischer, G., Wefer, G. (Eds.), Proxies in paleoceanography. Springer-Verlag, Berlin Heidelberg.

Dittert, N., Henrich, R., subm. Carbonate dissolution in the South Atlantic Ocean: Evidence by *Globigerina bulloides'* ultrastructure breakdown. Deep-Sea Res.

Dittert, N., Niebler, H.-S., Henrich, R., subm.-b. A 300 kyrs history of planktic foraminiferal distribution in the central equatorial Atlantic Ocean - paleo-environmental implications. Mar. Micropal.

Dokken, T.M., Hald, M., 1996. Rapid climatic shifts during isotope stages 2-4 in the Polar North Atlantic. Geology 24: 599-602.

Duplessy, J.C., Labeyrie, L., Paterne, M., Hovine, S., Fichefet, T., Duprat, J., Labracherie, M., 1996. High latitude deep water sources during the Last Glacial Maximum and the intensity of the global oceanic circulation. In: Wefer, G., Berger, W.H., Siedler, G., Webb, D.J. (Eds.), The South Atlantic: Present and past circulation. Springer-Verlag, Berlin Heidelberg, pp. 445-460.

Duplessy, J.C., Shackleton, N.J., Fairbanks, R.G., Labeyrie, L.D., Oppo, D., Kallel, N., 1988. Deepwater source variations during the last climatic cycle and their impact on the global deepwater circulation. Paleoceanography 3: 343-360.

Emerson, S., Bender, M., 1981. Carbon fluxes at the sediment-water interface of the deep-sea: Calcium carbonate preservation. J. Mar. Res. 39: 139-162.

Ericson, D.B., Wollin, G., 1968. Pleistocene climates and chronology in deep-sea sediments. Science 162: 1227-1234.

Farrell, J.W., Prell, W.L., 1989. Climatic change and $CaCO_3$ preservation: An 800,000 year bathymetric reconstruction from the central equatorial Pacific Ocean. Paleoceanography 4: 447-466.

Farrell, J.W., Prell, W.L., 1991. Pacific $CaCO_3$ preservation and $\delta^{18}O$ since 4 Ma: Paleoceanographic and paleoclimatic implications. Paleoceanography 6: 485-498.

Faugères, J.C., Mézerais, M.L., Stow, D.A.V., 1993. Contourite drift types and their distribution in the North and South Atlantic Ocean basins. Sedimentary Geology 82: 189-203.

Gamboa, L.A.P., Archer, R.T., Barker, P.F., 1983. Seismic stratigraphy and geologic history of the Rio Grande Gap and southern Brazil Basin. DSDP, Initial Reports 72: 481-498.

Gardner, J.V., Hays, J.D., 1976. Response of sea-surface temperatures and circulation to global climatic change during the past 200,000 years in the eastern equatorial Atlantic Ocean. Geol. Soc. Am. Mem. 145: 221-246.

Gordon, A.L., 1996. Communication between oceans. Nature 382: 399-400.

Gordon, A.L., Bosley, K.T., 1991. Cyclonic gyre in the tropical South Atlantic. Deep-Sea Res. 38: 323-343.

Guilderson, T.P., Fairbanks, R.G., Rubenstone, J.L., 1994. Tropical temperature variations since 20,000 years ago; modulating interhemispheric climate change. Science 263: 663-665.

Hay, W.W., 1970. Calcareous nannofossils from cores recovered on Leg 4. DSDP, Initial Reports 4: 455-501.

Hebbeln, D., Dokken, T., Andersen, E.S., Hald, M., Elverhoi, A., 1994. Moisture supply for northern ice-sheet growth during the Last Glacial Maximum. Nature 370: 357-360.

Hemleben, C., Spindler, M., 1983. Recent advances in research on living planktonic foraminifera. Utrecht Micropal. Bull. 30: 141-170.

Hemleben, C., Spindler, M., Anderson, O.R., 1989. Modern planktonic foraminifera. Springer-Verlag, New York, NY, pp. 363.

Henrich, R., 1989. Glacial/interglacial cycles in the Norwegian Sea: Sedimentology, paleoceanography, and evolution of late Pliocene to Quaternary northern hemisphere climate. In: Eldholm, O., Thiede, J., Taylor, E. (Eds.), Proceedings of the Ocean Drilling Program, Scientific Results. College Station, TX, 104, pp. 189-232.

Henrich, R., Kassens, H., Vogelsang, E., Thiede, J., 1989. Sedimentary facies of glacial-interglacial cycles in the Norwegian Sea during the last 350 ka. Mar. Geol. 86: 283-319.

Henrich, R., Wagner, T., Goldschmidt, P., Michels, K., 1995. Depositional regimes in the Norwegian-Greenland Sea: The last two glacial to interglacial transitions. Geol. Rdschau 84: 28-48.

Hubberten, H.-W., Meyer, G., 1989. Stable isotope measurements on foraminifera tests: Experiences with an automatic commercial carbonate preparation device. Terra abstracts 1: 80-81.

Imbrie, J., Berger, A., Boyle, E.A., Clemens, S.C., Duffy, A., Howard, W.R., Kukla, G., Kutzbach, J., Martinson, D.G., McIntyre, A., Mix, A.C., Molfino, B., Morley, J.J., Peterson, L.C., Pisias, N.G., Prell, W.L., Raymo, M.E., Shackleton, N.J., Toggweiler, J.R., 1993. On the structure and origin of major glaciation cycles 2. The 100,000-year cycle. Paleoceanography 8: 699-735.

Imbrie, J., Boyle, E.A., Clemens, S.C., Duffy, A., Howard, W.R., Kukla, G., Kutzbach, J., Martinson, D.G., McIntyre, A., Mix, A.C., Molfino, B., Morley, J.J., Peterson, L.C., Pisias, N.G., Prell, W.L., Raymo, M.E., Shackleton, N.J., Toggweiler, J.R., 1992. On the structure and origin of major glaciation cycles 1. Linear responses to Milankovitch forcing. Paleoceanography 7: 701-738.

Keeling, R.F., Piper, S.C., Heimann, M., 1996. Global and hemisphere $CO_2$ sinks deduced from changes in atmospheric $O_2$ concentration. Nature 381: 218-221.

Keigwin, L.D., 1976. Late Cenozoic planktonic foraminiferal biostratigraphy and paleoceanography of the Panama Basin. Micropaleontology 22: 419-422.

Keigwin, L.D., Curry, W.B., Lehman, S.J., Johnson, S., 1994. The role of the deep ocean in

North Atlantic climate change between 70 and 130 kyr ago. Nature 371: 323-326.

Keigwin, L.D., Jones, G.A., 1994. Western North Atlantic evidence for millennial-scale changes in ocean circulation and climate. J. Geophys. Res. 99: 12397-12410.

Kemle-von Mücke, S., 1994. Oberflächenwasserstruktur und -zirkulation des Südostatlantiks im Spätquartär. Ber. Fachbereich Geowiss., Univ. Bremen 55: 1-151.

Kennett, J.P., 1966. Foraminiferal evidence of a shallow calcium carbonate solution boundary, Ross Sea, Antarctica. Science 153: 191-193.

Kennett, J.P., Srinivasan, M.S., 1983. Neogene planktonic foraminifera. A phylogenetic atlas. Hutchinson Press, Stroudsburg, Penn., pp. 263.

Kinkel, H., Dittert, N., Henrich, R., subm. Calcareous plankton record in the equatorial Atlantic: A 300 kyrs record of climate feedback, productivity and dissolution. Palaeogeography, Palaeoclimatology, Palaeoecology.

Kipp, N.G., 1976. New transfer function for estimating past sea-surface conditions from sea bed distribution of planktonic foraminiferal assemblages in the North Atlantic. Geol. Soc. Am. Mem. 145: 3-42.

Kroopnick, P.M., 1985. The distribution of $^{13}C$ of $\Sigma CO_2$ in the World Oceans. Deep-Sea Res. 32: 57-84.

Le, J., Shackleton, N.J., 1992. Carbonate dissolution fluctuations in the western equatorial Pacific during the Late Quaternary. Paleoceanography 7: 21-42.

Levitus, S., Boyer, T., 1994. World Ocean Atlas 1994 Volume 4: Temperature. NOAA Atlas NESDIS 4: http://ingrid.ldgo.columbia.edu/SOURCES/.LEVITUS94/.

Malmgren, B.A., 1983. Ranking of dissolution susceptibility of planktonic foraminifera at high latitudes of the South Atlantic Ocean. Mar. Micropal. 8: 183-191.

Marszalek, D.S., Wright, R.C., Hay, W.W., 1969. Function of the test in Foraminifera. Trans. Gulf Coast Assoc. Geol. Soc. 19: 341-352.

Martin, W.R., Sayles, F.L., 1996. $CaCO_3$ dissolution in sediments of the Ceara Rise, western equatorial Atlantic. Geochim. Cosmochim. Acta 60: 243-263.

McIntyre, A., Ruddiman, W.F., Karlin, K., Mix, A.C., 1989. Surface water response of the equatorial Atlantic Ocean to orbital forcing. Paleoceanography 4: 19-55.

Mercier, H., Speer, K.G., Honnorez, J., 1994. Tracing the Antarctic Bottom Water through the Romanche and Chain Fracture Zones. Deep-Sea Res. 41: 1457-1477.

Mix, A.C., Morey, A.E., 1996. Climate feedback and Pleistocene variations in the Atlantic south equatorial current. In: Wefer, G., Berger, W.H., Siedler, G., Webb, D.J. (Eds.), The South Atlantic: Present and past circulation. Springer-Verlag, Berlin Heidelberg, pp. 503-525.

Mix, A.C., Ruddiman, W.F., McIntyre, A., 1986a. Late Quaternary paleoceanography of the tropical Atlantic 1: Spatial variability of annual mean sea-surface temperatures, 0-20,000 Years B.P. Paleoceanography 1: 43-66.

Mix, A.C., Ruddiman, W.F., McIntyre, A., 1986b. Late Quaternary paleoceanography of the tropical Atlantic 2: The seasonal cycle of sea-surface temperatures, 0-20,000 Years B.P. Paleoceanography 1: 339-353.

Moore, D.W., Hisard, P., McCreary, J., Merle, J., O'Brien, J., Picaut, J., Verstraete, J., Wunsch, C., 1978. Equatorial adjustment in the eastern Atlantic. Geophys. Res. Lett. 5: 638-640.

Murray, J., 1897. On the distribution of the pelagic foraminifera at the surface and on the floor of the ocean. Nat. Sci. 11: 17-27.

Murray, J.W., 1995. Microfossil indicators of ocean water masses, circulation and climate. In: Bosence, D.W.J., Alklison, P.A. (Eds.), Marine paleoenvironmental analysis from fossils. Geological Society Special Publication, 83, pp. 245-264.

Neftel, A., Moor, E., Oeschger, H., Stauffer, B., 1985. Evidence from polar ice cores for the increase in atmospheric $CO_2$ in the past two centuries. Nature 315: 45-47.

Neftel, A., Oeschger, H., Staffelbach, T., Stauffer, B., 1988. $CO_2$ record in the Byrd ice core 50,000 - 5,000 years BP. Nature 331: 609-611.

Niebler, H.-S., Gersonde, R., 1998. A planktic foraminiferal transfer function for the southern South Atlantic Ocean. Mar. Micropal. in press:

Oberhänsli, H., Bénier, C., Meinecke, G., Schmidt, H., Schneider, R., Wefer, G., 1992. Planktonic foraminifera as tracers of ocean currents in the eastern South Atlantic. Paleoceanography 7: 607-632.

Oeschger, H., Beer, J., Siegenthaler, U., Stauffer, B., Dansgaard, W., Langway, C.C., 1984. Late-glacial climate history from ice-cores. Am. Geophys. Union, Geophys. Monog. 29: 299-306.

Oppo, D.W., Lehman, S.J., 1993. Mid-depth circulation of the subpolar North Atlantic during the last glacial maximum. Science 259: 1148-1152.

Ottens, J.J., 1992. Planktic foraminifera as indicators of ocean environments in the Northeast Atlantic. FEBO B.V., Enschede, pp. 189.

Parker, F.L., 1962. Planktonic foraminiferal species in Pacific sediments. Micropaleontology 8: 219-254.

Parker, F.L., 1971. Distribution of planktonic foraminifera in recent deep-sea sediments. In: Funnell, B.M., Riedel, W.R. (Eds.), The micropaleontology of oceans. Cambridge University Press, Cambridge, pp. 289-307.

Parker, L.F., Berger, W.H., 1971. Faunal and solution patterns of planktonic foraminifera in surface sediments of the South Pacific. Deep-Sea Res. 18: 73-107.

Patterson, R.T., Fishbein, E., 1989. Re-examination of the statistical methods used to determine the number of point counts needed for micropaleontological quantitative research. J. Paleont. 63: 245-248.

Peterson, L.C., Prell, W.L., 1985. Carbonate dissolution in recent sediments of the eastern equatorial Indian Ocean: Preservation patterns and carbonate loss above the lysocline. Mar. Geol. 64: 259-290.

Peterson, R.G., Stramma, L., 1991. Upper-level circulation in the South Atlantic Ocean. Prog. Oceanog. 26: 1-173.

Pflaumann, U., Duprat, J., Pujol, C., Labeyrie, L.D., 1996. SIMMAX: A modern analog technique to deduce Atlantic sea surface temperatures from planktonic foraminifera in deep-sea sediments. Paleoceanography 11: 15-35.

Pflaumann, U., Krasheninnikov, V.A., 1978. Quaternary stratigraphy and planktonic foraminifers of the Eastern Atlantic, Deep Sea Drilling Project, Leg 41. DSDP, Initial Reports 41: 883-911.

Philander, S.G.H., 1979. Variability of the tropical oceans. Dynamics of Atmospheres and Oceans 3: 191-208.

Philander, S.G.H., Pacanowski, R.C., 1980. The generation of equatorial currents. J. Geophys. Res. 85: 1123-1136.

Philander, S.G.H., Pacanowski, R.C., 1981. The oceanic response to cross-equatorial winds (with application to coastal upwelling in low latitudes). Tellus 33: 201-210.

Philander, S.G.H., Pacanowski, R.C., 1986. A model of the seasonal cycle in the tropical Atlantic Ocean. J. Geophys. Res. 91: 14192-14206.

Puechmaille, C., 1994. Mg, Sr and Na fluctuations in the test of modern and recent *Globigerina bulloides*. Chem. Geol. 116: 147-152.

Ravelo, A.C., Fairbanks, R.G., Philander, S.G.H., 1990. Reconstructing tropical Atlantic hydrography using planktonic foraminifera and an ocean model. Paleoceanography 5: 409-431.

Reid, J.L., 1989. On the total geostrophic circulation of the South Atlantic Ocean: Flow patterns, tracers and transports. Prog. Oceanog. 23: 149-244.

Reid, J.R., 1996. On the circulation of the South Atlantic. In: Wefer, G., Berger, W.H., Siedler, G., Webb, D.J. (Eds.), The South Atlantic: Present and past circulation. Springer-Verlag, Berlin Heidelberg, pp. 13-44.

Richardson, P.L., Reverdin, G., 1987. Seasonal cycle of velocity in the Atlantic North Equatorial Counter Current as measured by surface drifters, current meters, and ship drifts. J. Geophys. Res. 92: 3691-3708.

Rind, D., Peteet, D.M., 1985. Terrestrial conditions at the last glacial maximum and CLIMAP sea-surface temperature estimates; are they consistent? Quat. Res. 24: 1-22.

Santschi, P.H., Bower, P., Nyffeler, U.P., Azevedo, A., Broecker, W.S., 1983. Estimates of the resistance to chemical transport posed by the deep-sea benthic boundary layer. Limnol. Oceanogr. 28: 899-912.

Sarnthein, M., 1971. Oberflächensedimente im Persischen Golf und Golf von Oman II. Quantitative Komponentenanalyse der Grobfraktion. "METEOR" Forsch.-Ergebnisse Reihe C: 1-113.

Sarnthein, M., Jansen, E., Weinelt, M., Arnold, M., Duplessy, J.C., Erlenkeuser, H., Flatoey, A., Johannessen, G., Johannessen, T., Jung, S., Koc, N., Labeyrie, L., Maslin, M., Pflaumann, U., Schulz, H., 1995. Variations in Atlantic surface ocean paleoceanography, 50° - 80°N: A time-slide recordof the last 30,000 years. Paleoceanography 10: 1063-1094.

Sarnthein, M., Winn, K., Jung, S.J.A., Duplessy, J.C., Labeyrie, L.D., Erlenkeuser, H., Ganssen, G., 1994. Changes in East Atlantic deepwater circulation over the last 30,000 years: Eight time slice reconstructions. Paleoceanography 9: 209-267.

Sautter, L.R., Thunell, R.C., 1991a. Planktonic foraminiferal response to upwelling and

seasonal hydrographic conditions: Sediment trap results from San Pedro Basin, Southern California Bight. J. Foram. Res. 21: 347-363.

Sautter, L.R., Thunell, R.C., 1991b. Seasonal variability in the $\delta^{18}O$ and $\delta^{13}C$ of planktonic foraminifera from an upwelling environment: Sediment trap results from the San Pedro Basin, Southern California Bight. Paleoceanography 6: 307-334.

Schmitz, W.J.j., 1995. On the interbasin-scale thermohaline circulation. Reviews in Geophysics 33: 151-173.

Schott, W., 1935. Die Foraminiferen in dem Äquatorialen Teil des Atlantischen Ozeans. Wiss. Ergebn. d. Deutschen Atl. Exp. Meteor 1925-1927 3: 1-135.

Shannon, L.V., Chapman, P., 1991. Evidence of Antarctic Bottom Water in the Angola Basin at 32°S. Deep-Sea Res. 38: 1299-1304.

Spero, H.J., 1992. Do planktic foraminifera accurately record shifts in the carbon isotopic composition of seawater carbon dioxide? Mar. Micropal. 19: 275-285.

Spero, H.J., Lea, D.W., 1996. Experimental determination of stable isotope variability in *Globigerina bulloides*: implications for paleoceanographic reconstructions. Mar. Micropal. 28: 231-246.

Stocker, T.F., Schmittner, A., 1997. Influence of $CO_2$ emission rates on the stability of the thermohaline circulation. Nature 388: 862-865.

Stute, M., Forster, M., Frischkorn, H., Serejo, A., Clark, J.F., Schlosser, P., Broecker, W.S., Bonani, G., 1995. Cooling of Tropical Brazil (5°C) during the Last Glacial Maximum. Science 269: 379-383.

Sundquist, E.T., 1985. Geological perspectives on carbon dioxide and the carbon cycle. In: Sundquist, E.T., Broecker, W.S. (Eds.), The carbon cycle and atmospheric $CO_2$: Natural variations Archean to Present. American Geophysical Union, Geophysical Monographs, 32, pp. 5-59.

Takayanagi, Y., Niitsuma, N., Sakai, T., 1968. Wall microstructure of *Globorotalia truncatulinoides* (d'Orbigny). Tohoku Univ Sci Repts, Series 2 (Geol.) 40: 141-170.

Talley, L.D., 1996. Antarctic Intermediate Water in the South Atlantic. In: Wefer, G., Berger, W.H., Siedler, G., Webb, D.J. (Eds.), The South Atlantic: Present and past circulation. Springer-Verlag, Berlin Heidelberg, pp. 219-238.

Thierstein, H.R., 1982. Terminal Cretaceous plankton extinctions: A critical assessment. Geol. Soc. Am. Spec. Publ. 190: 385-399.

Thierstein, H.R., Geitzenauer, K.R., Molfino, B., Shackleton, N.J., 1977. Global synchroneity of late Quaternary coccolith datum levels: Validation by oxygen isotops. Geology 5: 400-404.

Van Bennekom, A.J., Berger, G.W., 1984. Hydrography and silica budget of the Angola Basin. Neth. J. Sea Res. 17: 149-200.

Van Kreveld, S.A., 1996. Calcium carbonate dissolution indices on the northeast Atlantic sea floor. In: Van Kreveld-Alfane, S.A. (Ed.) Late Quaternary sediment records of mid-latitude Northeast Atlantic calcium carbonate production and dissolution. FEBO B.V., Enschede, pp. 135-184.

Van Leeuwen, R.J.W., 1989. Sea-floor distribution and Late Quaternary faunal patterns of planktonic and benthic foraminifers in the Angola Basin. Utrecht Micropal. Bull. 38: 287.

Verardo, D.J., McIntyre, A., 1994. Production and destruction: Control of biogenous sedimentation in the tropical Atlantic 0-300,000 years B.P. Paleoceanography 9: 63-86.

Verardo, D.J., Ruddiman, W.F., 1996. Late Pleistocene charcoal in tropical Atlantic deep-sea sediments: Climatic and geochemical significance. Geology 24: 855-857.

Wagner, T., Dupont, L., in press. Terrestrial OM in marine sediments: analytic approaches and eolian-marine records of the central Equatorial Atlantic. In: Fischer, G., Wefer, G. (Eds.), Proxies in paleoceanography. Springer-Verlag, Berlin Heidelberg, pp.

Warren, B.A., Speer, K.G., 1991. Deep circulation in the eastern South Atlantic Ocean. Deep-Sea Res. 38: 281-322.

Weinelt, M., Sarnthein, M., Pflaumann, U., Schulz, H., Jung, J.C., Erlenkeuser, A., 1996. Ice-free nordic seas during the last glacial maximum? Potential sites of deep-water formation. Paleoclimates 1: 283-309.

Wolff, T., Mulitza, S., Arz, H., Pätzold, J., Wefer, G., subm. Oxygen isotopes versus CLIMAP (18ka) temperatures: A comparison from the tropical Atlantic. Geology.

# Part II *Publications*

## Prologue

In order to derive climatic variations from sediments covering the last 300 kyrs modifications of planktic foraminiferal assemblages were investigated; as fundamental indicator of changes in surface water productivity, alterations in coccolithophore assemblages were examined on the same samples. To complete the picture of production of microorganisms in the surface water and their preservation in the sediment bulk parameters as $CaCO_3$, organic carbon, sedimentation rate, and sand content were studied, too (cf. Part II - chapters 1, 2).

Although the dissolution kinetics in the water column are well understood (e.g., Culberson and Pytkowicz 1968; Berner and Morse 1974; Keir 1980; Berelson et al. 1994), processes at the sediment pore-water interface are still under debate (e.g., Hales et al. 1994; Hales and Emerson 1996; Martin and Sayles 1996). In order to contribute to this particular topic we investigated planktic foraminifera *Globigerina bulloides*' ultrastructure and its prograding breakdown through the water column (cf. Part II - chapter 3).

Regarding the investigation of planktic foraminifera, some methods considered to be linked to carbonate dissolution display ecological rather than geochemical variations (see above). Hence, we applied several methods on sediment surface samples through the water column ranging from far above the carbonate lysocline to below the carbonate compensation depth. This yielded a compilation of methods and their limitation as paleoceanographic proxies (cf. Part II - chapter 4).

One of the most puzzling pecularities on determining organism assemblages is the number of specimens per sample to be investigated. Although there are various recommendations commonly applied, we can show that our approach improves further studies maximizing statistical significance and minimizing researchers' expenditure of energy (cf. Part II - chapter 5).

# 1. A 300 kyrs history of planktic foraminiferal distribution in the central equatorial Atlantic Ocean - paleo-environmental implications

Nicolas Dittert, Hans-Stefan Niebler, Rüdiger Henrich

*FB Geowissenschaften, Universität Bremen, Postfach 33 04 40, D-28334 Bremen, Germany*

## Abstract

A sediment core of the equatorial Atlantic Ocean (GeoB 1117-2) was investigated in order to reconstruct the paleo-environmental evolution during the last 300 kyrs by analysis of planktic foraminiferal assemblages.

All planktic foraminiferal assemblages are dominated by variations in the orbital eccentricity (100 kyrs) and precession (23 kyrs) periods; the 41 kyrs period (obliquity) is of minor importance. There is an obvious trend showing decreasing numbers of planktic foraminifera per gram sediment by about 50 % during the last 300 kyrs. Using a five-factor model, the transfer function technique displays two highly significant factors: (1) The subtropical-tropical factor which attains maximum loadings during all interglacials and the Holocene; (2) the warm-transitional factor which occurs with maximum loadings during glacial events. Highest estimated sea surface temperatures (SST's) are attained during interglacials, and lowest SST's occur during glacials. Glacial maxima are supposed to become warmer from oxygen isotope event 8.2 to 2.2 by about 2.5 °C. The difference between the modern and the Last Glacial Maximum SST amounts to about 6 °C for the central tropical South Atlantic. Two oceanic situations can be distinguished during the last 300 kyrs: (1) Cool and nutrient-rich waters are advected off the eastern boundary amplifying cooling in this area. Equatorial upwelling may be enhanced somewhat; however, the upwelling factor does not explain any significance; (2) warm and salty waters during interglacials with a deep thermocline and only moderate equatorial upwelling. Cool water advection is weak or absent in the equatorial Atlantic Ocean.

In order to check the reliability of our paleo-environmental data on calcite dissolution, some commonly used dissolution indices were applied to the core sediments. Although there is some indication for decreased calcite preservation, none of the indices accounts for a significant dissolution increase during the last 300 kyrs which would alter the

planktic foraminiferal assemblages and hence would fake our paleo-reconstructions.

## 1. Introduction

Regarding the reconstruction of past climate, shells of planktic foraminifera are one of the most abundant and significant calcite fossil remains used extensively for environmental reconstructions. They base on fossil evidence and provide evidence for climatic changes in a more than centennial tradition (e.g., Murray, 1897; Schott, 1935; Emiliani, 1955, etc.). The geographic distribution of living planktic foraminifera in surface waters and that of fossil assemblages in the geological record are intimately related to modern surface water temperatures (SST's) (Bé and Tolderlund, 1971; Bé, 1977; Vincent and Berger, 1981). Imbrie and Kipp (1971) first applied this relationship between planktic foraminifera and surface water hydrography to reconstruct past SST's. The first detailed studies of SST's in the equatorial Atlantic Ocean base on Imbrie and Kipp's method (CLIMAP, 1976; 1981; 1984; 1994); they suggest that the South Equatorial Current was cooler by 1 °C to 3 °C during the Last Glacial Maximum (LGM).

It has been known since the studies of Wüst (1935) that the water characteristics of the corrosive AABW are responsible for the pronounced abyssal calcium carbonate dissolution. Since the production of NADW is thought to be reduced during glacial periods (Curry and Oppo, 1997), AABW would expand in latitudinal and vertical distribution, and the lysocline would rise in the Brazil Basin, leading to an increase in carbonate dissolution (Bickert and Wefer, 1996). Usually, samples affected by calcite dissolution are excluded from the data set to avoid distortion of the parameters concerning environmental reconstructions (e.g., Pflaumann et al., 1996; Niebler and Gersonde, 1998). However, if the position of the modern calcite lysocline is known (Bainbridge, 1981) the "depth-transect approach" (e.g., Farrell and Prell 1989; Curry and Lohmann 1990; Bickert et al. 1997) provides qualitative and quantitative information on the intensity of calcite dissolution. Where the depth-transect crosses the lysocline the corresponding value of each dissolution index yields an excellent calibration of the modern to the fossil situation. Actually, if calcite dissolution becomes important the surface water parameters will fail. Vice versa, information on the degree and the latitudinal and the vertical extent of deep-water masses is attained (Dittert et al., subm.).

The main topic of this study is to reconstruct and to evaluate paleo-environmental patterns of the equatorial South Atlantic Ocean by analysis of planktic foraminiferal assemblages from the Brazil Basin during the last 300 kyrs. Therefore we have

investigated one sediment core (GeoB 1117-2) which is located at the southern rim of today's equatorial upwelling system and which is positioned well above the modern sedimentary calcite lysocline (about 4,300 m, Dittert and Henrich, subm.). The planktic foraminiferal assemblages alternate in orbital-to-suborbital cyclicity and enable us to estimate past surface water temperatures and modifications in surface water currents in the equatorial South Atlantic Ocean . In order to check the reliability of our core data we examined the surface sediments of the adjacent box corers. This also includes a depth-transect from the area above to the area below the modern calcite lysocline. Where the core data pass the calibration datums of the box corer transect calcite dissolution is supposed to bias surface water reconstructions.

## 2. Modern oceanic environment: An outline

### *2.1 Surface water circulation*

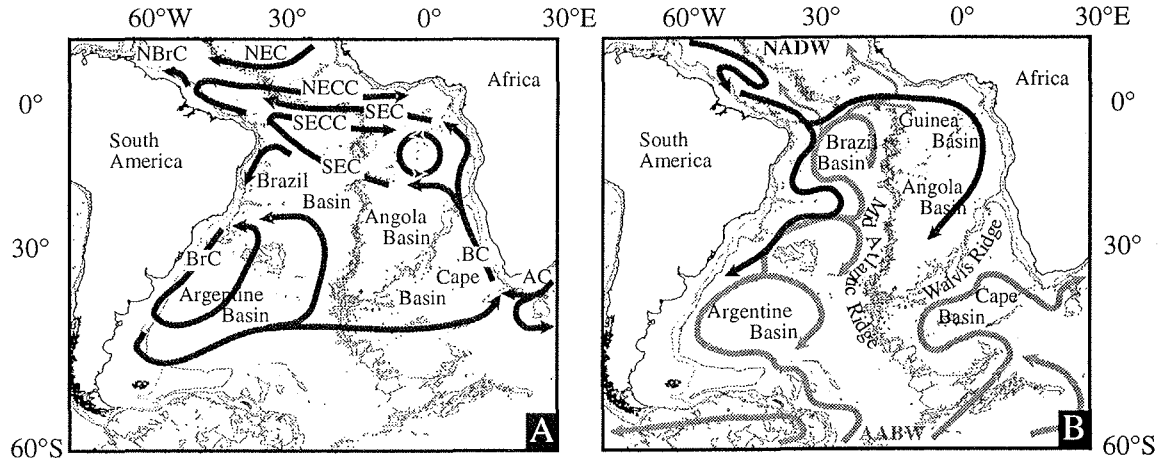


**Fig. 1:** Modern South Atlantic Ocean water mass distribution pathways at the working area: Surface waters (Fig. 1-A) with the South Equatorial Current (SEC) flowing westwards and the North Equatorial Counter Current (NECC), the South Equatorial Counter Current (SECC) flowing eastwards. Deep-water pathways (Fig. 1-B) with Antarctic Bottom Water (AABW; grey) coming from South and North Atlantic Deep Water (NADW; black) coming from North.

The surface water oceanography of the equatorial Atlantic (Fig. 1-A) is characterized by the westward flowing South Equatorial Current (SEC) and the eastward flowing South Equatorial Counter Current (SECC), the North Equatorial Current (NECC), and the Equatorial Undercurrent (EUC). Variations in the surface water oceanography are driven by the interaction of low-latitude trade- and monsoonal winds. During boreal winter, sea-surface temperatures are warmest in the eastern equatorial Atlantic (Philander, 1986). The intensification of the trade-winds in boreal spring in the western tropical

Atlantic (Philander and Pacanowski, 1986) causes massive transport of warm surface waters from the eastern to the western tropical Atlantic deepening the thermocline in the west, and lifting up the thermocline in the east. Additionally, an increased Ekman divergence results in stronger equatorial upwelling and productivity with maximum in boreal summer. In boreal autumn, the thermocline returns to its pre-upwelling state. Thus, the seasonally changing wind system reflects a combination of cool eastern-boundary waters advected westwards and a wave-like movement of the thermocline (Moore et al., 1978; Cane, 1979; Philander, 1979; Philander and Pacanowski, 1986). The seasonal cycle in the surface water circulation of the equatorial Atlantic stands for long-term variations induced by the precessional component of orbital forcing (Molfino and McIntyre, 1990).

### *2.2 Deep water circulation*

Today the circulation in the deep South Atlantic Ocean (Fig. 1-B) is dominated by interactions between the Antarctic Bottom Water (AABW) and the North Atlantic Deep Water (NADW) in contrasting extent. NADW is indicated by oxygen enriched, nutrient depleted water masses of high $CO_3^{2-}$ and low $CO_2$ contents. AABW can be distinguished as an extremely cold, oxygen depleted and nutrient enriched water mass of low $CO_3^{2-}$ and high $CO_2$ contents (Kroopnick, 1985; Boyle, 1988). Today's mixing zone between AABW and NADW in the South Atlantic is close to the 90 µmol/kg $CO_3^{2-}$ isoline (Bainbridge, 1981). The relatively warm and saline NADW roughly occupies the depth interval between 2,000 m and 4,000 m whereas below 4,000 m AABW is encountered. However, the geometry of deep-water masses in the South Atlantic Ocean is much more complex in detail. A strong east-west asymmetry in the deep-water structure is observed, which is related to deflections along topographic barriers like the Mid Atlantic Ridge, the Walvis Ridge, and the Rio Grande Rise. These barriers are partly incised by major deep-water conducts like the Romanche Fracture Zone which enable the inflow of NADW to the equatorial eastern Atlantic Ocean. With respect to the modern South Atlantic Ocean, the border of AABW with NADW and the hydrographic lysocline coincide (Bickert and Wefer, 1996).

### *2.3 Distribution patterns of planktic foraminifera*

The pioneer studies by Bé and Tolderlund (1971) and Bé (1977) define five zoogeographic provinces of planktic foraminifera in the World Ocean which are primarily influenced by ecology and temperature: tropical, subtropical, transitional, subpolar, and

polar. Additionally, most living species can be attributed to distinct water depths (Ravelo et al., 1990; Oberhänsli et al., 1992; Ottens, 1992). Due to the access of light and food, most of the spinose species are surface dwellers, or at least prefer to live in the upper part of the euphotic zone (e.g., *Globigerinoides* spp.). Non-spinose species preferentially live at sub-surface depths below 50 m (e.g., some *Globorotalia* spp.), and a few species inhibit depths below 100 m and even below 200 m (e.g., *G. theyeri* ). Some species prefer thermocline conditions (e.g., *N. dutertrei* ) and consequently follow the seasonally changing thermocline depth within the water column; other species (e.g., *G. bulloides* ) also correlate with high nutrient supply (Hemleben et al., 1989). That is, each species is assigned to discrete hydrographic conditions and, vice versa, reflects discrete hydrographic conditions which we use to reconstruct past equatorial Atlantic Ocean environments (Ravelo et al., 1990).

## 3. Material and methods

All sediment samples (Fig. 2) were collected during R/V *Meteor* cruise M9/4 (Wefer et al., 1989). The depth-transect is attributed to box corer samples (GeoB 1115 - 1119) from 2,921 m to 5,213 m water depth. One box corer (GeoB 1117-3) was sampled to achieve an undisturbed sediment surface of the gravity core GeoB 1117-2 (3°48.9' S - 14°53.8' W; 3,984 m water depth) at the same site. All data presented here are archived in the PANGAEA database at the Alfred Wegener Institute for Polar and Marine Research (http://www.pangaea.de).

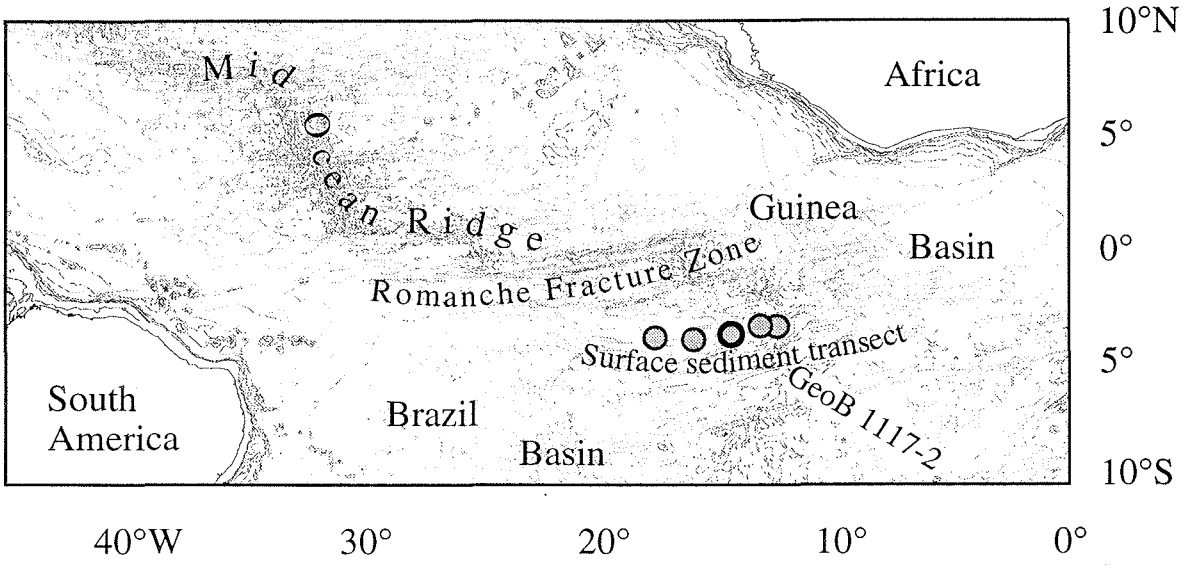


**Fig. 2:** Position of the sediment core GeoB 1117-2 (3,984 m; bold border) and the surface sediment transect (2,921 m down to 5,213 m water depth) ranging from the Mid Ocean Ridge into the Brazil Basin.

*Determination of bulk carbonate.* Total carbon (TC) and total organic (TOC) content of bulk sediments were measured with a LECO-CS 244 infrared analyzer. Therefore, 100 mg of freeze-dried and homogenized sediment were analyzed. For determination of TOC the same amount of sediment was acidified with 6n HCl and measured the same way. Calcium carbonate content was calculated in weight percentage of the bulk sample by:

$$CaCO_3 \text{ wt.-\%} = (\text{TC wt.-\%} - \text{TOC wt.-\%}) \cdot 8.33$$

*Species determination.* For foraminiferal counts, samples were freeze-dried, weighed, and washed through a 63 µm sieve under a gentle spray of water to prevent mechanical fragmentation. We base the faunal analysis on the fraction >150 µm according to the CLIMAP-conventions. After separating the fraction <150 µm, the samples were dry-sieved on a 212 µm, 355 µm, 500 µm, and 1,000 µm sieve-set in order to minimize sorting and to simplify counting. Each fraction was repeatedly split into subsamples using a microsplitter to obtain an aliquot of at least 300 non-fragmented planktic foraminiferal specimens (CLIMAP, 1984) which were identified and counted completely using an OLYMPUS SZ 40 binocular at 20× to 80× magnification. The taxonomy used follows that of Hemleben et al. (1989). Planktic foraminifera fragments, benthic foraminifera, radiolaria, and subordinately pteropods, rock fragments, and indeterminable particles were also counted on the same aliquot. All fauna-counts were converted into count percent and number of organisms per gram sediment (Mix, 1989). Due to statistical relevance, only species sensitive to temperature (e.g., Pflaumann et al., 1996), species with an relative abundance >2 % within at least 1 sample, and species with an occurrence within at least 5 samples were considered in the core (Imbrie and Kipp, 1971).

*Stratigraphy.* The stratigraphy of both the gravity core and the box corer is based on $\delta^{18}O$ measurements on tests of the benthic foraminifer *Cibicides wuellerstorfi.* All samples were analyzed using a Finnigan MAT 251 micromass spectrometer coupled with a Finnigan automated carbonate device at the University of Bremen. The raw data, age control points, and cross spectral analyses documenting the precision of the dating are presented by Bickert and Wefer (1996).

*Transfer function technique.* For surface water current reconstructions and paleo-temperature estimations within the transfer function method we follow the strategy of Niebler and Gersonde (1998). We apply a new transfer function which is based on selected data from the SPECMAP Archive 1 (1989/90), Pflaumann et al. (1996), Niebler and Gersonde (1998), and unpublished data from Niebler et al. (in prep.). This transfer-function ("F279-23-5") was developed for the tropical Atlantic and south Atlantic Ocean

(20°N-60°S), contains 279 surface sediment samples, requires 23 species and morphotypes and is based on a five factor model. Hydrographic data refer to Levitus and Boyer (1994) and Olbers et al. (1982). This transfer function technique results for each core depth in one paleo-temperature estimate and the associated communality. The communality describes the hallmark of good quality between the fossil data set and the reference data set (e.g., Malmgren and Haq, 1982; Davis, 1986). Due to the standard error of estimation ($\sigma_n$ =1.1 °C) temperatures are given with a precision of 0.5 °C.

*Preservation.* In order to avoid distortion of the parameters concerning environmental reconstructions the core was investigated on calcite dissolution. In detail these are (1) the *Globigerina bulloides* Dissolution Index (BDX, Dittert and Henrich, subm.) which gives evidence that *G. bulloides* ' ultrastructure will progressively break down with increasing carbonate dissolution. BDX was regarded over the last 140 kyrs; (2) the $CaCO_3$ content in weight percentage; (3) the rain ratio as the molar ratio of organic ($C_{org}$) to inorganic ($C_{carb}$) carbon (Berger and Keir, 1984); (4) the ratio of radiolaria vs. benthic foraminifera vs. planktic foraminifera (modified after Diester-Haass and Rothe, 1987); and (5) the foraminiferal dissolution index (FDX, Berger, 1979) which ranks planktic foraminifera according to their dissolution resistance. The depth-transect which was investigated earlier (Dittert et al., subm.) provides qualitative and quantitative information on the intensity of calcite dissolution in the sediment surface samples. Where the depth-transect crosses the lysocline the corresponding value of each dissolution index yields an excellent calibration of the modern to the fossil situation. Where the core data pass the calibration datums of the box corer transect calcite dissolution is supposed to bias surface water reconstructions.

*Cross spectral analysis.* We performed spectral analysis with the software package "AnalySeries 1.1" (Paillard et al., 1996). The analyzed time series were evenly resampled at 3 kyrs intervals and linearly detrended. As a record of global ice volume we used the $\delta^{18}O$ signal of the benthic foraminifera *C. wuellerstorfi* of the same core (Bickert and Wefer, 1996).

## 4. Results

*Planktic foraminifera.* The total number of planktic foraminifera per gram sediment varies from 27,000 to 191,000 specimens. Maximum numbers occur at the transition of oxygen isotope stages (OIS) 8/7 and at the oxygen isotope events (OIE) 7.1, 6.6, 6.4; minimum numbers occur at OIE 6.3, 5.4, and 2.1. Relative abundances and absolute

numbers of planktic foraminifera show a distinct orbital-to-suborbital modification (Figs. 3, 4). Moreover, there is an obvious trend from 110,000 (300 ka) to 54,000 (Recent) planktic foraminifera per gram sediment (Fig. 3).

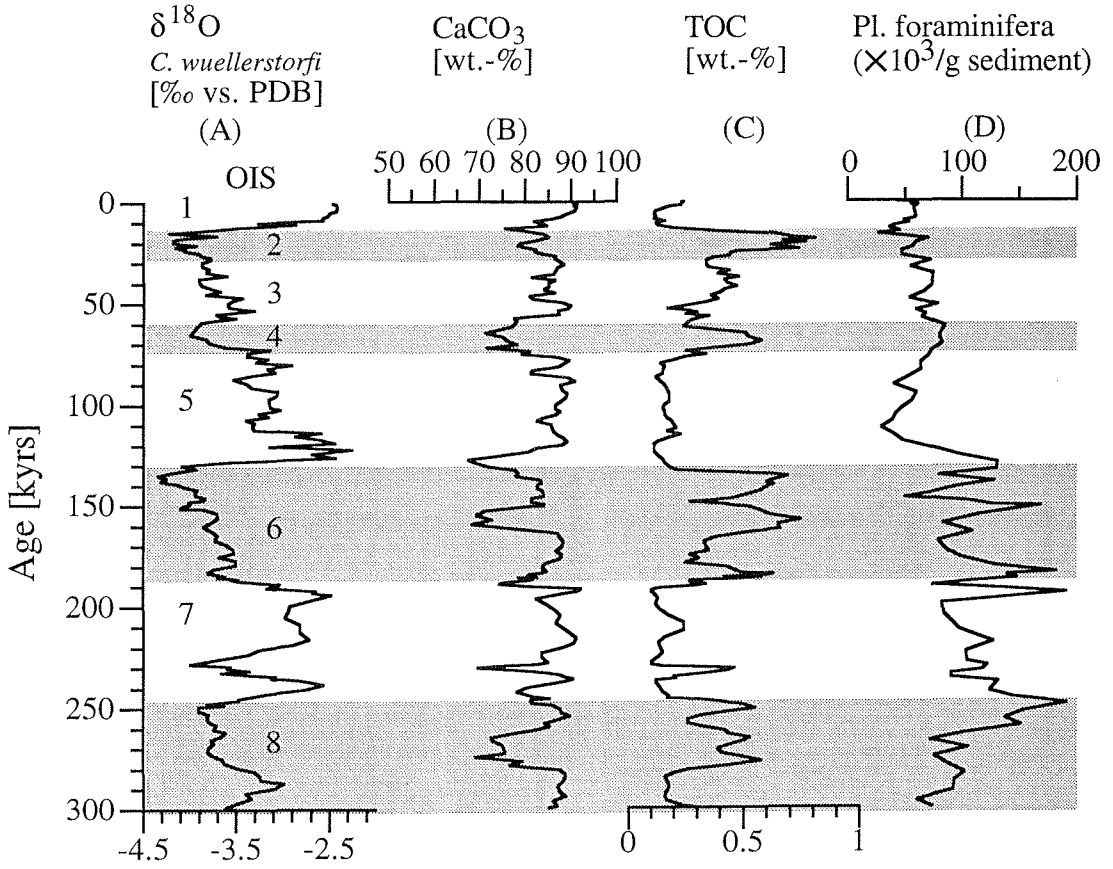


**Fig. 3:** $\delta^{18}O$, CaCO3 wt.-%, TOC wt.-%, and total number of planktic foraminifera during the last 300 kyrs showing a distinct glacial-to-interglacial modification.Glacials are put to grey bars.

The tropical species *G. sacculifer* (1 - 25 %), *P. obliquiloculata* (0 - 14 %), *G. menardii* (0 - 29 %), the subtropical representatives *G. ruber* (pink and white variety; 3 - 43 %), *G. rubescens* (pink and white variety; 0 - 7 %), *G. glutinata* (1 - 20 %), and *G. siphonifera* (0 - 6 %) attain maxima at interglacial maxima, particularly at OIS 7, 5, and during the Holocene; *G. rubescens* and *G. glutinata* attain only low values during the Holocene. Minima occur at glacial maxima of the OIS 8, 6, 4, and 2. *Globorotalia menardii* is missing completely from 155 ka to 126 ka and from 80 ka to 12 ka (cf. Ericson and Wollin, 1968; Berger et al., 1985). The subtropical species *G. truncatulinoides* dex. (0 - 6 %) mainly occurs at the transitions OIE 8.6/8.5, 7.2/7.1, 6.4/6.3, 4.2/4.1, and OIS 3/2 whereas it disappears during the Holocene. *Globorotalia truncatulinoides* dex. and *G. crassaformis* have only a minor contribution to the total number of planktic foraminifera. The transitional species *G. inflata* (0 - 37 %) attains maxima in glacials; it is nearly absent during the Holocene. Among the subpolar species,

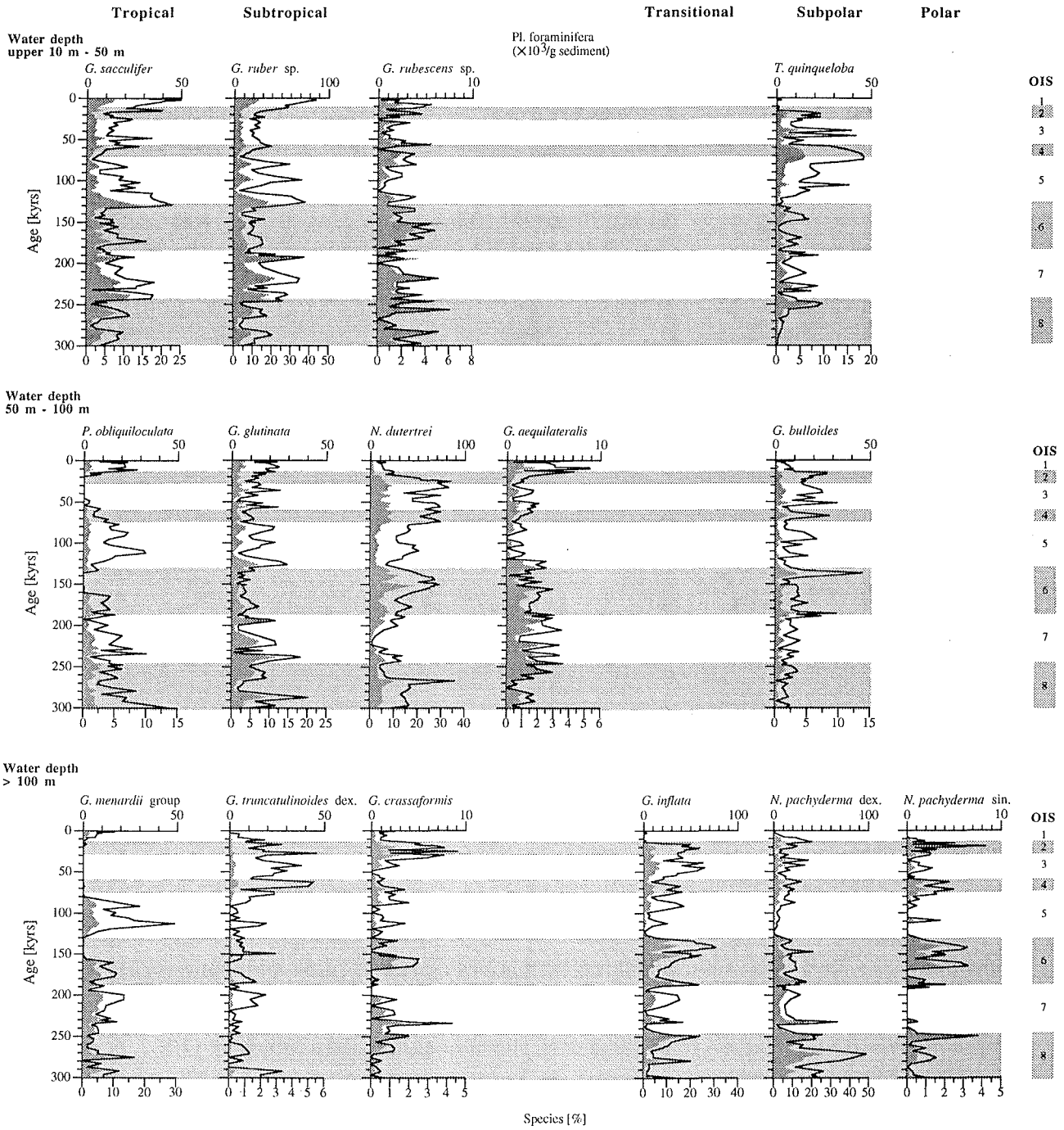


**Fig. 4:** Planktic foraminiferal species abundances during the last 300 kyrs distinguished into latitudinal and vertical distribution. Total numbers of planktic foraminifera per 1 g sediment are presented above (grey areas), species abundances are presented below (black lines). Mind the different scales! Glacials are put to grey bars.

*N. pachyderma* dex. (0 - 49 %) has its maximum occurrence during the glacial maxima of OIS 8 and the OIE 7.4; its abundance subsequently lowers. *Turborotalita quinqueloba* (0 - 18 %) mainly occurs during the transitions of OIS 7/6, 5/4, and 3/2. *Globigerina*

*bulloides* (0 - 14 %) has its maximum occurrence during the glacial events 6.2, 4.2, 2.2, and at the transition of OIS 7/6. All subpolar species are nearly absent during the Holocene. *Neogloboquadrina pachyderma* sin. (0 - 5 %) almost exclusively occurs at full glacial conditions. It is absent during the Holocene (Fig. 4).

*Transfer function technique.* We distinguished five factors: (1) the subtropical-tropical factor; (2) the warm-transitional factor; (3) the polar factor; (4) the upwelling factor; and (5) the subpolar factor. Actually, all five factors explain 93 % of the variance, but the factors three, four and five each only explain <4 % of the variance. The factor loadings of the subtropical-tropical factor (Fig. 5-A) range from 0.13 to 0.99, the loadings of the warm-transitional factor (Fig. 5-B) range from 0.03 to 0.87. Factor 1 attains its maximum loadings during all interglacials and the Holocene; minimum loadings occur during glacials. Factor 2 occurs with maximum loadings during glacial events and with minimum loadings during interglacials. During the Holocene this factor almost expires. Generally, amplitudes of factor 1 and factor 2 are high.

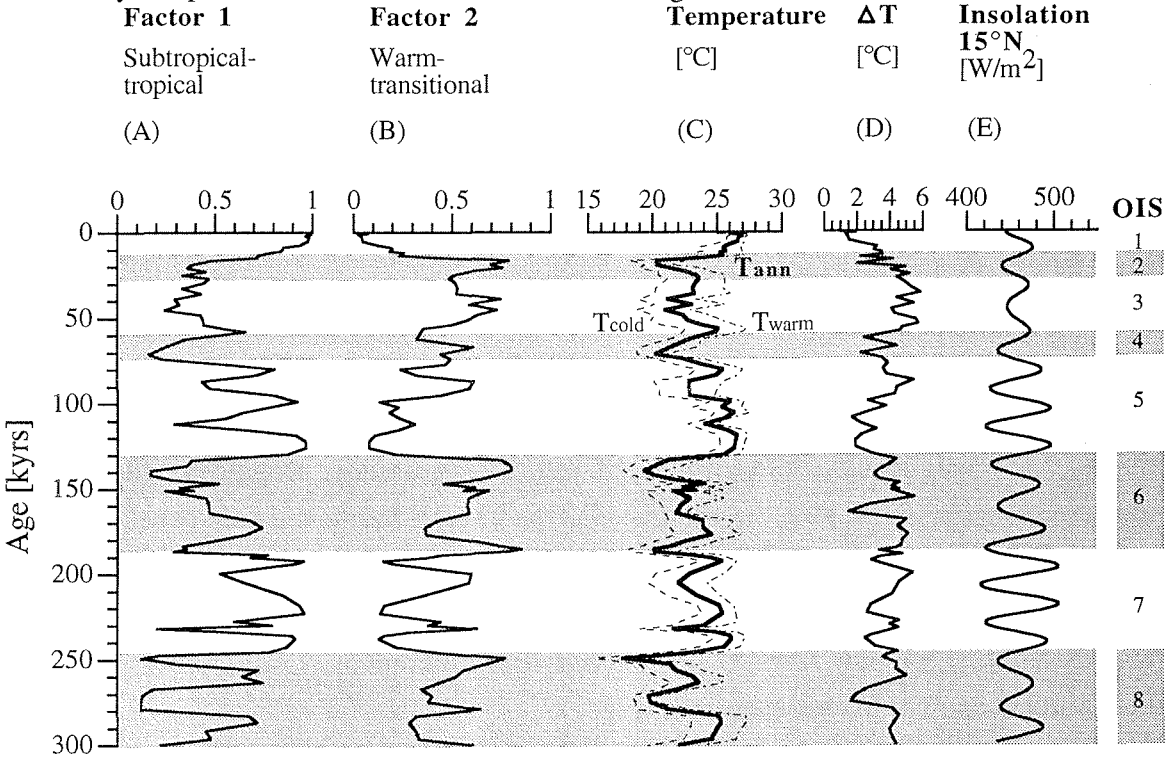


**Fig. 5:** Transfer function technique factors, estimated temperatures ($T_{warm}$, $T_{cold}$, $T_{annual\ mean}$; and $\Delta T$ referring to seasonality) and insolation at 15°N during the last 300 kyrs showing a distinct glacial-to-interglacial modification. Glacials are put to grey bars.

The estimated temperatures (Fig. 5-C) range from 19.1 °C to 27.5 °C ($T_{warm\ season}$), from 15.5 °C to 26.5 °C ($T_{cold\ season}$), and from 17.7 °C to 27.2 °C ($T_{annual\ mean}$). For all curves highest temperatures are attained in interglacials, and lowest temperatures are

attained during glacials. The difference between $T_{warm}$ and $T_{cold}$ ranges from 1.0 °C to 5.9 °C; highest $\Delta T$ generally coincide high loadings of the warm-transitional factor (Fig. 5-D).

*Sediment data and preservation studies.* BDX data for the last 140 kyrs show a moderate preservation without any strong dissolution impact; values range from 1.4 to 3.5. Minimum values occur at OIE 4.2, 2.2, and at the transition of OIS 6/5. Maximum values are attained at OIE 5.5, 5.4, and 5.1 (Fig. 6-A). The $CaCO_3$ content of the sediment ranges from 68 wt.-% to >92 wt.-% (Figs. 3-B, 6-B). Clear maximum values occur during interglacials, and minima are attained during glacials. The TOC content does not exceed 0.8 wt.-%; maximum values correspond to glacial, minimum values agree with interglacial conditions (Figs. 3-C, 6-C). The rain ratio shows only small variations; maximum values do not top 0.01 and coincide glacial OIS (Fig. 6-D). Regarding the assemblages >150 µm, planktic foraminifera range between 75 % and >90 %, benthic foraminifera attain values from 0 % to 15 %, and radiolaria occur with maximum values of 20 % of the total fauna. Major changes occur during glacials where the abundance of planktic foraminifera is lower, and the abundances of benthic foraminifera and radiolaria raise (Fig. 6-E). The composition of the planktic foraminiferal group can be roughly distinguished into thick- and thin-shelled species. Thick-shelled species attribute with >90 % to the total group during glacials; during interglacials values do not exceed 35 % (Fig. 6-F).

*Cross spectral analysis.* Most variation within the subtropical-tropical assemblage occurs in the 100 kyrs (eccentricity) and the 23 kyrs (precession) frequencies; however, the 41 kyrs frequency (obliquity) is of minor importance. Regarding the warm-transitional assemblage, only the 100 kyrs and the 23 kyrs frequencies are developed. For both assemblages the power decreases from the longer to the shorter periods. Only the subtropical-tropical and the warm-transitional factor attain coherence values >0.9. The factors three, four and five do not exceed 0.5 coherence; consequently, they are insignificant and not further examined (Fig. 7).

## 5. Discussion

*Paleo-environmental reconstructions.* The composition of the several assemblages of planktic foraminifera lastly gives evidence for the oceanic development of the equatorial Atlantic Ocean during the last 300 kyrs. Above all, the subtropical species *G. ruber* and the tropical species *G. sacculifer* (Figs. 4, 5) represent warm and salty surface water

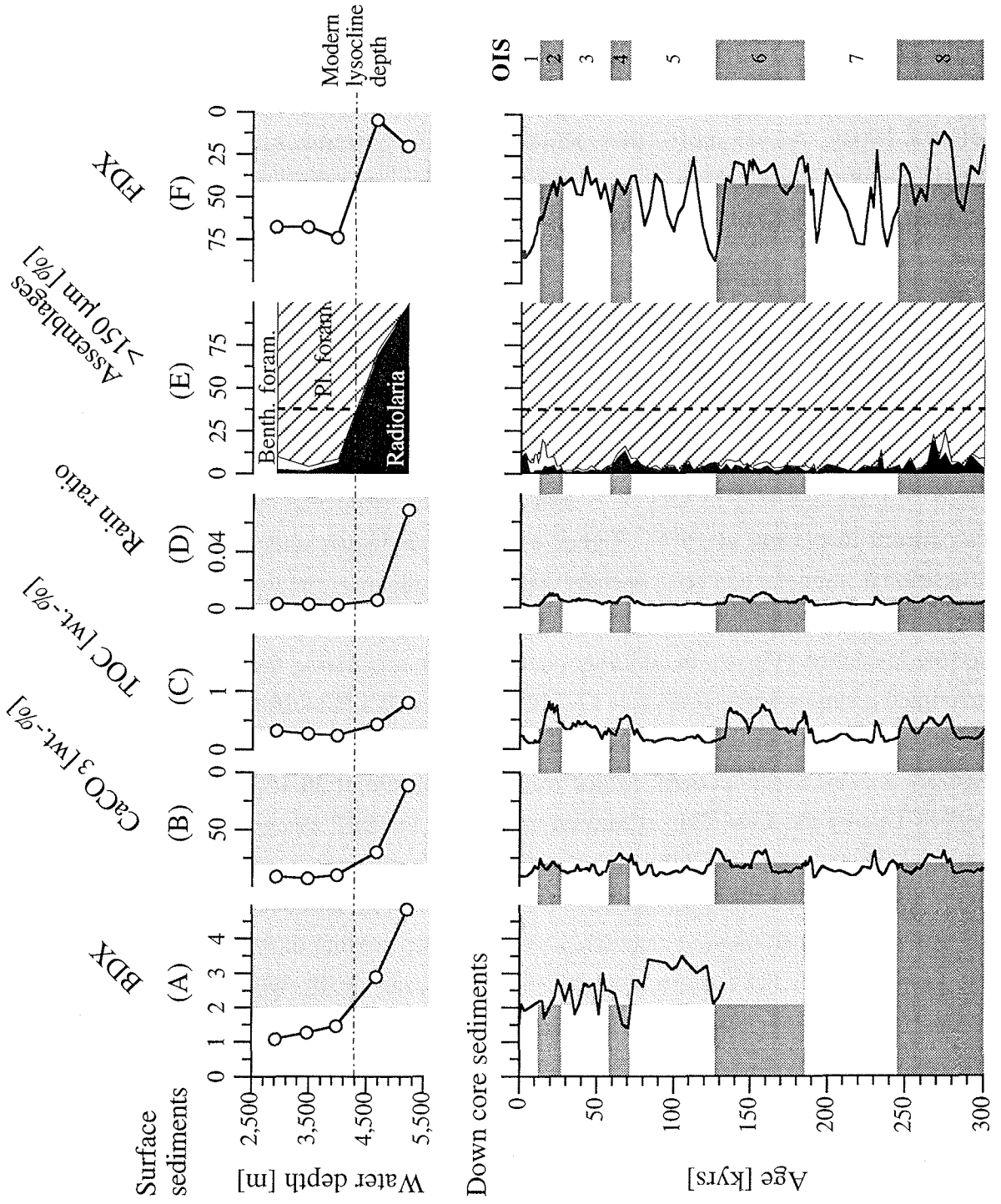


**Fig. 6:** Dissolution indices investigated to check whether fossil data are valid to reconstruct surface water environment parameters. Where the surface sediment data intersect the position of the modern lysocline (dotted-dashed line), calcite dissolution (light grey bars) is supposed to become important. Increasing dissolution is plotted towards right. This crossing was used as calibration for the fossil to the modern situation. Surface sediment dissolution proxies are presented above, down core dissolution proxies are presented below. Glacials are put to grey bars.

masses showing a deep thermocline (Parker and Berger, 1971; Kipp, 1976). *Turborotalita quinqueloba, G. bulloides*, and *N. pachyderma* correspond to cold water temperature and lower salinities (Bé and Hutson, 1977; Van Leeuwen, 1989; Oberhänsli et al., 1992). Additionally, they show a certain preference to nutrient enriched environments. For example, *N. pachyderma* sin. has its maximum occurrence at water temperatures <12 °C (Brummer and Kroon, 1988). Only *G. bulloides* tolerates temperature ranges from 4 °C to 22 °C (Niebler and Gersonde, 1998). However, Ganssen (1983), Pflaumann (1985), and Sautter and Thunell (1991) show, that optimum temperatures of about 15 °C and a high nutrient offer produce maximum number of specimens in *G. bulloides* and *N. pachyderma* dex. Higher relative abundances and absolute numbers of subtropical-tropical species are reflected by high loadings of the subtropical-tropical factor and by high estimated SST's. Maximum annual SST's (25 °C - 26.6 °C) are attained in OIS 7, 5 and during the Holocene which corresponds to maximum insolation at 15°N. Higher relative abundances and absolute numbers of transitional, subpolar and polar species yield high loadings of the warm-transitional factor and minimum annual SST's (17.7 °C - 20.4 °C) in OIS 8, 6, 4, and 2 which corresponds to low insolation (Fig. 5). In addition, our data show that during the last 300 kyrs glacial maxima become warmer (OIE 8.2: 17.7 °C; OIE 6.2: 19.3 °C; OIE 4.2: 20.3 °C; OIE 2.2: 20.4 °C). The modern annual SST of 26.6 °C reconstructed from the sediment surface sample is close to the modern surface water temperature of 26.4°C (Levitus and Boyer, 1994). During the Last Glacial Maximum (LGM) the SST estimation lowers down to 20.4 °C. This temperature difference ($\Delta SST_{modern - LGM}$) amounts to 4.9 °C ($T_{warm}$), 7.7 °C ($T_{cold}$), and 6.2 °C ($T_{ann}$). Our ΔSST approach the estimations reconstructed by other authors. Wolff et al. (subm.) calculate a distinct LGM cooling of 5.5 °C (winter) and 6.5 °C (summer) for the eastern tropical Atlantic Ocean (<20° W) via oxygen isotope investigations. Mix et al. (1986a; 1986b) and McIntyre et al. (1989) inferred an annual-average difference of 4 °C. However, these estimations recalculate temperatures for 0 m to 30 m water depths whereas our estimations refer to the surface water (0 m); this depth range would explain at least a part of the 1 °C to 2 °C temperature difference. CLIMAP's ΔSST estimates amount to only 1 °C to 3 °C (CLIMAP, 1976; 1981; 1984; 1994); this difference of about 4 °C to our SST's may be due to the relatively small data set used by CLIMAP. Discrepancies between the SST reconstructions for the tropical Atlantic and terrestrial temperature records caused serious obstacles, as the significantly lowered temperatures on land (about 5°C), and small changes in SST's (CLIMAP's 1 °C to 2° C) in the tropics could not be explained by a conclusive model. With huge data sets and improved transfer functions we now can show that our marine temperature signals, terrestrial temperature records (Rind and Peteet, 1985; Stute et al., 1995) and SST

reconstructions by coral records (Guilderson et al., 1994) all are of comparable magnitudes between the modern and the LGM tropical Atlantic Ocean.

Our paleo-environmental reconstruction admits us to distinguish two oceanic situations for the tropical Atlantic Ocean during the last 300 kyrs which both are of 23 kyrs and 100 kyrs cyclicity: (1) Cool water temperature, lower salinities and a somewhat higher nutrient supply corresponding to high loadings of the warm-transitional factor *G. bulloides* and *N. pachyderma*; and (2) warm and salty surface water masses with a deep thermocline indicated by high loadings of the subtropical-tropical factor as demonstrated by enhanced relative abundances and absolute numbers of *G. ruber, G. sacculifer* and *G. menardii* (Figs. 4, 5). That is, during glacials cool and nutrient-rich waters are advected off the eastern boundary, reach the equatorial Atlantic Ocean, and amplify cooling. Equatorial upwelling may be enhanced somewhat; however, the upwelling factor does not reach loadings that explain any significance. During interglacials the equatorial upwelling is moderate; cool water advection is weak or absent in the equatorial Atlantic Ocean. Mix and Morey (1996) who reconstructed Pleistocene variations in the Atlantic south equatorial current distinguished three significant factors. However, factor loadings indicate that upwelling and eastern boundary assemblages covary, and both upwelling and advection drive glacial cooling of the equatorial Atlantic Ocean.

*Assessment of the paleo-environmental reconstructions.* The modern sedimentary calcite lysocline at the core site is located at about 4,300 m (Dittert and Henrich, subm.) and the hydrographic calcite lysocline is not far above at about 4,150 m water depth (Bainbridge, 1981). How can we be sure that during the last 300 kyrs the lysocline did not raise and affect our samples by calcite dissolution biasing our paleo-environmental reconstructions? In the *South Atlantic Dissolution Experiment* (Dittert et al., subm.) we investigated some commonly used dissolution indices in a depth-transect of sediment surface samples to determine the qualitative and quantitative modification of these indices during increasing carbonate dissolution. Where the depth-transect crosses the calcite lysocline the corresponding value of each dissolution index yields an excellent calibration datum of the modern to the fossil situation. Applied to our down-core investigations, these indices reveal at which time the dissolution of sedimentary calcite increases (Fig. 6). In fact, the statements are not consistent. The ultrastructure investigations of *G. bulloides* (Fig. 6-A) show better preservation during glacials, whereas the $CaCO_3$ content and the Foraminiferal Dissolution Index (FDX) imply better preservation during interglacials (Figs. 6-B, E). Last not least, the rain ratio and the composition of assemblages >150 µm give no indication to enhanced dissolution at all (Figs. 6-D, E).

Enhanced calcite dissolution could be attributed to the productivity of marine organic

carbon in surface waters (Berger et al., 1994) which is supposed to be increased during glacials leading to intensified metabolic respiration (Emerson and Bender, 1981). Actually, the input of eolian terrigenous carbon contributes to the total organic carbon content (Verardo and Ruddiman, 1996; Wagner and Dupont, in press). Since it is inert, it is not available to calcite dissolution. On the other hand, enhanced calcite dissolution during interglacials could be attributed to maximum NADW production leading to enforced deep-water circulation (Gamboa et al., 1983). That is, the enhanced interchange between deep-water and sediment pore water might yield some calcite dissolution (Santschi et al., 1983; Le and Shackleton, 1992) which is monitored by the highly sensitive BDX (Dittert and Henrich, subm.). Regarding cross spectral analysis (Fig. 7), we can ascertain that there is a lack of coherent variations at the period of orbital tilt (41 kyrs) of the warm-transitional factor. As this period is clearly present in the oxygen isotope record, we infer that carbonate dissolution is not strongly affecting faunal investigations, because dissolution imparts a 41 kyrs rhythmic signal in calcite preservation indices similar to that of $\delta^{18}O$ in this region (Verardo and McIntyre, 1994; Mix and Morey, 1996).

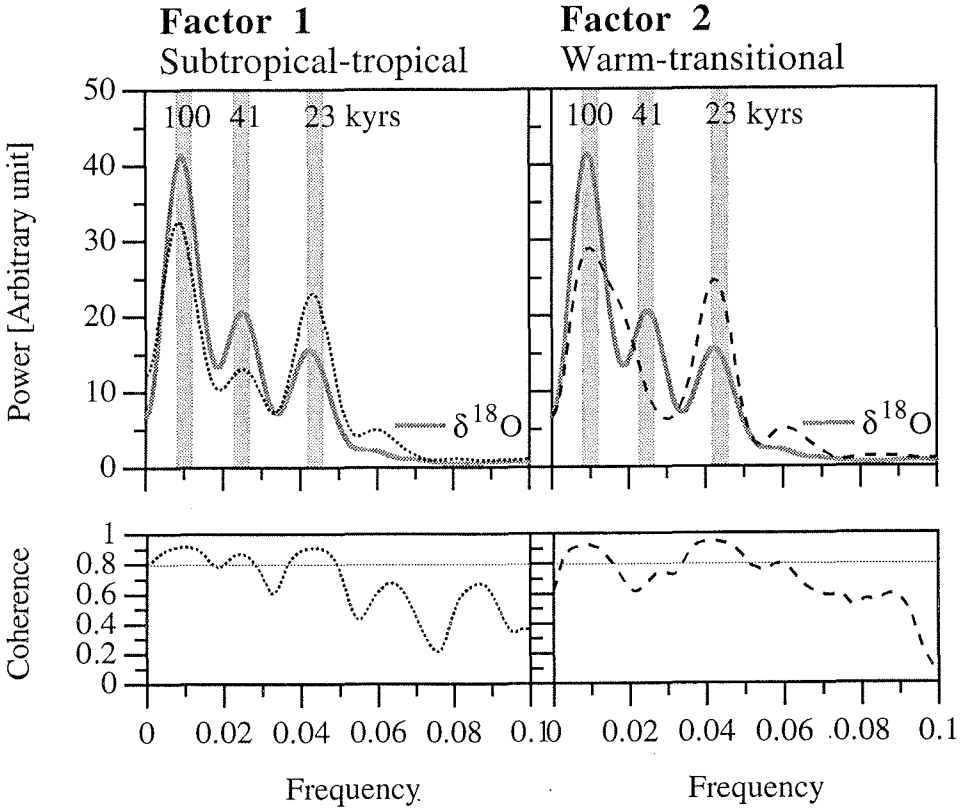


**Fig. 7:** Cross spectral analysis of the transfer function technique factors 1 and 2 showing cyclic variations within the main frequency domains of the earths orbital parameters (precession, obliquity, and eccentricity). Good significance is attained on coherence level >0.8; reference $\delta^{18}O$ is put to grey lines.

However, no index investigated gives clear evidence for such strong dissolution

increase which would be induced by the rise of the lysocline. That is, the site was dominated by the NADW influence during the last 300 kyrs, and the AABW never reached that location.

## 6. Conclusions

A sediment core of the equatorial Atlantic Ocean (GeoB 1117-2) was investigated in order to reconstruct the paleo-environmental development during the last 300 kyrs. All planktic foraminiferal assemblages are dominated by variations in the orbital eccentricity (100 kyrs) and precession (23 kyrs) periods, coherent with the global ice volume recorded in the $\delta^{18}O$ of the benthic foraminifera *Cibicides wuellerstorfi*. However, the 41 kyrs period (obliquity) is of minor importance. There is an obvious trend showing decreasing numbers of planktic foraminifera per gram sediment by about 50 % during the last 300 kyrs. Using a five-factor model, the transfer function technique displays two highly significant factors: (1) The subtropical-tropical factor which attains maximum loadings during all interglacials and the Holocene; (2) the warm-transitional factor which occurs with maximum loadings during glacial events; during the Holocene this factor almost expires. Highest estimated sea surface temperatures (SST's) are attained during interglacials, and lowest SST's occur during glacials. Glacial maxima are supposed to become warmer from oxygen isotope event 8.2 to 2.2 by about 2.5 °C. The difference between the modern and the Last Glacial Maximum SST amounts to about 6 °C for the central tropical South Atlantic. This temperature change is by some degrees higher than those reconstructed by CLIMAP. However, it is in accordance with most terrestrial and coral temperature records. Our paleo-environmental reconstruction admits us to distinguish two oceanic situations during the last 300 kyrs: During glacials, cool and nutrient-rich waters are advected off the eastern boundary, reach the equatorial Atlantic Ocean, and amplify cooling in this area. Equatorial upwelling may be enhanced somewhat; however, the upwelling factor does not reach loadings that explain any significance. During interglacials, the thermocline is deep and equatorial upwelling is only moderate. Cool water advection is weak or absent in the equatorial Atlantic Ocean.
In order to check the reliability of our paleo-environmental data on calcite dissolution, some commonly used dissolution indices were applied to the core sediments. Although there is some indication for worse calcite preservation, no index investigated gives evidence for a strong dissolution increase during the last 300 kyrs which would alter the planktic foraminiferal assemblages and hence would fake our paleo-reconstructions. These results corroborate earlier studies in the equatorial Atlantic (e.g., McIntyre et al., 1989; Mix and Morey, 1996; Kinkel et al., subm.).

**Acknowledgements**

We appreciate the kind assistance of the crews and masters of R/V METEOR on numerous cruises to The South Atlantic. The authors are indebted to P.J. Müller who kindly provided the carbonate and organic carbon data, to T. Bickert who supplied oxygen isotope and stratigraphy data, H. Heilmann, R. Henning, and C. Wienberg for marvellous technical collaboration. We are grateful to K.-H. Baumann, H. Kinkel, and H. Meggers for constructive comments. This investigation was funded by the Deutsche Forschungsgemeinschaft. This is SFB 261 contribution no. xxx at Bremen University.

## 7. References

Bainbridge, A.E., 1981. GEOSECS Atlantic Expedition, Hydrographic Data, 1972-1973. National Science Foundation, Superintendent of Documents, US Government Printing Office, Washington, DC, pp. 121.

Bé, A.W.H., 1977. An ecological, zoogeographic and taxonomic review of recent planktonic foraminifera. In: Ramsay, A.T.S. (Ed.) Oceanic Micropaleontology. Academic Press, London, 1, pp. 1-100.

Bé, A.W.H., Hutson, W.H., 1977. Ecology of planktonic foraminifera and biogeographic patterns of life and fossil assemblages in the Indian Ocean. Micropaleontology 23: 369-414.

Bé, A.W.H., Tolderlund, D.S., 1971. Distribution and ecology of living planktonic foraminifera in surface waters of the Atlantic and Indian Oceans. In: Funnell, B.M., Riedel, W.R. (Eds.), The micropaleontology of oceans. Cambridge University Press, Cambridge, pp. 105-149.

Berger, W.H., 1979. Preservation of foraminifera. In: Lipps, J.H., Berger, W.H., Buzas, M.A., Douglas, R.G., Ross, C.A. (Eds.), Foraminiferal ecology and palecology. Society of Economic Paleontologists and Mineralogists, Houston, 6, pp. 105-155.

Berger, W.H., Herguera, J.C., Lange, C.B., Schneider, R., 1994. Paleoproductivity: Flux proxies versus nutrient proxies and other problems concerning the quaternary productivity record. In: R. Zahn, e.a. (Ed.) Carbon cycling in the glacial ocean: Constains on the ocean´s role in global change. (NATO ASI Series) Springer-Verlag, Berlin Heidelberg, 117, pp. 385-412.

Berger, W.H., Keir, R.S., 1984. Glacial-Holocene changes in atmospheric $CO_2$ and the deep-sea record. In: Hansen, J.E., Takahashi, T. (Eds.), Climate processes and climate sensitivity. Geophys. Monogr. 29, Maurice Ewing Series, Washington, DC, 5, pp. 337-351.

Berger, W.H., Killingley, J.S., Metzler, C.V., Vincent, E., 1985. Two-step deglaciation: $^{14}C$-dated high-resolution $\delta^{18}O$ records from the tropical Atlantic Ocean. Quat. Res. 23: 258-271.

Bickert, T., Cordes, R., Wefer, G., 1997. Late Pliocene to Mid-Pleistocene (2.6-1.0 M.Y.) carbonate dissolution in the western equatorial Atlantic: Results of Leg 154, Ceara Rise. Proc. ODP, Sci. Results 154: 229-237.

Bickert, T., Wefer, G., 1996. Late Quaternary deep water circulation in the South Atlantic: Reconstruction from carbonate dissolution and benthic stable isotopes. In: Wefer, G., Berger, W.H., Siedler, G., Webb, D.J. (Eds.), The South Atlantic: Present and past circulation. Springer-Verlag, Berlin Heidelberg, pp. 599-620.

Boyle, E.A., 1988. Vertical oceanic nutrient fractionation and glacial/interglacial $CO_2$ cycles. Nature 331: 55-56.

Brummer, G.J.A., Kroon, E., 1988. Genetically controlled planktonic foraminiferal coiling ratios as tracers of past ocean dynamics. In: Brummer, G.J.A., Kroon, E. (Eds.), Planktonic foraminifers as tracers of ocean-climate history: Ontogeny, relationships and preservation of modern species and stable isotopes, phenotypes and assemblage distribution in different watermasses. Free University Press, Amsterdam, pp. 293-298.

Cane, M.E., 1979. The response of an equatorial ocean to simple wind stress patterns: II. Numerical results. J. Mar. Res. 37: 253-299.

CLIMAP Project members, 1976. The surface of the ice-age earth. Science 191: 1131-1137.

CLIMAP Project members, 1981. Seasonal Reconstructions of the Earth's Surface at the last glacial maximum. Geol. Soc. Am. Bull., MC Series 36: 1-18.

CLIMAP Project members, 1984. The last interglacial ocean. Quat. Res. 21: 123-224.

CLIMAP Project members, 1994. CLIMAP 18k database. IGBP Pages/World Data Center-A for paleoclimatology data contribution series #94-NOAA/NGDC Paleoclimatology Program, Boulder, CO.

Seasonal Reconstructions of the Earth's Surface at the last glacial maximum. Geol. Soc. Am. Bull., MC Series 36: 1-18.

Curry, W.B., Lohmann, G.P., 1990. Reconstructing past particle fluxes in the tropical Atlantic Ocean. Paleoceanography 5: 487-506.

Curry, W.B., Oppo, D.W., 1997. Synchronous, high frequency oscillations in tropical sea surface temperatures and North-Atlantic Deep Water production during the last glacial cycle. Paleoceanography 12: 1-14.

Davis, J.C., 1986. Statistics and data analysis in geology. John Wiley & Sons, New York, NY, pp. 646.

Diester-Haass, L., Rothe, P., 1987. Plio-Pleistocene sedimentation on the Walvis Ridge, Southeast Atlantic (DSDP Leg 75, Site 532) - Influence of surface currents, carbonate dissolution and climate. Mar. Geol. 77: 53-85.

Dittert, N., Baumann, K.-H., Bickert, T., Henrich, R., Huber, R., Kinkel, H., Meggers, H., subm. Carbonate dissolution in the deep sea: Methods, quantification and paleoceanographic application. In: Fischer, G., Wefer, G. (Eds.), Proxies in paleoceanography. Springer-Verlag, Berlin Heidelberg,.

Dittert, N., Henrich, R., subm. Carbonate dissolution in the South Atlantic Ocean: Evidence by *Globigerina bulloides* ultrastructure breakdown. Deep-Sea Res.

Emerson, S., Bender, M., 1981. Carbon fluxes at the sediment-water interface of the deep-sea: Calcium carbonate preservation. J. Mar. Res. 39: 139-162.

Emiliani, C., 1955. Pleistocene temperatures. J. of Geology 63: 538-578.

Ericson, D.B., Wollin, G., 1968. Pleistocene climates and chronology in deep-sea sediments. Science 162: 1227-1234.

Farrell, J.W., Prell, W.L., 1989. Climatic change and $CaCO_3$ preservation: An 800,000 year bathymetric reconstruction from the central equatorial Pacific Ocean. Paleoceanography 4: 447-466.

Gamboa, L.A.P., Archer, R.T., Barker, P.F., 1983. Seismic stratigraphy and geologic history of the Rio Grande Gap and southern Brazil Basin. DSDP, Initial Reports 72: 481-498.

Ganssen, G., 1983. Dokumentation von küstennahem Auftrieb anhand stabiler Isotope in rezenten Foraminiferen vor Nordwest-Afrika. "Meteor" Forsch.-Ergebn. C 37: 1-46.

Guilderson, T.P., Fairbanks, R.G., Rubenstone, J.L., 1994. Tropical temperature variations since 20,000 years ago; modulating interhemispheric climate change. Science 263: 663-665.

Hemleben, C., Spindler, M., Anderson, O.R., 1989. Modern planktonic foraminifera. Springer-Verlag, New York, NY, pp. 363.

Imbrie, J., Kipp, N.G., 1971. A new micropaleontological method for quantitative paleoclimatology: application to a Late Pleistocene Carribean core. In: Turekian, K.K. (Ed.) Late Cenocoic glacial ages. (Memorial Lectures) Yale University Press, New Haven, 43, pp. 71-181.

Kinkel, H., Dittert, N., Henrich, R., subm. Calcareous plankton record of the Equatorial Atlantic: A 300 kyrs record of climate feedback, productivity and dissolution. Palaeogeogr., Palaeoclimatol., Palaeoecol.

Kipp, N.G., 1976. New transfer function for estimating past sea-surface conditions from sea bed distribution of planktonic foraminiferal assemblages in the North Atlantic. Geol. Soc. Am. Mem. 145: 3-42.

Kroopnick, P.M., 1985. The distribution of $^{13}C$ of $\Sigma CO_2$ in the World Oceans. Deep-Sea Res. 32: 57-84.

Le, J., Shackleton, N.J., 1992. Carbonate dissolution fluctuations in the western equatorial Pacific during the Late Quaternary. Paleoceanography 7: 21-42.

Levitus, S., Boyer, T., 1994. World Ocean Atlas 1994 Volume 4: Temperature. NOAA Atlas NESDIS 4: http://ingrid.ldgo.columbia.edu/SOURCES/.LEVITUS94/.

Malmgren, B.A., Haq, B.U., 1982. Assessment of quantitative techniques in paleobiogeography. Mar. Micropal. 7: 213-236.

McIntyre, A., Ruddiman, W.F., Karlin, K., Mix, A.C., 1989. Surface water response of the equatorial Atlantic Ocean to orbital forcing. Paleoceanography 4: 19-55.

Mix, A.C., 1989. Influence of productivity variations on long-term atmospheric $CO_2$. Nature 337: 541-544.

Mix, A.C., Morey, A.E., 1996. Climate feedback and Pleistocene variations in the Atlantic south equatorial current. In: Wefer, G., Berger, W.H., Siedler, G., Webb, D.J. (Eds.), The

South Atlantic: Present and past circulation. Springer-Verlag, Berlin Heidelberg, pp. 503-525.

Mix, A.C., Ruddiman, W.F., McIntyre, A., 1986a. Late Quaternary paleoceanography of the tropical Atlantic 1: Spatial variability of annual mean sea-surface temperatures, 0-20,000 Years B.P. Paleoceanography 1: 43-66.

Mix, A.C., Ruddiman, W.F., McIntyre, A., 1986b. Late Quaternary paleoceanography of the tropical Atlantic 2: The seasonal cycle of sea-surface temperatures, 0-20,000 Years B.P. Paleoceanography 1: 339-353.

Molfino, B., McIntyre, A., 1990. Precessional forcing of nutricline dynamics in the equatorial Atlantic. Science 249: 766-769.

Moore, D.W., Hisard, P., McCreary, J., Merle, J., O'Brien, J., Picaut, J., Verstraete, J., Wunsch, C., 1978. Equatorial adjustment in the eastern Atlantic. Geophys. Res. Lett. 5: 638-640.

Murray, J., 1897. On the distribution of the pelagic foraminifera at the surface and on the floor of the ocean. Nat. Sci. 11: 17-27.

Niebler, H.-S., Gersonde, R., 1998. A planktic foraminiferal transfer function for the southern South Atlantic Ocean. Mar. Micropal. in press.

Niebler, H.-S., Salvignac, M.-E., Duprat, J., Gersonde, R., Sieger, R., Labracherie, M., in prep. Planktic foraminifers in deep-sea sediments: Different size-fraction delimitations to estimate paleotemperatures.

Oberhänsli, H., Bénier, C., Meinecke, G., Schmidt, H., Schneider, R., Wefer, G., 1992. Planktonic foraminifera as tracers of ocean currents in the eastern South Atlantic. Paleoceanography 7: 607-632.

Olbers, D., Gouretski, V., Seib, G., Schröter, J., 1982. Hydrographic atlas of the Southern Ocean. Alfred Wegener Institute for Polar and Marine Research, Bremerhaven, pp. 82.

Ottens, J.J., 1992. Planktic foraminifera as indicators of ocean environments in the Northeast Atlantic. FEBO B.V., Enschede, pp. 189.

Paillard, D., Labeyrie, L., Yiou, P., 1996. Macintosh program performs time-series analysis. AGU 379.

Parker, L.F., Berger, W.H., 1971. Faunal and solution patterns of planktonic foraminifera in surface sediments of the South Pacific. Deep-Sea Res. 18: 73-107.

Pflaumann, U., 1985. Transfer-function '134/6' - a new approach to estimate sea-surface temperatures and salinities of the eastern North Atlantic from the planktonic foraminifers in the sediment. "METEOR" Forsch.-Ergebnisse C: 37-71.

Pflaumann, U., Duprat, J., Pujol, C., Labeyrie, L.D., 1996. SIMMAX: A modern analog technique to deduce Atlantic sea surface temperatures from planktonic foraminifera in deep-sea sediments. Paleoceanography 11: 15-35.

Philander, S.G.H., 1979. Variability of the tropical oceans. Dynamics of Atmospheres and Oceans 3: 191-208.

Philander, S.G.H., 1986. Unusual conditions in the tropical Atlantic Ocean in 1984. Nature 322: 236-238.

Philander, S.G.H., Pacanowski, R.C., 1986. A model of the seasonal cycle in the tropical

Atlantic Ocean. J. Geophys. Res. 91: 14192-14206.

Ravelo, A.C., Fairbanks, R.G., Philander, S.G.H., 1990. Reconstructing tropical Atlantic hydrography using planktonic foraminifera and an ocean model. Paleoceanography 5: 409-431.

Rind, D., Peteet, D.M., 1985. Terrestrial conditions at the last glacial maximum and CLIMAP sea-surface temperature estimates; are they consistent? Quat. Res. 24: 1-22.

Santschi, P.H., Bower, P., Nyffeler, U.P., Azevedo, A., Broecker, W.S., 1983. Estimates of the resistance to chemical transport posed by the deep-sea benthic boundary layer. Limnol. Oceanogr. 28: 899-912.

Sautter, L.R., Thunell, R.C., 1991. Seasonal variability in the $\delta^{18}O$ and $\delta^{13}C$ of planktonic foraminifera from an upwelling environment: Sediment trap results from the San Pedro Basin, Southern California Bight. Paleoceanography 6: 307-334.

Schott, W., 1935. Die Foraminiferen in dem Äquatorialen Teil des Atlantischen Ozeans. Wiss. Ergebn. d. Deutschen Atl. Exp. Meteor 1925-1927 3: 1-135.

SPECMAP, A.N.1., 1989/90. Compiled by Duffy, A., Imbrie, J., Mix, A. C. and McIntyre, A. NSF SPECMAP Project, Brown University, Providence, Rhode Island: 1.4 Mega Bytes.

Stute, M., Forster, M., Frischkorn, H., Serejo, A., Clark, J.F., Schlosser, P., Broecker, W.S., Bonani, G., 1995. Cooling of Tropical Brazil (5°C) during the Last Glacial Maximum. Science 269: 379-383.

Van Leeuwen, R.J.W., 1989. Sea-floor distribution and Late Quaternary faunal patterns of planktonic and benthic foraminifers in the Angola Basin. Utrecht Micropal. Bull. 38: 287.

Verardo, D.J., McIntyre, A., 1994. Production and destruction: Control of biogenous sedimentation in the tropical Atlantic 0-300,000 years B.P. Paleoceanography 9: 63-86.

Verardo, D.J., Ruddiman, W.F., 1996. Late Pleistocene charcoal in tropical Atlantic deep-sea sediments: Climatic and geochemical significance. Geology 24: 855-857.

Vincent, E., Berger, W.H., 1981. Planktonic foraminifera and their use in paleoceanography. In: Emiliani, C. (Ed.) The oceanic lithosphere. John Wiley & Sons, New York, NY, 7, pp. 1025-1119.

Wagner, T., Dupont, L., in press. Terrestrial OM in marine sediments: analytic approaches and eolian-marine records of the central Equatorial Atlantic. In: Fischer, G., Wefer, G. (Eds.), Proxies in paleoceanography. Springer-Verlag, Berlin Heidelberg, pp.

Wefer, G., Bleil, U., Schulz, H.D., cruise participants, 1989. Bericht über die Meteor-Fahrt M9-4, Dakar-Santa Cruz, 19.2.-16.3.1989. Ber. Fachbereich Geowiss., Univ. Bremen 7: 1-103.

Wolff, T., Mulitza, S., Arz, H., Pätzold, J., Wefer, G., subm. Oxygen isotopes versus CLIMAP (18ka) temperatures: A comparison from the tropical Atlantic. Geology.

Wüst, G., 1935. Schichtung und Zirkulation des atlantischen Ozeans. Dtsch. Atlant. Exp. "Meteor", 1925-1927, Wiss. Ergeb. 2.

# 2. Calcareous plankton record in the Equatorial Atlantic: A 300 kyrs record of climate feedback, productivity and dissolution

Hanno Kinkel, Nicolas Dittert, and Rüdiger Henrich

*FB Geowissenschaften, Universität Bremen, Postfach 330 440, D-28334 Bremen, Germany*

## Abstract

A sediment core from the southern equatorial Atlantic (GeoB 1117-2) was investigated to reconstruct the surface water circulation and its impact on productivity of calcareous plankton (planktic foraminifera and coccolithophores) during the last 300 kyrs.

The floral and faunal records show significant changes in surface water circulation which can be attributed (1) to advection of cool and nutrient rich water masses from higher latitudes and (2) to equatorial upwelling intensity. Cross-spectral analysis revealed that both processes show cyclic variations within the orbital frequency domains of eccentricity and precession, and to a minor degree within the obliquity band.

Since the sediment core is situated just about the modern lysocline, carbonate dissolution due to an reduction in NADW (North Atlantic Deep Water) production and stronger influence of AABW (Antarctic Bottom Water) is likely to have influenced carbonate sedimentation during peak glacials.

While the floral and faunal assemblages seem to be robust and only slightly affected by carbonate dissolution, the total numbers of planktic foraminifera and coccoliths, which should provide us with information on the productivity of calcareous plankton, partly seem to be biased by carbonate dissolution.

*Keywords:* calcareous nannoplankton; planktic foraminifera; paleoceanography; South Atlantic Ocean

## 1. Introduction

Surface water circulation and productivity changes in the equatorial Atlantic have been

the focus of numeral studies (McIntyre et al., 1989; Mix, 1989; Molfino and McIntyre, 1990; Struck et al., 1993; Sikes and Keigwin, 1994; McIntyre and Molfino, 1996; Mix and Morey, 1996; Schneider et al., 1996). Usually stable isotopes, planktic foraminifera and calcium carbonate or organic carbon records are used to reconstruct the paleoceanography of the equatorial Atlantic.

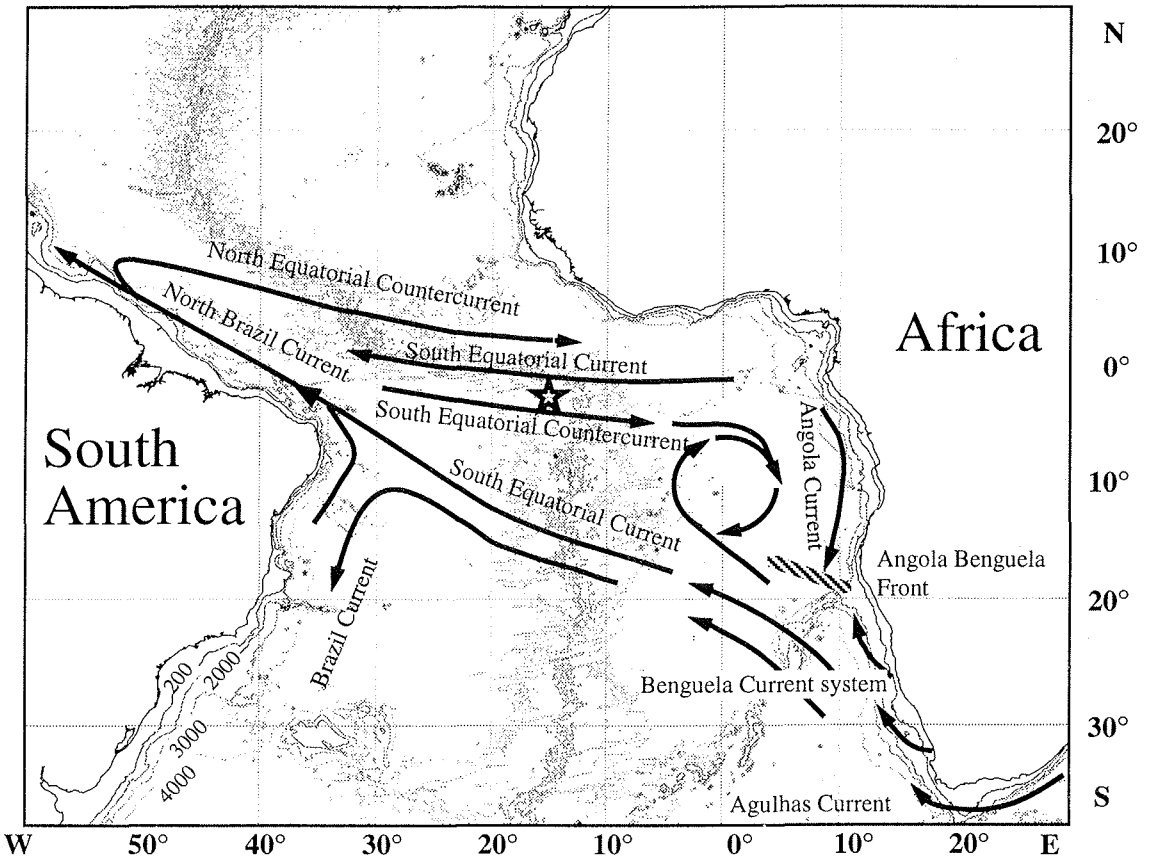


**Fig. 1:** Position of the sediment core GeoB 1117-2 and a sketch of the surface water circulation pattern, adapted from various authors.

The tropical Atlantic is a key area for understanding global thermohaline circulation as it transfers huge amounts of heat from the Southern to the Northern Hemisphere (Gordon, 1986; Gordon, 1996; Macdonald and Wunsch, 1996). Additionally, the equatorial upwelling area, associated with the South Equatorial Current, is a highly productive regime which contributes significantly to the global export productivity (Berger et al., 1989). Nowadays it may not be as productive in terms of carbon produced per area compared to the highly productive areas as the North Atlantic where massive blooms occur regularly or the intensive upwelling zones of the continental margins along the eastern boundary currents. Since the tropical oceans cover by far the largest area, their contribution to the global carbon cycle is important (Longhurst, 1993; Monger et al., 1997). It was suggested that an increase in paleoproductivity in the equatorial Atlantic is

likely to influence the global atmospheric $CO_2$ concentration as recorded in ice core inclusions (Mix, 1989; Struck et al., 1993; Mix and Morey, 1996).

Calcareous plankton contributes largely to the particle flux in the investigated area (Fischer and Wefer, 1996), thus, its sedimentary record should provide information on the productivity changes in the past. Yet, we have to keep in mind that the calcium carbonate record in the tropical Atlantic is susceptible to carbonate dissolution reflecting the glacial- interglacial fluctuations of deep-water circulation patterns (Verardo and McIntyre, 1994; Bickert and Wefer, 1996).

We have chosen a sediment core (GeoB 1117-2; 3°34'S - 14°54'W, 3,984 m; Fig. 1) from the southern rim of today's equatorial upwelling system and situated above the modern Carbonate Compensation Depth (CCD). Both surface- and deep-water circulation patterns are considered to have experienced significant changes during the last 300 kyrs in concert with global climate changes.

We present data of the two dominant calcareous plankton groups, planktic foraminifera and coccolithophores, to reconstruct their faunal and floral response to changing surface water circulation as well as their productivity record.

## 2. Present and past equatorial Atlantic oceanography

### *2.1. Surface water circulation*

The surface water oceanography of the equatorial Atlantic is characterized by the westward flowing South Equatorial Current (SEC) and the eastward flowing South Equatorial Counter Current (SECC), the North Equatorial Current (NECC) and the Equatorial Undercurrent (EUC). The westward flow of the SEC is mainly controlled by the intensification of westward directed tradewinds in boreal spring in the western tropical Atlantic (Philander and Pacanowski, 1986). This causes a massive transport of warm surface waters from the eastern tropical Atlantic, one of the major pathways of oceanic heat transport to the northern hemisphere within the Atlantic. As a result of the wind induced westward flow of the SEC, the thermocline is uplifted in the eastern tropical Atlantic and a corresponding deepening is observed in the western tropical Atlantic. The seasonal uplift of the thermocline which is at its maximum in boreal summer causes an elevated nutrient flux, which results in a productivity increase within the photic zone. Besides thermocline uplift, additional nutrient flux to the photic zone results from the a wind driven equatorial divergence and shear mixing between the EUC and the SEC. During boreal autumn the thermocline has returned to its pre-upwelling state. More recently a comprehensive summary between the physical ocean dynamics and the

observed phytoplankton response in the Equatorial Atlantic was given by Monger et al. (1997).

This seasonal cycle in the surface water circulation of the equatorial Atlantic is an analogon for long-term variations by the precessional component of orbital forcing (Molfino and McIntyre, 1990). Perihelion centered on boreal winter (December) is equivalent to maximum divergence, while perihelion centered on boreal summer is equivalent to minimum divergence (McIntyre et al., 1989). The intensified heating of the African continent during June perihelion causes an uplift of air and relative low pressure in this region. As a result, a monsoonal effect is caused with meridional winds from the south.

The importance of the equatorial Atlanticís surface water circulation for northward directed heat transport is a key for reconstructing and modeling past global climates (Webb et al., 1997). Discrepancies between the SST reconstruction for the tropical Atlantic (CLIMAP, 1981; 1984; Sikes and Keigwin, 1994) and terrestrial temperature records (Rind and Peteet, 1985; Stute et al., 1995) caused serious obstacles, as the significantly lowered temperatures on land (about 5 °C) and small changes in SST (<2 °C) in the tropics could not be explained by a conclusive model. More recently, CLIMAP's SST reconstructions were challenged by coral records from the Atlantic (Guilderson et al., 1994) as well as from the Pacific (Beck et al., 1997) which had the same magnitude as the terrestrial temperature records.

### *2.2. Deep-water circulation*

Today, the circulation in the deep South Atlantic Ocean is dominated by interactions between the AABW and the NADW in contrasting extent. NADW is indicated by oxygen enriched, nutrient depleted water masses of high $CO_3^{2-}$ and low $CO_2$ contents. AABW can be distinguished as an extremely cold, oxygen depleted and nutrient enriched water mass of low $CO_3^{2-}$ and high $CO_2$ contents (Kroopnick, 1985; Boyle, 1988). Today's mixing zone between AABW and NADW in the South Atlantic is close to the 90 µmol/kg $CO_3^{2-}$ isopleth (Bainbridge, 1981). The relatively warm and saline NADW occupies the depth interval between 2,000 m and 4,000 m, while below 4,000 m AABW is encountered. With respect to the modern South Atlantic Ocean, the border of AABW with NADW and the hydrographic lysocline coincide (Bickert and Wefer, 1996). Since the production of NADW is thought to be reduced during glacials periods (Curry and Oppo, 1997), the lysocline will rise in the Brazil Basin leading to an increase in carbonate dissolution (Bickert and Wefer, 1996).

## 3. Material and methods

The gravity core was retrieved from the ocean floor during R/V METEOR cruise M9-4 (Wefer et al., 1989). In addition, a giant box corer was retrieved and sampled to achieve an undisturbed sediment surface which usually is not the case in the gravity core. To achieve a composite record all sediment parameters were used.

### *3.1. Stratigraphy*

Stable oxygen and carbon isotopes of the epibenthic foraminifera *Cibicides wuellerstorfi* were analyzed at the University of Bremen (Bickert, 1992). All samples were analyzed using Finnigan MAT 251 micromass spectrometer coupled with a Finnigan automated carbonate device. The reproducibility of the measurements, as referred to an internal carbonate standard (Solnhofen limestone), is ±0.07 ‰. The conversion to the PDB - scale was performed using the international standards NBS 18, 19 and 20. To achieve a complete time series a composite record was established using all sediment parameters measured in the sediment sequences, in the giant box corer, and the gravity core. The age model is based on the graphic correlation between the $\delta^{18}O$ record of the core and the SPECMAP standard record (Imbrie et al., 1984).

### *3.2. Sedimentation and mass accumulation rates*

Except transfer functions (Mix, 1989; Lebreiro et al., 1997) all methods for reconstructing paleoproductivity are based on mass accumulation rates of bulk parameters. Sedimentation rates were determined by linear interpolation between age control points of the $\delta^{18}O$ record and the SPECMAP stack (Bickert, 1992). To elucidate the paleofluxes of various sediment components like calcium carbonate, organic carbon, planktic foraminifera, and coccolithophores, it is necessary to calculate their accumulation rates (AR). AR was calculated after the method of van Andel et al. (Van Andel et al., 1975). The accuracy of AR strongly depends on the preciseness of the age model applied. The correlation coefficient between the oxygen isotope record in core GeoB 1117-2 and the SPECMAP standard record is extremely high ($r^2>0.98$). Nevertheless, there are a few outstanding maxima in sedimentation rates (Fig. 2) which are far above the expected variance. Since these maxima are also observed in the global distributed sediment cores that were used for the standard records, it is likely that they are artefacts due to a non-linear climate response to orbital forcing (Bickert, 1992).

### 3.3. Planktic foraminifera

For foraminiferal counts, samples were freeze-dried, weighed, and washed through a 63 µm sieve under a gentle spray of water to prevent mechanical fragmentation. We base the faunal analysis on the fraction >150 µm according to the CLIMAP-conventions. After separating the fraction <150 µm, the samples were dry-sieved on a 212 µm, 355 µm, 500 µm, and 1,000 µm sieve-set in order to minimize sorting and to simplify counting. Each fraction was repeatedly split into subsamples using a microsplitter to obtain an aliquot of at least 300 non-fragmented planktic foraminiferal specimens (CLIMAP, 1984) which were identified and counted completely using an OLYMPUS SZ 40 binocular at 20× to 80× magnification. The taxonomy used follows that of Hemleben et al. (1989). Planktic foraminifera fragments, benthic foraminifera, radiolaria, and subordinately pteropods, rock fragments, and indeterminable particles were also counted on the same aliquot. All fauna-counts were converted into count percent and number of organisms per gram sediment (Mix, 1989).

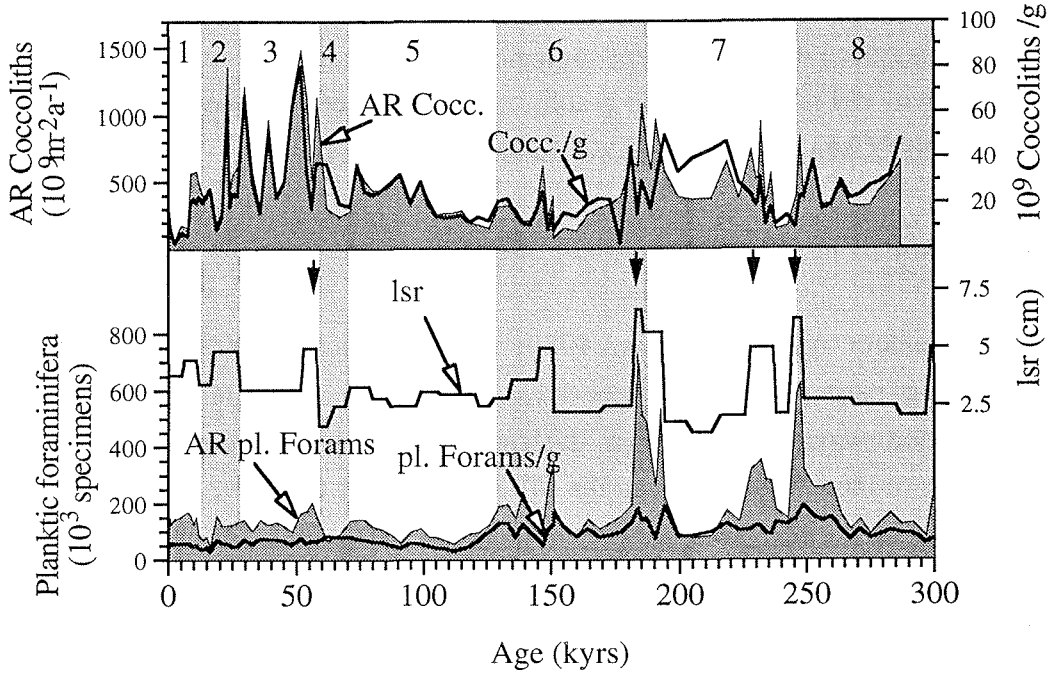


**Fig. 2:** Downcore distribution of the absolute numbers of coccoliths per gram sediment, coccolith accumulation rate, absolute numbers and accumulation rates of planktic foraminifera and the linear sedimentation rates (from Bickert, 1992).

### 3.4. Coccoliths

For preparation of sediment samples a combined dilution/filtering technique as described by (Andruleit, 1996) was used. A small amount of sediment was weighed and

brought into suspension. After dilution with a rotary splitter, the suspension was filtered through polycarbonate membrane filters (Schleicher&Schuell™, 50 mm diameter, 0.4 µm pore size). A monolayer of all sediment particles was successively studied by SEM. All coccoliths were recorded in numbers per gram dry sediment. In general, the taxonomy of Jordan and Kleijne (1994) was used.

Coccolith numbers were then converted to coccosphere units, assuming that coccospheres of *E. huxleyi* are covered by 24 coccoliths; coccospheres of the genus *Gephyrocapsa* bear 14 coccoliths, and coccospheres of *F. profunda* carry 75 coccoliths. This data contain own observations on living coccolithophores from the South Atlantic as well as from various other sources (e.g., Knappertsbusch, 1993; Young, subm.). Although it is known that the number of coccoliths per coccosphere is not constant, and that especially *E. huxleyi* is known to produce multiple layers of coccoliths and even to shed coccoliths during its life cycle, these values seem to be a reasonable average.

### *3.5. Spectral analysis*

We performed spectral analysis with the software package "AnalySeries 1.1" (Paillard et al., 1996). The analyzed timeseries were evenly resampled at 3 kyr intervals and linearly detrended. As a record of global ice volume, we used the $\delta^{18}O$ signal of the benthic foraminifer *C. wuellerstorfi* of the same core (Bickert and Wefer, 1996).

### *3.6. Carbonate and carbon content*

Calcium carbonate and organic carbon contents of the bulk sediment were determined with a Leco - CS 244. Therefore, 100 mg of freeze-dried and homogenized sediment was analyzed. For determination of the organic carbon content, the same amount of sediment was acidified with 6n HCl and measured the same way. The carbonate content is calculated by subtracting the organic carbon content from the total carbon content.

## 4. Results

### *4.1. Planktic foraminifera*

The absolute number of planktic foraminifera per gram sediment varies from 27,000 to 191,000 specimens. Maximum numbers occur at the transition of isotope stages 8/7 and at the oxygen isotope events 7.1, 6.6, 6.4; minimum numbers occur at isotope events 6.3, 5.4, and 2.1. Relative abundances and absolute numbers of planktic foraminifera

show a distinct orbital-to-suborbital modification. Moreover, there is an obvious trend from 110,000 (300 ka) to 54,000 (Recent) planktic foraminifera per gram sediment.

The subtropical representative *G. ruber* (pink and white variety; 3 - 43 %) attains maxima at interglacial maxima, particularly at isotope stages 7, 5, and during the Holocene. Among the subpolar species, *N. pachyderma* dex. (0 - 49 %) has its maximum occurrence during the glacial maxima of isotope stage 8 and the isotope event 7.4; its abundance subsequently lowers. It is nearly absent during the Holocene. *Neogloboquadrina pachyderma* sin. (0 - 5 %) almost exclusively occurs at full glacial conditions. It is absent during the Holocene (cf. Dittert et al., subm.).

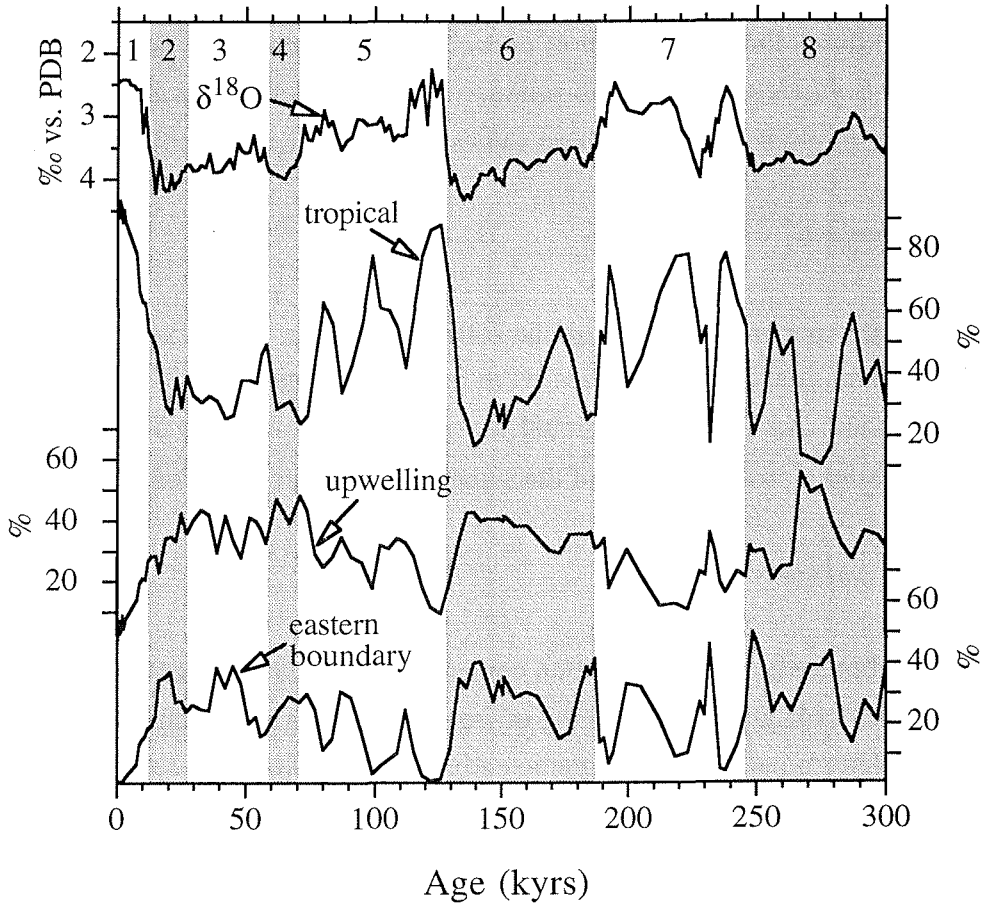


**Fig. 3:** Downcore distribution of the planktic foraminifera assemblages according to Mix and Morey (1996), species composition of the assemblages is listed in Table 1.

Mix and Morey (1996) distinguished three assemblages of planktic foraminifera, based on down core factor analysis of a set of sediment cores from the tropical Atlantic and Pacific Ocean. The use of down core sediment samples rather than surface sediment samples was chosen to avoid "no-analogue" situations, which are a general problem of modern analog and transfer techniques applied to foraminiferal counts. The three

assemblages are defined as: 1) warm-tropical-, 2) upwelling-, and 3) the eastern boundary assemblage. These assemblages are related to the major surface circulation processes in the tropical Atlantic. The first assemblage is representative for warm surface water masses with a deep thermocline; the second is attributed to an upwelling intensity with a shallow thermocline and reduced surface water temperature, whereas the third assemblage reflects the advection of cold and nutrient rich water masses via the eastern boundary currents.

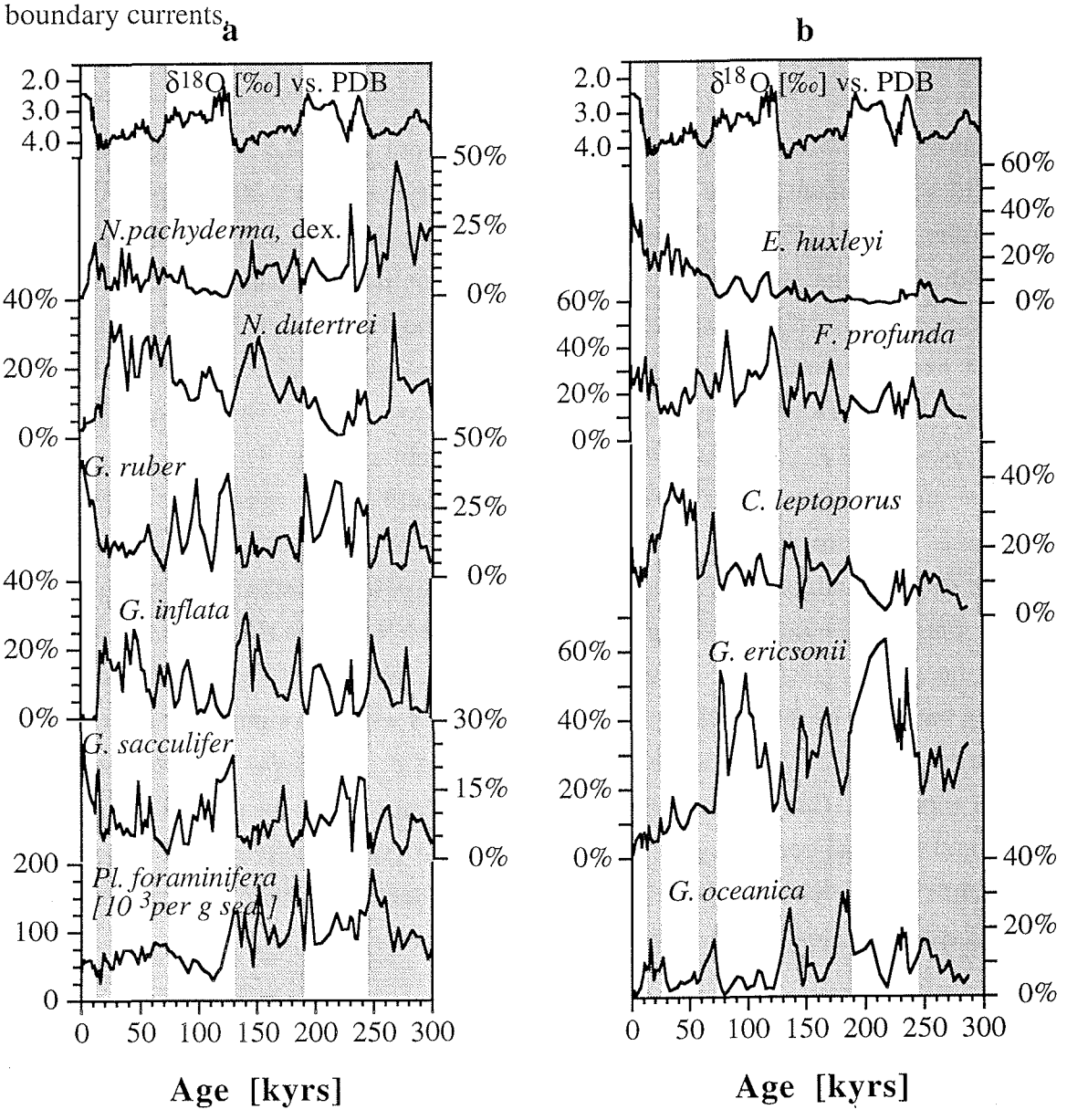


**Fig. 4:** Downcore distribution of the relative abundance of the most common coccolithophore and planktic foraminifera species. Mind the different scales!

Highest abundance of the tropical group occurs in isotope stages 7, 5, and during the Holocene which corresponds up to 96 % of the whole assemblage (Fig. 3). Lowest

values in general occur during all glacials stages and substages. The upwelling assemblage has maximum abundances in isotope stages 8, 6, and 4 which corresponds up to 55 % of the total assemblage (Fig.3). Minimum values occur during interglacials. The eastern boundary assemblage amounts up to 50.2 % of the total assemblage in isotope stage 8.1. Minimum values occur in isotope stage 5.5 and during the Holocene (Fig. 3).

### *4.2. Coccoliths*

Coccolith numbers in core GeoB 1117-2 vary from about 2.5 x $10^9$ up to 80 x $10^9$ coccoliths/g sediment, while accumulation rates vary from 60 x $10^9$ up to 1,500 x $10^9$ coccoliths $m^{-2}$ $a^{-1}$ (Fig. 2). In general, variability in numbers of coccoliths resemble coccolith accumulation rates, with slight disagreement in isotope stage 4 and more larger disagreements in early isotope stage 6 and throughout stage 7. Highest numbers and highest accumulation rates occur during isotope stage 2 and 3. Lowest values are indicative for the Holocene as well as for oxygen isotope stage 5. During isotope stage 5 *G. ericsonii* and *F. profunda* dominate the assemblage (Fig. 4). Here, *G. ericsonii* reaches abundances of up to 54 %, while it shows subordinate abundance in Holocene sediments. A sharp drop in the abundance of this species is observed at the oxygen isotope stage boundary 5/4. Contemporaneously relative abundances of *E. huxleyi* began to rise until they reach their maximum values of 44 % in the Holocene. In addition, abundances of *F. profunda* show a cyclic variation throughout the record with values varying between 10 % and 48 %. Highest abundances with two significant peaks appear in isotope stage 5. In general, lower abundances of *F. profunda* are observed in the glacial intervals. *Calcidiscus leptoporus* reach almost 40 % in isotope stage 3, and additional maxima occur in glacial stages 6 and 4. A similar pattern can be seen in the abundance of *G. oceanica* which reveals significant maxima up to 26 % in glacial stages 6, 4, 2, and subordinate abundances in the rest of the record.

## 5. Discussion

Planktic foraminifera and coccoliths are the major components of the sediments in the investigated core, whereas siliceous microfossils (e.g. diatoms) are only a subordinated component (Gingele, 1992). Terrigenous sediments, in general eolian transported fine (< 2 μm) and silt fraction (<63 μm), can reach 25 wt.-% of the total sediment in glacial periods (Gingele and Dahmke, 1994). Although these high percentages correlate well with low carbonate contents, and therefore a concentration effect due to carbonate

dissolution may be assumed, a two- to threefold increase in accumulation rates of terrigenous matter indicates stronger eolian transport during glacials, which has been reported by various authors from nearby sediment cores (Gingele, 1992; deMenocal et al., 1993; Ruddiman, 1997).

Since Imbrie and Kipp (1971) used planktic foraminifera to reconstruct past sea surface temperatures, a lot of authors turned to that method with different approaches (Mix et al., 1986a; 1986b; Pflaumann et al., 1996). Although the reliability of these methods increased with the growing numbers of calibration points (core top samples), the problem of "no-analogue" situations (Hutson, 1977) remained; a problem, that is unfortunately very apparent in the tropical oceans (Mix et al., 1986a; 1986b; Ravelo et al., 1990). Mix and Morey (1996) tried to avoid this problem by investigating planktic foraminiferal assemblages from a set of downcore samples from sites in the tropical Atlantic and Pacific Ocean instead of investigating surface sediments or core tops. This approach resulted in the establishment of three planktic foraminifera assemblages which allow to deduce long-term variations of the equatorial current system, as proposed before by Ravelo et al. (1990). Moreover these three assemblages are supposed to be insensitive to carbonate dissolution (Mix and Morey, 1996).

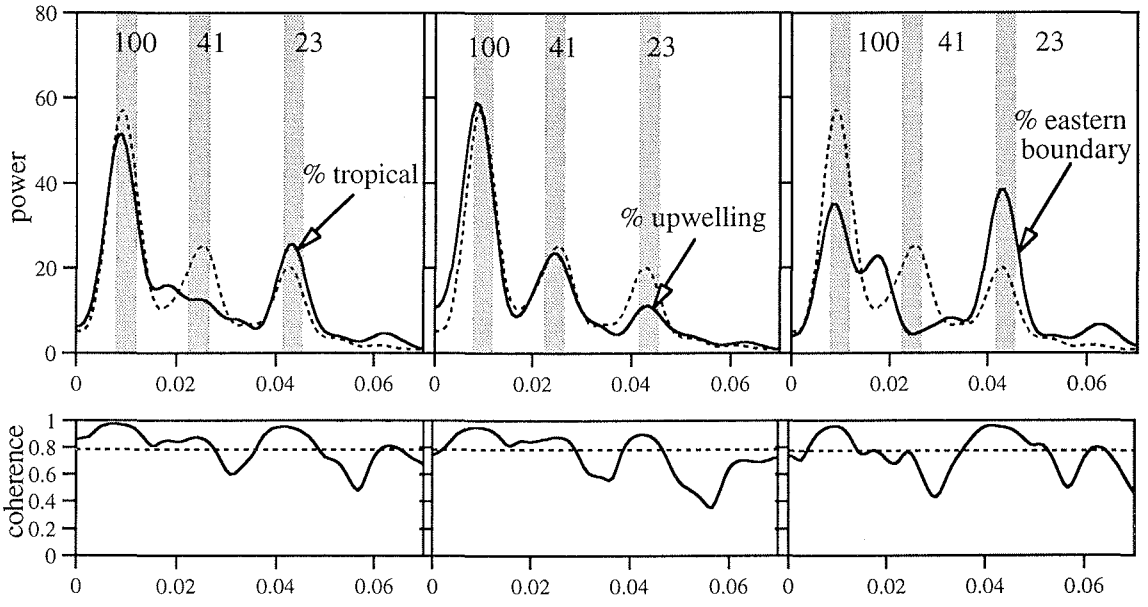


**Fig. 5:** Cross spectral analysis between the planktic foraminifera assemblages (solid line) and the stable oxygen isotope record of *C. wuellerstorfi* (dashed line). The coherency is plotted in the lower panel with the 80% confidence level indicated with the dashed line.

Cross-spectral analysis of the planktic foraminifera assemblages reveal cyclic variations within the main frequency domains of the earth's orbital parameters

(precession, obliquity, and eccentricity). However, it is obvious from the drawings of the downcore results, that the main periodicities between the assemblages are different (Fig. 3). Spectral analysis revealed significant differences in the main periodicities for each assemblage (Fig. 5). The tropical and eastern boundary assemblages are dominated by variations in the orbital eccentricity (100 kyrs) and precession (23 kyrs) periods coherent with global ice volume recorded in the $\delta^{18}O$ of *C. wuellerstorfi*. It is apparent, that most variation within the tropical assemblage occurs in the 100 kyrs period with maxima aligned to a minimum in ice volume (Fig. 3). All three orbital periodicities (eccentricity, obliquity, and precession) are observed in the spectra of the upwelling assemblage with decreasing power from the longer to the shorter periods. In contrast, the eastern boundary assemblage spectra show most power in the precession band and weaker power in the eccentricity band, whereas no variation is observed in the obliquity band (Fig. 5). These results corroborate earlier studies in the equatorial Atlantic (McIntyre et al., 1989; Mix and Morey, 1996).

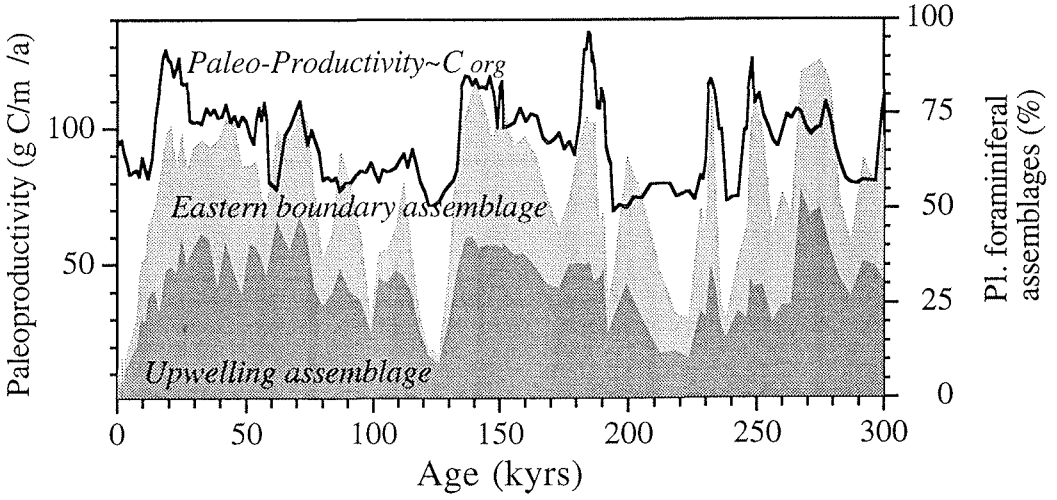


**Fig. 6:** Comparison between the relative abundance of the upwelling and eastern boundary assemblages (shaded areas) with the paleoproductivity estimations, based on organic carbon accumulation rates (from Bickert, 1992).

Comparison between the abundance of the three planktic foraminiferal assemblages to the numbers of planktic foraminifera per gram sediment does not reveal any significant linear correlation. However, we noticed obvious trends with high numbers of foraminifera per gram sediment being typical for higher abundances of the tropical assemblages (not plotted). The opposite is true for both, eastern boundary and upwelling assemblages. These results would severely bias productivity estimations based on AR $CaCO_3$ (Brummer and Van Eijden, 1992; Rühlemann et al., 1996; Van Kreveld et al., 1996) if we assume that an increase in the abundance of upwelling and eastern boundary

assemblages should indicate higher productivity. However, in areas which remain more or less oligotrophic through time, this approach seems to provide reasonable results (Brummer and Van Eijden, 1992; Rühlemann et al., 1996). A more reasonable relationship is revealed by the comparison between the abundance of the upwelling and eastern boundary assemblages with the TOC record and the paleoproductivity estimations (Sarnthein et al., 1992) based on organic carbon accumulation rates (Fig. 6).

In addition, we tested the use of absolute numbers of coccoliths and coccolith accumulation rates to reconstruct paleoproductivity. An increase in coccolith numbers and accumulation rates should provide reliable information on an enhanced productivity in the surface water masses, although it remains questionable whether or not coccolithophores reflect the gross productivity of phytoplankton in surface water masses?

If we take a look at the data available on coccolithophore productivity in the modern oceans, it appears that coccolithophores do react to increased nutrient levels, due to upwelling or frontal systems in open and coastal oceans (Kleijne et al., 1989; Ziveri et al., 1994; Kinkel et al., subm.). Nevertheless, it seems to be obvious that coccolithophores may appear in second place within an ecological succession of phytoplankton groups in their ability to use nutrients in surface waters following fast growing phytoplankton like diatoms (Young, 1994). This is supported by results of plankton samples (Garcia-Soto et al., 1995; Giraudeau and Bailey, 1995) and sediment trap studies (Samtleben et al., 1995) which showed that coccolithophores began to thrive and dominate phytoplankton communities after diatoms utilized most of the nutrients and a postupwelling or seasonal stratification of the water column occurred. Today, coccolithophores react to upwelling activity in the tropical Atlantic along the equator which is documented in plankton and surface sediment samples (Kinkel et al., subm.). Albeit, the differences between the equatorial Atlantic upwelling area and the oligotrophic areas seem to be more distinguished by the composition of coccolith assemblages than by the numbers of coccoliths (Kinkel et al., subm.). Our downcore results indicate that enhanced coccolithophore productivity indeed did not occur simultaneously with maximum TOC-contents and paleoproductivity estimations (Figs. 7, 2, 6). However, we still assume that coccolith numbers and accumulation rates indicate increased productivity, at least of coccolithophores, during late isotope stage 8, early stage 7, at stage boundary 6/7, during substage 6.3, late stage 5, and stage 3. Moreover, the maximum in coccolith numbers and accumulation rates are observed just before and after TOC values reach their maximum. This leads to the conclusion that optimum growth conditions of coccolithophores may occur just before or after gross productivity was at its maximum. Yet, we have to keep in mind that organic carbon contents in the tropical Atlantic can be

overestimated, as reasonable proportions of the organic carbon fraction may be added to the record by eolian transport of terrigenous organic matter (Verardo and Ruddiman, 1996; Wagner and Dupont, in press). The eolian transport of terrigenous matter is supposed to be increased during glacial times when wind speeds reach their maximum; nonetheless, the proportion of terrestrial organic carbon to total organic carbon is still under debate.

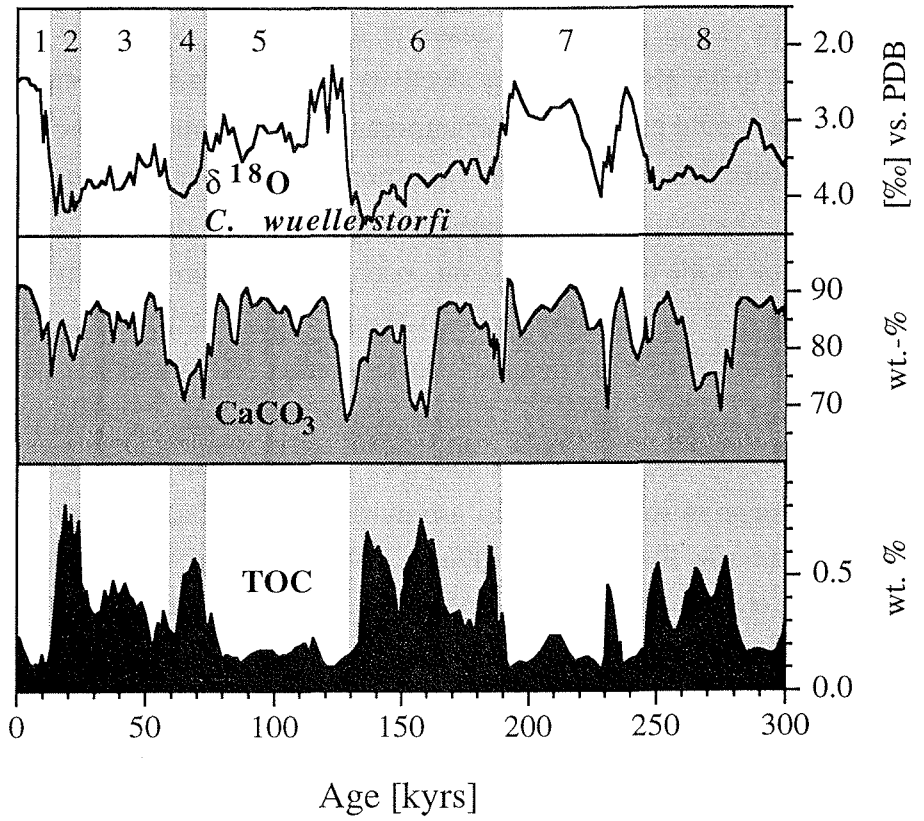


**Fig. 7:** Downcore distribution of stable oxygen isotopes of the epibenthic foraminifera *C. wuellerstorfi* (from Bickert and Wefer, 1996), $CaCO_3$ and organic carbon contents (wt.-%); from Bickert (1992).

The minima in coccolith numbers and accumulation rates in stages 6, 4, and 2 are likely to be influenced by an increase in carbonate dissolution as recorded by the sand content (Bickert and Wefer, 1996). This is corroborated by the results of Dittert et al. (subm.) who demonstrated that except for extreme conditions during peak glacials the lysocline did not raise above the core site.

Comparison between the relative abundance of *F. profunda* and the numbers of coccoliths or coccolith accumulation rates reveal opposite trends with maxima in coccolithophore numbers and accumulation rates more or less coherent with minima in the relative abundance of *F. profunda* (Fig. 8). This gives further support to the conceptual model of Molfino and McIntyre (1990) who suggested that high abundances of *F.*

*profunda* indicate a deep thermocline and nutricline leading to a decrease in coccolithophore productivity in the upper photic zone where the majority of coccolithophores grow. This conceptual model was applied successfully by other authors (Ahagon et al., 1993; Okada and Matsuoka, 1996; Bassinot et al., 1997; Beaufort et al., 1997) but it was never shown that other proxies reacted in the same manner or opposite to the *F. profunda* signal.

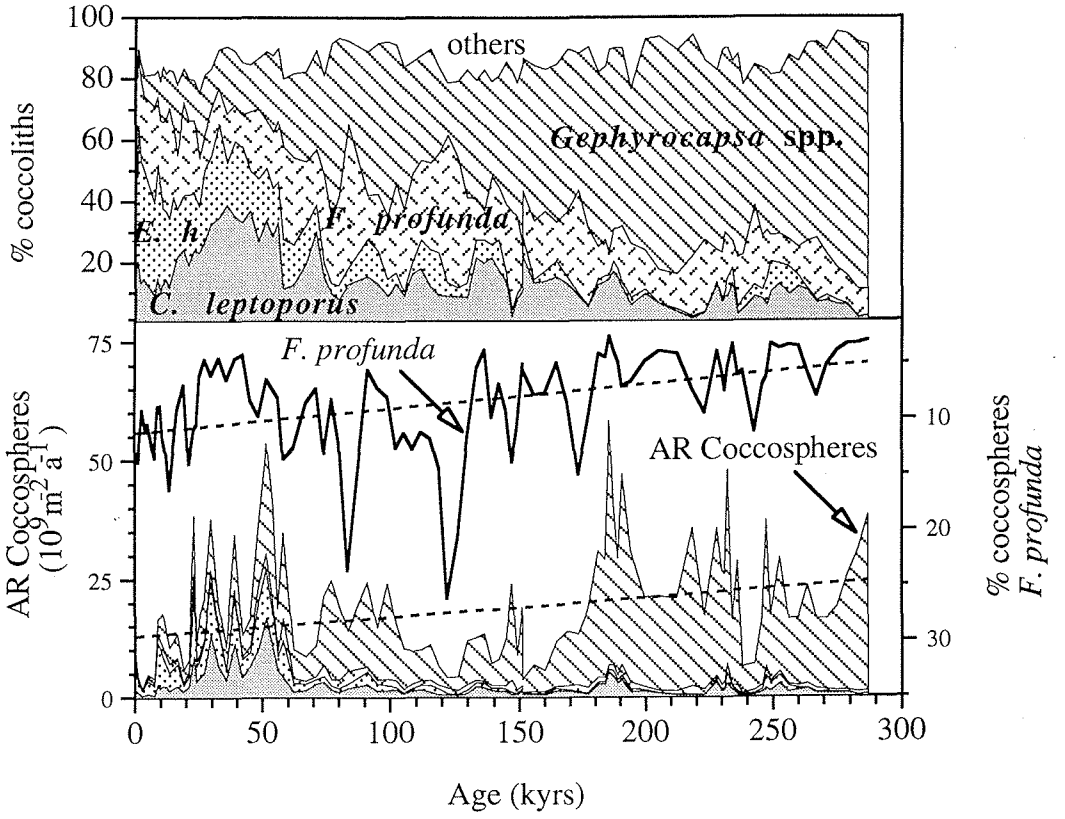


**Fig. 8:** Downcore distribution of the rel. abundance of coccoliths of the most common coccolithophore species (upper panel). The distribution pattern of the calculated coccosphere accumulation rate as well as the relative abundance of *F. profunda* after recalculating all coccoliths to coccospheres (lower panel).

Yet, an obstacle remains if we look at the relative abundance of *F. profunda* and the number of coccoliths or coccolith accumulation rates, respectively. It is obvious that on average,the relative abundance of *F. profunda* slightly increases over the last 300 kyrs (Figs. 4, 8) while the same is true for the coccolith numbers and accumulation rates (Fig. 2) although an opposite trend would be expected. A similar trend can be observed in the abundance of *F. profunda* in a sediment core of the Indian Ocean (Beaufort et al., 1997) over the last 300 kyrs. We therefore converted the most common species (*E. huxleyi*, *C. leptoporus*, *F. profunda*, and *Gephyrocapsa* spp.) which in general make up more than 80 % of the total coccolith assemblage (Fig. 8) into coccosphere units. It was suggested

before that ecological interpretation of coccolith assemblages may be biased if only coccoliths are taken into account instead of recalculating the organism level of entire cells (Giraudeau, 1992a; 1992b; Pujos, 1992). Our recalculations did not change the general picture but two significant modifications are notified: First of all, the increase in the coccosphere abundance of *F. profunda* over the last 300 kyrs is not as strong as in the coccolith abundance. Nevertheless, it is still notable. Second, the trend in the coccosphere accumulation rates of the most important species is opposite to that of the coccolith accumulation rates. This is reasonable as *C. leptoporus* and *E. huxleyi* are the major contributors to the coccosphere accumulation rates in sediments younger than oxygen isotope stage 4, whereas mainly species of the genus *Gephyrocapsa* contribute to the coccosphere accumulation rates in older sediments. Both *C. leptoporus* and *E. huxleyi* bear significantly more coccoliths per coccosphere (30 and 24, respectively) than coccospheres of the genus *Gephyrocapsa* which on an average only bear 14 coccoliths per coccosphere.

If we compare this result to our coccolith and foraminifera data we can conclude that the relative abundance data seem to be robust and generally are not influenced by carbonate dissolution. A stronger impact of carbonate dissolution influences the absolute numbers calcareous microfossils. Numbers of planktic foraminifera seem to be much stronger affected by carbonate dissolution than numbers of coccoliths which are more likely to reflect surface water productivity.

## 6. Conclusions

The investigation of different faunal and floral assemblages together with a set of bulk parameters (TOC, $CaCO_3$) in a sediment core from the southern Equatorial Atlantic provided details on the influence of surface water circulation patterns in the investigated area and its impact on the sedimentation of planktic foraminifera and coccolithophores.

Spectral analysis revealed significant variance at the 100 kyrs and the 23 kyrs periodicities which are typical for paleoceanographic reconstructions of the tropical Atlantic Ocean. As most variability and power is observed in the 23 kyrs band of the eastern boundary assemblage, we assume that advection of cold and nutrient rich water masses via the eastern boundary currents is the most important feature in surface water circulation above the investigated site. In addition, upwelling intensity is controlled by the relationship between the meridional (monsoonal) and zonal (tropical easterlies) wind stress. Minima in upwelling intensity are monitored by the increase in the relative abundance of the coccolithophore *F. profunda* as well as the tropical planktic foraminiferal assemblage represented by (Fig. 9). Both are positively correlated to the

insolation over the North African landmass with maxima indicating a warm and deep surface layer associated to a deep thermocline due to more meridional wind stress. In contrast, low insolation values leads to more zonal wind stress which will cause a thermocline uplift and increased nutrient supply leading to a rise in productivity.

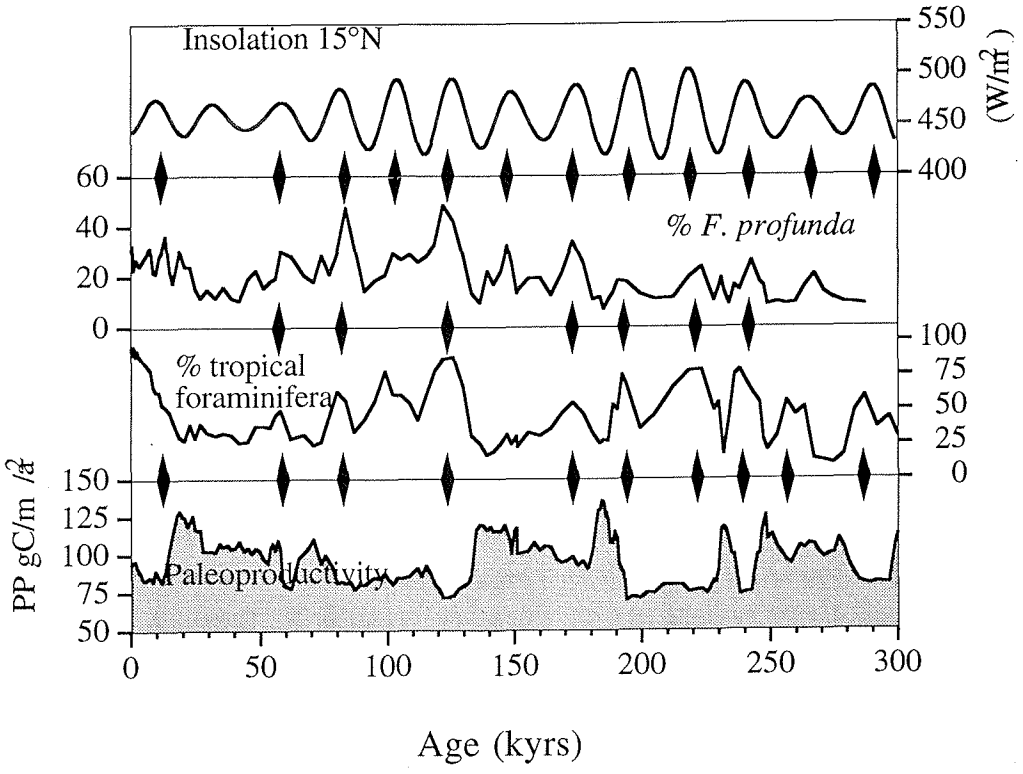


**Fig. 9:** Comparison between the relative abundance of the *F. profunda* (coccolithophore), *G. ruber* (planktic foraminifer) and the insolation at 15°N (after Bergér and Loutre, 1991).

Our data do not allow a distinct separation between the eastern boundary and the upwelling mechanism. As there is much more variability in the eastern boundary dynamics, we assume that this is the driving force in the surface water circulation at this site that interacts with upwelling activity and provides it with additional nutrients.

Although carbonate sedimentation seems to be dominated by the tropical planktic foraminifera, coccolithophores contribute largely to the carbonate sedimentation in times of higher surface water productivity even though the carbonate dissolution reduces these signals during peak glacial times.

## 7. Acknowledgement

We like to thank C. Wienberg for technical assistance. P.J. Müller kindly provided the carbonate and organic carbon data, oxygen isotopes and stratigraphy were given by T.

Bickert. We like to thank K.-H. Baumann and R. Huber for helpful comments on the manuscript. This is SFB 261 contribution No. xxx.

## 8. References

Ahagon, N., Tanaka, Y., Ujiie, H., 1993. Florisphaera profunda, a possible nannoplankton indicator of late Quaternary changes in sea-water turbidity at the northwestern margin of the Pacific. Mar. Micropal. 22: 255-273.

Andruleit, H., 1996. A filtration technique for quantitative studies of coccoliths. Micropaleontology 42: 403-406.

Bainbridge, A.E., 1981. GEOSECS Atlantic Expedition, Hydrographic Data, 1972-1973. National Science Foundation, Superintendent of Documents, US Government Printing Office, Washington, DC, pp. 121.

Bassinot, F.C., Beaufort, L., Vincent, E., Labeyrie, L., 1997. Changes in the dynamics of western equatorial Atlantic surface currents and biogenic productivity at the "Mid-Pleistocene Revolution" (930 ka). In: Shackleton, N.J., Curry, W.B., Richter, C., Bralower, T.J. (Eds.), Proceedings of the Ocean Drilling Program, Scientific Results. College Station, TX (Ocean Drilling Program), 154, pp. 269-284.

Beaufort, L., Lancelot, Y., Camberlin, P., Cayre, O., Vincent, E., Bassinot, F., Labeyrie, L., 1997. Insolation cycles as a major control of equatorial Indian Ocean primary production. Science 278: 1451-1454.

Beck, J.W., Récy, J., Taylor, F., Edwards, R.L., Cabioch, G., 1997. Abrupt changes in early Holocene tropical sea surface temperatures derived from coral records. Nature 385 705-707.

Berger, W.H., Smetacek, V.S., Wefer, G., 1989. Ocean productivity and paleoproductivity - An overview. In: Berger, W.H., Smetacek, V.S., Wefer, G. (Eds.), Productivity of the ocean: Present and past. John Wiley & Sons, New York, NY, pp. 1-34.

Bickert, T., 1992. Rekonstruktion der spätquartären Bodenwasserzirkulation im östlichen Südatlantik über stabile Isotope benthischer Foraminiferen. Ber. Fachbereich Geowiss., Univ. Bremen 27: 1-205.

Bickert, T., Wefer, G., 1996. Late Quaternary deep water circulation in the South Atlantic: Reconstruction from carbonate dissolution and benthic stable isotopes. In: Wefer, G., Berger, W.H., Siedler, G., Webb, D.J. (Eds.), The South Atlantic: Present and past circulation. Springer-Verlag, Berlin Heidelberg, pp. 599-620.

Boyle, E.A., 1988. Vertical oceanic nutrient fractionation and glacial/interglacial $CO_2$ cycles. Nature 331: 55-56.

Brummer, G.-J.A., Van Eijden, A.J.M., 1992. "Blue-ocean" paleoproductivity estimates from pelagic carbonate mass accumulation rates. Mar. Micropal. 19: 99-117.

CLIMAP project members, 1981. Seasonal Reconstructions of the Earth's Surface at the last glacial maximum. Geol. Soc. Am. Bull., MC Series 36: 1-18.

CLIMAP project members, 1984. The last interglacial ocean. Quat. Res. 21: 123-224.

Curry, W.B., Oppo, D.W., 1997. Synchronous, high frequency oscillations in tropical sea surface temperatures and North-Atlantic Deep Water production during the last glacial cycle. Paleoceanography 12: 1-14.

deMenocal, P.B., Ruddiman, W.F., Pokras, E.M., 1993. Influences of high- and low-latitude processes on African terrestrial climate: Pleistocene eolian records from equatorial Atlantic Ocean Drilling Program Site 663. Paleoceanography 8: 209-242.

Dittert, N., Niebler, H.-S., Henrich, R., subm. A 300 kyrs history of planktic foraminiferal distribution in the central equatorial Atlantic Ocean - paleo-environmental implications. Mar. Micropal.

Fischer, G., Wefer, G., 1996. Seasonal and interannual particle fluxes in the eastern tropical Atlantic from 1989 to 1991: ITCZ migrations and upwelling. In: Ittekot, V., Schäfer, P., Honjo, S., Depetris, P.J. (Eds.), Particle Flux in the Ocean. John Wiley & Sons, New York, NY.

Garcia-Soto, C., Fernández, E., Pingree, R.D., Harbour, D.S., 1995. Evolution and structure of a coccolithophore bloom in the Western English Channel. Journal of Plankton Research 17: 2011 - 2036.

Gingele, F., 1992. Zur Klimaabhängigen Bildung biogener und terrigener Sedimente und ihrer Veränderung durch Frühdiagenese im zentralen östlichen Atlantik. Berichte, Fachbereich Geowissenschaften 202 S.

Gingele, F.X., Dahmke, A., 1994. Discrete barite particles and barium as tracers of paleoproductivity in South Atlantic sediments. Paleoceanography 9: 151-168.

Giraudeau, J., 1992a. Coccolith paleotemperature and paleosalinity estimates in the Caribbean Sea for the Middle-Late Pleistocene (DSDP Leg 68 - Hole 502 B). Memorie di Scienze Geologiche 43: 375 - 387.

Giraudeau, J., 1992b. Distribution of recent nannofossil beneath the Benguela system: Southwest African continental margin. Mar. Geol. 108: 219-237.

Giraudeau, J., Bailey, G.W., 1995. Spatial dynamics of coccolithophore communities during an upwelling event in the southern Benguela System. Cont. Shelf Res. 15: 1825-1852.

Gordon, A.L., 1986. Interocean exchange of thermocline water. J. Geophys. Res. 91: 5037-5046.

Gordon, A.L., 1996. Communication between oceans. Nature 382: 399-400.

Guilderson, T.P., Fairbanks, R.G., Rubenstone, J.L., 1994. Tropical temperature variations since 20,000 years ago; modulating interhemispheric climate change. Science 263: 663-665.

Hemleben, C., Spindler, M., Anderson, O.R., 1989. Modern planktonic foraminifera. Springer-Verlag, New York, NY, pp. 363.

Hutson, W.H., 1977. Transfer functions under no-analog conditions: Experiments with Indian Ocean planktonic foraminifera. Quat. Res. 8: 355-367.

Imbrie, J., Hays, J.D., Martinson, D.G., McIntyre, A., Mix, A.C., Morley, J.J., Pisias, N.G., Prell, W.L., Shackleton, N.J., 1984. The orbital theory of Pleistocene climate: Support from a revised chronology of the marine $\delta^{18}O$ record. In: Berger, A., Imbrie, J., Hays, J.,

Kukla, G., Saltzman, B. (Eds.), Milancovitch and climate - Part I. D. Reidel, Dordrecht, pp. 269-305.

Imbrie, J., Kipp, N.G., 1971. A new micropaleontological method for quantitative paleoclimatology: application to a Late Pleistocene Carribean core. In: Turekian, K.K. (Ed.) Late Cenocoic glacial ages. (Memorial Lectures) Yale University Press, New Haven, 43, pp. 71-181.

Jordan, R.W., Kleijne, A., 1994. A classification system for living coccolithophores. In: Winter, A., Siesser, W.G. (Eds.), Coccolithophores. Cambridge University Press, Cambridge, pp. 83-105.

Kinkel, H., Baumann, K.-H., Cepek, M., subm. Living and Late Quaternary coccolithophores from the equatorial Atlantic: Response to surface water productivity. Mar. Micropal.

Kleijne, A., Kroon, D., Zevenboom, W., 1989. Phytoplankton and foraminiferal frequencies in northern Indian Ocean and Red Sea surface waters. Neth. J. Sea Res. 24: 531-539.

Knappertsbusch, M., 1993. Geographic distribution of living and Holocene coccolithophores in the Mediterranean sea. Mar. Micropal. 21 (1-3): 219-247.

Kroopnick, P.M., 1985. The distribution of $^{13}C$ of $\Sigma CO_2$ in the World Oceans. Deep-Sea Res. 32: 57-84.

Lebreiro, S.M., Moreno, J.C., Abrantes, F.F., Pflaumann, U., 1997. Productivity and paleoceanographic implications on the Tore Seamount (Iberian Margin) during the last 225 kyr: Foraminiferal evidence. Paleoceanography 12: 718-727.

Longhurst, A., 1993. Seasonal cooling and blooming in tropical oceans. Deep-Sea Res. 40: 2145-2177.

Macdonald, A.M., Wunsch, C., 1996. An estimate of global ocean circulation and heat fluxes. Nature 382: 436-439.

McIntyre, A., Molfino, B., 1996. Forcing of Atlantic equatorial and subpolar millenial cycles by precession. Science 274: 1867-1870.

McIntyre, A., Ruddiman, W.F., Karlin, K., Mix, A.C., 1989. Surface water response of the equatorial Atlantic Ocean to orbital forcing. Paleoceanography 4: 19-55.

Mix, A.C., 1989. Influence of productivity variations on long-term atmospheric $CO_2$. Nature 337: 541-544.

Mix, A.C., Morey, A.E., 1996. Climate feedback and Pleistocene variations in the Atlantic south equatorial current. In: Wefer, G., Berger, W.H., Siedler, G., Webb, D.J. (Eds.), The South Atlantic: Present and past circulation. Springer-Verlag, Berlin Heidelberg, pp. 503-525.

Mix, A.C., Ruddiman, W.F., McIntyre, A., 1986a. Late Quaternary paleoceanography of the tropical Atlantic 1: Spatial variability of annual mean sea-surface temperatures, 0-20,000 Years B.P. Paleoceanography 1: 43-66.

Mix, A.C., Ruddiman, W.F., McIntyre, A., 1986b. Late Quaternary paleoceanography of the tropical Atlantic 2: The seasonal cycle of sea-surface temperatures, 0-20,000 Years B.P. Paleoceanography 1: 339-353.

Molfino, B., McIntyre, A., 1990. Precessional forcing of nutricline dynamics in the equatorial Atlantic. Science 249: 766-769.

Monger, B., McClain, C., Murtugudde, R., 1997. Seasonal phytoplankton dynamics in the eastern tropical Atlantic. J. Geophys. Res. 102: 12,389-12,411.

Okada, H., Matsuoka, M., 1996. Lower-photic nannoflora as an indicator of the late Quaternary monsoonal paleo-record in the tropical Indian Ocean. In: Moguilevsky, A., Whatley, R. (Eds.), Microfossils and Oceanic Environments. Aberystwyth Press, Aberystwyth, pp. 231-245.

Paillard, D., Labeyrie, L., Yiou, P., 1996. Macintosh program performs time-series analysis. AGU 379.

Pflaumann, U., Duprat, J., Pujol, C., Labeyrie, L.D., 1996. SIMMAX: A modern analog technique to deduce Atlantic sea surface temperatures from planktonic foraminifera in deep-sea sediments. Paleoceanography 11: 15-35.

Philander, S.G.H., Pacanowski, R.C., 1986. The mass and heat budget in a model of the tropical Atlantic. J. Geophys. Res. 91: 14212-14220.

Pujos, A., 1992. Calcareous nannofossils of Plio-Pleistocene sediments from the northwestern margin of tropical Africa. In: Summerhayes, C.P., Prell, W.L., Emeis, K.C. (Eds.), Upwelling systems: Evolution since the Early Miocene. (Geological Society Special Publication.) Geological Society of America, Avon, 64, pp. 343-358.

Ravelo, A.C., Fairbanks, R.G., Philander, S.G.H., 1990. Reconstructing tropical Atlantic hydrography using planktonic foraminifera and an ocean model. Paleoceanography 5: 409-431.

Rind, D., Peteet, D.M., 1985. Terrestrial conditions at the last glacial maximum and CLIMAP sea-surface temperature estimates; are they consistent? Quat. Res. 24: 1-22.

Ruddiman, W.F., 1997. Tropical Atlantic terrigenous fluxes since 25.000 yrs B.P. Mar. Geol. 136: 189-207.

Rühlemann, C., Frank, M., Hale, W., Mangini, A., Mulitza, S., Müller, P.J., Wefer, G., 1996. Late Quaternary productivity changes in the western equatorial Atlantic: Evidence from 230Th-normalized carbonate and organic carbon accumulation rates. Mar. Geol. 135: 127-152.

Samtleben, C., Schaefer, P., Andruleit, H., Baumann, A., Baumann, K.-H., Kohly, A., Matthiessen, J., Schröder-Ritzau, A., 1995. Plankton in the Norwegian-Greenland Sea: From living communities to sediment assemblages - an actualistic approach. Geol. Rdschau 84: 108-136.

Sarnthein, M., Pflaumann, U., Ross, R., Thiedemann, R., Winn, K., 1992. Transfer functions to reconstruct ocean paleoproductivity: A comparison. In: Summerhayes, C.P., Prell, W.L., Emeis, K.C. (Eds.), Upwelling systems: Evolution since the early Miocene. Geological Society Special Publication, 64, pp. 411-427.

Schneider, R.R., Müller, P.J., Ruhland, G., Meinecke, G., Schmidt, H., Wefer, G., 1996. Late Quaternary surface temperatures and productivity in the east-equatorial South Atlantic: response to changes in Trade / Monsoon wind forcing and surface water advection. In: Wefer, G., Berger, W.H., Siedler, G., Webb, D. (Eds.), The South Atlantic: Present and Past

Circulation. Springer-Verlag, Berlin Heidelberg, pp. 527-551.

Sikes, E.L., Keigwin, L.D., 1994. Equatorial Atlantic sea surface temperature for the last 30 kyr: A comparison of $U^{k}_{37}$, $\delta^{18}O$ and foraminiferal assemblage temperature estimates. Paleoceanography 9: 31-45.

Struck, U., Sarnthein, M., Westerhausen, L., Barnola, J.M., Raynaud, D., 1993. Ocean-atmosphere carbon exchange: impact of the "biological pump" in the Atlantic equatorial upwelling belt over the last 330,000 years. Palaeogeogr., Palaeoclimatol., Palaeoecol. 103: 41-56.

Stute, M., Forster, M., Frischkorn, H., Serejo, A., Clark, J.F., Schlosser, P., Broecker, W.S., Bonani, G., 1995. Cooling of Tropical Brazil (5°C) during the Last Glacial Maximum. Science 269: 379-383.

Van Andel, T.H., Heath, G.R., Moore, T.C., 1975. Cenozoic history and paleoceanography of the central equatorial Pacific Ocean. Geol. Soc. Am. Mem. 143: 1-134.

Van Kreveld, S.A., Knappertsbusch, M., Ottens, J., Ganssen, G.M., Van Hinte, J., 1996. Biogenic carbonate and ice-rafted debris (Heinrich Layer) accumulation in deep sea sediments from a North East Atlantic piston core. Marine Geology ??? xxx:

Verardo, D.J., McIntyre, A., 1994. Production and destruction: Control of biogenous sedimentation in the tropical Atlantic 0-300,000 years B.P. Paleoceanography 9: 63-86.

Verardo, D.J., Ruddiman, W.F., 1996. Late Pleistocene charcoal in tropical Atlantic deep-sea sediments: Climatic and geochemical significance. Geology 24: 855-857.

Wagner, T., Dupont, L., in press. Terrestrial OM in marine sediments: analytic approaches and eolian-marine records of the central Equatorial Atlantic. In: Fischer, G., Wefer, G. (Eds.), Proxies in paleoceanography. Springer-Verlag, Berlin Heidelberg, pp.

Webb, R.S., Rind, D.H., Lehman, S.J., Healy, R.J., Sigman, D., 1997. Influence of ocean heat transport on the climate of the Last Glacial Maximum. Nature 385: 695-699.

Wefer, G., Bleil, U., Schulz, H.D., cruise participants, 1989. Bericht über die Meteor-Fahrt M9-4, Dakar-Santa Cruz, 19.2.-16.3.1989. Ber. Fachbereich Geowiss., Univ. Bremen 7: 1-103.

Young, J.R., subm. Calculation of coccolith volume and its use in calibration of carbonate flux estimates. Deep-Sea Res.

Young, J.R., 1994. Functions of coccoliths. In: Winter, A., Siesser, W.G. (Eds.), Coccolithophores. Cambridge Acedemic Press, Cambridge, pp. 63-82.

Ziveri, P., Thunell, R.C., Rio, D., 1994. Export production of coccolithophores in an upwelling region: Results from San Pedro Basin, Southern California borderlands. Mar. Micropal. 24: 335-358.

# 3. Carbonate dissolution in the South Atlantic Ocean: Evidence by *Globigerina bulloides*' ultrastructure breakdown

NICOLAS DITTERT* AND RÜDIGER HENRICH

**Abstract**—Ultrastructure dissolution susceptibility of the planktic foraminifer, *Globigerina bulloides*, carbonate ion content of the water column, calcium carbonate content of the sediment surface, and rain ratio derived from sediment surface samples were investigated in order to reconstruct the position of the hydrographic and the sedimentary calcite lysocline and the CCD in the modern South Atlantic Ocean. Carbonate ion data from the water column refer to the GEOSECS locations 48, 103, and 109, calcium carbonate data come from 19 GeoB sediment surface samples of 4 transects into the Brasil-, the Guinea-, and the Cape Basins. Regarding *G. bulloides,* we will present a new (pale-)oceanographic tool, namely the *Globigerina bulloides* Dissolution Index (BDX). Further, we will give evidence a) for progressive *G. bulloides*' ultrastructural breakdown with increasing carbonate dissolution even above the lysocline; b) for a sharp BDX increase at the top of the sedimentary lysocline; and c) for the total erase of this species at the bottom of the lysocline or the CCD. BDX puts us in the position to distinguish the upper open ocean and the upwelling influenced continental margin above from the deep ocean below the sedimentary lysocline. Water column carbonate ion data, sedimentary calcite data, and rain ratio appear to be good proxies in order to confirm BDX. As shown by BDX both the hydrographic lysocline (in the water column) and the sedimentary lysocline (at the sediment pore-water interface) mark the boundary between the carbonate ion undersaturated and highly corrossive AABW and the carbonate ion saturated NADW of the modern South Atlantic.

## INTRODUCTION

The thermohaline circulation of the global oceans (Broecker and Denton, 1989; Broecker, 1997) is an essential factor determining the climate on the earth and is crucial for understandimg climate change. It contributes substantially to the global transport of heat and water and is important for the global carbon cycle. Since the oceans cover over 70 % of the earth's surface, and since deep- and intermediate waters of the oceans contain about 60 times more $CO_2$ than the atmosphere (Broecker and Peng, 1982), they represent "sleeping giants" in the control of increased $CO_2$ in the atmosphere. Regarding the

* Fachbereich 5 - Geowissenschaften, Universität Bremen, Postfach 33 04 40, D-28334 Bremen, Germany

reconstruction of the deep-water circulation in the South Atlantic, judgement of both position and thickness of the calcite lysocline are of major climatic importance (Archer, 1996). They are determined by characteristic extent and corrosivity of Antarctic Bottom Water (AABW) and North Atlantic Deep Water (NADW) whose different impact is reflected by distinct preservation patterns of calcareous sediments.

Our main objective is it to determine top and bottom of the modern sedimentary calcite lysocline and its inter-basin variations by means of the ultrastructure dissolution susceptibility of the planktic foraminifer, *Globigerina bulloides* d'Orbigny 1826. We investigated 19 sediment surface samples of four transects into the Brasil-, the Guinea-, and the Cape Basin. This led us to the *Globigerina bulloides* Dissolution Index (BDX) which is based on the recognition of preservation features in the ultrastructure of planktic foraminiferal tests at the SEM (Bé *et al.*, 1975) and has been evaluated for *Neogloboquadrina pachyderma* (Henrich, 1989; Baumann and Meggers, 1996) and for *G. bulloides* (Van Kreveld, 1996) at high latitudes.

*Oceanographic sketch*

Today the circulation in the deep South Atlantic Ocean is dominated by interactions between the AABW and the NADW in contrasting extent. NADW is indicated by oxygen enriched, nutrient depleted water masses of high $CO_3^{2-}$ and low $CO_2$ contents. AABW can be distinguished as an extremely cold, oxygen depleted and nutrient enriched water mass of low $CO_3^{2-}$ and high $CO_2$ contents (Kroopnick, 1985; Boyle, 1988). Today's mixing zone between AABW and NADW in the South Atlantic is close to the 90 µmol/kg $CO_3^{2-}$ isoline (Bainbridge, 1981). The relatively warm and saline NADW occupies the depth interval between 2,000 m and 4,000 m, while below 4,000 m AABW is encountered. With respect to the modern South Atlantic Ocean, the border of AABW with NADW and the hydrographic lysocline coincide (Bickert and Wefer, 1996). Other deep water reconstructions (e.g., Bainbridge, 1976; Takahashi *et al.*, 1980; Reid, 1996) elucidate the contrasting influence of the carbonate ion depleted, $CO_2$ ameliorated, and corrosive AABW. That is, below the lysocline destruction and dissolution of calcareous sediments become progressively more intense due to the predominance of the AABW. Dissolution subsequently increases proportional to the fourth power of $\Delta CO_3^{2-}$ (Keir, 1980) until the rate of calcite sedimentation is totally compensated for by the rate of calcite dissolution (Bramlette, 1961; Archer, 1996).

## MATERIAL AND METHODS

Sediment surface samples (giant box core) were collected during R/V METEOR cruises M9/4, M12/1, M20/2 (Wefer *et al.*, 1989; Wefer *et al.*, 1990; Schulz *et al.*, 1992) at water depths from 1,007 m down to 5,213 m (Fig. 1; Table 1). Total carbon (TC) and total organic carbon (TOC) content of bulk sediments were measured with a LECO-CS 244 infrared analyzer. Calcium carbonate content was calculated in weight percentage of the bulk sample by: $CaCO_3$ % (w/w) = (TC % (w/w) - TOC % (w/w)) · 8.33 (1), whereas the rain ratio is determined by the molar ratio of organic ($C_{org}$) to anorganic ($C_{carb}$) carbon (Berger and Keir, 1984).

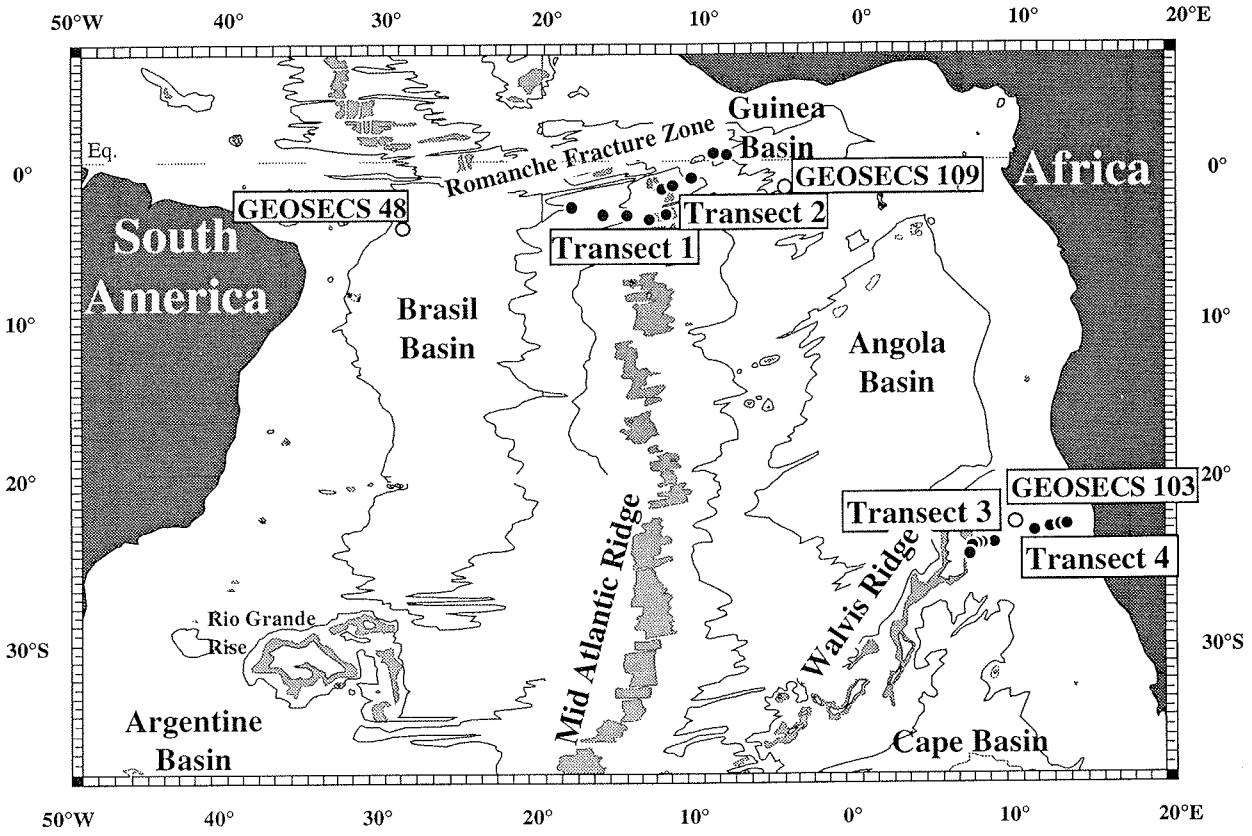


Fig. 1. General map of the investigated areas; for data consult Table 1.

For dissolution investigations, the samples were washed through a 63 µm sieve under a weak spray of water to protect them from additional fragmentation. The whole sample >63 µm was sieved on a 150 µm sieve (Imbrie and Kipp, 1971) according to paleoceanographic and paleoclimatic investigation conventions (CLIMAP, 1976). The taxonomy used follows that of Hemleben et al. (1989). The number of *G. bulloides* specimens to be investigated is settled on the confidence limit of 95 %. Consequently, for determination of dissolution stages regarding ultrastructural breakdown, at least 40 *G.*

*bulloides* specimens per sample were hand-picked and mounted on a carbon tape, glued on SEM stub, and then gold coated. On the apertural side of the test the ultimate and the penultimate chambers were investigated using ZEISS DSM 940A at 9 mm working distance and 9kV accelerating voltage. Overview investigations were carried out at 200× magnification, ultrastructure investigations were executed at 3,000× magnification.

*Table* 1. *Locations and water depths of the investigated surface sediment samples (0-1 cm) and GEOSECS stations 48, 103, 109*

| Sample | Latitude | Longitude | Depth [m] |
|---|---|---|---|
| Transect 1: MOR - Brasil Basin | | | |
| GeoB 1115-4 | 03.558°S | 12.580°W | 2,921 |
| GeoB 1116-1 | 03.623°S | 13.187°W | 3,471 |
| GeoB 1117-3 | 03.817S | 14.903°W | 3,977 |
| GeoB 1118-2 | 03.560°S | 16.432°W | 4,675 |
| GeoB 1119-2 | 02.998°S | 18.378°W | 5,213 |
| GEOSECS 48 | 04.000°S | 29.000°W | 11 - 5,075 |
| Transect 2: MOR - Guinea Basin | | | |
| GeoB 1106-5 | 01.760°S | 12.552°W | 2,471 |
| GeoB 1105-3 | 01.665°S | 12.428°W | 3,231 |
| GeoB 1104-5 | 01.016°S | 10.705°W | 3,724 |
| GeoB 1103-3 | 00.602°N | 09.263°W | 4,321 |
| GeoB 1102-3 | 00.515°N | 08.588°W | 4,779 |
| GEOSECS 109 | 02.000°S | 04.500°W | 2 - 5,132 |
| Transect 3: Walvis Ridge - Cape Basin | | | |
| GeoB 1217-1 | 24.945°S | 06.725°E | 2,007 |
| GeoB 1207-2 | 24.598°S | 06.855°E | 2,593 |
| GeoB 1208-1 | 24.492°S | 07.113°E | 2,971 |
| GeoB 1209-1 | 24.512°S | 07.283°E | 3,303 |
| GeoB 1211-1 | 24.473°S | 07.537°E | 4,089 |
| GeoB 1212-2 | 24.332°S | 08.250°E | 4,669 |
| GEOSECS 103 | 23.995°S | 08.503°E | 5 - 4,572 |
| Transect 4: Cape Basin - Namibia Continental Margin | | | |
| GeoB 1709-3 | 23.588°S | 10.758°E | 3,837 |
| GeoB 1710-2 | 23.430°S | 11.703°E | 2,987 |
| GeoB 1711-5 | 23.317°S | 12.462°E | 1,964 |
| GeoB 1712-2 | 23.255°S | 12.803°E | 1,007 |

As based on SEM evidence, *G. bulloides* ultrastructure distinguishes two principal surface textures, namely the reticulate and the crystalline morphotype. We differentiate five dissolution stages by the distinct preservation features of spines, spine bases, ridges,

interpore areas, and pores which each get worse shaped regarding progressing dissolution:

Dissolution stage $R_1$: High spines with well preserved spine bases (Plate I R1-1); round pores (Plate I R1-2); smooth interpore area (Plate I R1-3); intact ridges (Plate I R1-4).

Dissolution stage $R_2$: Slightly denuded spine bases and/or ridges (Plate I R2-1); broaden or funnel-like pores (Plate I R2-2); etched interpore areas (Plate I R2-3); reduced spine bases (Plate I R2-4).

Dissolution stage $R_3$: Peeled calcite layers (Plate I R3-1); formation of haircracks (Plate I R3-2); strongly undermined spine bases (Plate I R3-3); strongly reduced spine bases and/or ridges (Plate I R3-4).

Dissolution stage $R_4$: Partial removal of the surface layer (Plate I R4-1); forced formation of cracks and holes on ridges and/or spine bases (Plate I R4-2); pores becoming interconnected (Plate I R4-3); missing spine bases and/or ridges (Plate I R4-4).

Dissolution stage $R_5$: Specimens are preserved not even as fragments which is equivalent to absent due to dissolution.

Specimens of the crystalline morphotype appeared subordinately, and progressing dissolution hence can be defined almost exclusively by worsening of the calcite crystalls:

Dissolution stage $C_1$: Sharp crystal edges (Plate I C-1).

Dissolution stage $C_2$: Weakly rounded edges; pitted surface (Plate I C-2).

Dissolution stage $C_3$: Stronger rounded edges; slightly distorted crystallites (Plate I C-3).

Dissolution stage $C_4$: Rounded edges and angles; buried pores; completely distorted crystallites (Plate I C-4).

Dissolution stage $C_5$: Specimens are preserved not even as fragments which is equivalent to absent due to dissolution.

Dissolution stages $R_0$ and $C_0$ were not observed in surface sediment samples. Each BDX value between one and five was calculated weighted on the frequency of appearance per sample:

$$BDX = \sum (BDX') \,/\, \text{number of investigated tests} \qquad (2.1)$$

$$BDX' = \sum (A_{1\text{-}5}) \,/\, \text{number of features per test obtained} \qquad (2.2)$$

$A_{1\text{-}5}$ ... preservation features

The top of the hydrographic calcite lysocline was estimated by the intercept of seawater carbonate ion content and the concentration of carbonate ions in equilibrium with seawater (saturation state: $\Delta CO_3^{2-} = 0$ µmol/kg) for calcite mineral phase as proposed by Takahashi *et al.* (1980) and Broecker and Takahashi (1978). The thickness of the sedimentary calcite lysocline covers the range from 10 µmol/kg (Broecker and Peng, 1982) to the $\Delta CO_3^{2-}$ at the carbonate compensation depth ($\Delta CO_3^{CCD}$) sensu Archer (1996).

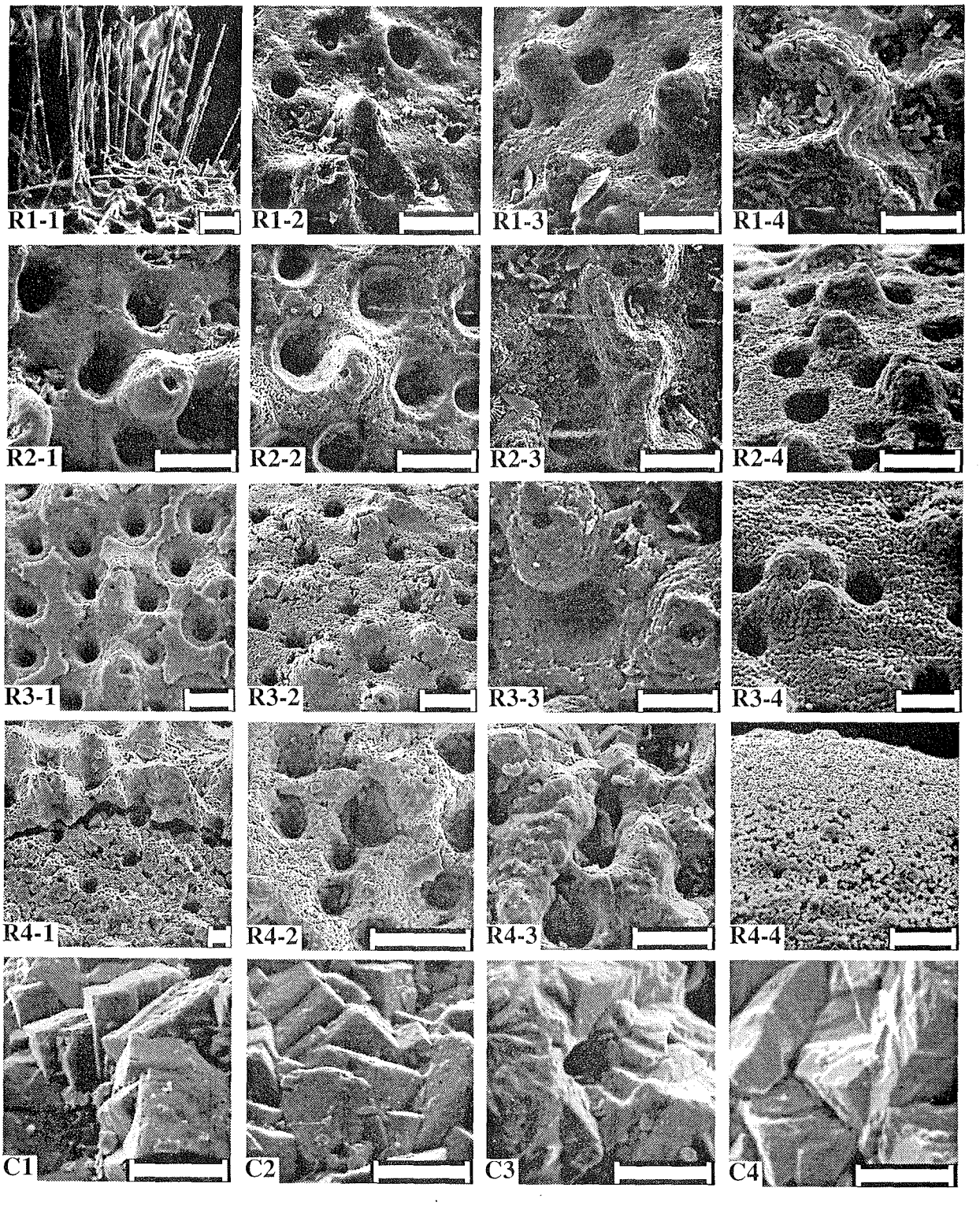


Plate I. Progressive dissolution stages of *Globigerina bulloides*; the reticulate tests ($R_1$ to $R_4$) as well as the crystalline tests ($C_1$ to $C_4$) worsen in preservation features due to increasing dissolution. Pores become frayed, spine bases and ridges denude until they are dissolved totally, hair-cracks make the tests disintegrating into fragments, and smooth interpore areas convert to rugged appearance.

## RESULTS

### Globigerina bulloides *Dissolution Index*

Each sample is represented by BDX values showing a Gaussian distribution. Standard deviation ranges from 0.31 to 0.41 (Fig. 2). Transect 1 (Brasil Basin) BDX values increase from 1.1 to 5 with a distinct shift from 1.5 to 2.9 below 3.977 m ($\sigma_n$=0.31). Transect 2 (Guinea Basin) BDX values intensify from 1.1 to 2 ($\sigma_n$=0.41); transect 3 (Cape Basin) BDX values increase from 0.7 to 2.6 ($\sigma_n$=0.38); transect 4 (Namibia Continental Margin) BDX values raise from 0.9 to 2.4 ($\sigma_n$=0.39). BDX values versus water depth show a significantly linear correlation regarding the Guinea Basin transect ($r^2$=0.981), the Cape Basin transect ($r^2$=0.812), and the Namibia Continental Margin transect ($r^2$=0.999). Brasil Basin transect data show a meaningfully exponential correlation ($r^2$=0.933).

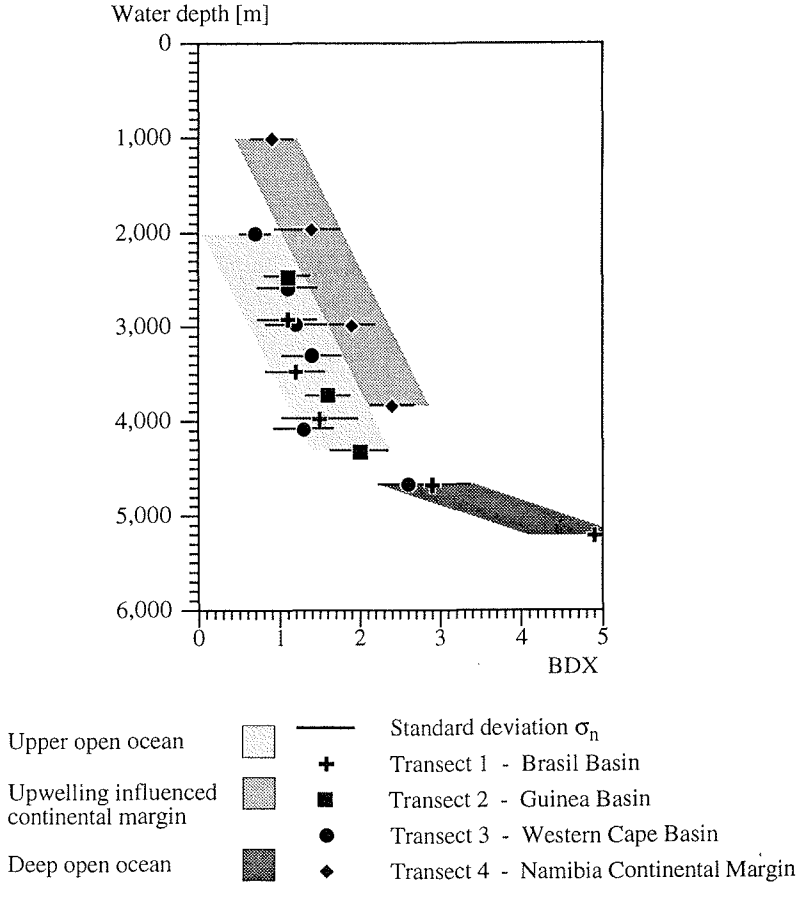


Fig. 2. *Globigerina bulloides* Dissolution Index (BDX) versus water depth. BDX raises with increasing water depth due to increasing carbonate dissolution. Clusters of BDX values distinguish the upper open ocean and the upwelling influenced continental margin above the lysocline from the deep ocean below the lysocline. BDX shows strong increase at the lysocline and total erase of *G. bulloides* at the CCD.

*Geochemical parameters*

The calcium carbonate content (Fig. 3) of the sediment surface samples decreases at all investigated transects with increasing water depth. Transect 1 (Brasil Basin) $CaCO_3$-values drop from 98.5 % to 11.5 %; transect 2 (Guinea Basin) $CaCO_3$-values decrease from 98.2 % (w/w) to 79.6 % (w/w); transect 3 (western Cape Basin) $CaCO_3$-values diminish from 96.4 % (w/w) to 50.3 % (w/w); transect 4 (Namibia Continental Margin) $CaCO_3$-values decrease from 97.5 % (w/w) to 4.2 % (w/w).

In comparison to inorganic carbon, the organic carbon content (Fig. 3) of the sediment surface samples increases with respect to the Brasil Basin transect (0.16 % (w/w) to 0.8 % (w/w)), the Guinea Basin transect (0.14 % (w/w) to 0.48 % (w/w)), and the western Cape Basin transect (0.1 % (w/w) to 0.44 % (w/w)). Continental margin $C_{org}$-values decrease from 5.69 % (w/w) down to 0.24 % (w/w).

The rain ratio (Fig. 3) raises regarding the Brasil Basin transect from 0.002 to 0.069; regarding the Guinea Basin transect from 0.001 to 0.006; regarding the Cape Basin transect from 0.001 to 0.009. Namibia continental margin rain ratio first drops from 0.067 down to 0.003 and subsequently increases to 0.121.

## DISCUSSION

Globigerina bulloides *Dissolution Index*

As can be visualized immediately by looking at the photographs, the ultrastructure of *G. bulloides* worsens in regular patterns due to increasing carbonate dissolution (Plate I). Regarding the reticulate morphotype, spines and spine bases become reduced, spine bases and ridges become denuded, pores become funnel-like, the surface becomes chapped until complete parts will crack off. Regarding the crystalline morphotype edges and angles grow round, pores become buried, and at last crystals become completely distorted. However, in order to attain a specific dissolution stage not all preservation features of one preservation category have to occur. Applying equation (2.1) BDX values result in non-integer numbers which allow us to document even minor differences in the dissolution extent.

If regarded as data clusters BDX values can be assigned to three different oceanic realms (Fig. 2). The first cluster covers dissolution stages 1 and 2 and is found in surface sediments of the upper open ocean from 2,000 m to 4,300 m. The second cluster contains dissolution stages 2.5 to 5 and indicates the deep open ocean from 4,600 m to 5,300 m water depth. Between these two clusters where dissolution becomes rapidly stronger until

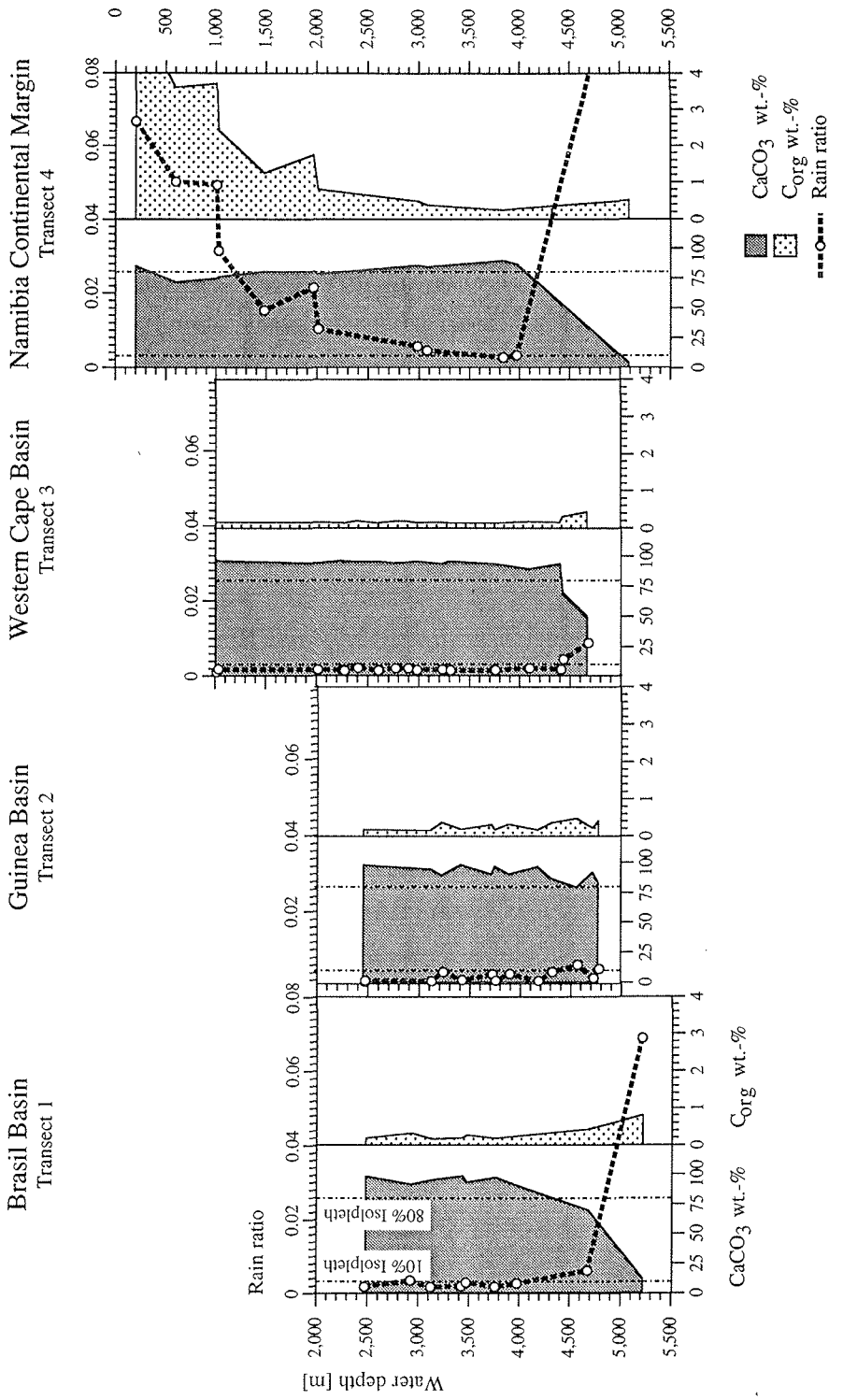


Fig. 3. Modification of $CaCO_3$ wt.-%, $C_{org}$ wt.-%, and rain ratio versus water depth. High rain ratio may be put down to the facts that a) productivity of organic carbon is enlarged vigorously which may lead to supralysoclinal dissolution, and that b) $CaCO_3$ values decrease due to sublysoclinal dissolution. Where the rain rate of calcitic and noncalcitic material is constant and neither productivity nor dilution are enhanced, rain ratio of organic to anorganic carbon remains constant and low. Data refer to GeoB surface sediment samples.

even fragments are completely dissolved we locate the border between upper and deep open ocean, namely the sedimentary lysocline. The third cluster includes dissolution stages 0.9 to 2.4 and is found in sediments of the upwelling influenced continental margin from 1,000 m to 3,900 m water depth. This area is reflected by high productivity within the Benguela system where significantly higher amounts of organic carbon than in the open ocean are delivered to the depth. Metabolic activities of benthic organisms lead to respiration and remineralization and subsequently to $CO_2$ enrichment at the sediment pore-water interface. This metabolic driven carbonate dissolution which was earlier described as supralysoclinal dissolution (Emerson and Bender, 1981; Jahnke *et al.*, 1994; Freiwald, 1995; Martin and Sayles, 1996) results in a higher basic dissolution potential.

The dissolution stages $R_1$ to $R_5$ (reticulate morphotype) and $C_1$ to $C_5$ (crystalline morphotype) based on our *G. bulloides* examinations are comparable to those of *G. bulloides* ("no dissolution" to "severe dissolution") investigated by Van Kreveld (1996) and to those of *Neogloboquadrina pachyderma* ($D_0$ "no dissolution" to $D_4$ "severe dissolution") introduced by Henrich *et al.* (1989) and Henrich (1989). Similar to our examinations on *G. bulloides*, sediment investigations on *G. bulloides* (Van Kreveld, 1996) and laboratory experiments on *Globigerinoides trilobus* (Hecht *et al.*, 1975) show that the initial dissolution first reduces spines and affects spine bases (Plate I).

Other micropaleontological approaches undertaken to reconstruct the sedimentary lysocline depth include (1) percent fragmented planktic foraminiferal tests (e.g., Keigwin, 1976; Le and Shackleton, 1992); (2) proportions of solution susceptible and solution resistant planktic foraminifera species (e.g., Schott, 1935; Berger, 1979; Boltovskoy and Totah, 1992); (3) the ratio of one organism group to another (e.g., Kennett, 1966; Hay, 1970; Parker, 1971; Berner, 1977; Peterson and Prell, 1985). Actually, each of these parameters is a potential dissolution index, but their variations are controlled by ecological rather than by geochemical factors (see compilation by Dittert *et al.*, subm.) Berger et al. (1982) developped the "elbow" model which illustrates the rapidly increasing dissolution at the lysocline basing on the relationship between foraminiferal preservation states and amount of calcite dissolution as a function of water depth. With our BDX tool we are able to expand Berger's "elbow" model and may distinguish the upper part into the upper open ocean and the upwelling influenced continental margin realm. At the bend we position the top of the sedimentary lysocline, and dissolution stage 5 corresponds to the CCD (Figs. 2, 4).

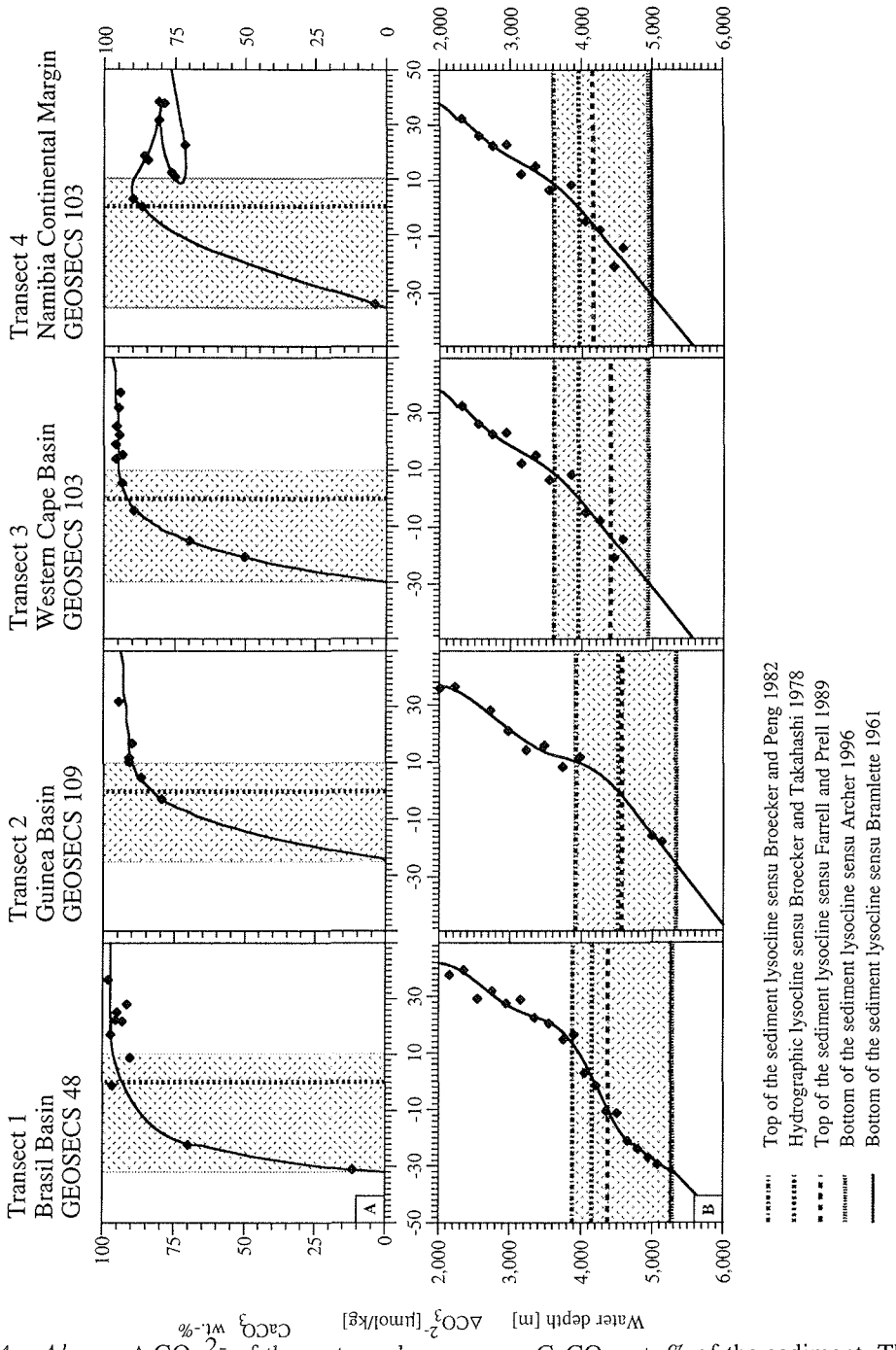


Fig. 4. *Above*: $\Delta CO_3^{2-}$ of the water column versus $CaCO_3$ wt.-% of the sediment. The top of the sedimentary calcite lysocline is defined by $\Delta CO_3^{2-}$ = 10 µmol/kg; the bottom of the sedimentary calcite lysocline is defined as the zero intercept of the $\%CaCO_3$ versus $\Delta CO_3^{2-}$ relation. The top of the hydrographic calcite lysocline horizon was estimated by the intercept of seawater carbonate ion content and the concentration of carbonate ions in equilibrium with seawater (saturation state $\Delta CO_3^{2-}$ = 0 µmol/kg) for calcite mineral phase (dotted line). *Below*: $\Delta CO_3^{2-}$ of the water column versus water depth below 2,000 m. Applying several methods, the top and the bottom of the hydrogryphic and the sedimentary calcite lysocline were calculated. The dotted area marks the thickness of the lysocline. $\Delta CO_3^{2-}$ values refer to GEOSECS locations 48, 103, and 109, whereas the calcium carbonate data come from GeoB sediment surface samples.

*Geochemical parameters*

In order to assess the BDX tool we seeked methods, which support our results. By means of the carbonate ion content of the water column (Takahashi *et al.*, 1980) and the calcium carbonate content of the sediment surface samples our conclusions were confirmed. The carbonate ion content at GEOSECS station 48 (Brasil Basin) ranges from 235 µmol/kg at the water surface to 77 µmol/kg at 5,075 m water depth. In the Guinea Basin (GEOSECS station 109) the values decrease from 247 µmol/kg at the water surface to 90 µmol/kg at 5,132 m. At GEOSECS station 103 (Cape Basin) the carbonate ion content drops from 219 µmol/kg at the water surface to 84 µmol/kg at 4,572 m. According to the equation introduced by Broecker and Takahashi (1978) the calcite saturation in the water column raises from 48 µmol/kg at the water surface to 114 µmol/kg at 5,500 m water depth.

Using several geochemical approaches we were able to determine the position of hydrographic and sedimentary lysocline as well as the CCD (Fig. 4). The hydrographic lysocline sensu Broecker and Takahashi (1978) is situated highest in the Cape Basin (transects 3 and 4) at 3,900 m and in the Brasil Basin at 4,150 m. In the Guinea Basin it is located at 4,500 m water depth (Fig. 4, 5). The reconstruction from sedimentary calcite (Figs. 3, 4) locates the top of the sedimentary lysocline 50 m to 450 m below the hydrographic lysocline. The 80 % isopleth (Fig. 4, Farrell and Prell, 1989) varies from 4,150 m (Namibia continental margin) to 4,350 m (Brasil Basin) to 4,400 m (western Cape Basin) to 4,550 m (Guinea Basin). Since at the hydrographic lysocline $\Delta CO_3^{2-}$ becomes zero, above the hydrographic lysocline the seawater is per definitionem supersaturated with respect to carbonate ion content. Nevertheless, $\Delta CO_3^{2-}$ of 10 µmol/kg is obviously enough to disturb the carbonate equilibrium persistently (Broecker and Peng, 1982). This leads to a sedimentary lysocline depth of 3,900 m in the Brasil- and the Guinea Basin (transects 1, 2) and 3,600 m in the Cape Basin (transects 3 and 4).

The bottom of the sedimentary lysocline sensu Archer (1996) varies from 4,900 m (Cape Basin) to 5,300 m (Brasil-; Guinea Basins). The 10 % isopleth (Figs. 3, 4) which is a marker of both the sediment lysocline bottom and the CCD sensu Bramlette (1961) varies from 4,900 m (Namibia continental margin) to 5,300 m (Brasil Basin). That is, in the Guinea Basin and the Cape Basin the CCD is not attained. Where the carbonate content drops below 10 % (w/w), we can ascertain that both the geochemical and the sedimentary reconstructions lead to a corresponding depth of the bottom of the lysocline. Presumably, this accordance is due to the fact that the 10 % isopleth and the zero intercept of the $\%CaCO_3$ versus $\Delta CO_3^{2-}$ relation coincide approximately with the progressive dissolution increase of $\Delta CO_3^{2-}$ (Keir, 1980) below the top of the lysocline.

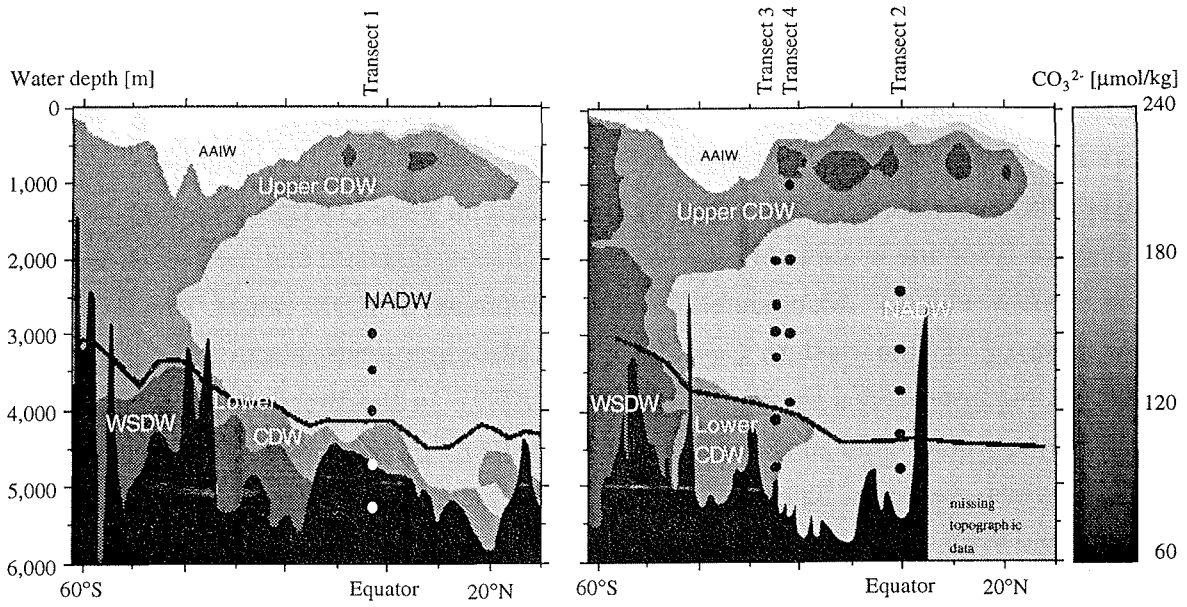


Fig. 5. Present-day stratification of the main water masses in the South Atlantic as displayed by $CO_3^{2-}$ ion content. Carbonate ion distribution refers to Geochemical Ocean Section Study data (GEOSECS, Bainbridge, 1981). The lysocline depth (black line) was calculated according to Broecker and Takahashi (1978). In the western section of the South Atlantic carbonate ion content decreases continually southwards due to the strong influence of AABW. Consequently, the lysocline raises from 4,000 m up to 3,000 m. In the eastern section of the South Atlantic, North Atlantic Deep Water (NADW) is stopped southwards at the Walvis Ridge and at the SW Indian Ridge. Hence, the lysocline raises in steps. Dots indicate the position of the sample locations.
CDW...Circumpolar Deep Water; AAIW...Antarctic Intermediate Water; NADW...North Atlantic Deep Water; WSDW ... Weddell Sea Deep Water; AABW ... Antarctic Bottom Water (WSDW + Lower CDW)

Another clue for the assessment of the lysocline depth is the influence of organic carbon. Our results show, that at the open ocean realm of all three South Atlantic basins the amount of sedimentary $C_{org}$ is below 1 % (w/w) (Fig. 3). However, the rain ratio increases rapidly at distinct water depths. Where the values exceed 0.004, the top of the lysocline sensu Farrell and Prell (1989) is attained exactly (Fig. 3). At the continental margin it will be noticed immediately that even in lower water depths high amounts of organic carbon (up to 5.69 % (w/w)) are present, which is to explain by the enormous productivity of the Benguela upwelling system. The high rain ratio (up to 0.067) and the smooth break of carbonate content (down to 71 % (w/w)) at water depths of 350 m down to 1,400 m lead us to assume a certain amount of supralysoclinal dissolution (Emerson and Bender, 1981; Jahnke *et al.*, 1994).

*Comparison of* Globigerina bulloides *Dissolution Index and geochemical parameters*

As we can show by the increase of the BDX values above the lysocline (Fig. 2), carbonate dissolution obviously affects *G. bulloides*' ultrastructure even at supersaturation state as it was stated by Broecker and Peng (1982). According to BDX values the lysocline is attained only by transect 1 (Brasil Basin) and transect 3 (western Cape Basin) which is documented by a rapid increase of BDX values. Regarding the Brasil Basin and the western Cape Basin our lysocline reconstruction through BDX matches the approaches by Farrell and Prell (1989). In the Brasil Basin BDX values increase between 3,977 m (GeoB 1117-3) and 4,675 m (GeoB 1118-2) by leaps and bounds which covers the calculated sedimentary lysocline depth of 4,350 m (according to Farrell and Prell, 1989). In the western Cape Basin BDX values increase between 4,089 m (GeoB 1211-1) and 4,669 m (GeoB 1212-2) which covers the calculated depth of 4,400 m (according to Farrell and Prell, 1989). However, the exact determination of the lysocline depth through BDX is not possible due to the low sample density. The most severe deviation from BDX involves the method by Broecker and Peng (1982) which locates the sedimentary lysocline several hundred meters above the hydrographic lysocline (Fig. 4). As confirmed by BDX and the approach by Farrell and Prell (1989) the statical view of the 10 µmol/kg border (Broecker and Peng, 1982) underestimates the depth of the sedimentary lysocline vigorously in comparison to the hydrographic lysocline (Broecker and Takahashi, 1978). Nevertheless, dissolution even becomes evident at supersaturation state (Fig. 2). We attribute that offset between the hydrographic lysocline and the sedimentary lysocline to the fact that dissolution mostly occurs at the sediment pore water interface rather than in the water column. That is, at this interface $[CO_3^{2-}]$ is very likely to be higher than at the equivalent water depth in the water column (Le and Shackleton, 1992). According to BDX values the CCD is attained only by transect 1 (Brasil Basin) which is shown by dissolution stage 5 at about 5,213 m (Fig. 2). Our reconstruction fits the approaches by Archer (1996) and Bramlette (1961) which locate the CCD at about 5,300 m (Fig. 4).

Regarding the top and the bottom of the sedimentary calcite lysocline, all reconstructions show a consistent picture which we attribute to the bottom water distribution (Fig. 5). While AABW - as a composite of Weddell Sea Deep Water and Lower Circumantarctic Deep Water - is moving more or less unhampered northwards within the Brasil Basin, it is orographically detained within the Cape- and the Guinea Basins by the Mid Atlantic Ridge and the Walvis Ridge (Fig. 1). The inflow of AABW into the Guinea Basin is restricted to only small quantities passing the sills through the Romanche-, the Chain Fracture Zone and the Walvis Passage (Van Bennekom and

Berger, 1984; Shannon and Chapman, 1991; Warren and Speer, 1991; Mercier *et al.*, 1994). Consequently, the deepest parts of the Guinea Basin are filled almost exclusively by $O_2$ ameliorated, $CO_2$ depleted, and carbonate ion saturated NADW (Kroopnick, 1985). The Cape Basin, although located eastwards of the Mid Atlantic Ridge, is dominated by AABW below 4,000 m due to a bottom water passage, which allows AABW to enter the basin from the south (Reid, 1989). Therefore, lysocline depth and sublysoclinal carbonate dissolution pattern in the open ocean seem to depend on both the influence of the corrosive AABW and the asymmetry of its oceanographic distribution (Figs. 1, 5).

## CONCLUSIONS

Ultrastructure dissolution susceptibility of the planktic foraminifer, *G. bulloides*, carbonate ion content of the water column, calcium carbonate content of the sediment surface, and rain ratio derived from sediment surface samples were used to reconstruct the position of hydrographic and sedimentary calcite lysocline as well as the CCD in the modern South Atlantic Ocean. Carbonate data from the water column refer to the GEOSECS locations 48, 103, and 109, calcium carbonate data come from 19 GeoB sediment surface samples of four transects into the Brasil-, the Guinea-, and the Cape Basins. Our results lead to following conclusions:

1) *G. bulloides*' undergoes remarkably ultrastructural breakdown with increasing carbonate dissolution even above the lysocline which we converted into *Globigerina bulloides* Dissolution Index (BDX).

2) We give evidence for a sharp BDX increase at the top of the sedimentary lysocline and for the total erase of this species at the bottom of the lysocline or the CCD. Additionally, BDX puts us in the position to distinguish the upper open ocean and the upwelling influenced continental margin above from the deep ocean below the sedimentary lysocline.

3) Water column carbonate ion data, sedimentary calcite data, and rain ratio assess BDX to go for a valuable (pale-)oceanographic proxy in order to confirm BDX. For future work our new tool BDX may enable us to derive Pleistocene lysocline fluctuations from gravity core samples.

4) As shown by BDX both the hydrographic lysocline (in the water column) and the sedimentary lysocline (at the sediment pore-water interface) mark the boundary between the carbonate ion undersaturated and highly corrossive AABW and the carbonate ion saturated NADW of the modern South Atlantic.

*Acknowledgements*—We thank H. Meggers, S. Mulitza and H.-S. Niebler for constructive comments and careful review of the manuscript. Finally, we thank M. Matthies and R. Schlotte, who assisted the processing of the GEOSECS data set, and H. Heilmann, R. Henning, and C. Wienberg for technical collaboration. This investigation was funded by the German Research Foundation (SFB No. 261). This is SFB 261 contribution no. xxx at Bremen University.

## REFERENCES

Archer, D. E. (1996) An Atlas of the distribution of calcium carbonate in sediments of the deep sea. *Global Biogeochemical Cycles*, **10**(1), 159-174.

Bainbridge, A. E. (1976) *GEOSECS Atlantic Expedition, Sections and Profiles*. National Science Foundation, Superintendent of Documents, US Government Printing Office, Washington, DC.

Bainbridge, A. E. (1981) *GEOSECS Atlantic Expedition, Hydrographic Data, 1972-1973*. National Science Foundation, Superintendent of Documents, US Government Printing Office, Washington, DC, 121 pp.

Baumann, K.-H. and Meggers, H. (1996) Paleoceanographical change in the Labrador Sea during the last 3.1 MY: Evidence from calcareous plankton records. In *Microfossils and Oceanic Environments,* A. Moguilevsky and R. Whatley (eds), pp. 131-154. Aberystwyth-Press, Aberystwyth.

Bé, A. W. H., Morse, J. W. and Harrison, S. M. (1975) Progressive dissolution and ultrastructural breakdown of planktonic foraminifera. In *Dissolution of Deep-Sea Carbonates,* W. V. Sliter, A. W. H. Bé and W. H. Berger (eds), pp. 27-55. Cushman Found. Foram. Res. Spec. Publ., Ithaka, NY.

Berger, W. H. (1979) Preservation of foraminifera. In *Foraminiferal Ecology and Palecology,* J. H. Lipps, W. H. Berger, M. A. Buzas, R. G. Douglas and C. A. Ross (eds), pp. 105-155. Society of Economic Paleontologists and Mineralogists, Houston.

Berger, W. H., Bonneau, M.-C. and Parker, F. L. (1982) Foraminifera on the deep-sea floor: lysocline and dissolution rate. *Oceanologica Acta*, **5**(2), 249-258.

Berger, W. H. and Keir, R. S. (1984) Glacial-Holocene changes in atmospheric $CO_2$ and the deep-sea record. In *Climate processes and climate sensitivity,* J. E. Hansen and T. Takahashi (eds), pp. 337-351. Geophys. Monogr. 29, Maurice Ewing Series, Washington, DC.

Berner, R. A. (1977) Sedimentation and dissolution of pteropods in the ocean. In *The Fate of Fossil Fuel $CO_2$ in the Oceans,* N. R. Andersen and A. Malahoff (eds), pp. 243-260. Plenum Press, New York, NY.

Bickert, T. and Wefer, G. (1996) Late Quaternary deep water circulation in the South Atlantic: Reconstruction from carbonate dissolution and benthic stable isotopes. In *The South Atlantic: Present and past circulation,* G. Wefer, W. H. Berger, G. Siedler and D. J. Webb (eds), pp. 599-620. Springer-Verlag, Berlin Heidelberg.

Boltovskoy, E. and Totah, V. I. (1992) Preservation index and preservation potential of some foraminiferal species. *Journal of Foraminiferal Research*, **22**(3), 267-273.

Boyle, E. A. (1988) Vertical oceanic nutrient fractionation and glacial/interglacial CO2 cycles. *Nature*, **331**, 55-56.

Bramlette, M. N. (1961) Pelagic sediments. In *Oceanography,* M. Sears (ed) pp. 345-366. AAAS Publication, New York, NY.

Broecker, W. S. (1997) Thermohaline Circulation, the Achilles Heel of our climate system: Will man made $CO_2$ upset the current balance? *Science*, **278**, 1582-1588.

Broecker, W. S. and Denton, G. H. (1989) The role of ocean-atmosphere reorganizations in glacial cycles. *Geochimica et Cosmochimica Acta*, **53**, 2465-2501.

Broecker, W. S. and Peng, T. H. (1982) *Tracers in the Sea.* Eldigio Press, New York, NY, 689 pp.

Broecker, W. S. and Takahashi, T. (1978) The relationship between lysocline depth and in situ carbonate ion concentration. *Deep-Sea Research*, **25F**(1), 65-95.

CLIMAP Project members (1976) The surface of the ice-age earth. *Science*, **191**(4232), 1131-1137.

d'Orbigny, A. (1826) Tableau méthodique de la classe des Céphalopodes. *Annales des Sciences Naturelles*, **7**, 245-314.

Dittert, N., Baumann, K.-H., Bickert, T., Henrich, R., Huber, R., Kinkel, H., Meggers, H. and Müller, P. J. (subm.) Carbonate dissolution in the deep sea: Methods, quantification and paleoceanographic application. In *Proxies in paleoceanography,* G. Fischer and G. Wefer (eds), Springer-Verlag, Berlin Heidelberg.

Emerson, S. and Bender, M. (1981) Carbon fluxes at the sediment-water interface of the deep-sea: Calcium carbonate preservation. *Journal of Marine Research*, **39**, 139-162.

Farrell, J. W. and Prell, W. L. (1989) Climatic change and $CaCO_3$ preservation: An 800,000 year bathymetric reconstruction from the central equatorial Pacific Ocean. *Paleoceanography*, **4**(4), 447-466.

Freiwald, A. (1995) Bacteria-induced carbonate degradation: A taphonomic case study of *Cibicides lobolatus* from a high-boreal carbonate setting. *Palaios*, **10**, 337-346.

Hay, W. W. (1970) Calcareous nannofossils from cores recovered on Leg 4. *Initial Report Deep Sea drilling Project*, **4**, 455-501.

Hecht, A. D., Eslinger, E. V. and Garmon, L. B. (1975) Experimental studies on the dissolution of planktonic foraminifera. *Cushman Foundation For Foraminiferal Research Special Publication*, **13**, 56-96.

Hemleben, C., Spindler, M. and Anderson, O. R. (1989) *Modern planktonic foraminifera.* Springer-Verlag, New York, NY, 363 pp.

Henrich, R. (1989) Glacial/interglacial cycles in the Norwegian Sea: Sedimentology, paleoceanography, and evolution of late Pliocene to Quaternary northern hemisphere climate. In *Proceedings of the Ocean Drilling Program, Scientific Results,* O. Eldholm, J. Thiede and E. Taylor (eds), pp. 189-232. College Station, TX.

Henrich, R., Kassens, H., Vogelsang, E. and Thiede, J. (1989) Sedimentary facies of glacial-interglacial cycles in the Norwegian Sea during the last 350 ka. *Marine Geology*, **86**, 283-319.

Imbrie, J. and Kipp, N. G. (1971) A new micropaleontological method for quantitative paleoclimatology: application to a Late Pleistocene Carribean core. In *Late Cenocoic glacial ages,* K. K. Turekian (ed) pp. 71-181. Yale University Press, New Haven.

Jahnke, R. A., Craven, D. B. and Gaillard, J. F. (1994) The influence of organic matter diagenesis on $CaCO_3$ dissolution at the deep-sea floor. *Geochimica et Cosmochimica Acta*, **58**, 2799-2809.

Keigwin, L. D. (1976) Late Cenozoic planktonic foraminiferal biostratigraphy and paleoceanography of the Panama Basin. *Micropaleontology*, **22**, 419-422.

Keir, R. S. (1980) The dissolution kinetics of biogenic calcium carbonates in seawater. *Geochimica et Cosmochimica Acta*, **44**, 241-252.

Kennett, J. P. (1966) Foraminiferal evidence of a shallow calcium carbonate solution boundary, Ross Sea, Antarctica. *Science*, **153**(3732), 191-193.

Kroopnick, P. M. (1985) The distribution of $^{13}C$ of $\Sigma CO_2$ in the World Oceans. *Deep-Sea Research*, **32**(1), 57-84.

Le, J. and Shackleton, N. J. (1992) Carbonate dissolution fluctuations in the western equatorial Pacific during the Late Quaternary. *Paleoceanography*, **7**, 21-42.

Martin, W. R. and Sayles, F. L. (1996) $CaCO_3$ dissolution in sediments of the Ceara Rise, western equatorial Atlantic. *Geochimica et Cosmochimica Acta*, **60**(2), 243-263.

Mercier, H., Speer, K. G. and Honnorez, J. (1994) Tracing the Antarctic Bottom Water through the Romanche and Chain Fracture Zones. *Deep-Sea Research*, **41**, 1457-1477.

Parker, F. L. (1971) Distribution of planktonic foraminifera in recent deep-sea sediments. In *The micropaleontology of oceans,* B. M. Funnell and W. R. Riedel (eds), pp. 289-307. Cambridge University Press, Cambridge.

Peterson, L. C. and Prell, W. L. (1985) Carbonate dissolution in recent sediments of the eastern equatorial Indian Ocean: Preservation patterns and carbonate loss above the lysocline. *Marine Geology*, **64**, 259-290.

Reid, J. L. (1989) On the total geostrophic circulation of the South Atlantic Ocean: Flow patterns, tracers and transports. *Progress in Oceanography*, **23**, 149-244.

Reid, J. R. (1996) On the circulation of the South Atlantic. In *The South Atlantic: Present and past circulation,* G. Wefer, W. H. Berger, G. Siedler and D. J. Webb (eds), pp. 13-44. Springer-Verlag, Berlin Heidelberg.

Schott, W. (1935) Die Foraminiferen in dem Äquatorialen Teil des Atlantischen Ozeans. *Wissenschaftliche Ergebnisse der Deutschen Atlantik Expedition Meteor 1925-1927*, **3**, 1-135.

Schulz, H. D. and cruise participants (1992) Bericht und erste Ergebnisse über die Meteor-Fahrt M20/2, Abidjan-Dakar, 27.12.1991-3.2.1992. *Berichte, Fachbereich Geowissenschaften, Universität Bremen*, **25**, 1-173.

Shannon, L. V. and Chapman, P. (1991) Evidence of Antarctic Bottom Water in the Angola Basin at 32°S. *Deep-Sea Research*, **38**, 1299-1304.

Takahashi, T., Broecker, W. S., Bainbridge, A. E. and Weiss, R. F. (1980) *Carbonate chemistry of the Atlantic, Pacific and Indian Oceans: The results of the GEOSECS expeditions 1972-1978.* Lamont-Doherty Geological Observatory, Palisades, NY, 211 pp.

Van Bennekom, A. J. and Berger, G. W. (1984) Hydrography and silica budget of the Angola Basin. *Netherlands Journal of Sea Research*, **17**, 149-200.

Van Kreveld, S. A. (1996) Calcium carbonate dissolution indices on the northeast Atlantic sea floor. In *Late Quaternary sediment records of mid-latitude Northeast Atlantic calcium carbonate production and dissolution,* S. A. Van Kreveld-Alfane (ed) pp. 135-184. FEBO B.V., Enschede.

Warren, B. A. and Speer, K. G. (1991) Deep circulation in the eastern South Atlantic Ocean. *Deep-Sea*

*Research*, **38**(Suppl. 1), 281-322.

Wefer, G., Bleil, U. and cruise participants (1990) Bericht über die Meteor-Fahrt M12/1, Kapstadt-Funchal, 13.3.1990-14.4.1990. *Berichte, Fachbereich Geowissenschaften, Universität Bremen*, **11**, 1-66.

Wefer, G., Bleil, U., Schulz, H. D. and cruise participants (1989) Bericht über die Meteor-Fahrt M9-4, Dakar-Santa Cruz, 19.2.-16.3.1989. *Berichte, Fachbereich Geowissenschaften, Universität Bremen*, **7**, 1-103.

# 4. Carbonate dissolution in the deep-sea: Methods, quantification and paleoceanographic application

N. Dittert, K.-H. Baumann, T. Bickert, R. Henrich, R. Huber, H. Kinkel and H. Meggers

*Fachbereich Geowissenschaften, Universität Bremen, 28334 Bremen, Germany*

**Abstract:** Understanding spatial and temporal changes in oceanic carbonate dissolution and preservation patterns is of key importance for testing models which seek to explain past changes in atmospheric $p\ CO_2$ and surface water $P\ CO_2$ through changes in the global carbon cycle.

As part of the *South Atlantic Dissolution Experiment*, three deep-sea transects covering areas above and below the calcite lysocline into the Brazil- and through the Cape Basin were investigated. Our work includes (1) determination of sediment surface assemblages of coccolithophores and planktic foraminifera; (2) SEM ultrastructure analysis of planktic foraminifera *Globigerina bulloides*; and (3) comparative assessment of different carbonate dissolution proxies.

We find that all dissolution proxies are able to distinguish the area above the top of the calcite lysocline from the area below. Moreover, some parameters are qualified to distinguish the upper continental margin of upwelling areas from the open ocean. Regarding three different oceanographic regimes, only the carbonate ion content and the percentage of sediment carbonate content put us in the position to determine the total scale of the lysocline. If these parameters are not available, a combination of the *Globigerina bulloides* Dissolution Index, the *Calcidiscus leptoporus - Emiliania huxleyi* Dissolution Index, and the rain ratio give the best approach to the authentic conditions.

## *Prologue*

By publishing his article "On the Distribution of the Pelagic Foraminifera at the Surface and on the Floor of the Ocean" as a monthly review of scientific progress, Murray (1897) laid the foundations of a topic that still occupies scientists 100 years later: he realized that the gradual disappearance of calcareous shells with increasing water depths is due to the solvent action of deep-sea water. The importance of the ocean as one principal global carbon reservoir and the close relationship between $CO_2$ and climatic change led oceanographers and paleoceanographers to explore intensively the balance between

biogenic production and $CaCO_3$ accumulation-dissolution through time.

## Introduction

As early as in the late 19th century Murray and Renard (1891) realized that the distribution and character of *Globigerina* ooze are governed by the bio-/zoogeography of the living organisms in surface currents and by the chemistry of deep-sea water that is responsible for the modification of the sediment and organism assemblages. In particular, they noted that dissolution works selectively, and that below a depth of about 4,000 m in the central Pacific it destroys essentially all calcareous matter. In addition, Murray (1897) explained the different shell dissolution patterns observed by the powerful solvent action of decaying organic matter on carbonates. With expanded knowledge in micropaleontology, changes in faunal composition recorded in pelagic sequences could be explained to be dependent on both changes in the composition of the living assemblages and in the intensity of dissolution and resulting fragmentation of the tests (Schott 1935).
Even before this, Philippi (1910) already had established the hypothesis of increased activity of Antarctic Bottom Water during glacials based on an enhanced carbonate dissolution. However, one obstacle in recognizing that carbonate dissolution in the eastern tropical Pacific was in fact less important during glacials than during interglacials was the (mistaken) notion of *Globigerina* sp. as being highly resistant to dissolution and of *Globorotalia* sp. as being highly susceptible to it (Arrhenius 1952). The reverse has been shown to be correct (Berger 1967). In contrast to the situation in the equatorial Pacific, Olausson (1965) showed that interglacials can be assigned to high-carbonate stages and glacials to low-carbonate stages in the Atlantic.
The first demonstration that the long-term exposure of calcite crystals to sea water on deep-sea moorings revealed information on the depth dependence of dissolution rate and calcite saturation was given by Peterson (1966). Milliman (1975) repeated Peterson's experiment in the North Atlantic using aragonite, low and high Mg calcite and confirmed that each of these carbonate varieties had its own lysocline occurrence at critical levels of undersaturation.
Berger (1967, 1968) ranked planktic foraminifera species collected from sediment samples according to dissolution resistance as a basis for forming dissolution indices. Furthermore, he exposed samples which were derived from sediment and from plankton tows on a taut wire buoy (same mooring as that used by Peterson 1966) at different depths in the central Pacific, in order to assess the effects of dissolution on foraminiferal shells. Additional information on the dissolution of planktic organisms were delivered by

investigations on coccolithophores (Hay 1970) as well as on pteropods (Berner 1977). Comparison of laboratory experiments with surface sediment samples indicated differential preservation of coccolithophore species in oceanic sediments (McIntyre and McIntyre 1971). Further evidence of differential dissolution among shells from analyses of living specimens and fossil shells has been obtained by in-situ experiments using sediment traps (Honjo and Erez 1978) and by laboratory experiments (Bé et al. 1975); comparisons between water column communities and sediment assemblages (including in-situ investigations) were performed by Vilks (1975).
With technological progress and the invention of scanning electron microscopy, Bé et al. (1975) started investigations of foraminiferal ultrastructure reaction to carbonate dissolution. They elaborated various species-specific SEM dissolution indices. This approach has been evaluated for *Neogloboquadrina pachyderma* (Henrich 1989; Baumann and Meggers 1996) and for *Globigerina bulloides* (Van Kreveld 1996; Dittert and Henrich subm). For both species the progressive ultrastructural breakdown with increasing dissolution could be shown.

In order to outline the essentials for carbonate dissolution in the deep-sea, a brief review on the carbon dioxide system and on the deep-water circulation in the world oceans will be presented. Many different methodical approaches were established as dissolution proxies in the past. We will contemplate the most important ones regarding the use of bulk sediment parameters and the use of calcareous micro- and nannoplankton. Since the history of "*Carbonate dissolution in the deep-sea*" covers more than one hundred years, only a few scientists who improved the comprehension of that complex topic can be mentioned. An excellent summary on previous studies is given by Boltovskoy (1991).
This leads up to the *South Atlantic Dissolution Experiment*, where the mentioned parameters are tested for their usefulness at three surface sediment transects into the Brazil Basin and through the Cape Basin. At last, we will elucidate the advantages and disadvantages of several dissolution proxies.

## Some aspects on the carbon dioxide system and carbonate dissolution

The carbon dioxide flux between atmosphere and ocean surface water is governed by molecular diffusion. Thereby the direction and magnitude of the $CO_2$ flux depend on the gas exchange coefficient of carbon, the thickness of the surface water boundary layer, the solubility coefficient, and the partial pressure difference between sea water and air (Liss 1973; Millero 1979; Liss and Merlivat 1986; Maier-Reimer and Hasselmann 1987). Only

about 1% of dissolved $[CO_2]_{aqua}$ occurs as $H_2CO_3$, the rest of the $CO_2$ exists in the form of different ions. Representatives of inorganic carbon are carbonic acid, bicarbonate and carbonate. Coccolithophores, foraminifers, pteropods, and a few other organisms build calcium carbonate shells or skeletons. Calcification can proceed both from carbonate and bicarbonate ions. In any case, it tends to drive $CO_2$ from the ocean to the atmosphere (Gattuso et al. 1993).

The transfer of calcium carbonate particles from the mixed layer to the deep ocean was introduced as carbonate pump or alkalinity pump (Berger 1982). The vertical distribution of organic carbon in the ocean is mainly controlled by photosynthesis, feeding, respiration, and decay (Berger et al. 1989) which contribute to the biological pump (Revelle 1944). With respect to the water column, $Ca^{2+}$ varies relatively little, hence the calcite saturation state is controlled by the concentration of $CO_3^{2-}$, temperature, and water pressure. Position and thickness of the saturation horizon in the water column can be defined as the difference $\Delta CO_3^{2-}$ between the concentration of carbonate *in situ* and the concentration of saturated carbonate ion for the mineral phase calcite (Broecker and Takahashi 1978).

Carbonate dissolution in the water column (Culkin 1965; Edmont 1970; Murray and Riley 1971) and at the sediment pore water interface (Santschi et al. 1983; Le and Shackleton 1992) depend on the disequilibrium of the total carbon dioxide content ($\Sigma CO_2$). It is balanced with $HCO_3^-$ and $CO_3^{2-}$ and driven by the alkalinity (Fig. 1; Baes 1982). The water depth in which the sea water carbonate ion content and the concentration of carbonate ions in equilibrium with sea water for calcite mineral phase intercept was introduced as the hydrographic calcite lysocline (Broecker and Takahashi 1978) - also known as "Peterson's level" (Berger 1975). It is stated that an undersaturation of about 10 µmol/kg is enough to dissolve almost all the calcite descending to the sea-floor (Broecker and Peng

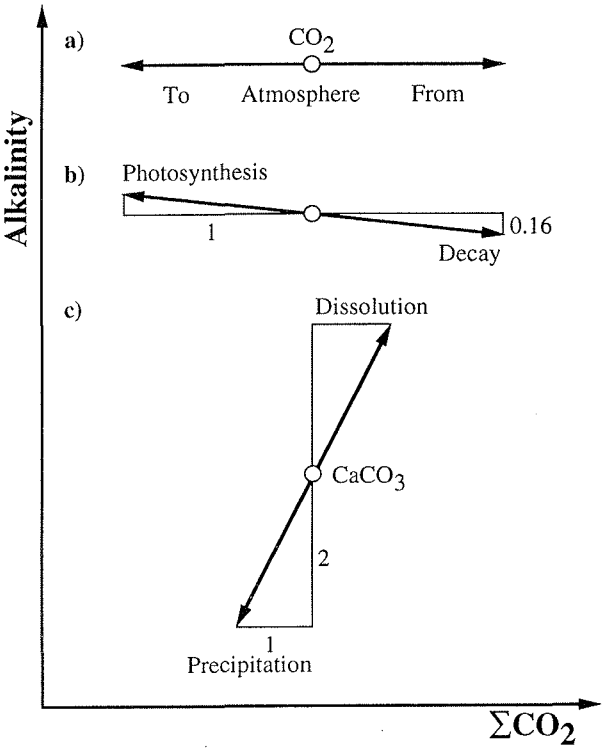


**Fig. 1.** $\Sigma CO_2$-alkalinity-vector-diagram which describes changing alkalinity and total carbon content according to a) supply and withdrawal of $CO_2$ to/from the atmosphere; b) enhanced photosynthesis or decay; c) increased $CaCO_3$ precipitation or dissolution (modified after Baes 1982).

1982). The depth at which the effects of dissolution first appear in the sediments is termed sedimentary lysocline (Berger 1975), foraminiferal lysocline (Berger 1968), or coccolith lysocline (Berger 1973a), respectively. Keir (1980) discovered that dissolution becomes progressively more intense in proportion to the fourth power of $\Delta CO_3^{2-}$ below the lysocline. Where undersaturation is large enough so that the rate of calcite sedimentation is totally compensated for by the rate of calcite dissolution, the carbonate compensation depth (CCD) is attained (Bramlette 1961), which is described by Archer (1996) as the zero intercept of the $\%CaCO_3$ versus $\Delta CO_3^{2-}$ relation.

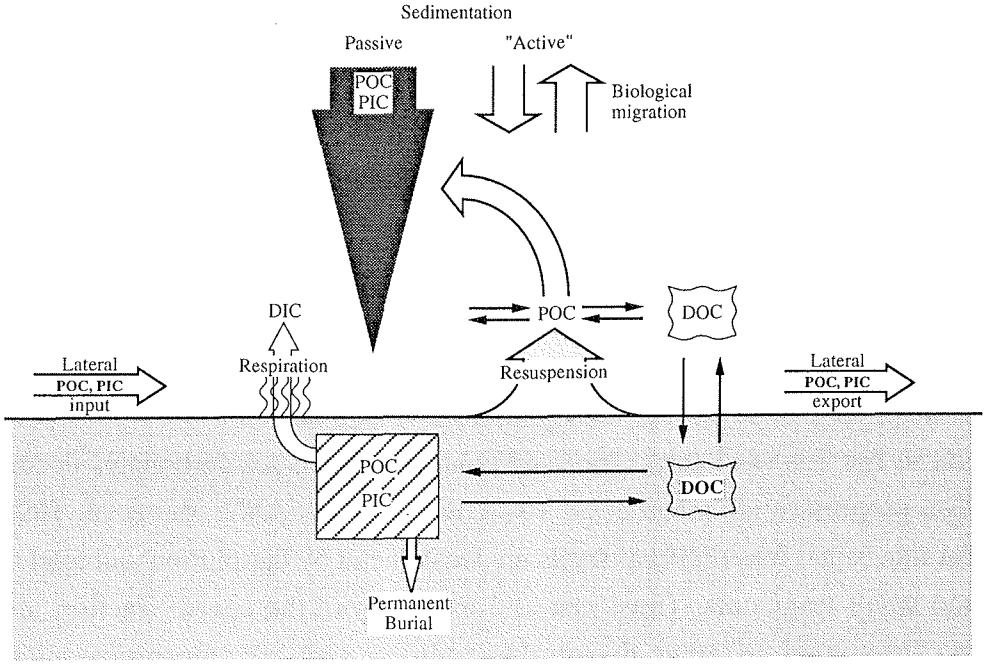


**Fig. 2.** Carbon fluxes at the benthic boundary layer (from JGOFS 1989).
I ... Inorganic; O ... Organic; C ... Carbon; P ... Particulate; D ... Dissolved

The by far greatest fraction of the organic carbon arriving at the sea-floor is respired as $CO_2$ or remineralized to other organic compounds by benthic organisms (Reimers 1989). This metabolic $CO_2$ generated by organisms which live within the sediment may contribute to the dissolution of calcite even above the lysocline, known as supralysoclinal dissolution (Emerson and Bender 1981; Jahnke et al. 1994; Freiwald 1995). Other parts of the vertical and horizontal flux to the sediment are degraded or resuspended and recycled back into the ocean (Fig. 2). The remaining material is perturbed in the uppermost centimeters and decimeters of the sediment by benthic organisms. Molecular diffusion alone, coupled with the low solubility of calcite, would yield extremely low dissolution rates. The benthic mixing process continually accumulates new calcite into the

sediment eliminating the necessity for a long diffusion path (Broecker and Peng 1982). At last, the benthic boundary layer (Santschi et al. 1983) is the site of carbon removal from the ocean-atmosphere system and constitutes the historical record of the carbon flux - perhaps distorted by the process of diagenesis - from which paleoceanographic and paleoclimatic changes are deciphered (Jumars et al. 1989). Long records of carbonate fluctuations exhibit long-term trends in dissolution (e. g., the Mid-Brunhes dissolution cycle) which are thought to be associated with global changes in the carbon reservoir of the oceans (Vincent 1981; Farrell and Prell 1991; Bassinot et al. 1994; Bickert et al. 1997). Thus, for reconstructing the deep-water chemistry in the past, both the respiratory effect and the global trend have to be considered to extract the true deep-water properties from dissolution records.

## The use of bulk sediment parameters as dissolution proxies

Quantitative reconstruction of carbonate dissolution to times of the past is not a simple matter. It requires the determination of the fraction of calcite rained to the sea-floor which survived dissolution. Unfortunately, among the several criteria used to judge the state of preservation of the calcite most remain qualitative. One indicator is the weight percentage of the coarse fraction (>63 μm). The sand content of deep-sea carbonates decreases as dissolution progresses (Johnson et al. 1977; Berger et al. 1982; Wu et al. 1990). The reason for this is that foraminiferal shells are weakenend by dissolution and tend to break down into small fragments. Thus, material moves from the coarse fraction into finer fractions. Inspection of other dissolution indices, such as calcareous micro- and nannoplankton dissolution proxies (see chapter below), investigated in deep-sea sediments by several authors (e.g., Hebbeln et al. 1990; Yasuda et al. 1993), shows a good agreement with the sand content records of each study. However, other sediment related studies on the deep-sea rise reveal that foraminiferal fragmentation and hence the percentage of the fine fraction increases before the significant overall loss of carbonate begins, and thus may be more sensitive to changes in bottom water or pore water corrosiveness than bulk carbonate. For instance, Peterson and Prell (1985) showed that about 60 % of the non-fragmented sand-sized planktic foraminifera were already broken at the lysocline level, whereas no more than 20 % to 30 % of carbonate has been lost. This mismatch in sensitivities may be due to the transfer of carbonate during the fragmentation from larger to smaller size fractions. Furthermore, changes in the rain ratio between nannofossil placoliths and foraminiferal shells could bias the relative portion of the coarse fraction without any changes in dissolution (e.g., Bickert and Wefer 1996).

Therefore, the sand content is not an unambiguous proxy for dissolution and requires calibration with other dissolution indices prior to the interpretation of its variation with time.

A potentially more quantitative index of calcite dissolution is the percentage of $CaCO_3$ in the sediment. Of course, variations in the percentage of $CaCO_3$ in a single core cannot be simply interpreted as an index of preservation because the relative abundance of carbonate is controlled by the balance of productivity over dissolution and by dilution due to the influx of non-carbonate sedimentary components. Only in the ideal situation, where the rain rate of calcitic and of noncalcitic material are constant in space and time, the amount of calcite lost to dissolution could be calculated from the percentage $CaCO_3$ in the sediment. Otherwise, for each time interval of interest, the calcite content of the sediment from above the lysocline has to be used as the reference for the amount of dissolution which has occurred in cores from the transition zone (the "depth-transect approach"; e.g., Farrell and Prell 1989; Curry and Lohmann 1990; Bickert et al. 1997). However, the fact that $CaCO_3$-contents of supralysoclinal sediment average to about 90 % in the world ocean (Archer 1996) raises the problem that quite large amounts of dissolution create only very small changes in the carbonate content. For example, if a sediment which, in the absence of dissolution, would have a calcite content of 90 % were to lose half of its calcite to dissolution, its $CaCO_3$-content would drop to only 82 %. Because of this, even small variations in the ratio of the rain rate of calcite to the rain rate of non-calcite would lead to substantial errors in the extent of dissolution.

One way out of this dilemma could be the conversion of $CaCO_3$ % (w/w) to $CaCO_3$ mass accumulation rate (MAR), which corrects for the effect of dilution in the sediment. According to van Andel et al. (1975) the $CaCO_3$-MAR is calculated as:

$$CaCO_3\text{-MAR } (g/cm^2/ky) = CaCO_3 \text{ \% (w/w)} \cdot DBD\ (g/cm^3) \cdot SR\ (cm/ky) \qquad (1)$$

This calculation requires estimates of dry bulk densities (DBD) for the sediments and sedimentation rates (SR). DBD, if not measured directly, might be calculated using the empiric equation of Ruddiman and Janecek (1989). The major problem comes from the SR, which is commonly derived by linear interpolation between stratigraphic datums based on oxygen isotope, paleomagnetic and biostratigraphic events. Especially, if the variance of the carbonate content is low, the $CaCO_3$-MAR will be dominated by the SR changes, which depend on the resolution of the age model and which are mostly difficult to reproduce the sediment accumulation variability with time.

Two other processes are at work which could bias the interpretations based on the $CaCO_3$-content. The first of these consists in the winnowing of sediment by currents which carry away the fine material and thereby enrich the coarse material (mainly shells). This raises the $CaCO_3$-content (Wu et al. 1990). The other is deposition by turbidity and

boundary currents. As currents often originate along the continental margins, the debris they carry is usually very low in $CaCO_3$. To avoid the impacts of these processes, quiet zones on the sea-floor must be carefully chosen as the localities for such studies.
Regarding all these potential complications, how should one carry out a reliable quantification of calcite dissolution in the deep-sea? Significant progress has been made in modelling the diagenesis of $CaCO_3$ in sediments, on diagenetic scales of centimeters (Emerson and Bender 1981; Archer et al. 1989; Keir 1990; Hales et al. 1994), basin-wide scales (Emerson and Archer 1990), and global scales (Keir 1990; Archer and Maier-Reimer 1994). The models have reached the point where even small variations of the carbonate distribution on the sea-floor might be interpretable or serve to differentiate model formulations and assumptions. Archer (1996) converted available sedimentary data into a format suitable for validating models of $CaCO_3$-dynamics in the ocean. He related the distribution of sedimentary calcite in the deep-sea to a new gridded field of water column $\Delta CO_3^{2-}$ in an attempt to reveal regional variations in calcite preservation and thus the shape of the calcite lysocline. As a result, the lysocline has been found thicker (i.e., has a greater contrast in $\Delta CO_3^{2-}$ between the high- and low-calcite sediments) in the western Pacific and in the Atlantic Oceans than it is in the eastern equatorial Pacific. This pattern is consistent with the model's response to varying rates of dilution caused by terrigenous material. In low latitudes, calcite can be preserved to -30 µmol/kg $CO_3^{2-}$, whereas calcite is depleted from higher latitude sediments by a rate of -10 µmol/kg $CO_3^{2-}$. This gradient is smaller than the glacial/interglacial shift as required by the "rain ratio model" for generating lower atmospheric $p\,CO_2$ (Archer and Maier-Reimer 1994). This implies that the model requires an application of conditions in glacial times which have no analog in today's ocean. This conclusion rules out that the modern ocean carbonate system not necessarily validates models of $CaCO_3$-dynamics in the past. This is especially true for the preservation events at the onset of each interglaciation and for the dissolution events at the onset of each glaciation, recorded in dissolution records in the deep of the Indian and Pacific Ocean, which require the additional examination of compensation processes in the carbonate system on different time scales.

## The use of calcareous micro- and nannoplankton as dissolution proxies

### *Comparative analysis of dissolution proxies derived from planktic and benthic foraminifera*

The preservation potential of planktic foraminifera strongly depends on the internal wall

structure, which consists of small, anhedral crystals on the proximal side, larger crystals toward the distal side, and in some partially deep-living species, large crystals, forming the calcite crust (Bé et al. 1975). The shell containing the largest crystals is the most resistant one. In some cases, a very smooth distal calcite layer ("cortex"; e.g., *Pulleniatina obliquiloculata*) covers the outside of the test. It retards dissolution for some time, protecting the underlying crust.

Berger (1967; 1968) investigated samples from a mooring (Peterson 1966) as well as plankton and sediment samples. He finds that carbonate dissolution changes species diversity, test size distribution, content of damaged shells, and average particle weight of an assemblage. Moreover, he establishes the ranking of planktic foraminiferal species with respect to their preservation potential. Investigations on the shell calcite show that the ratio of elements such as Na, Mg, Sr, F, V, U versus Ca decrease in the course of dissolution in some planktic foraminiferal species (Bender et al. 1975; Rosenthal and Boyle 1993; Hastings 1994; Russell et al. 1994; Nürnberg 1995). The reason is that chambers, keel and "cortex" are each secreted in different depths displaying a distinct chemical water composition, and dissolution removes the most "impure" calcite parts first and faster than pure calcite (Brown and Elderfield 1996). As the foraminiferal assemblage is changed qualitatively and quantitatively due to dissolution, the perturbation of the record makes the interpretation difficult, and some method must be found to indicate the extent of bias caused by dissolution (Hemleben et al. 1989).

There are routinely measured micropaleontological and sedimentological methods considered to be linked to carbonate dissolution and preservation. These methods include determination of (1) percentage of fragmented planktic foraminifera tests (e.g., Keigwin 1976; Le and Shackleton 1992); (2) proportions of solution susceptible and solution resistant planktic foraminifera species (e.g., Schott 1935; Berger 1979; Boltovskoy and Totah 1992); (3) the ratio of benthic to planktic foraminifera (e.g., Parker and Berger 1971; Hooper et al. 1991); (4) the ratio of agglutinating to calcifying foraminifera (e.g., Kennett 1966; Murray 1989): (5) the ratio of radiolaria to foraminifera (Peterson and Prell 1985); (6) the ratio of pteropods to foraminifera (Berner 1977); (7) the ratio of coccoliths to foraminifera (e.g., Hay 1970; Hsü and Andrews 1970). Each of these parameters is a potential dissolution index, but their variations may partly be controlled by ecological or other factors (e.g., productivity, winnowing). Thus mostly, a multi-method approach was used in carbonate dissolution-studies.

Several similar rankings of the solubility of planktic foraminifera (Table 1) were derived from sediment samples, from taut wire buoys, from mooring experiments, and from laboratory experiments. This ranking depends on chamber structure, test size, thickness of the shell, development of a "cortex", dimension of aperture, existence of spines, width

of pores, fragility of sutures (Berger 1979; Henrich and Wefer 1986). It is stated that *Globigerinoides ruber* is one of the most solution-susceptible species whereas *Neogloboquadrina* sp. belongs to the rather solution-resistant species.

**Table 1.** Dissolution ranking of planktic foraminifera based on previous work by several authors: low numbers correspond to least resistance and vice versa. If data of all authors are standardized, genus-dependent resistance with respect to dissolution becomes obvious:
(least resistant)

*Globigerinoides sp. < Globigerina sp. < Globigerinella sp. < Globigerinita sp. < Globorotalia sp.*

(most resistant)

| Species | | SCHOTT (1935) | PARKER &BERGER (1971) | BERGER (1979) | MALMGREN (1983) | BERGER (1970) | THUNELL & HONJO (1981) | BOLTOVSKOY & TOTAH (1992) |
|---|---|---|---|---|---|---|---|---|
| Way of investigation: | | | Sediment ranking | | | Taut wire buoy | Mooring | Laboratory |
| ***Hastigerina*** | *pelagica* | | 3 | 4 | | | 6 | |
| ***Globigerina*** | *bulloides* | | 31 | 21 | 63 | 36 | 17 | |
| | *falconensis* | | 49 | 43 | | | | |
| *Turborotalita* | *humilis* | | 100 | 89 | | 100 | | |
| | *quinqueloba* | | 29 | 25 | 13 | 41 | | |
| *Globoturborotalita* | *rubescens* | | 11 | 11 | | 18 | | |
| | *tenella* | | 14 | 18 | | 27 | | |
| ***Globigerinella*** | *adamsi* | | 20 | | | | | |
| | *calida* | | 34 | 46 | | | 33 | |
| | *digitata* | | 63 | 61 | | | 11 | |
| | *siphonifera* | | 17 | 36 | | 14 | 22 | 45 |
| *Orbulina* | *universa* | 50 | 54 | 39 | | 9 | 39 | |
| ***Globigerinita*** | *glutinata* | | 43 | 50 | 50 | 45 | | 18 |
| | *uvula* | | 40 | | 25 | | | |
| *Candeina* | *nitida* | | 51 | | | 50 | 28 | |
| *Tenuitella* | *iota* | | 46 | 54 | | | | |
| ***Globigerinoides*** | *conglobatus* | | 26 | 32 | | 32 | 61 | 64 |
| | *ruber* | | 9 | 14 | | 5 | 44 | 9 |
| | *sacculifer* | 25 | 23 | 29 | | 23 | 56 | 55 |
| | *(trilobus)* | | | | | | | 27 |
| *Sphaeroidinella* | *dehiscens* | | 94 | 75 | | 91 | 100 | 82 |
| ***Globoquadrina*** | *conglomerata* | | 66 | 64 | | | | 73 |
| *(Neo-)* | *dutertrei* | | 83 | 86 | | 73 | 67 | 36 |
| *(Neo-)* | *pachyderma* | | 86 | 100 | 37 (dex.) / 100 (sin.) | 77 | | |
| ***Globorotalia*** | *crassaformis* | | 77 | 82 | | 86 | 94 | |
| | *hirsuta* | | 69 | | | 55 | | |
| | *inflata* | | 74 | 96 | 88 | 64 | 72 | |
| | *menardii* | 75 | | 68 | | | 50 | |
| | *scitula* | | 57 | 57 | | | | |
| | *truncatulinoides* | | 71 | 93 | 75 | 59 | 78 | |
| | *tumida* | 100 | 97 | 79 | | 95 | 89 | 91 |
| *Berggrenia* | *pumilio* | | 89 | | | | | |
| *Globorotaloides* | *hexagonus* | | 60 | | | | | |
| *Pulleniatina* | *obliquiloculata* | | 91 | 71 | | 82 | 83 | 100 |

According to Berger (1973b), benthic foraminifera are approximately three times less susceptible to dissolution than planktic foraminifera. Unfortunately, the information available on the dissolution of benthic foraminifera is scarce and fragmentary. Corliss and Honjo (1981) compiled a table of the relative susceptibility of benthic foraminifera to

dissolution. It should be noted that at least some planktic foraminifera are more resistant than certain benthic ones (Adelseck 1977; Boltovskoy and Totah 1992).
Another method is based on the ratio of the number of insoluble organic linings of five benthic foraminifera species to the number of calcareous shells of the same species (De Vernal et al. 1992). Maximum concentrations of organic linings correspond with a minimum of well-preserved shells and vice versa. The known relation between calcareous shells and their organic linings may lead to a dissolution index.

*Dissolution of calcareous nannoplankton assemblages*

Due to their small size, delicate ultrastructure, and complex sedimentation processes, relatively little work was done on coccolith dissolution as compared to planktic foraminifera. An early attempt to establish a preservation index was made by Roth and Thierstein (1972) who set up four categories of etching to express the preservation state of a coccolith assemblage. Among others, Hay (1970) stated that coccoliths show the best resistance to dissolution in deep waters especially compared with planktic foraminifera and other carbonate secreting invertebrates. He found - confirmed by early results of the Deep Sea Drilling Project - coccoliths to be more abundant close to the CCD than foraminifera. However, the results of Berger (1973b), Roth and Coulbourn (1982), and Paull et al. (1988) suggest that the dissolution behavior of coccoliths and foraminifera is rather similar, although differences in range of resistance cannot be excluded.
The occurrence of well-preserved coccoliths far below the CCD was then explained by protective chemosorptive coatings (Chave and Suess 1970) or organic membranes (McIntyre and McIntyre 1971). Fecal pellet transport is the most likely explanation for this phenomenon (Honjo 1975). Moreover, transport by fecal pellets is the most important process in transferring small phytoplankton skeletons from the photic zone to the ocean floor and therefore is a major component in the global carbon, carbonate, and silica cycles (Honjo 1976; Honjo et al. 1982). On the other hand, almost no information is available whether and how digestion processes in the guts of copepods or other zooplankton could lead to the dissolution of calcium carbonate after incorporation (Nejstgaard et al. 1994). Investigations on living coccolithophore communities have shown that malformation is a common feature in the biomineralization of coccoliths (Kleijne 1990; Giraudeau et al. 1993).
This incomplete formation of coccoliths already influences their preservation within the water column. In addition, heavily corroded specimens often occurred as well (Young 1994; Baumann et al. 1997).

Roth and Coulbourn (1982) explained the problems of defining a coccolith lysocline via the composition of a coccolith assemblage with the predominance of solution resistant species in both well and badly preserved coccolith assemblages. This is in contrast to foraminiferal assemblages that are usually predominated by more fragile forms should they be well preserved. All studies on coccolith dissolution are based on visual examination or ranking of the coccolith assemblages according to their preservation state. More recently Matsouoka et al. (1991) tried to use the disintegration of the distal and proximal shields of *Calcidiscus leptoporus* to establish a dissolution index.

## The South Atlantic dissolution experiment

In the following, several of the methods presented in the first part of this publication were applied on three depth transects in the South Atlantic extending a) from the Mid-Atlantic Ridge into the Brazil Basin, b) from the Walvis Ridge into the Cape Basin, and c) from the Namibian Continental Margin into the Cape Basin (Fig. 7, Table 2). In particular, these methods include the bulk sediment parameters, i.e. absolute and relative weigths of the coarse fraction (>63 µm), rain ratio, and carbonate content. With respect to planktic foraminifera, the number of fragments of single species and the number of fragments of all species, the ratio of dissolution resistant to dissolution susceptible species, the weighted occurrence and the ratio of several species, the ultrastructural breakdown of a single species, the ratio of planktic foraminifera to radiolaria as well as benthic foraminifera were applied as investigation methods. Furthermore, the carbonate ion content of the water column versus the saturation state of calcite in sea water and a nannofossil dissolution index were used. The purpose of the dissolution experiment was to compare the pattern of carbonate dissolution in both the open ocean and the coastal upwelling zones in particular consideration of the applicability of dissolution proxies.

**Table 2.** Locations and water depths of the investigated core-top samples (0-1 cm) and GEOSECS sattions 48,103.

| Giant box core | Latitude | Longitude | Water depth [m] |
|---|---|---|---|
| Transect 1: MOR - Brasil Basin | | | |
| GeoB 1115-4 | 3°33.5'S | 12°34.8'W | 2,921 |
| GeoB 1116-1 | 3°37.4'S | 13°11.2'W | 3,471 |
| GeoB 1117-3 | 3°49.0'S | 14°54.2'W | 3,977 |
| GeoB 1118-2 | 3°33.6'S | 16°25.9'W | 4,675 |
| GeoB 1119-2 | 2°59.9'S | 18°22.7'W | 5,213 |
| GEOSECS 48 | 4°00.0'S | 29°00.0'W | 11 - 5,075 |
| Transect 2: Walvis Ridge - Cape Basin | | | |
| GeoB 1217-1 | 24°56.7'S | 6°43.5'E | 2,007 |
| GeoB 1207-2 | 24°35.9'S | 6°51.3'E | 2,593 |
| GeoB 1208-1 | 24°29.5'S | 7°06.8'E | 2,971 |
| GeoB 1209-1 | 24°30.7'S | 7°17.0'E | 3,303 |
| GeoB 1211-1 | 24°28.4'S | 7°32.2'E | 4,089 |
| GeoB 1212-2 | 24°19.9'S | 8°15.0'E | 4,669 |
| GEOSECS 103 | 23°59.7'S | 8°30.2'E | 5 - 4,572 |
| Transect 3: Cape Basin - Namibia Continental Margin | | | |
| GeoB 1709-3 | 23°35.3'S | 10°45.5'E | 3,837 |
| GeoB 1710-2 | 23°25.8'S | 11°42.2'E | 2,987 |
| GeoB 1711-5 | 23°19.0'S | 12°22.7'E | 1,964 |
| GeoB 1712-2 | 23°15.3'S | 12°48.2'E | 1,007 |

## Deep-water circulation and carbonate dissolution

Regarding the modern distribution patterns of $CaCO_3$ in deep-sea sediments (Fig. 3), the Atlantic Ocean (Biscaye et al. 1976) generally exhibits a better calcium carbonate preservation in deeper waters than the Pacific (Berger et al. 1976) and the Indian Oceans (Kolla et al. 1976). Accordingly, the saturation horizon is deepest in the western Atlantic Ocean (~4,500 m), intermediate in the western Indian Ocean (~3,500 m) and shallowest in the northernmost Pacific Ocean (~1,000 m) due to different vertical mixing processes within the water column (Broecker and Peng 1982). Additionally, the CCD is shallower in the Pacific and the Indian Oceans than in the Atlantic Ocean.

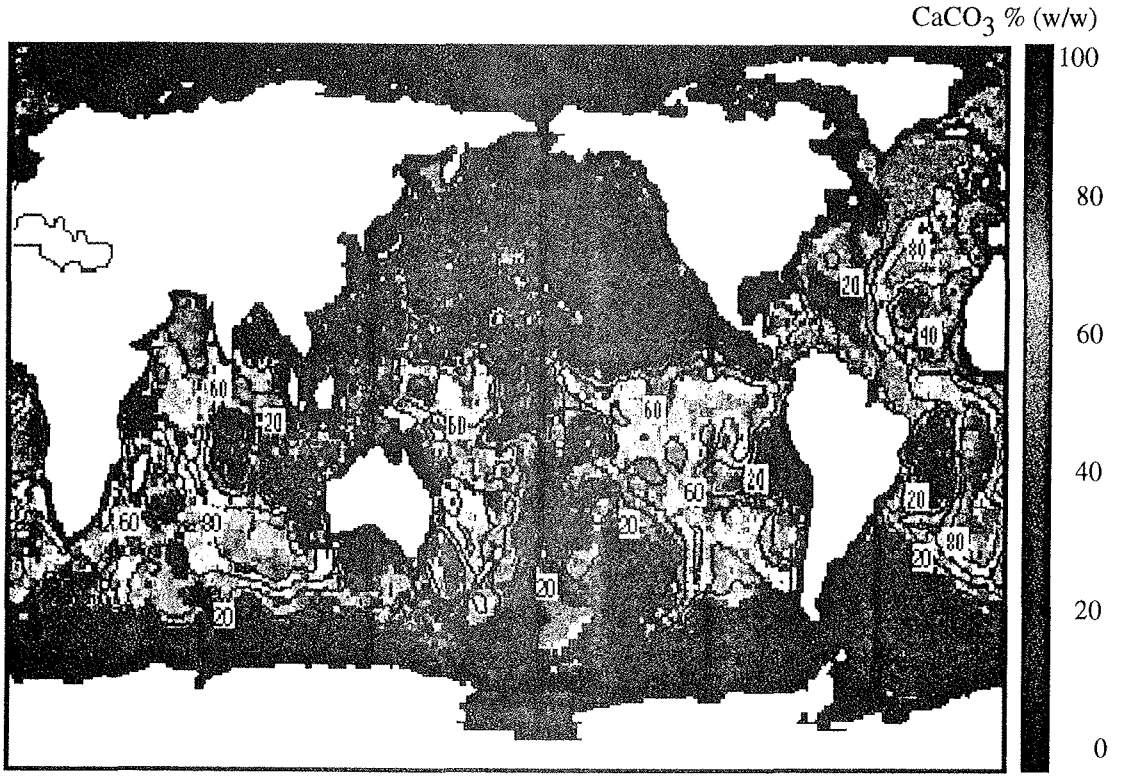


**Fig. 3.** Calcium carbonate ($CaCO_3$ % (w/w)) distribution in surface sediments of the Atlantic, Pacific and Indian Oceans (from Archer 1996).

The global deep-waters are driven by thermohaline processes, characterized and separated by unambiguous water features. The overriding factor is the age of each water mass. It strongly depends on both the distance to the source area and the alteration of the water mass on the pathway to and through the deep ocean. Plots of $C^{14}C$ (Fig. 4) versus apparent oxygen utilization (AOU), versus North Atlantic Deep Water (NADW) share in the deep-water, and versus inorganic carbon ($\Sigma CO_2$) for various deep-water types show

a strong dependence of each parameter on the distance to the deep-water source area (Broecker and Peng 1982). The water mass alterations result from molecular diffusion (Liss 1973), turbulent mixing (Liss and Merlivat 1986), and respiration activity of benthic organisms (Reimers 1989; Berelson et al. 1990).

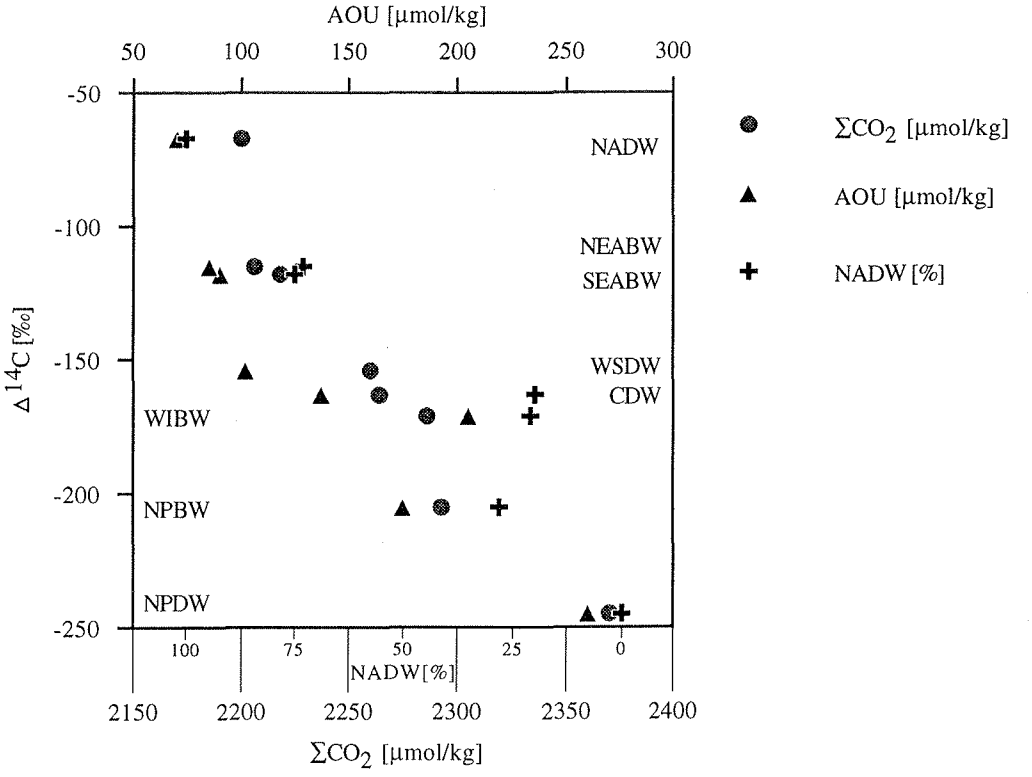


**Fig. 4.** Plots of $\Delta^{14}C$ versus apparent oxygen utilization (AOU), versus North Atlantic Deep Water (NADW) proportion in the deep water, and versus inorganic carbon content ($\Sigma CO_2$) for various deep water types show strong correlation ($r^2>0.9$): The more distant a distinct deep water type from the source area, the lower the amount of NADW, the more oxygen is respired, and the higher the content of $\Sigma CO_2$ will be (modified after Broecker and Peng 1982).
NADW...North Atlantic Deep Water, NEABW/SEABW ... North-, Southeast Atlantic Bottomwater, WSDW ... Weddell Sea Bottom Water, CDW ... Circumpolar Deep Water, WIBW ... West Indian Bottom Water, NPBW/NPDW ... North Pacific Bottom/Deep Water

NADW is characterized by oxygen enriched, nutrient depleted water masses of high $CO_3^{2-}$ and low $CO_2$ contents. Antarctic Bottom Water (AABW) can be distinguished as an extremely cold, oxygen depleted and nutrient enriched water mass of low $CO_3^{2-}$ and high $CO_2$ contents (Reid 1989; Boyle 1988). Today's mixing zone between AABW and NADW in the South Atlantic is close to the 90 µmol/kg $CO_3^{2-}$ isoline (Fig. 5; Bainbridge 1981). The carbonate ion content of GEOSECS station 48 ranges from 235 µmol/kg at 11 m to 77 µmol/kg at 5,075 m with a distinct minimum of 69 µmol/kg at 512 m water depth. According to equation (2), values for calcite saturation increase from 48 µmol/kg

at 11 m to 107 µmol/kg at 5,075 m water depth. The carbonate ion content curve intersects the calcite saturation at about 4,150 m. At these points $\Delta CO_3^{2-}$ becomes zero. The carbonate ion content of GEOSECS station 103 ranges from 219 µmol/kg at 5 m to 84 µmol/kg at 4,572 m with a distinct minimum of 63 µmol/kg at 613 m water depth. The carbonate ion content curve intersects the calcite saturation at about 4,000 m. It has been known since the studies of Wüst (1935) that the water characteristics of the corrosive AABW are responsible for the pronounced abyssal calcium carbonate dissolution. Furthermore, the asymmetry in deep-water distribution is responsible for the modern pattern of carbonate dissolution driving the positions of the calcite lysocline and the CCD (Berger 1968).

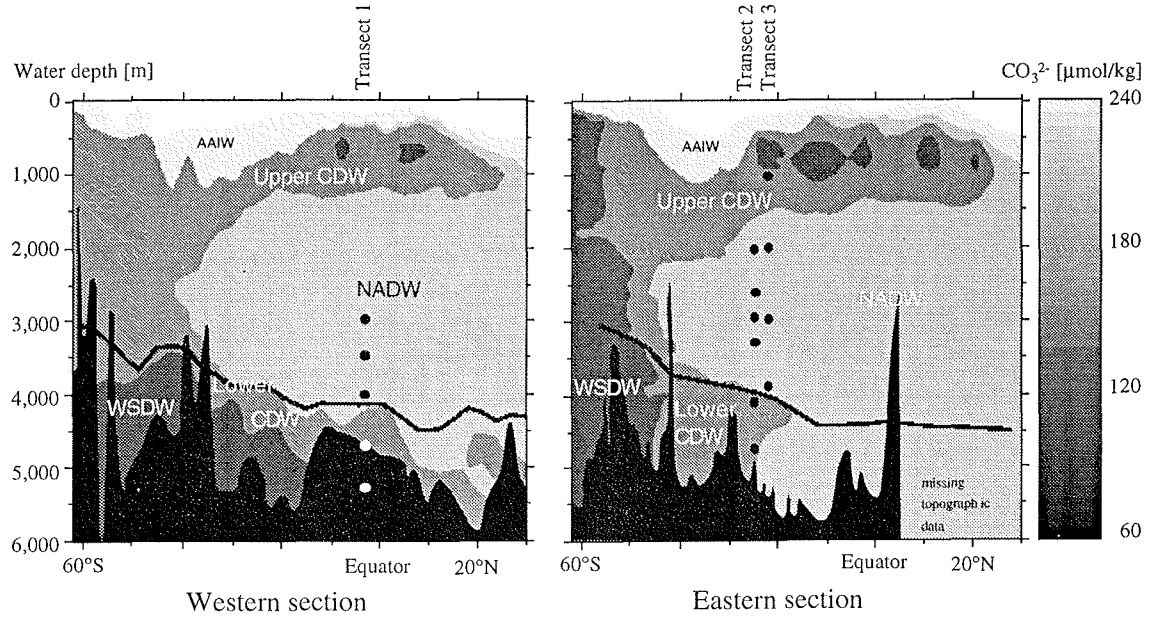


**Fig. 5.** Present-day stratification of the main water masses in the South Atlantic as displayed by $CO_3^{2-}$ ion content. Carbonate ion distribution refers to Geochemical Ocean Section Study data (GEOSECS; Bainbridge 1981). The lysocline depth (black line) was calculated according to Broecker and Takahashi (1978). In the western section of the South Atlantic, the carbonate ion content continually decreases southwards due to the strong influence of AABW. Consequently, the lysocline raises from 4,000 m up to 3,000 m. In the eastern section of the South Atlantic, North Atlantic Deep Water (NADW) is stopped in the South at the Walvis Ridge and at the SW Indian Ridge. Hence, the lysocline rises in steps. Dots indicate the position of the sample locations.
CDW...Circumpolar Deep Water; AAIW...Antarctic Intermediate Water; NADW...North Atlantic Deep Water; WSDW ... Weddell Sea Deep Water; AABW ... Antarctic Bottom Water (WSDW + Lower CDW)

Today, two domains of deep-water production can be distinguished. NADW is formed in the Baffin Bay, the Labrador Sea, and the Norwegian-Greenland Sea. The advected warm water evaporates, becomes more saline, cools and sinks down, carrying

atmospheric carbon with it. From there, NADW extends far southwards across the equator into the South Atlantic and is subsequently distributed into the Indian and the Pacific Oceans via the Antarctic Circumpolar Current (ACC). The second major deep-water source is subdivided into the dense Weddell Sea Deep Water (WSDW) - which is derived from surface water and after making contact with air is cooled and becomes more saline when sea ice is formed - and the lighter Circumpolar Deep Water (CDW) which is derived from the upwelled currents recirculated around Antarctica (Rhein et al. 1996). The density characteristics of these water masses cause the NADW to divide the CDW into an upper and a lower branch (UCDW, LCDW; (Reid 1989). WSDW and LCDW form the AABW which is distributed into the Atlantic, the Indian, and the Pacific Oceans via the ACC (McCartney 1992).

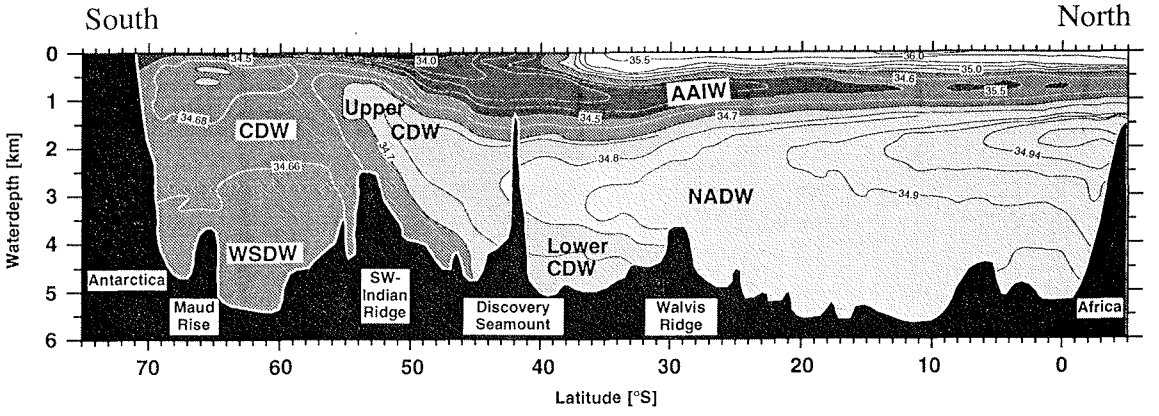


**Fig. 6.** Present-day stratification of main ocean water masses in the South Atlantic as displayed by salinity contour lines [‰] at a north-south transect along the Greenwich Meridian (modified after Reid 1989).

CDW...Circumpolar Deep Water; AAIW...Antarctic Intermediate Water; NADW...North Atlantic Deep Water; WSDW ... Weddell Sea Deep Water; AABW ... Antarctic Bottom Water (WSDW + Lower CDW)

The western Atlantic ocean receives deep-water directly both from the northern and the southern production area. The relatively warm and saline NADW occupies the depth interval between 2 km and 4 km, whereas AABW is located below 4 km (Fig. 6). The only path where AABW can enter the western North Atlantic is on the route through the Equatorial Channel into the Guiana Basin. In the eastern Atlantic, the Walvis Ridge and the Mid-Atlantic Ridge bar AABW from entering the Angola Basin. Only small quantities of AABW pass the sills eastwards through the Romanche- (Van Bennekom and Berger 1984; Warren and Speer 1991), the Chain Fracture Zone (Mercier et al. 1994), and the Walvis Passage (Connary and Ewing 1972; Shannon and Chapman 1991). Thus, even the deepest parts of these basins are filled almost exclusively by NADW. In contrast, the Cape Basin, although located east of the Mid-Atlantic Ridge, is dominated by AABW

below 4,000 m due to a bottom water passage which allows AABW to enter the basin from the South.

The Indian and the Pacific Oceans are supplied mainly from the southern source whereas NADW is added only secondary via the ACC. The North Pacific Deep Water (NPDW) is the abyssal water mass most abroad from the two domains of deep-water production. Hence, it carries almost no NADW. Likewise, NPDW contains the largest amount of $CO_2$, because oxygen is respired almost totally on its abyssal way to the northern edges of the Pacific Ocean, which results in sub- to anoxic pore water.

## Samples and methods

All sediment surface samples from giant box cores were collected on R/V *Meteor* cruises (Wefer et al. 1989; Wefer et al. 1990; Schulz et al. 1992) at water depths from 1,007 m down to 5,213 m (Fig. 7; table 2).

The first transect (GeoB 1115-1119) extends from 3°33'S - 12°35'W over about 345 nm to the West (2,921 m to 5,213 m water depth) and belongs to the tropical biogeographic faunal province sensu Bé (1977). The second transect (GeoB 1207-1217) streches from 24°57'S - 6°44'E over about 85 nm to the East (2,007 m to 4,669 m water depth); the third transect (GeoB 1709-1712) ranges from 23°15'S - 12°48'E over about 120 nm to the West (1,007 m to 3,837 m water depth). Transect 2 and transect 3 belong to the subtropical biogeographic faunal province. Hence, all samples within each transect should be characterized by a more or less identical faunal association except for the easternmost sample (GeoB 1712), which is located beneath the cold, nutrient rich, and highly productive Benguela Coastal Current system.

The top of the hydrographic lysocline horizon was determined sensu Takahashi et al. (1980) and Broecker and Takahashi (1978) given by the relationship:

$$(CO_3^{2-})^{calcite}\ [\mu mol/kg] = 90 \cdot e^{[0.16 \cdot (\text{Water depth [km]} - 4)]} \qquad (2)$$

The thickness of the calcite lysocline covers the range from 10 µmol/kg (sensu Broecker and Peng 1982) to the $\Delta CO_3^{2-}$ at the CCD ($\Delta CO_3^{CCD}$) sensu Archer (1996a).

A LECO CS-125 infrared analyzer was used in order to measure the total carbon (TC) and the total organic carbon (TOC) content of bulk sediments. Calcium carbonate content was calculated in weight percentage of the bulk sample according to the following equation:

$$CaCO_3\ \%\ (w/w) = (TC\ \%\ (w/w) - TOC\ \%\ (w/w)) \cdot 8.33 \qquad (3)$$

The rain ratio (Berger and Keir 1984) is determined by the molar ratio of organic ($C_{org}$) to inorganic ($C_{carb}$) carbon.

For grain-size analysis as well as for foraminiferal counts, samples were washed through a 63 µm sieve under a gentle spray of water to prevent additional fragmentation. The whole sample >63 µm was sieved on a 150 µm, 212 µm, 355 µm, 500 µm, and a 1,000 µm sieve-set according to the CLIMAP-conventions (Imbrie and Kipp 1971). Each fraction was repeatedly split into subsamples using a microsplitter to obtain an aliquot of at least 300 non-fragmented planktic foraminifera specimens (CLIMAP 1984) that were identified and counted completely; fragments, benthic foraminifera and radiolaria were also counted on the same aliquot. Meanwhile, it is common to examine the >150 µm fraction in paleoceanographic and paleoclimatic investigations (CLIMAP 1976). The taxonomy used follows that of Hemleben et al. (1989).

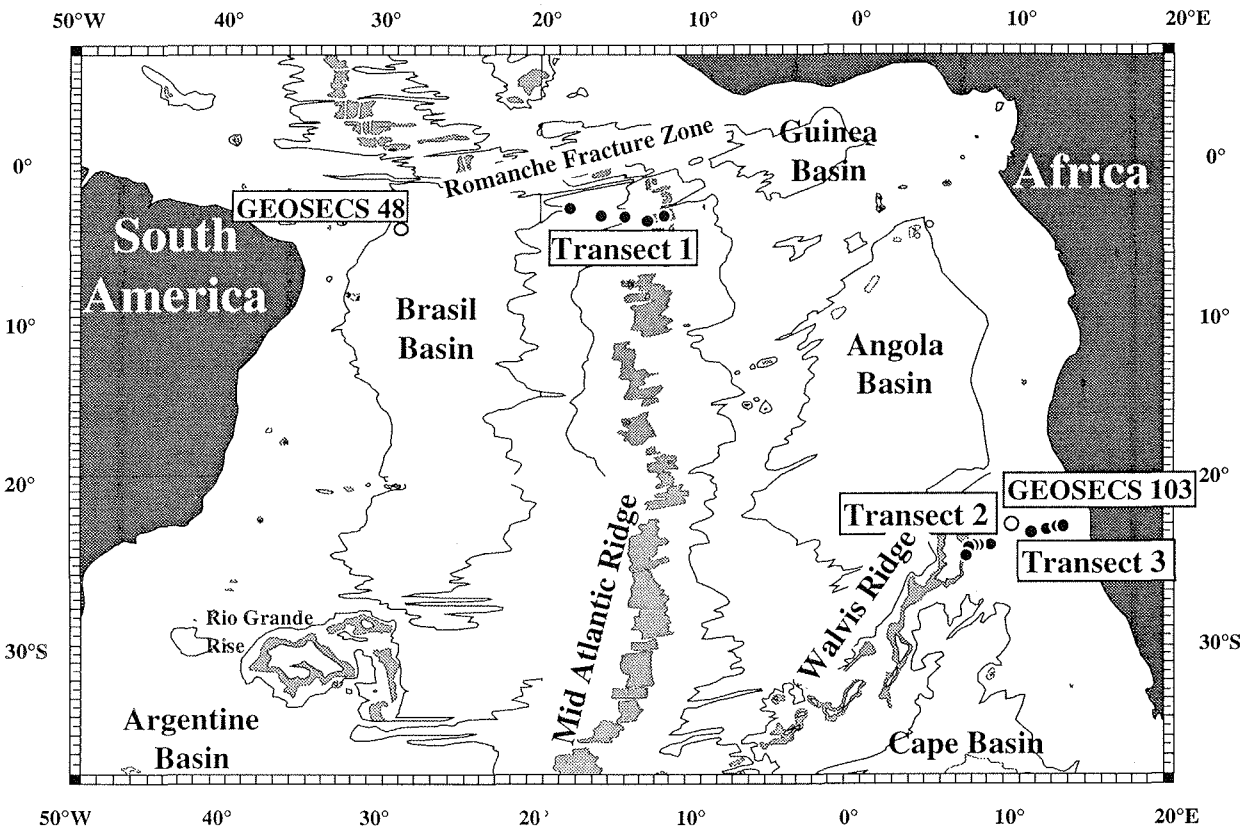


**Fig. 7:** General map of the investigated areas; for data consult table 2.

For the determination of dissolution stages according to ultrastructural breakdown, in each of the 5 fractions at least 40 *Globigerina bulloides* specimens were hand-picked and mounted on a carbon tape, glued onto a SEM stub, and then coated with Au-Pd. The apertural side of the non-fragmented test, the last and the penultimate chambers were examined using ZEISS Digital Scanning Microscope 940 A. The five dissolution stages correspond to "undissolved test surface" (stage 0) until "preserved not even as fragments" which is equivalent to "absent due to dissolution" (stage 5). Each *G. bulloides*

Dissolution Index (BDX) between zero and five was calculated weighted on the frequency of appearance per sample according to Dittert and Henrich (subm):

$$BDX = \sum (BDX') \,/\, \text{number of investigated tests} \quad (4)$$

$$BDX' = \sum (A_{0\text{-}5}) \,/\, \text{number of aspects per test obtained}$$

$A_{0\text{-}5}$ ... dissolution aspects of stage 0 to 5 per test

Fragments are counted if at least 50 % of the single chamber is preserved. The absolute and relative frequencies of skeletal fragments, the ratio of benthic to planktic foraminifera, and the ratio of radiolaria to planktic foraminifera were calculated according to Diester-Haass and Rothe (1987):

$$\text{Fragmentation Index} = F / (F+W) \quad (5.1)$$

$$\text{Benthic to planktic foraminifera Index} = B / (B+P) \quad (5.2)$$

$$\text{Radiolaria to planktic foraminifera Index} = R / (R+P) \quad (5.3)$$

F ... number of fragmented planktic foraminifera tests

W ... number of non-fragmented planktic foraminifera tests

B ... number of benthic foraminifera

P ... number of planktic foraminifera

R ... number of radiolaria

According to the dissolution-resistance, Berger (1979) defined a foraminiferal dissolution index (FDX; Table 1):

$$FDX = \sum (R_i \cdot P_i) / \sum P_i \quad (6)$$

$R_i$ ... rank of species i

$P_i$ ... percentage of species i

Ecological factors may bias results referring to faunal investigations; nevertheless, the loss of foraminifera was estimated on the assumption that the initial association within a transect is invariant and altered only by dissolution, not by changing productivity.

In order to describe the effect of carbonate dissolution on calcareous nannoplankton, the ratio of two coccolithophore species, *Emiliania huxleyi* and *Calcidiscus leptoporus*, was chosen. Both species occur frequently in modern sediments of the investigation area and appear to have a similar biogeographic distribution pattern (see Baumann et al., this volume). Hence, ecological factors that could influence this ratio are more or less excluded. The coccoliths formed by both species are placoliths, i.e., they consist of a proximal and a distal shield joined by a central column. *E. huxleyi* is a relatively fragile form with slots separating the single elements of the proximal shield, a large central pore, and a distal shield that is build up of delicate T-shaped elements. In contrast, *C. leptoporus* is a very solution-resistant form with heavily calcified distal and proximal shields, where no slots between the single elements occur and the connecting central tube is very narrow. Carbonate dissolution will have a stronger effect on *E. huxleyi* than on *C. leptoporus* and, therefore, the ratio of these two species will change with increasing carbonate dissolution. This *Calcidiscus leptoporus* - *Emiliania huxleyi* Dissolution Index

(CEX) is calculated as: $CEX = \%E.\ huxleyi\ /\ (\%E.\ huxleyi + \%C.\ leptoporus)$ (7)

## Results

*Bulk parameters.* The sediment $CaCO_3$-content extends from 94.6 % (w/w) at 2,471 m to 0.9 % (w/w) at 7,622 m (transect 1 - equatorial Atlantic) and from 96.4 % (w/w) at 1,023 m to 50.3 % (w/w) at 4,669 m water depth (transect 2 - Walvis Ridge). The 80 % isopleth intersects $CaCO_3$-values of transect 1 and 2 at about 4,300 m, whereas the 10 % isopleth crosses $CaCO_3$-values of transect 1 at about 5,100 m water depth (Fig. 8A, left side). Transect 3 (continental margin) $CaCO_3$-values amount to 88.3 % (w/w) at 167 m, reach a first minimum at 603 m with 40.6 % (w/w), attain a distinct maximum at 1,006 m with 97.5 % (w/w) and lastly come down to 4.2 % (w/w) at 5,086 m water depth. The 80 % isopleth crosses $CaCO_3$-values three times at about 200 m, 2,000 m, and at about 4,100 m, whereas the 10 % isopleth intersects transect 3 at about 5,000 m (Fig. 8A, right side).

With respect to GEOSECS station 48, the top of the hydrographic calcite lysocline can be set to 4,150 m, whereas the top of the sediment calcite lysocline appears at about 4,300 m; the bottom of the sediment calcite lysocline can be obtained at about 5,100 m water depth (transect 1) which corresponds to -40 µmol/kg $\Delta CO_3^{2-}$ (Fig. 8A, B, left side). According to transect 2, the bottom of the lysocline cannot be estimated due to absent sediment samples. Regarding GEOSECS station 103, the top of the hydrographic calcite lysocline can be set to 4,000 m, whereas the top of the sediment calcite lysocline appears at about 4,100 m (transect 3); the bottom of the sediment calcite lysocline is considered to be located at about 5,000 m water depth which corresponds to -30 µmol/kg $\Delta CO_3^{2-}$. Because there are no values below -30 µmol/kg $\Delta CO_3^{2-}$, this estimation is somewhat uncertain (Fig. 8A, B, right side). We should note, that GEOSECS station 103 possibly belongs to the pelagic ocean rather than to the continental margin and consequently $CO_3^{2-}$ values may bias our results to some extent.

With respect to transect 1, the grain size fraction 63 µm - 150 µm increases from 15 % at 2,921 m to 70 % at 5,213 m water depth, the fractions 150 µm - 355 µm remain mostly unchanged, and the fractions >355 µm decrease from 60 % to about 10 %. In transect 2 as well as in transect 3, size fractions do not vary greatly. Fluctuations amount to 10 % maximum (Fig. 9, above).Dry bulk density decreases from 0.6 g/cm$^3$ to 0.2 g/cm$^3$ (transect 1) and from 0.9 g/cm$^3$ to 0.3 g/cm$^3$ (transect 2). Only in transect 3 could a significant increase be detected. Values rise from 0.4 g/cm$^3$ to 0.8 g/cm$^3$ (Fig. 9, above). The rain ratio increases from 0.002 to about 0.07 with a distinct shift at 4,779 m water

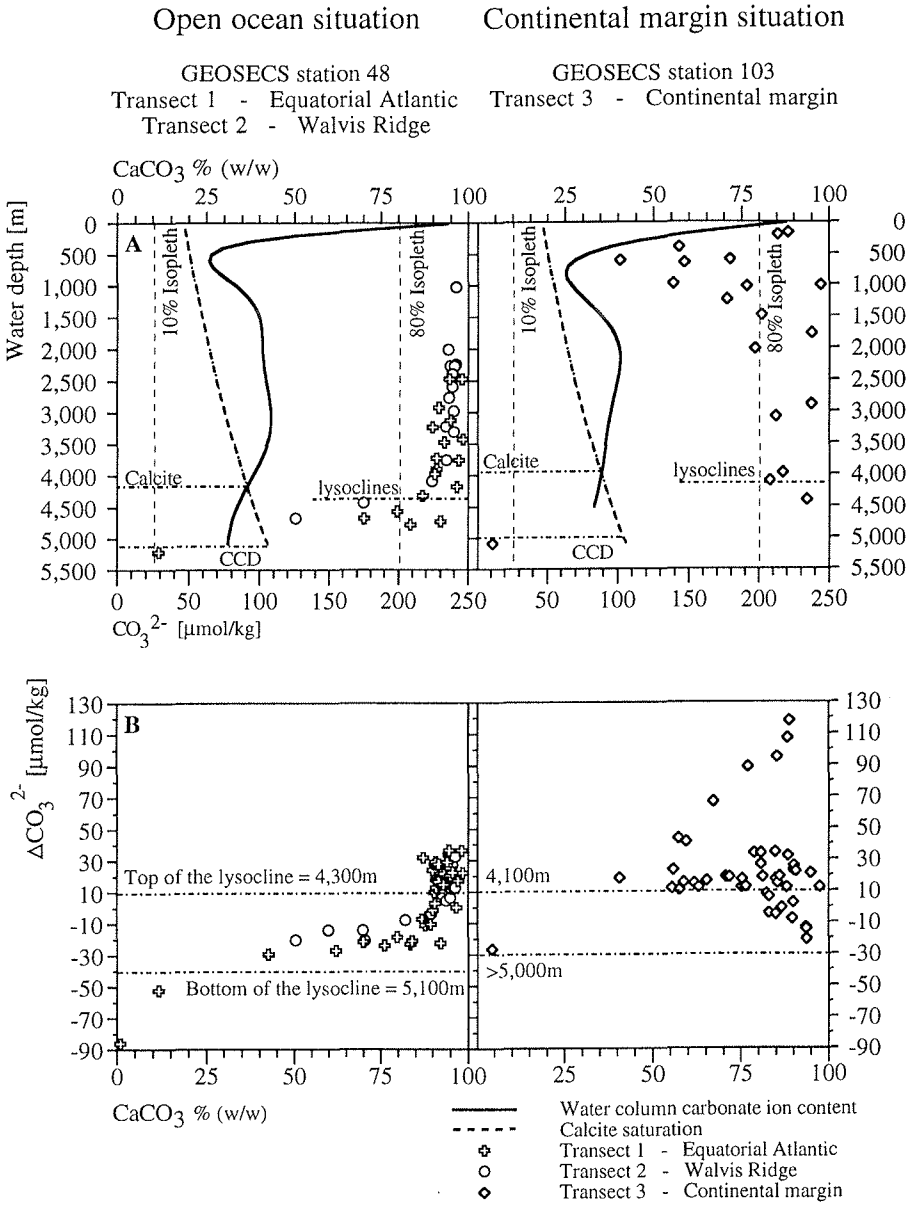


**Fig. 8.** The top of the hydrographic lysocline is determined by the intercept of seawater carbonate ion content ($CO_3^{2-}$) and the concentration of carbonate ions in equilibrium with seawater (saturation state) for calcite mineral phase. The top of the lysocline as obtained from the sediment can be described as the 80 % $CaCO_3$ isopleth (A) sensu Farrell and Prell (1989). The top of the calcite lysocline at the continental margin is higher than in the open ocean due to stronger influence of the AABW and due to the respiration effects at the continental margin of the coastal ocean within the classical upwelling area of the Benguela system induced by enormous productivity, high export and rapid sedimentation.

The thickness of the calcite lysocline (B) covers the range from 10 µmol/kg sensu Broecker and Peng (1982) to the $\Delta CO_3^{2-}$ at the CCD ($\Delta CO_3^{CCD}$) which is the zero intercept of the $CaCO_3$ % (w/w) versus $\Delta CO_3^{2-}$ relation sensu Archer (1996), i.e. $\Delta CO_3^{2-}$ (%$CaCO_3$ = 0). The calcite lysocline at the continental margin (transect 3) is thicker than in the open ocean (transects 1, 2) due to the higher calcium carbonate production and dissolution within the Benguela system. Water carbonate ion content refers to GEOSECS stations 48, 103 (Takahashi et al. 1980). Sediment calcite content ($CaCO_3$ % (w/w)) refers to GeoB locations.

depth (transect 1). In transect 2, modifications are not that sharp. The shift occurs at about 4,089 m towards 0.01. The most recognizable changes occur in transect 3, where the rain ratio decreases from 0.05 to about 0.002 building an interim maximum of 0.02 at 1,964 m water depth (Fig. 9 below; Fig. 13C).

*Planktic foraminifera parameters.* The modification of organism assemblages can be expressed by the number of radiolaria, benthic and planktic foraminifera >150 µm per gram sediment (Fig. 10, above). Transect 1 is characterized by a strong decrease in planktic foraminifera from 15,000 down to 4,000 tests; benthic foraminifera increase from 500 to 3,000 tests, and radiolaria increase from 150 to 360,000 tests per gram sediment. The most vigorous shift can be seen at about 3,977 m water depth. A similar picture is given in transect 2. Planktic foraminifera decrease from 14,000 to 4,500 tests, benthic foraminifera increase from 600 to 1,100 tests, and radiolaria increase from 100 to about 4,000 tests per gram sediment. A totally different situation occurs in transect 3: Planktic foraminifera increase from 17,000 to 45,000 tests, benthic foraminifera decrease from 1,800 to 500 tests, and radiolaria drop from 600 to 200 tests per gram sediment.

Looking at the modification of planktic foraminiferal assemblages, thick- and thin shelled varieties can be related to each other (Fig. 10, below). In transect 1, thick-shelled planktic foraminifera amount to 25 % at 2,921 m and increase to about 80 % at 5,213 m with an interim peak of 95 % at 4,675 m water depth. In transect 2, the amount of 60 % thick-shelled varieties at 2,007 m rises to 85 % at 4,669 m water depth. A similar picture appears in transect 3 where 25 % thick-shelled tests at 1,007 m increase to 40 % at 3,837 m water depth.

The ratio of dissolution susceptible to resistant planktic foraminifera shows a consistent trend in all three transects. Values remain consistently low from 1,007 m to 4,089 m, shift from about 0.2 to 0.6 and 0.8 at 4,670 m and drop then to 0.6 at 5,213 m water depth (Figs. 11A, F). The ratio of radiolaria to planktic foraminifera starts with about zero at 1,007 m and shifts at 4,089 m to about 1 at 5,213 m water depth (Fig. 11C). In a similar manner, the ratio of benthic to planktic foraminifera begins with about zero at 1,007 m and jumps at 4,089 m to about 0.5 at 5,213 m water depth (Fig. 11D). The foraminiferal dissolution index (FDX) commences at about 4.5 at 1,007 m rises at 4,089 m to 7 at 4,675 m and decreases to about 6 at 5,213 m water depth with respect to transects 1 and 3. Transect 2 starts on a higher level with 6 at 2,007 m and increases with a low slope to about 7 at 4,669 m water depth (Fig. 11B). Likewise, the fragmentation index of the sum of planktic foraminifera remains mostly unchanged from 1,007 m to 3,977 m and then shifts from 0.3 to 0.8 at 4,675 m, then decreasing to 0.4 at 5,213 m water depth according to transects 1 and 3. Values of transect 2 increase from 0.2 at 2,007 m to 0.8 at 4,089 m, then drop to 0.2 at 4,700 m water depth (Fig. 11E). Looking

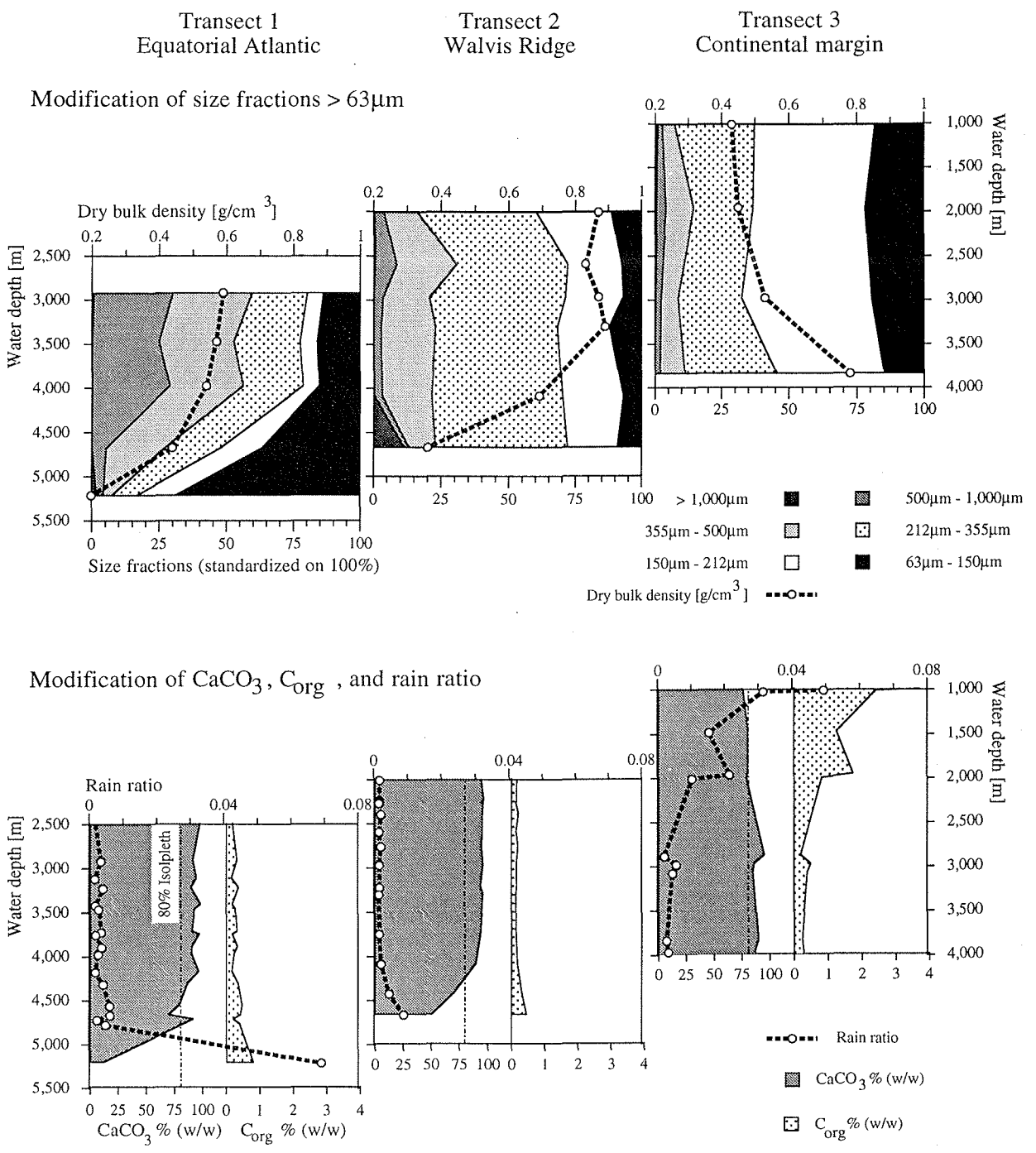


**Fig. 9.** *Above.* Modification of the grain size fractions ( >63 µm) and the dry bulk density show that at the top of the calcite lysocline size fractions are partly dominated by smallest fractions. Dry bulk density decreases due to the lower part of calcareous (2.7 g/cm$^3$) tests and the higher amount of opal skeletons (2.1 g/cm$^3$).

*Below.* Modification of $CaCO_3$ % (w/w), $C_{org}$ % (w/w), and rain ratio. High rain ratio may be attributed to the fact that a) productivity of organic carbon is enlarged vigorous what leads to supralysoclinal dissolution, and b) $CaCO_3$ values decrease due to sublysoclinal dissolution. Where the rain rate of calcitic and noncalcitic material are constant and neither productivity nor dilution are enhanced, rain ratio of organic to inorganic carbon remains constant and low.

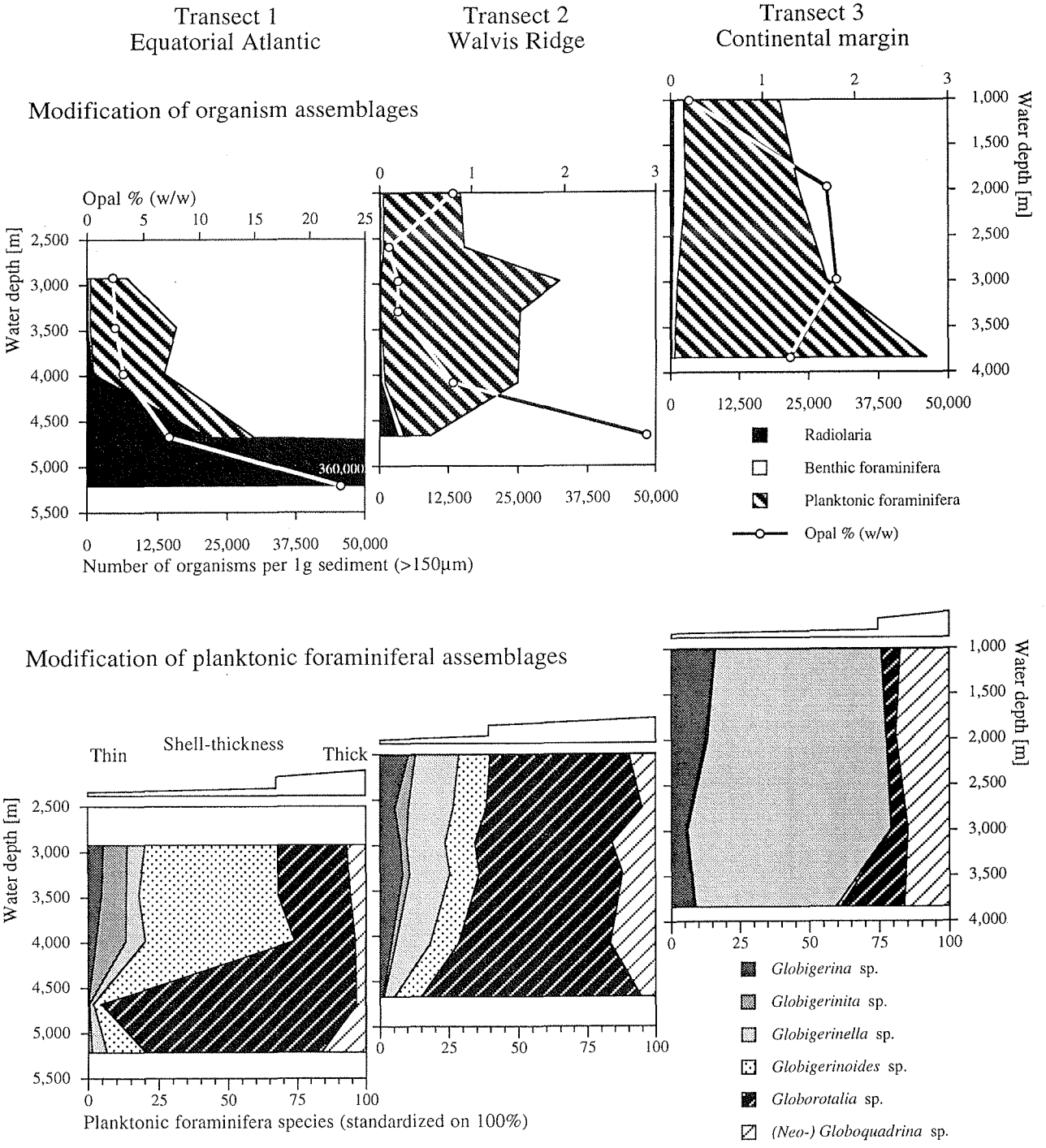


**Fig. 10.** *Upper panel.* Modification of organism assemblages show that the number of planktic foraminifera decreases whereas the number of benthic foraminifera and radiolaria increases at the top of the calcite lysocline. Furthermore, this is reflected by the rising amount of opal % (w/w). In the area of enhanced supralysoclinal dissolution the same picture is given resulting from respiration effects at the continental margin of the coastal ocean. This may be explained with enormous productivity, high export and rapid sedimentation of organic carbon.

*Lower panel.* Modification of planktic foraminiferal assemblages, expressed by the ratio of thick- to thin-shelled species. At the top of the calcite lysocline the amount of thick-shelled varieties increases drastically. Towards the CCD, the ratio is disturbed due to the deteriorated data base.

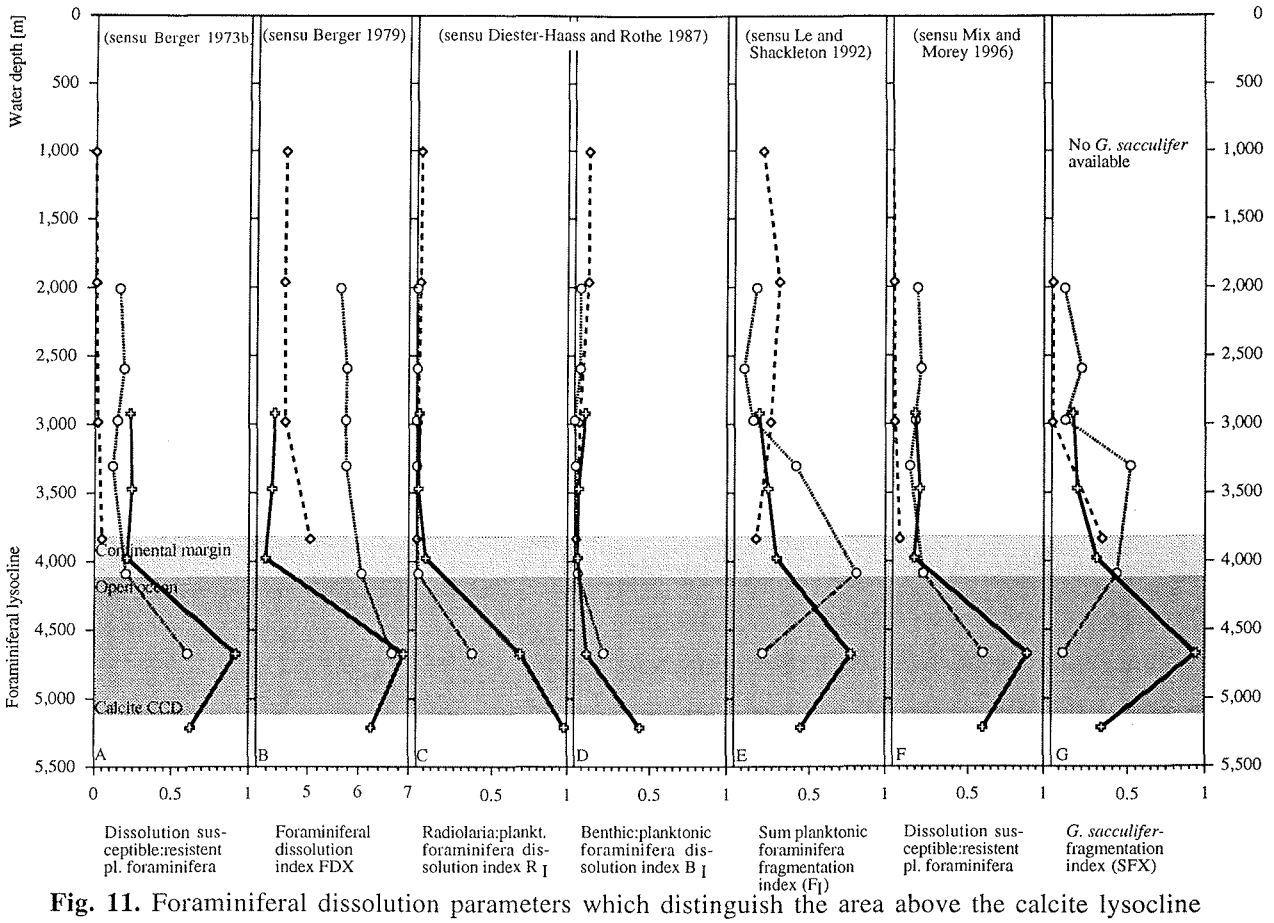


**Fig. 11.** Foraminiferal dissolution parameters which distinguish the area above the calcite lysocline from the area below, irrespective of whether they are derived from the open ocean or the continental margin transects. Increase of dissolution can be obtained at the top of the lysocline; towards the CCD, the parameters are disturbed due to the deteriorated data base.

at the fragmentation of *Globigerina sacculifer* tests, the values of all transects slightly increase from about zero at 2,007 m to 0.9 at 4,089 m. Transect 2 values drop to 0.1 at 4,669 m whereas transect 1 values rise to 0.9 at 4,675 m and then drop to 0.3 at 5,213 m water depth (Fig. 11G).

Regarding the development of fragmentation, about 60 percent of the sand-sized planktic foraminifera assemblage may be fragmented, whereas just 20 percent or less of the initial $CaCO_3$-content are lost (Fig. 12).

*New approaches.* The *Globigerina bulloides* Dissolution Index (BDX) increases from 1 at 2,007 m to about 2 at 4,089 m with respect to transects 1 and 2. Below, the values increase to 5 at 5,213 m water depth. According to transect 3, values increase from 1 at 1,007 m to about 3 at 3,837 m water depth (Fig. 13A). The *Calcidiscus leptoporus* - *Emiliania huxleyi* Dissolution Index (CEX) decreases from 0.8 at 2,007 m to 0.5 at 4,089 m and then shifts to about 0.2 at 5,213 m water depth with respect to transects 1 and 2. According to transect 3, values drop from 0.8 at 1,007 m to about 0.6 at 3,977 m

water depth (Fig. 13B).

## Discussion

In general, all parameters applied to the carbonate dissolution in the deep ocean contain both striking advantages and limiting handicaps. First of all, we were able to distinguish three quite different environments. The open ocean realms refer to the environments above and below the top of the lysocline, which is reflected by all parameters of each transect, no matter whether they are derived from the equatorial Atlantic, the Walvis Ridge or the continental margin samples. The continental margin realm is characterized by the strong productivity of the surface waters due to the coastal upwelling which is connected to the Benguela Current.

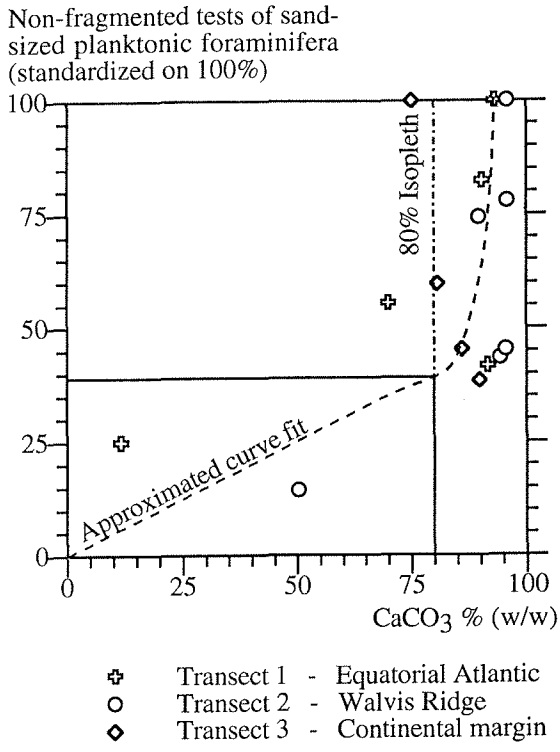


**Fig. 12.** The plot of $CaCO_3$ % (w/w) versus the number of non-fragmented tests of sand-sized planktic foraminifera clarifies that about 60 % of the assemblage is fragmented, whereas only 20 % or less of the initial $CaCO_3$ content are lost.

The best lysocline reconstruction is obtained on the basis of the carbonate ion content measured within the water column. This leads to the exact determination of the hydrographic lysoclines with respect to calcite (Fig. 8A). GEOSECS data position the hydrographic lysocline with respect to calcite at a depth of 4,150 m for the open ocean and at a depth of 4,000 m for the continental margin. Our results corroborate the calculations by Broecker and Takahashi (1978) who concluded that the hydrographic lysoclines are located where carbonate ion concentration in the water column plotted against the water depth intersects the carbonate saturation curve. Moreover, the same depths are attained following the concept by Broecker and Peng (1982) who set the top of the lysocline at 10 µmol/kg $\Delta CO_3^{2-}$. On the other hand, our investigations show, that the 'sedimentary' lysocline which coincides with the bend in the slope of the sediment $CaCO_3$-content versus water depth curve (Berger 1975), is positioned at 4,300 m for the open ocean and 4,100 m water depth for the continental margin realm (Fig. 8A).

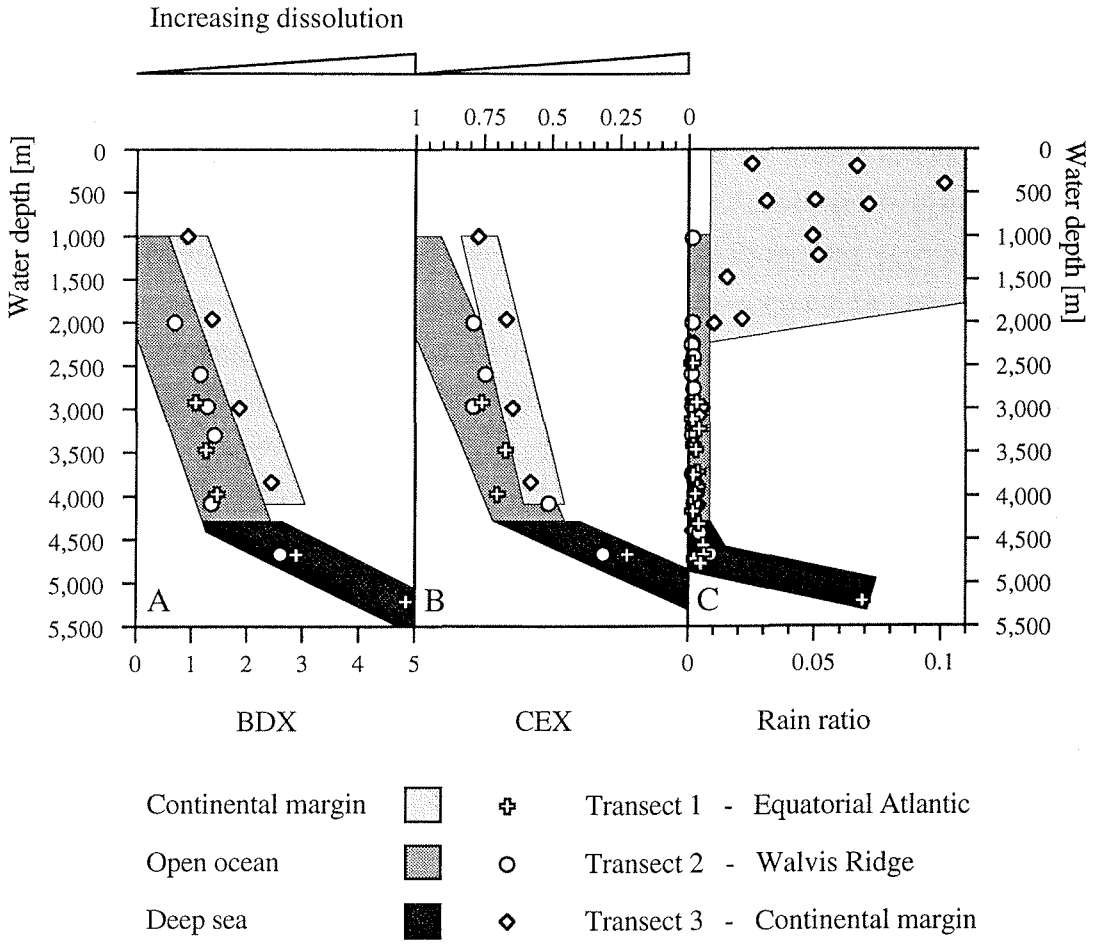


**Fig. 13.** *A. Globigerina bulloides* dissolution index (BDX) intensifies with increasing water depths and steady decrease of $\Delta CO_3^{2-}$ within the water column. BDX increases by about one dissolution stage towards the calcite lysocline. BDX values increase drastically in samples below the lysocline. However, the investigated tests of the equatorial Atlantic and the Walvis Ridge transect above the lysocline show an offset of about one dissolution stage less than at comparable depths of the continental margin.

*B. Calcidiscus leptoporus - Emiliania huxleyi* dissolution index (CEX) shows the same pattern as BDX.

*C.* The rain ratio of organic to inorganic carbon can serve as a useful tool. Low values (<0.01) above the lysocline and strongly increasing values (>0.01) below represent the open ocean situation, whereas high values (>>0.01) in the upper few thousand meters of the water column stand for the continental margin realm. The high rain ratio may be explained as follows: a) the productivity of organic carbon is enlarged leading to supralysoclinal dissolution, and b) the carbonate values decrease due to sublysoclinal dissolution. Where the rain rate of calcitic and noncalcitic material are constant and neither productivity nor dilution are enhanced, rain ratio of organic to inorganic carbon remains constant and low.

Additionally, these results comply to the concept by Farrell and Prell (1989) who define the top of the sediment lysocline by the 80 % $CaCO_3$-isopleth (Fig. 8A). At the same depths, we observed the 'foram' lysocline (Figs. 10, 11) which is based upon morphology and association of planktic foraminifera (Berger 1968). We put that offset

between the hydrographic lysocline and the sedimentary and the 'foram' lysocline due to the fact that dissolution mostly occurs at the sediment pore water interface rather than in the water column. That is, at this interface [$CO_3^{2-}$] is very likely to be higher than at the equivalent water depths in the water column (Le and Shackleton 1992). Nevertheless, we are not able to give any evidence for the position of the aragonite lysocline due to missing indicators such as pteropods. The bottom of the lysocline was determined by two different concepts which both set it to a depth of 5,100 m for the open ocean and at about 5,000 m water depth for the continental margin. Here, carbonate undersaturation reaches such low values that the rate of calcite sedimentation is nearly totally compensated for by the rate of calcite dissolution (Bramlette 1961; Archer 1996). Hence, the thickness of the lysocline is calculated as about 800 m for the open ocean and more than 900 m water depth for the continental margin (Fig. 8B). Where the carbonate content falls below 10 % (w/w), we can ascertain that both the geochemical and the sedimentary reconstructions of each transect lead to a corresponding depth of the bottom of the lysocline. Presumably, this accordance is due to the fact that the 10 % isopleth and the zero intercept of the %$CaCO_3$ versus $\Delta CO_3^{2-}$ relation coincide approximately with the progressive dissolution increase to the fourth power of $\Delta CO_3^{2-}$ (Keir 1980) below the top of the lysocline. But it has to be emphasized that the percentage of $CaCO_3$ as a single dissolution parameter cannot be simply interpreted as an index of preservation. Some general aspects must be regarded: 1) the rain rate and the accumulation rate of carbonate and non-carbonate particles; 2) the extent to which sea water is saturated with $CaCO_3$; 3) the amount of organic matter buried with $CaCO_3$; 4) whether the carbonate particles have an organic coating to retard dissolution; 5) whether there are currents to stir the layer of dissolution around the $CaCO_3$-particles (Le and Shackleton 1992). Only in the ideal situation, where the rain rate of carbonate and non-carbonate material is constant, can the amount of calcite lost to dissolution be calculated from the percentage $CaCO_3$ in the sediment (Farrell and Prell 1989; Curry and Lohmann 1990; Bickert et al. 1997).

Another method to distinguish the three environments leads to the new approaches made here. The continuous increase of dissolution stages of *Globigerina bulloides* ultrastructure with increasing water depths complies to the concept of perpetual decrease of $\Delta CO_3^{2-}$ within the water column (Broecker and Takahashi 1978). For all transects, dissolution increases by about one dissolution stage towards the calcite lysocline. Samples below the lysocline drastically increase in BDX values. However, the investigated tests of the equatorial Atlantic and the Walvis Ridge transect above the lysocline show an offset of about one dissolution stage less than at comparable depths of the continental margin (Fig. 13A). This is due to the strong productivity of organic and inorganic carbon within the Benguela upwelling system which yields higher benthic

respiration rates and hence a larger contribution to carbonate dissolution (Berger et al. 1987). However, each realm can be distinguished by discrete clusters. The important point is that this parameter does not depend on the ecology of the surface water, i.e., if there are tests broken without being affected by dissolution - whatever the reason may be - they will raise micropaleontological parameters and additionally they even will change the fragmentation index towards stronger dissolution (Dittert and Henrich subm).

The *Calcidiscus leptoporus* - *Emiliania huxleyi* Dissolution Index (CEX) shows comparable results. Considering the investigated areas, *Emiliania huxleyi* and *Calcidiscus leptoporus* show rather similar ecological behavior in response to nutrient distribution and temperature. Consequently, the changing ratio of these two species can be attributed to their different dissolution susceptiblity. Hence, we are able to form clusters which separate the continental margin from the open ocean realm above and below the lysocline. That is, CEX values rise steadily with increasing water depths above the lysocline and then turn to stronger dissolution below the lysocline. Due to higher productivity, CEX values are offset by about 0.1 towards stronger dissolution above the lysocline at the continental margin (Fig. 13B). However, in surface waters which are distinctly more nutrient-depleted or cooler, CEX may fail.

The rain ratio of organic to inorganic carbon can serve as a useful tool. Our results show, that rain ratio forms clusters which are comparable to BDX and CEX. Low values (<0.01) above the lysocline and strongly increasing values (>0.01) below represent the open ocean situation, whereas high very values (>>0.01) in the upper few thousand meters of the water column stand for the continental margin realm. This supports the concept of Berger (1991) who describes maximum values of organic carbon for the upper continental margin of the coastal ocean within the classical upwelling areas on the basis of a combination of enormous productivity, high export and rapid sedimentation (Fig. 9, below). On the other hand, oxidation of such an immense amount of organic carbon deposits results in (1) a successive $CO_2$ release which lowers the pH of pore water; (2) reduced oxygen content; and (3) supralysoclinal dissolution of carbonates. Consequently, a high rain ratio may be attributed to the fact that a) productivity of organic carbon is intensified which leads to supralysoclinal dissolution, and b) carbonate values decrease due to sublysoclinal dissolution. Where the rain rate of carbonate and non-carbonate material is constant and neither productivity nor dilution are enhanced, the rain ratio of organic to inorganic carbon remains constant and low. All three situations can clearly be distinguished in separate clusters (Fig. 13C). Questions on the origin of organic carbon may arise if the eolian supply of terrigenous organic material related to the trade winds was of some importance in the deep Equatorial Atlantic (Verardo and Ruddiman 1996); furthermore, riverine particulate organic carbon deposited nearshore might enforce the

total organic carbon signal (Emerson and Hedges 1988). However, extended input of land-derived organic carbon would raise the total organic carbon content and consequently also increase the rain ratio towards higher values with respect to both the open ocean and the continental margin.

In contrast, most of the parameters dealing with planktic foraminifera are only qualified to determine the position of the lysocline. No matter whether it concerns the modification of grain size distribution of the sand fraction (Fig. 9, above), the modification of organism assemblages (Fig. 10, upper panel), the variation of planktic foraminifera assemblages (Fig. 10, lower panel), the ratio of dissolution susceptible to resistant planktic foraminifera (Figs. 11A, B, F), the ratio of radiolaria to planktic foraminifera (Fig. 11C), the ratio of benthic to planktic foraminifera (Fig. 11D), or the fragmentation of planktic foraminifera (Figs. 11E, G), the calcite lysocline can be positioned at about 4,300 m for the open ocean transects and at about 4,100 m water depth for the continental margin transect. The reasons why the continental margin situation cannot be distinguished are diverse. If there were intermediate water currents they might blow out lighter particles, i.e. finer grain-size fractions, fragments, and radiolaria. This would bias the results of grain-size investigations as well as the results of micropaleontological examinations towards less dissolution (Diester-Haass and Müller 1979). In a similar way, most samples below 4,675 m water depth (Fig. 11) present a distorted picture of less dissolution. We ascribe this to the fact that the number of organisms to be investigated is too small due to the effects of dissolution, i.e. the total decreases under the minimum that is required for statistical relevance (CLIMAP 1984).

In order to establish BDX and CEX as global dissolution proxies, we will apply these parameters on further realms which include continental margin situations outside the upwelling areas and regions with modified bottom water influence.

## Conclusions

Carbonate dissolution in the deep ocean was determined by using sea water carbonate ion data, bulk sediment parameters, and calcareous micro- and nannoplankton parameters as dissolution proxies. Investigation areas were the open ocean regime specified by two transects into the western Brazil Basin and the western Cape Basin. The continental margin realm is characterized by one transect into the eastern Cape Basin. Carbonate ion contents were measured between 5 m and 5,075 m water depth. The sediment surface samples are derived from water depths between 1,007 m and 5,213 m.

We can conclude that all parameters are capable of distinguishing the area above from the

area below the top of the calcite lysocline. Beyond that, some parameters are suited to distinguish the upper continental margin of the coastal ocean within an upwelling area controlled by enormous productivity, high export and rapid sedimentation. In detail, these are the carbonate ion content of the water column and the weight percentage of sediment $CaCO_3$-content (Fig. 8), the rain ratio (Fig. 9, below; Fig. 13C), the *Globigerina bulloides* Dissolution Index (BDX; Fig. 13A), and the *Calcidiscus leptoporus - Emiliania huxleyi* Dissolution Index (CEX; Fig. 13B).

Regarding the three different oceanographic regimes, only the carbonate ion content and the percentage of sediment carbonate content put us in the position to determine top, bottom, and thickness of the lysocline. If these parameters are not available, a combination of BDX, CEX and rain ratio (Fig. 13) gives the best approach to the authentic conditions.

According to the investigated transects, the top of the calcite lysocline can be set to about 4,300 m in the open ocean realm of the Brazil- and the western Cape Basin. It reflects the modern boundary between the North Atlantic Deep Water and the corrosive Antarctic Bottom Water, subsequently leading to sublysoclinal dissolution. The thickness of the lysoclines amount to about 800 m. With respect to the continental margin of the eastern Cape Basin, the lysocline is situated at about 4,100 m water depth; the lysocline thickness becomes >900 m. It reflects the high amount of organic matter buried with $CaCO_3$, induced by coastal upwelling processes of the Benguela Current, subsequently leading to sublysoclinal dissolution as well as to supralysoclinal dissolution.

## Acknowledgements

We appreciate the kind assistance of the crews and masters of R/V METEOR on numerous cruises to The South Atlantic. The authors are indebted to M. Matthies and R. Schlotte, who assisted the processing of the GEOSECS data set, as well as to H. Heilmann, R. Henning, and C. Wienberg for technical collaboration. B. Diekmann contributed Fig. 6. This research benefitted from many discussions with colleagues at Bremen University. Finally, we are grateful to W. H. Berger for constructive comments. The investigations were funded by the Deutsche Forschungsgemeinschaft. This is SFB 261.contribution no. xxx at Bremen University.

## References

Adelseck CG (1977) Dissolution of deep-sea carbonate: Preliminary calibration of preservational and morphological aspects. Deep-Sea Res 25:1167-1185

Archer DE (1996) An Atlas of the distribution of calcium carbonate in sediments of the deep-sea. Global Biogeochem Cycles 10(1):159-174

Archer DE, Emerson S, Reimer C (1989) Dissolution of calcite in deep-sea sediments: pH and $O_2$ microelectrode results. Geochim Cosmochim Acta 53:2831-2846

Archer DE, Maier-Reimer E (1994) Effect of deep-sea sedimentary calcite preservation on atmospheric $CO_2$ concentration. Nature 367:260-264

Arrhenius GOS (1952) Sediment Cores from the East Pacific - Fasc. 1. Rep Swed Deep-Sea Exped 1947-1948 5:1-227

Baes CFJ (1982) Effects of ocean chemistry and biology. In: Clark WC (ed) Carbon dioxide Review 1982. Oxford University Press, Oxford, 488 pp

Bainbridge AE (1981) GEOSECS Atlantic Expedition, Hydrographic Data, 1972-1973. National Science Foundation, Superintendent of Documents, US Government Printing Office, Washington, DC, 121 pp

Bassinot FC, Beaufort L, Vincent E, Labeyrie LD, Rostek F, Müller PJ, Quidelleur X, Lancelot Y (1994) Coarse fraction fluctuations in pelagic carbonate sediments from the tropical Indian Ocean: A 1,500 kyr record of carbonate dissolution. Paleoceanography 9(4):579 - 600

Baumann K-H, Andruleit H, Schröder-Ritzrau A, Samtleben C (1997) Spatial and temporal dynamics of coccolithophore communities during low production phases (spring-early summer) in the Norwegian-Greenland Sea. In: Hass HC, Kaminski MA (eds) Contributions to the micropaleontology and paleoceanography of the northern North Atlantic. Grzybowski Foundation Special Publication, Kraków, 5:227-243

Baumann K-H, Meggers H (1996) Paleoceanographical change in the Labrador Sea during the last 3.1 MY: Evidence from calcareous plankton records. In: Moguilevsky A, Whatley R (eds) Microfossils and Oceanic Environments. Aberystwyth-Press, Aberystwyth, 131-154

Bé AWH (1977) An ecological, zoogeographic and taxonomic review of recent planktonic foraminifera. In: Ramsay ATS (ed) Oceanic Micropaleontology. Academic Press, London, 1:1-100

Bé AWH, Morse JW, Harrison SM (1975) Progressive dissolution and ultrastructural breakdown of planktonic foraminifera. In: Sliter WV, Bé AWH, Berger WH (eds) Dissolution of Deep-Sea Carbonates. Cushman Found. Foram. Res. Spec. Publ., Ithaka, NY, 13:27-55

Bender ML, Lorens RB, Williams DF (1975) Na, Mg, Sr in the tests of planktonic foraminifera. Micropaleontology 21:448-459

Berelson WM, Hammond DE, Cutter GA (1990) *In situ* measurements of calcium carbonate dissolution rates in deep-sea sediments. Geochim Cosmochim Acta 54:3013-3020

Berger WH (1967) Foraminiferal ooze: Solution at depths. Science 156(3773):383-385

Berger WH (1968) Planktonic foraminifera: Selective solution and paleoclimatic interpretation. Deep-Sea Res 15:31-43

Berger WH (1970) Planktonic foraminifera: Selective solution and the lysocline. Mar Geol 8:111-138

Berger WH (1973a) Deep-sea carbonates: Evidence for a coccolith lysocline. Deep-Sea Res 20:917-921

Berger WH (1973b) Deep-sea carbonates: Pleistocene dissolution cycles. J Foram Res 3(4):187-195

Berger WH (1975) Deep-sea carbonates: Dissolution profiles from foraminiferal preservation. In: Sliter WV, Bé AWH, Berger WH (eds) Cushman Foundation For Foraminiferal Research Special Publication. Cushman Found Foram Res Spec Publ, Ithaka, NY, 13:82-86

Berger WH (1979) Preservation of foraminifera. In: Lipps JH, Berger WH, Buzas MA, Douglas RG, Ross CA (eds) Foraminiferal Ecology and Palecology. Society of Economic Paleontologists and Mineralogists, Houston, 6:105-155

Berger WH (1982) Increase of carbon dioxide in the atmosphere during deglaciation: the coral reef hypothesis. Naturwissenschaften 69:87-88

Berger WH (1991) Produktivität des Ozeans aus geologischer Sicht: Denkmodelle und Beispiele. Z Dt Geol Ges 142:149-178

Berger WH, Adelseck CG, Mayer LA (1976) Distribution of carbonate in surface sediments of the Pacific Ocean. J Geophys Res 81(C):2617-2627

Berger WH, Bonneau M-C, Parker FL (1982) Foraminifera on the deep-sea floor: lysocline and dissolution rate. Oceanol Acta 5(2):249-258

Berger WH, Fischer K, Lai C, Wu G (1987) Ocean productivity and organic carbon flux. Part I. Overview and maps of primary production and export production. Scripps Inst. Oceanogr., Univ. Calif., 67 pp

Berger WH, Keir RS (1984) Glacial-Holocene changes in atmospheric $CO_2$ and the deep-sea record. In: Hansen JE, Takahashi T (eds) Climate processes and climate sensitivity. Geophys. Monogr. 29, Maurice Ewing Series, Washington, DC, 5:337-351

Berger WH, Smetacek VS, Wefer G (1989) Ocean productivity and paleoproductivity - An overview. In: Berger WH, Smetacek VS, Wefer G (eds) Productivity of the Ocean: Present and Past. John Wiley & Sons, New York, NY, 1-34

Berner RA (1977) Sedimentation and dissolution of pteropods in the ocean. In: Andersen NR, Malahoff A (eds) The Fate of Fossil Fuel $CO_2$ in the Oceans. Plenum Press, New York, NY, 243-260

Bickert T, Cordes R, Wefer G (1997) Late Pliocene to Mid-Pleistocene (2.6-1.0 M.Y.) carbonate dissolution in the western equatorial Atlantic: Results of Leg 154, Ceara Rise. Proc ODP, Sci Results 154:229-237

Bickert T, Wefer G (1996) Late Quaternary deep water circulation in the South Atlantic: Reconstruction from carbonate dissolution and benthic stable isotopes. In: Wefer G, Berger WH, Siedler G, Webb DJ (eds) The South Atlantic: Present and past circulation. Springer-Verlag, Berlin Heidelberg, 599-620

Biscaye PE, Kolla V, Turekian KK (1976) Distribution of calcium carbonate in surface sediments of the Atlantic Ocean. J Geophys Res 81(C5):2595-2603

Boltovskoy E (1991) La destruction des tests de foraminifères (experiences de laboratoire). Revue de Micropaléontologie 34(1):19-25

Boltovskoy E, Totah VI (1992) Preservation index and preservation potential of some foraminiferal species. J Foram Res 22(3):267-273

Boyle EA (1988) Vertical oceanic nutrient fractionation and glacial/interglacial CO2 cycles. Nature 331:55-56

Bramlette MN (1961) Pelagic sediments. In: Sears M (ed) Oceanography. AAAS Publication, New York, NY, 67:345-366

Broecker WS, Peng TH (1982) Tracers in the Sea. Eldigio Press, New York, NY, 689 pp

Broecker WS, Takahashi T (1978) The relationship between lysocline depth and in situ carbonate ion concentration. Deep-Sea Res 25F(1):65-95

Brown SJ, Elderfield H (1996) Variations in Mg/Ca and Sr/Ca ratios of planktonic foraminifera caused by postdepositional dissolution: Evidence of shallow Mg-dependent dissolution. Paleoceanography 11(5):543-551

Chave KE, Suess E (1970) Calcium carbonate saturation in sea water: Effects of dissolved organic matter. Limnol Oceanogr 15:633-637

CLIMAP Project members (1976) The surface of the ice-age earth. Science 191(4232):1131-1137

CLIMAP Project members (1984) The last interglacial ocean. Quat Res 21:123-224

Connary SD, Ewing M (1972) The nepheloid layer and bottom circulation in the Guinea and Angola Basins. In: Gordon AL (ed) Studies in physical oceanography: a tribute to Georg Wüst on his 80th birthday. Gordon and Breach, New York, NY, 2:169-184

Corliss BH, Honjo S (1981) Dissolution of deep-sea benthic foraminifera. Micropaleontology 27(4):356-378

Culkin F (1965) The major ion components of seawater. In: Riley JP, Skirrow G (eds) Chemical oceanography. Academic Press, New York, NY, 1:121-162

Curry WB, Lohmann GP (1990) Reconstructing past particle fluxes in the tropical Atlantic Ocean. Paleoceanography 5:487-506

De Vernal A, Bilodeaul G, Hillaire-Marcel C, Kassou N (1992) Quantitative Assessment of Carbonate Dissolution in Marine Sediments from Foraminifer Linings vs. Shell Ratios: Davis Strait, Northwest North Atlantic. Geology 20:527-530

Diester-Haass L, Müller PJ (1979) Processes influencing sand fraction composition and organic matter content in surface sediments off W Africa (12-19°N). "Meteor" Forsch-Ergebn C 31:21-47

Diester-Haass L, Rothe P (1987) Plio-Pleistocene sedimentation on the Walvis Ridge, Southeast Atlantic (DSDP Leg 75, Site 532) - Influence of surface currents, carbonate dissolution and climate. Mar Geol 77:53-85

Dittert N, Henrich R (subm) Carbonate dissolution in the South Atlantic Ocean: Evidence by *Globigerina bullloides*' ultrastructure breakdown: Deep-Sea Res

Edmont JM (1970) High precision determination of titration alkalinity and total carbon dioxide content of seawater by potentiometric titration. 17:737-750

Emerson S, Archer D (1990) Calcium carbonate preservation in the ocean. Phil Trans R Soc Lond A 331:29-40

Emerson S, Bender M (1981) Carbon fluxes at the sediment-water interface of the deep-sea: calcium carbonate preservation. J Mar Res 39:139-162

Emerson S, Hedges JI (1988) Processes controlling the organic carbon content of open ocean sediments. Paleoceanography 3(5):621-634

Farrell JW, Prell WL (1989) Climatic change and $CaCO_3$ preservation: An 800,000 year bathymetric reconstruction from the central equatorial Pacific Ocean. Paleoceanography 4(4):447-466

Farrell JW, Prell WL (1991) Pacific $CaCO_3$ preservation and $\delta^{18}O$ since 4 Ma: paleoceanographic and paleoclimatic implications. Paleoceanography 6(4):485-498

Freiwald A (1995) Bacteria-induced carbonate degradation: A taphonomic case study of *Cibicides lobolatus* from a high-boreal carbonate setting. Palaios 10:337-346

Gattuso J-P, Pichon M, Delesalle B, Frankignoulle M (1993) Community metabolism and air-sea $CO_2$ fluxes in a coral reef ecosystem (Moorea, French Polynesia). Mar Ecol Prog Ser 96:259-267

Giraudeau J, Monteiro PMS, Nikodemus K (1993) Distribution and malformation of living coccolithophores in the northern Benguela upwelling system off Namibia. Mar Micropal 22:93-110

Hales B, Emerson S, Archer D (1994) Respiration and dissolution in the sediments of the western North Atlantic: estimates from models of *in situ* microelectrode measurements of pore water oxygen and pH. Deep-Sea Res 41(4):695-719

Hastings DW (1994) Vanadium in the ocean: A marine mass balance and paleoseawater record. PhD Thesis:1-177

Hay WW (1970) Calcareous nannofossils from cores recovered on Leg 4. DSDP, Initial Reports 4:455-501

Hebbeln D, Wefer G, Berger WH (1990) Pleistocene dissolution fluctuations from apparent depth of deposition in core ERDC-127P, West-Equatorial Pacific. Mar Geol 92:165-176

Hemleben C, Spindler M, Anderson OR (1989) Modern planktonic foraminifera. Springer, New York, NY, 363 pp

Henrich R (1989) Glacial/interglacial cycles in the Norwegian Sea: Sedimentology, paleoceanography, and evolution of late Pliocene to Quaternary northern hemisphere climate. In: Eldholm O, Thiede J, Taylor E (eds) Proceedings of the Ocean Drilling Program, Scientific Results. College Station, TX, 104:189-232

Henrich R, Wefer G (1986) Dissolution of biogenic carbonates: Effects of skeletal structure. Mar Geol 71:341-362

Honjo S (1975) Dissolution of suspended coccoliths in the deep-sea water column and sedimentation of coccolith ooze. In: Sliter WV, Bé AWH, Berger WH (eds) Dissolution of Deep-Sea Carbonates. Cushman Found Foram Res Spec Publ, Ithaka, NY, 13:114-120

Honjo S (1976) Coccoliths: production, transportation and sedimentation. Mar Micropal 1(1):65-79

Honjo S, Erez J (1978) Dissolution rates of calcium carbonate in the deep ocean; an in-situ experiment in the North Atlantic Ocean. Earth Planet Sci Lett 40:287-300

Honjo S, Manganini SJ, Cole JJ (1982) Sedimentation of biogenic matter in the deep ocean. Deep-Sea Res 29(5A):609-625

Hooper PWP, Funnell BM, Weaver PPE (1991) Late Miocene-Early Pliocene planktonic foraminifera and paleoceanography of the North Atlantic. J Micropaleontol 9:145-152

Hsü KJ, Andrews JE (1970) Lithology. In: Bader RG (ed) Initial Report DSDP. National Science Foundation, Superintendent of Documents, US Government Printing Office, Washington, DC, 3:445-453

Imbrie J, Kipp NG (1971) A new micropaleontological method for quantitative paleoclimatology: application to a Late Pleistocene Carribean core. In: Turekian KK (ed) Late Cenocoic glacial ages. (Memorial Lectures) Yale University Press, New Haven, 43:71-181

Jahnke RA, Craven DB, Gaillard JF (1994) The influence of organic matter diagenesis on $CaCO_3$ dissolution at the deep-sea floor. Geochim Cosmochim Acta 58:2799-2809

JGOFS (1989) Canadian National Programme for the Joint Global Ocean Flux Study. The Canadian Committee for JGOFS, Halifax, 28 pp

Johnson TC, Hamilton EL, Berger WH (1977) Physical properties of calcareous ooze: Control by dissolution at depth. Mar Geol 24:259-277

Jumars PA, Altenbach AV, De Lange GJ, Emerson SR, Hargrave BT, Müller PJ, Prahl FG, Reimers CE, Steiger T, Suess E (1989) Transformation of Seafloor-arriving Fluxes into the Sedimentary Record. In: Berger WH, Smetacek VS, Wefer G (eds) Productivity of the Ocean: Present and Past. John Wiley & Sons, New York, NY, 291-311

Keigwin LD (1976) Late Cenozoic planktonic foraminiferal biostratigraphy and paleoceanography of the Panama Basin. Micropaleontology 22:419-422

Keir RS (1980) The dissolution kinetics of biogenic calcium carbonates in seawater. Geochim Cosmochim Acta 44:241-252

Keir RS (1990) Reconstructing the ocean carbon system variation during the last 150,000 years according to the Antarctic nutrient hypothesis. Paleoceanography 5(3):253-276

Kennett JP (1966) Foraminiferal evidence of a shallow calcium carbonate solution boundary, Ross Sea, Antarctica. Science 153(3732):191-193

Kleijne A (1990) Distribution and malformation of extant calcareous nannoplankton in the Indonesian Seas. Mar Micropal 16:293-316

Kolla V, Bé AWH, Biscaye PE (1976) Calcium carbonate distribution in surface sediments of the Indian Ocean. J Geophys Res 81(C15):2605-2616

Le J, Shackleton NJ (1992) Carbonate dissolution fluctuations in the western equatorial Pacific during the Late Quaternary. Paleoceanography 7:21-42

Liss PS (1973) Process of gas exchange across an air-water interface. Deep-Sea Res 20:221-238

Liss PS, Merlivat L (1986) Air-sea gas exchange rates: introduction and synthesis. In: Ménard-Buat P (ed) The role of air-sea exchange in geochemical cycling. NATO ASI Series, Dordrecht Boston, C185:113-127

Maier-Reimer E, Hasselmann K (1987) Transport and storage of $CO_2$ in the Ocean - An inorganic ocean-circulation carbon cycle model. Clim Dyn 2:63-90

Malmgren BA (1983) Ranking of dissolution susceptibility of planktonic foraminifera at high latitudes of the South Atlantic Ocean. Mar Micropal 8:183-191

Matsuoka H, McIntyre A, Molfino A, Verardo B (1991) A sensitive dissolution indicator *Calcidiscus leptoporus*: Concordance with climate-forced dissolution at orbital time scales. EOS 72(44):271

McCartney MS (1992) Recirculating components to the Deep Boundary of the Northern North Atlantic. Prog Oceanog 29:283-383

McIntyre A, McIntyre R (1971) Coccolith concentrations and differential solution in Oceanic Sediments. In: Funnell BM, Riedel WR (eds) The micropaleontology of oceans. Cambridge University Press, London, 253-261

Mercier H, Speer KG, Honnorez J (1994) Tracing the Antarctic Bottom Water through the Romanche and Chain Fracture Zones. Deep-Sea Res 41:1457-1477

Millero FJ (1979) The thermodynamics of the carbonate system in seawater. Geochim Cosmochim Acta 43:1651-1661

Milliman JD (1975) Dissolution of aragonite, Mg-calcite, and calcite in the North Atlantic Ocean. Geology 3(8):461-462

Mix AC, Morey AE (1996) Climate feedback and Pleistocene variations in the Atlantic south equatorial current. In: Wefer G, Berger WH, Siedler G, Webb DJ (eds) The South Atlantic: Present and Past Circulation. Springer-Verlag, Berlin Heidelberg, 503-525

Murray CN, Riley JP (1971) The solubility of gases in distilled water and seawater. IV. Carbon dioxide. Deep-Sea Res 18:533-541

Murray J (1897) On the distribution of the pelagic foraminifera at the surface and on the floor of the ocean. Nat Sci 11(65):17-27

Murray J, Renard AF (1891) Deep-sea deposits based on the specimens collected during the voyage of H.M.S. *Challenger* in the years 1872-1876. London, 525 pp

Murray JW (1989) Syndepositional dissolution of calcareous foraminifera in modern shallow-water Sediments. Mar Micropal 15:117-121

Nejstgaard JC, Witte HJ, Van-der-Wal P, Jacobsen A (1994) Copepod grazing during a mesocosm study of an *Emiliania huxleyi* (Prymnesiophyceae) bloom. Sarsia 79(4):369-377

Nürnberg D (1995) Magnesium in tests of *Neogloboquadrina pachyderma,* sinistral from high northern and southern latitudes. J Foram Res 25(4):350-368

Olausson E (1965) Evidence of climatic changes in North Atlantic deep-sea cores, with remarks on isotopic paleotemperature analysis. In: Sears M (ed) Progress in Oceanography. Pergamon Press, London, 3:221-252

Parker LF, Berger WH (1971) Faunal and solution patterns of planktonic foraminifera in surface sediments of the South Pacific. Deep-Sea Res 18:73-107

Paull CK, Hills SJ, Thierstein HR (1988) Progressive dissolution of fine carbonate particles in pelagic sediments. Mar Geol 81:27-40

Peterson LC, Prell WL (1985) Carbonate dissolution in recent sediments of the eastern equatorial Indian Ocean: Preservation patterns and carbonate loss above the lysocline. Mar Geol 64:259-290

Peterson MNA (1966) Calcite: Rates of dissolution in a Vertical profile in the central Pacific. Science 154(3756):1542-1544

Philippi E (1910) Die Grundproben der Deutschen Südpolar-Expedition 1901-1903. Deutsch Südpolar-Exped 1901-1903 2:411-616

Reid JL (1989) On the total geostrophic circulation of the South Atlantic Ocean: Flow patterns, tracers and transports. Prog Oceanog 23:149-244

Reimers CE (1989) Control of benthic fluxes by particulate supply. In: Berger WH, Smetacek VS, Wefer G (eds) Productivity of the Ocean: Present and Past. John Wiley & Sons, New York, NY, 217-233

Revelle R (1944) Marine bottom samples collected in the Pacific Ocean by the 'Carnegie' on its seventh cruise. Carnegie Inst Wash Publ 556(2-1):1-133

Rhein M, Schott F, Fischer J, Send U, Stramma L (1996) The deep water regime in the equatorial Atlantic. In: Wefer G, Berger WH, Siedler G, Webb DJ (eds) The South Atlantic: Present and past circulation. Springer-Verlag, Berlin Heidelberg, 261-271

Rosenthal Y, Boyle EA (1993) Factors controlling the fluoride content of planktonic

foraminifera: An evaluation of its paleoceanographic applicability. Geochim Cosmochim Acta 57:335-346

Roth PH, Coulbourn WT (1982) Floral and solution patterns of coccoliths in surface sediments of the North Pacific. Mar Micropal 7:1-52

Roth PH, Thierstein HR (1972) Calcareous nannoplankton. DSDP, Initial Reports 14:421-486

Ruddiman WF, Janecek TP (1989) Pliocene-Pleistocene biogenic and terrigenous fluxes at equatorial Atlantic Sites 662, 663 and 664. Proc ODP, Sci Results 108:211-240

Russell AD, Emerson S, Nelson BK, Erez J, Lea DW (1994) Uranium in foraminiferal calcite as a recorder of seawater uranium concentrations. Geochim Cosmochim Acta 58:671-681

Santschi PH, Bower P, Nyffeler UP, Azevedo A, Broecker WS (1983) Estimates of the resistance to chemical transport posed by the deep-sea benthic boundary layer. Limnol Oceanogr 28:899-912

Schott W (1935) Die Foraminiferen in dem Äquatorialen Teil des Atlantischen Ozeans. Wiss Ergebn d Deutschen Atl Exp Meteor 1925-1927 3:1-135

Schulz HD, cruise participants (1992) Bericht und erste Ergebnisse über die Meteor-Fahrt M20/2, Abidjan-Dakar, 27.12.1991-3.2.1992. Ber FB Geo Univ Bremen 25:1-173

Shannon LV, Chapman P (1991) Evidence of Antarctic Bottom Water in the Angola Basin at 32°S. Deep-Sea Res 38:1299-1304

Takahashi T, Broecker WS, Bainbridge AE, Weiss RF (1980) Carbonate chemistry of the Atlantic, Pacific and Indian Oceans: The results of the GEOSECS expeditions 1972-1978. Lamont-Doherty Geological Observatory, Palisades, NY, 211 pp

Thunell RC, Honjo S (1981) Calcite dissolution changes in the South Atlantic Ocean: Response to initiation of northern hemisphere glaciation. Paleoceanography 4:565-583

Van Andel TH, Heath GR, Moore TC (1975) Cenozoic history and paleoceanography of the central equatorial Pacific Ocean. Geol Soc Am Mem 143:1-134

Van Bennekom AJ, Berger GW (1984) Hydrography and silica budget of the Angola Basin. Neth J Sea Res 17:149-200

Van Kreveld SA (1996) Calcium carbonate dissolution indices on the northeast Atlantic sea floor. In: Van Kreveld-Alfane SA (ed) Late Quaternary sediment records of mid-latitude Northeast Atlantic calcium carbonate production and dissolution. FEBO B.V., Enschede, 135-184

Verardo DJ, Ruddiman WF (1996) Late Pleistocene charcoal in tropical Atlantic deep-sea sediments: Climatic and geochemical significance. Geology 24(9):855-857

Vilks G (1975) Comparison of *Globorotalia pachyderma* (EHRENBERG) in the water column and sediments of the Canadian Arctic. J Foram Res 5:313-325

Vincent E (1981) Carbonate stratigraphy of Hess Rise, Central North Pacific and paleoceanographic implications. Mar Biol 62:571-606

Warren BA, Speer KG (1991) Deep circulation in the eastern South Atlantic Ocean. Deep-Sea Res 38(Suppl. 1):281-322

Wefer G, Bleil U, cruise participants (1990) Bericht über die Meteor-Fahrt M12/1, Kapstadt-Funchal, 13.3.1990-14.4.1990. Ber FB Geo Univ Bremen 11:1-66

Wefer G, Bleil U, Schulz HD, cruise participants (1989) Bericht über die Meteor-Fahrt M9-4, Dakar-Santa Cruz, 19.2.-16.3.1989. Ber FB Geo Univ Bremen 7:1-103

Wu G, Herguera JC, Berger WH (1990) Differential dissolution: Modification of late Pleistocene oxygen isotope records in the western Equatorial Pacific. Paleoceanography 5(4):581-594

Wüst G (1935) Die Stratosphäre. Wiss Ergebn d Deutschen Atl Exp Meteor 1925-1927 6(1-2):1-288

Yasuda M, Berger WH, Wu G, Burke S, Schmidt H (1993) Foraminiferal preservation record for the last million years: Site 805, Ontong Java Plateau. Proc ODP, Sci Results 130:491-508

Young JR (1994) Variations in *Emiliania huxleyi* coccolith morphology in samples from the Norwegian EHUX experiment. Sarsia 79:417-425

# 5. Foraminiferal assemblages made anonymous - a reflection on quantitative research

**Nicolas Dittert and Reiner Schlotte**

*Fachbereich Geowissenschaften, Universität Bremen, 28334 Bremen, Germany*

**ABSTRACT:** The basis of quantitative research within marine micropaleontology is the producing of sample proportions, which have to represent the whole sample. We will present a major error distorting generally scientific results. Namely, this is the minimal number of individuals to be determined in order to attain statistically reliable evidence on species distribution (diversity, evenness) within a sample. Subsequently, we will show both how to minimize labour and how to maximize statistic meaningfulness using suitable tools.

That is, depending on (1) the maximum number of species to be expected within a sample and (2) the importance of single species regarding a given assemblage, the number of individuals to be determined ranges from tens to several hundreds.

## INTRODUCTION

Until today, there is still considerable confusion in the micropaleontological community regarding the statistical significance of rarer species, and whether variation in the total number of species between given samples has any bearing on the number of counts required. The relation between number of species and number of individuals occurring in a random sample of any organism assemblage is of major importance within many fields of micropaleontology. Among them, a multitude of applications are conceivable: a) the mapping of surface water assemblages in order to infer general and latitudinal biogeographic zonations (e.g., Baumann and Mathiessen 1992); b) climatic reconstructions through Transfer Function and Modern Analog Technique in order to estimate past sea-surface conditions (e.g., Kipp 1976; Pflaumann et al. 1996); c) the constructing of bio- and chronostratigraphies (e.g., Castradori 1993); d) the determination of extinction events (e.g., Thierstein 1982) and dominance changes of related species (e.g., Thierstein et al. 1977) etc.

Most of these applications base on the examination of species diversity as a function of the number of species present (cf. species richness or abundance) and the evenness with which the individuals are distributed among these species (cf. species equitability). In fact, there are a large number of those indices which we do not consider here; Hurlbert (1971) has given a critical and extensive review. For various practical reasons, micropaleontologists typically examine only a certain proportion, or split, of the total microfossil assemblage in any given sample. The number of individuals to be determined varies from researcher to researcher, depending on the degree of precision required for a particular study. In order to keep count results comparable, many researchers remind of uniform and standardized proceedings. The absolute number of individuals generally examined varies between 200 and >1,000 per sample. However, most workers usually count approximately 300 individuals. This latter figure was propunded by Phleger (1960) who, based on experience and on an equation derived by Dryden (1931) for counting heavy mineral grains, suggested that 300 individuals provide sufficient accuracy for most quantitative examinations.

This publication's target is to improve quantitative research and - attention to statistics - to avoid (1) wasting of time due to the working on too large sample sizes and (2) thwaring of maximum precision due to the working on too small sample sizes.

## METHODS

In order to determine recent and late Quaternary sediment assemblages of planktic foraminifera we investigated 279 sediment samples of the Brazil-, the Guinea-, and the Cape Basin. Each of the samples was washed through a 63 µm sieve; the whole sample >63 µm was sieved on a 150 µm, 212 µm, 355 µm, and a 500 µm sieve-set according to the CLIMAP-conventions (Imbrie and Kipp 1971). Since below 150 µm most planktic foraminifera are hardly determinable any more (e.g., Jansen and Bjørklund 1985), we examined the >150 µm fraction in behalf of paleoceanographic and paleoclimatic investigations (CLIMAP 1976).

### Approach 1:

We recorded the species assemblages by identifying and counting each fraction containing up to 1,000 individuals completely. Fractions containing too much material were repeatedly split into subsamples using a microsplitter to obtain an aliquot of about 1,000 planktic foraminiferal individuals. Afterwards, they were identified and counted

completely. During determining the individuals we have recorded with which individual $n_i$ which different species $i$ was counted (Text-fig. 1). It can be detected immediately that the first two rows always be equal (0: no individuals - no species; 1: first individual - first species). Only the third row bears real new information. For data processing reason (approach 2) even the first two rows were recorded.

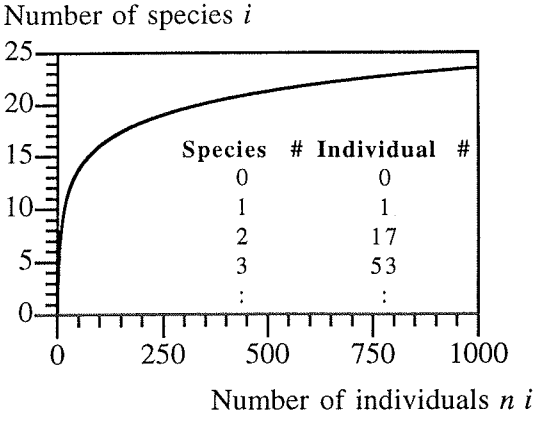


TEXT-FIGURE 1

Schematic plot of individuals $n_i$ vs. species $i$ for any given random sample developing during individual determination.

## Approach 2:

Investigating a certain sample proportion there is no guarantee that all species representing the total sample - or even better the real conditions - are recorded. Hence, we let a computer simulate the researchers work making him "count" and "determine" a given random sample individual by individual. Our objective was to find whether there is a maximum diversity increment by which the already existing diversity of a samlpe might increase. Thus, a function was fitted at the results of *approach 1* count by count in order to get an estimation $A$ for the true number of species and - through the speed $B$ by which the number of species $i$ approaches its limit - for the abundance of each species. Through variation of the parameters $A$ and $B$, the sum $S$ of the squares of differences be minimized:

$$i = A \cdot (1 - e^{(-B \cdot n)}) \quad \text{with } A, B > 0 \qquad (1)$$

Consequently:

$$n = -1/B \cdot \ln(1 - i/A)$$

and:

$$S = \sum_i \frac{[n_i - (-1/B) \cdot \ln(1 - i/A)]^2}{\sigma_{n_i}^2}$$

$$= \sum_i \frac{[n_i + (1/B) \cdot \ln(1 - i/A)]^2}{\sigma_{n_i}^2} \overset{!}{=} \min$$

If a function $f$ with respect to a parameter $x$ becomes minimum, its derivative $\partial f / \partial x$ will become zero:

$$0 \overset{!}{=} \frac{\partial}{\partial B} S \text{ ; regarding } B \text{ a non-linear problem is attained}$$

which can be solved directly on any given estimation of $A$:

$$= \sum_i \frac{2 \cdot [n_i + (1/B) \cdot \ln(1 - i/A)] \cdot (-1/B^2) \cdot \ln(1 - i/A)}{\sigma_{n_i}^2}$$

$$= (-2/B^2) \cdot \sum_i \frac{[n_i + (1/B) \cdot \ln(1 - i/A)] \cdot \ln(1 - i/A)}{\sigma_{n_i}^2}$$

$$= (-2/B^2)\cdot\left\{\sum_i \frac{n_i}{\sigma_{n_i}^2}\cdot\ln(1-i/A)+(1/B)\cdot\sum_i\frac{\ln^2(1-i/A)}{\sigma_{n_i}^2}\right\}$$

$$-\sum_i \frac{n_i}{\sigma_{n_i}^2}\cdot\ln(1-i/A) = (1/B)\cdot\sum_i\frac{\ln^2(1-i/A)}{\sigma_{n_i}^2}$$

$$B = -\frac{\sum_i \frac{\ln^2(1-i/A)}{\sigma_{n_i}^2}}{\sum_i \frac{n_i}{\sigma_{n_i}^2}\cdot\ln(1-i/A)}$$

How do we have to select $\sigma_{n_i}$? On the one hand, $n_i$ is known exactly because counted; thus, for each $i$ we can set $\sigma = 1$. Consequently:

$$B_1 = -\frac{\sum_i \ln^2(1-i/A)}{\sum_i n_i\cdot\ln(1-i/A)} \qquad \text{and} \qquad S_1 = \sum_i\left[n_i + (1/B)\cdot\ln(1-i/A)\right]^2$$

On the other hand, the selection of the foraminifera to be counted next is a random procedure; consequently $\sigma_{n_i}^2 = n_i$ is indicated. Thus:

$$B_2 = -\frac{\sum_i \frac{\ln^2(1-i/A)}{n_i}}{\sum_i \ln(1-i/A)} \qquad \text{and} \qquad S_2 = \sum_i \frac{\left[n_i + (1/B)\cdot\ln(1-i/A)\right]^2}{n_i}$$

If we let the deviation of $i$ serve as a hallmark of good quality:

$$T = \sum_i\left[i - A\cdot(1-e^{(-B\cdot n_i)})\right]\cdot(1-e^{(-B\cdot n_i)})$$

we now can determine the estimation $A$ for the true number of species:

$$0 \overset{!}{=} \frac{\partial}{\partial A}T$$

$$= \sum_i 2\cdot\left[i - A\cdot(1-e^{(-B\cdot n_i)})\right]\cdot(1-e^{(-B\cdot n_i)})$$

$$= 2\cdot\left\{\sum_i i\cdot(1-e^{(-B\cdot n_i)}) - A\cdot\sum_i(1-e^{(-B\cdot n_i)})^2\right\}$$

$$A = \frac{\sum_i i\cdot(1-e^{(-B\cdot n_i)})}{\sum_i(1-e^{(-B\cdot n_i)})^2}$$

This function yields an estimation of the minimum number of individuals to be counted depending on the number of species and its distribution expected. We assume a certain part $p$ of species not represented in the sample, the existing part be $n'$. Consequently, the abundance $p_i$ of each species present corresponds to the true abundance

$$p_i' = (1-p)\cdot p_i \qquad (2)$$

Consequently: $$1 = p + \sum_n p_i' = p + \sum_n k \cdot p_i = p + k \cdot \sum_n p_i = p + k \cdot 1 \longrightarrow k = 1 - p \qquad (3)$$

The true diversity $D$ splits into the part $D_S$ including each species present and the part $D_P$ including each species yet not present: $$D = D_S + D_P \qquad (4)$$

Looking at $D_S$ we can infer: $$D_S = -\sum_n p_i' \cdot \ln p_i' \qquad (5)$$

$$= -\sum_n (1-p) \cdot p_i' \cdot \ln(1-p) \cdot p_i'$$

$$= -(1-p) \cdot \sum_n p_i \cdot \left[\ln(1-p) - \ln p_i\right]$$

$$= -(1-p) \cdot \left[\sum_n p_i \cdot \ln(1-p) + \sum_n p_i \ln p_i\right]$$

$$= -(1-p) \cdot \left[\ln(1-p) + \sum_n p_i - D\right]$$

$$= -(1-p) \cdot \left[D - \ln(1-p)\right]$$

If $p<<1$ we can estimate: $$D_S = -(1-p) \cdot \left[D - \underbrace{\ln(1-p)}_{\approx -p}\right] \qquad (6)$$

$$\approx (1-p) \cdot \left[D + p\right]$$

If additionally $p<<D$ we further simplify to: $D_S \approx (1-p) \cdot D$

That is, $D_S$ is properly smaller than $D$ if $D$ is sufficiently large and $p$ is sufficiently small. But, what about $D_P$ ? The highest possible diversity is attained if the sample is equally distributed, that is, if $p_j = p / n'$ is complied: $$D_P = -\sum_{n'} p_j \cdot \ln p_j \qquad (7)$$

$$\leq -\sum_{n'} \frac{p}{n'} \cdot \ln \frac{p}{n'}$$

$$= -p \cdot \ln \frac{p}{n'}$$

$$= p \cdot \left[\ln n' - \ln p\right] = D_{\max}$$

Obviously this term may grow without restraint on open species numbers $n'$. In real conditions the number of species is limited; thus $D_{max}$ gives maximum diversity increment by which the diversity in the sample might increase provable.

## RESULTS

After counting and determining all individuals of all samples (approach 1) we ranked groups of identical species numbers and entered them into the model (approach 2). After simulation we attained the results both for conservatively determined and modelled species distribution (Text-figs. 2, 3).

**Approach 1:**

The one part of the samples is characterized by an extremely steep gradient at the beginning of the individual determination (Text-fig. 2). During the first 160 individual counts about 75 % to 90 % of all occurring species were identified (samples with 3, 5, 6, 7, 8, 9, 10, 12 species). The determination of the remaining 10 % to 25 % of all occurring species took further 100 to 280 individual counts. The second part of the samples is indicated by a smooth gradient at the beginning of the individual determination (samples with 11, 13, 15, 16, 20, 32, 34 species). Here, the number of species increases consecutively during the first 488 individual counts until the maximum number of species is attained.

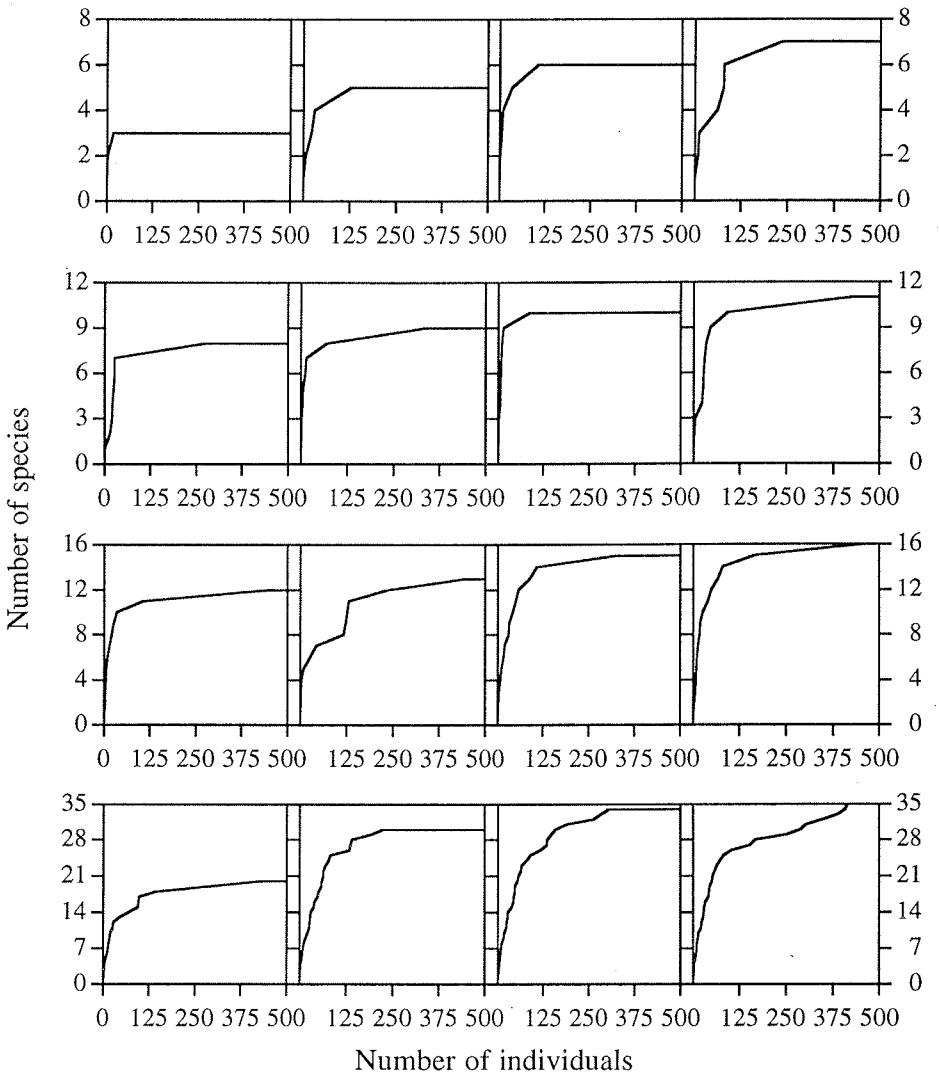


TEXT-FIGURE 2
Numbers of species versus individuals determined in random samples demonstrate different gradients due to different maximum number of species.

**Approach 2:**

During an unlimited number of runs the model calculated the maximum diversity increment by which the already existing diversity of a samlpe might increase by perpetual variation of the parameters *A*, *B*, and *S* (equation 1). All samples resulted in sepearte graphs (basing on the appropriate data) for $D_{max}$ (Text-fig. 3) and for the best fit with respect to both model and conservatively determined samples (Text-fig. 2). For all samples $D_{max}$ and the best fit coincide; the maximum diversity increment provable ranges from 0.1 and 0.7 species and -0.4 and -1.9 species. In the latter case, the theoretical situation of species decline appears which bears no equivalent with real conditions for the number of individuals or species occurred in a sample per se will not diminish.

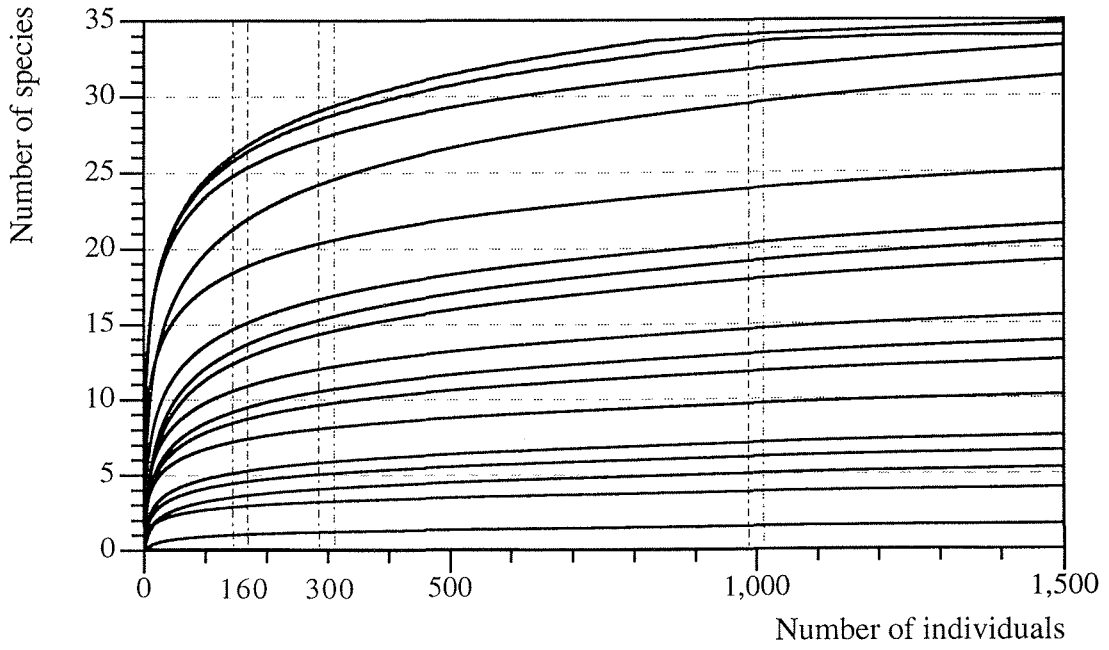


TEXT-FIGURE 3

Numbers of species versus individuals calculated by the model basing on counts determined in random samples show that the number of individuals to be determined depends on the number of species occuring in the sample. In order to comply with statistical requests, a minimum number of species can be deduced.

## DISCUSSION

During species determination the number of individuals versus number of species increases by leaps and bounds until the maximum value approaches an asymptote (Text-fig. 2). If a sample is distributed stochastically the relation between species and individuals increases as an exponential function (Text-figs. 1, 3). Where the curve

flattens the diversity does not change significantly any longer. By counting up to 1,000 individuals we actually comply with the request of several authors (e.g., Sarnthein 1971; Pflaumann 1975; Meggers and Baumann 1997) although in many cases too much individuals were determined (Text-figs. 2, 3). On the other hand, if we only had determined 160 individuals (e.g., Boltovskoy et al. 1996) or 300 individuals (e.g., McIntyre and Bé 1967; ImbrieKipp 1971; Buzas 1990; Bodén 1991; Giraudeau 1993; Pflaumann et al. 1996) the statistical requests would not have been performed.

Determining the exact species diversity of a random sample requires the determination of (1) *all* species and (2) *all* individuals per species. However, the basic problem regarding quantitative research is that a random sample not necessarily consists of all species representing the sample area - which mostly is attributed to the accuracy of sampling method and sample size. Additionally, there is no guarantee that not at least one species has been lost during processing. That is, the number of species encountered in a sample is at least partly dependent on sample size and split number (Murray 1995). Since the minimum size of counts to be investigated strongly depends on the diversity of a sample, it is questionable whether (1) uneconomic too much or (2) statistically too little individuals were determined (Weinholz 1987). Consequently, determining fixed numbers of individuals never show the demanded maximum time-statistics-efficiency.

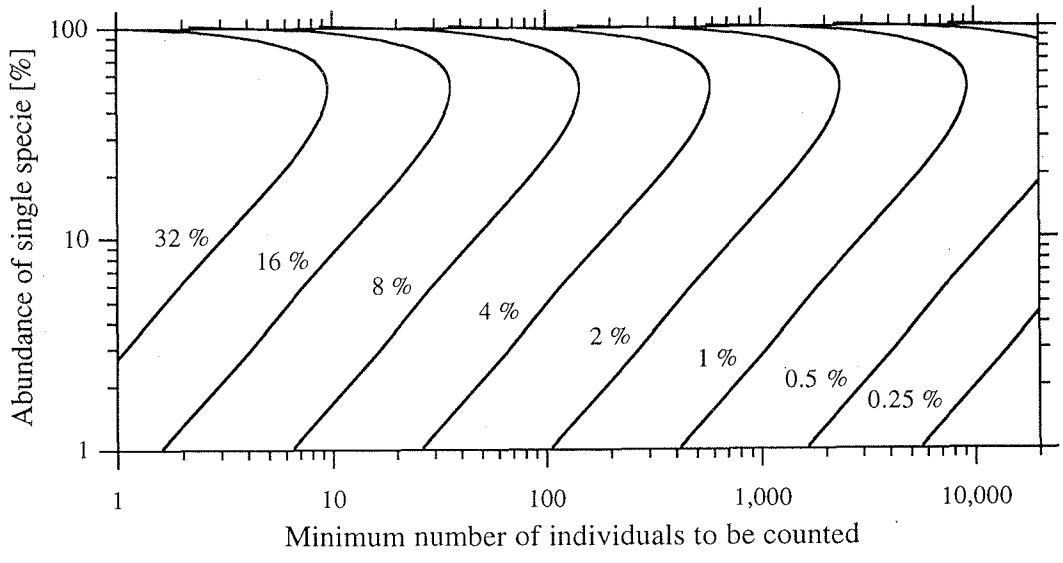


TEXT-FIGURE 4

Abundance of single species versus minimum numbers of individuals to be counted. A species occuring by 5 % of the total sample requires about 100 counts accepting an 4 % error; if only 2 % error are acceptable 450 specimens have to be counted; more than thousand individuals must be counted if the acceptable error falls below 1 % (modified after Patterson and Fishbein 1989).

Comparing conservatively and model determined samples there is a good agreement with only a little deviation. This leads to a high precision with respect to the model results. Consequently, regarding micropaleontological investigations we propose a strategy which is suitable for all belongings concerning organism assemblages as mentioned above. Since in real conditions the number of species is limited, and we can presuppose a certain knowledge or expectation on the number of species occuring in an area, we are able to determine the maximum diversity increment (equations 1-7). Subsequently, we are able to determine the minimum number of individuals to be determined until the statistically requested accuracy is attained (Text-fig. 3). Depending on the number of species expected to occurr maximum within a sample the number of individuals to be determined ranges from tens to several hundreds. However, for belongings of extinction events, dominance changes etc. we propose the approach by Patterson and Fishbein (1989, Text-fig. 4). They refer to Buzas et al. (1982) who found that most species tallied in paleontological analyses are rare and many of these rarer species are important regarding paleoceanographic interpretations as mentioned above. They recommend that researchers count at least 50 individuals regarding indicator species having an abundance of approximately 50 % or greater and counts of several thousands for defining species that comprise 1 % of a sample.

## ACKNOWLEDGEMENTS

We appreciate the kind assistance of the crews and masters of R/V METEOR on numerous cruises to The South Atlantic. The authors are indebted to H. Meggers, who participated the sample counting, as well as to H. Heilmann, R. Henning, and C. Wienberg for technical collaboration. The investigations were funded by the Deutsche Forschungsgemeinschaft. This is SFB 261 contribution no. xxx at Bremen University.

## REFERENCES

Baumann, K.-H. and Mathiessen, J., 1992. Variations in surface water mass conditions in the Norwegian Sea: evidence from Holocene coccolith and dinoflagellate cyst assemblage. Marine Micropaleontology, 20 : 129-146.

Bodén, P., 1991. Reproducibility in the random settling method for quantitative diatom analysis. Micropaleontology, 37 (3): 313-319.

Boltovskoy, E., Boltovskoy, D., Correa, N., Brandini, F., 1996. Planktic foraminifera from the southwestern Atlantic (30°-60°S): Species-specific patterns in the upper 50 m. Marine Micropaleontology, 28 : 53-72.

Buzas, M.A., 1990. Another look at confidence limits for species proportions. Journal of Paleontology, 64 (5): 842-843.

Buzas, M.A., Koch, S.J., Culver, S.J., Sohl, N.F., 1982. On the distribution of species occurrence. Paleobiology, 8 : 142-150.

Castradori, D., 1993. Calcareous nannofossil biostratigraphy and biochronology in eastern Mediterranean deep-sea cores. Rivista Italiana Di Paleontologia E Stratigrafia, 99 (1): 107-126.

CLIMAP project members, 1976. The surface of the ice-age earth. Science, 191 (4232): 1131-1137.

Dryden, A.L., 1931. Accuracy in percentage representations of heavy mineral frequency. Proceedings of the National Academy of Science, 17 : 233-238.

Giraudeau, J., 1993. Planktonic foraminiferal assemblages in surface sediments from the southwest African continental margin. Marine Geology, 110 (1-2): 47-62.

Hurlbert, S.H., 1971. The nonconcept of species diversity: a critique and alternative parameters. Ecology, 52 (4): 577-586.

Imbrie, J. and Kipp, N.G., 1971. A new micropaleontological method for quantitative paleoclimatology: Application to a Late Pleistocene Carribean core. In: K.K. Turekian (Ed.) Late Cenocoic glacial ages: 71-181. New Haven: Yale University Press.

Jansen, E. and Bjørklund, K.R., 1985. Surface ocean circulation in the Norwegian Sea, 15,000 B.P. to Present. Boreas, 14 : 243-257.

Kipp, N.G., 1976. New transfer function for estimating past sea-surface conditions from sea bed distribution of planktonic foraminiferal assemblages in the North Atlantic. Geological Society of America Memories, 145 : 3-42.

McIntyre, A. and Bé, A.W.H., 1967. Modern coccolithophoridae of the Atlantic Ocean - I. Placoliths and Cyrtoliths. Deep-Sea Research, 14 : 561-597.

Meggers, H. and Baumann, K.-H., 1997. Late Pliocene/Pleistocene calcareous plankton and paleoceanography of the North Atlantic. In: H.-C. Hass and M.A. Kaminski (Eds.), Contributions to the micropaleontology and paleoceanography of the northern North Atlantic: 39-50. Kraków: Grzybowski Foundation Special Publication.

Murray, J.W., 1995. Microfossil indicators of ocean water masses, circulation and climate. In: D.W.J. Bosence and P.A. Alklison (Eds.), Marine paleoenvironmental analysis from fossils: 245-264. Geological Society Special Publication.

Patterson, R.T. and Fishbein, E., 1989. Re-examination of the statistical methods used to determine the number of point counts needed for micropaleontological quantitative research. Journal of Paleontology, 63 (2): 245-248.

Pflaumann, U., 1975. Late Quaternary stratigraphy based on planktobic foraminifera off Senegal. "METEOR" Forsch.-Ergebnisse, C (23): 1-46.

Pflaumann, U., Duprat, J., Pujol, C., Labeyrie, L.D., 1996. SIMMAX: A modern analog technique to deduce Atlantic sea surface temperatures from planktonic foraminifera in deep-sea sediments. Paleoceanography, 11 (1): 15-35.

Phleger, F.B., 1960. Ecology and distribution of recent foraminifera. John Hopkins Press, Baltimore, VA, 297 pp.

Sarnthein, M., 1971. Oberflächensedimente im Persischen Golf und Golf von Oman II. Quantitative Komponentenanalyse der Grobfraktion. "METEOR" Forschungs-Ergebnisse, Reihe C (5): 1-113.

Thierstein, H.R., 1982. Terminal Cretaceous plankton extinctions: A critical assessment. Geological Society of America Special Publication, 190 : 385-399.

Thierstein, H.R., Geitzenauer, K.R., Molfino, B., Shackleton, N.J., 1977. Global synchroneity of late Quaternary coccolith datum levels: Validation by oxygen isotops. Geology, 5 : 400-404.

Weinholz, P., 1987. FOCOS - eine Methode zum Zählen von Mikrofossilien mit Hilfe eines Personal-Computers. Berichte aus dem Sonderforschungsbereich 313, Christian-Albrechts-Universität zu Kiel, 6 : 5-16.

# Part III *Conclusions and contemplations*

## Conclusions

This PhD thesis is the result of three years research on the topics *Late Quaternary planktic foraminifera assemblages in the South Atlantic Ocean* and *Preservational aspects regarding carbonate dissolution.* In order to determine a calibration of the modern to the fossil situation four surface sediment depth-transects into the Brazil-, the Guinea-, and the western and eastern Cape Basin were investigated. However, Late Quaternary paleoceanographic and paleoclimatic aspects were focussed on the central equatorial Atlantic Ocean and the time frame of 300 kyrs. The main results of this work are summed up as follows.

*1. A 300 kyrs history of plankton distribution in the central equatorial Atlantic Ocean - climate feedback, productivity and dissolution*

Late Quaternary planktic foraminiferal and coccolithophorid assemblages of the equatorial Atlantic Ocean are dominated by variations in the periods of orbital eccentricity (100 kyrs) and precession (23 kyrs), coherent with the global ice volume recorded in the $\delta^{18}O$ of the benthic foraminifer *Cibicides wuellerstorfi*. However, the 41 kyrs period (obliquity) is of minor importance. There is an obvious trend showing decreasing numbers of planktic foraminifera per gram sediment by about 50 % during the last 300 kyrs. Using a five-factor model, the transfer function technique displays two highly significant factors: (1) The subtropical-tropical factor which attains maximum loadings during all interglacials and the Holocene; (2) the warm-transitional factor which occurs with maximum loadings during glacial events; during the Holocene this factor almost expires. Highest estimated sea surface temperatures (SST's) are attained during interglacials, and lowest SST's occur during glacials. Glacial maxima are supposed to become warmer from oxygen isotope event 8.2 to 2.2 by about 2.5 °C. The difference between the modern and the Last Glacial Maximum SST amounts to about 6 °C for the central tropical South Atlantic. Paleo-environmental reconstructions distinguish two oceanic situations during the last 300 kyrs: During glacials, advection of cold and nutrient enriched water masses via the eastern boundary currents is the most important feature in surface water circulation above the investigated site (GeoB 1117-2/3). In addition,

equatorial upwelling which is controlled by the relationship between the meridional (monsoonal) and zonal (tropical easterlies) wind stress may be enhanced somewhat; however, the upwelling factor does not reach loadings that explain any significance. Minima in upwelling intensity are monitored by the increase in the relative abundance of the coccolithophore *F. profunda* as well as of the tropical planktic foraminiferal assemblage; both are positively correlated to the insolation over the North African landmass. During interglacials the thermocline is deep and equatorial upwelling is only moderate. Cool water advection is weak or absent in the equatorial Atlantic Ocean.

Data do not allow a distinct separation between the eastern boundary and the upwelling mechanism. Since there is much more variability in the warm-transitional fauna, it is assumed that eastern boundary dynamics are the driving force in the surface water circulation at this site, interacting with the upwelling activity and providing it with further nutrients. However, today's equatorial upwelling activity is much smaller than that of the continental margin upwelling systems. The investigations of site GeoB 1117-2/3 which is located at the southern rim of the modern equatorial upwelling area indicate that this domain was not extended or moved significantly during glacial times.

Although carbonate sedimentation seems to be dominated by the subtropical-tropical planktic foraminiferal assemblage, coccolithophores contribute largely to the carbonate sedimentation in times of higher surface water productivity. Some dissolution proxies point to a slender decrease in carbonate preservation during glacials, others do not. However, no index investigated gives evidence for strong dissolution increase during the last 300 kyrs which would alter the planktic foraminiferal assemblages and hence would fake paleo-reconstructions.

## *2. Carbonate dissolution in the deep-sea*

### *2.1 Evidence by* Globigerina bulloides' *ultrastructure breakdown*

In order to reconstruct the position of the hydrographic and the sedimentary calcite lysocline as well as the CCD in the modern South Atlantic Ocean the ultrastructure dissolution susceptibility of the planktic foraminifer *G. bulloides* was investigated. *Globigerina bulloides* undergoes remarkably ultrastructural breakdown with increasing carbonate dissolution even above the lysocline which was converted into the *Globigerina bulloides* Dissolution Index (BDX). There is evidence for a sharp BDX increase at the top of the sedimentary lysocline and for the total erase of this species at the bottom of the lysocline or the CCD, respectively. Additionally, BDX puts us in the position to distinguish the upper open ocean and the upwelling influenced continental margin above

the sedimentary lysocline from the deep ocean below the sedimentary lysocline. Water column carbonate ion data, sedimentary calcite data, and the rain ratio assess BDX to go for a valuable paleoceanographic proxy. As shown by BDX, both the hydrographic lysocline (in the water column) and the sedimentary lysocline (at the sediment pore water interface) mark the boundary between the carbonate ion undersaturated, highly corrosive AABW and the carbonate ion saturated NADW of the modern South Atlantic Ocean.

*Globigerina bulloides'* stable isotope composition ($\delta^{13}C$, $\delta^{18}O$) was investigated in samples of four sediment surface depth-transects into the Brazil-, the Guinea-, and into the Cape Basin (covering areas above and below the calcite lysocline) to find out whether there are patterns which are correlated to carbonate dissolution. Regarding carbon isotope composition, both $\delta^{13}C$ and $\delta^{18}O$ values generally raise with increasing water depth. However, the ratio of carbon versus oxygen isotopes displays rather strong correlation between Brazil- and Guinea Basin and between Western Cape Basin and Namibia Continental Margin, respectively, which can be attributed to different surface water temperatures in the equatorial and the southeast Atlantic surface waters. Because a major part of the $^{12}C$ enriched phytoplankton is respired and remineralized within the first 200 m of the water colum each new secreted chamber of *G. bulloides* becomes isotopically lighter. Consequently, if a test undergoes dissolution (either supralysoclinal or below the lysocline) through a layer-by-layer removal of shell material the remaining test will become isotopically heavier with respect to $^{13}C$. The present results show an increase of 0.4 ‰ and 0.76 ‰ per 1,000 m water depth for carbon and oxygen isotopes, respectively. However, carbonate dissolution lastly does not affect the known relationship between carbon and oxygen stable isotopes regarding surface water temperature reconstruction.

After investigating BDX on sediment surface samples, this tool was applied on down-core samples from the sediment core GeoB 1117-2/3 during the last 140 kyrs. Actually, the results cause serious obstacles as BDX is supposed to indicate better calcite preservation during glacials and worse calcite preservation during interglacials in the central equatorial Atlantic. Since the production of NADW is thought to be reduced during glacial periods, the northwards directed AABW would expand in latitudinal and vertical distribution in the Brazil Basin. Consequently, the southwards directed NADW velocity at the core-site lessens. During interglacials the onset of NADW production accelerates the southwards directed bottom water; the currents to stir the layer of dissolution around the $CaCO_3$ particles are stimulated. Even under (super-) saturated conditions as displayed by $\Delta CO_3^{2-}$ data the preservation of calcite worsens somewhat. Since there is evidence that the core site never was influenced directly by AABW, BDX is supposed to serve as deep-water circulation index under carbonate (super-) saturated

conditions.

*2.2 Methods, quantification and paleoceanographic application*

Carbonate dissolution in the deep ocean was determined by using sea-water carbonate ion data, bulk sediment parameters, and calcareous micro- and nannoplankton parameters as dissolution proxies. Investigation areas were the open ocean regime specified by two transects into the western Brazil Basin and the western Cape Basin. The continental margin realm is characterized by one transect into the eastern Cape Basin. The sediment surface samples are derived from water depths between 1,007 m and 5,213 m.

All parameters are capable of distinguishing the area above from the area below the top of the calcite lysocline. Beyond that, some parameters are suited to distinguish the upper continental margin of the coastal ocean within an upwelling area controlled by enormous productivity, high export and rapid sedimentation. In detail, these are the carbonate ion content of the water column and the weight percentage of sediment $CaCO_3$-content, the rain ratio, the *Globigerina bulloides* Dissolution Index (BDX), and the *Calcidiscus leptoporus* - *Emiliania huxleyi* Dissolution Index (CEX).

Regarding the three different oceanographic regimes, only the carbonate ion content and the percentage of sediment carbonate content put us in the position to determine top, bottom, and thickness of the lysocline. If these parameters are not available, a combination of BDX, CEX and rain ratio gives the best approach to the authentic conditions.

According to the investigated transects, the top of the calcite lysocline can be set to about 4,300 m in the open ocean realm of the Brazil- and the western Cape Basin. It reflects the modern boundary between the NADW and the corrosive AABW, subsequently leading to sublysoclinal dissolution. The thickness of the lysoclines amount to about 800 m. With respect to the continental margin of the eastern Cape Basin, the lysocline is situated at about 4,100 m water depth; the lysocline thickness becomes >900 m. It reflects the high amount of organic matter buried with $CaCO_3$, induced by coastal upwelling processes of the Benguela Current, subsequently leading to sublysoclinal dissolution as well as to supralysoclinal dissolution.

## Contemplations

For further investigations of planktic foraminifera in the South Atlantic Ocean with respect to the preservational potential some suggestions should be taken into account:

➥ The investigation of some more surface sediment depth-transects in the South Atlantic Ocean would refine the methodical approach of BDX. Either, it would contribute to the main target of the subproject B3 *Calcareous plankton and carbonate budget.* The investigation of a core transect at about lysocline depths would show in which way and in which extent calcite was lost due to dissolution which lastly results in the carbonate budget over time in this area.

Yet, there remains the question whether the critical sill depth of the Romanche Fracture Zone (~ 3,850 m) was activated during glacial times or not. The investigation of a core transect at about lysocline depths (as mentioned above) would yield the final solution.

As the ancient conflict of scientific opinions regarding temperature difference between the modern and LGM SST's for the western tropical Atlantic Ocean is still smouldering, the investigation of core transects (time slices) along the equator was worthwhile.

➥ (1) *Globigerina bulloides* belongs to the species adapted also to nutrient rich conditions and moderate to low temperatures in upwelling areas; (2) *G. bulloides* presumably will loose its index status (BDX) in other basins of the South Atlantic due to missing upwelling conditions; (3) there are research studies recently carried out dealing with carbonate dissolution effects on planktic foraminiferal shells in the laboratory (Marilyn Vautravers; Université de Bordeaux). Consequently, additional species from sediment surface samples should be investigated with respect to their ultrastructural breakdown behavior. After many debates with other colleagues I bring up to discussion some species to be investigated: *G. truncatulinoides* and *N. dutertrei* (index species for gyre situation), *G. crassaformis* (shallow thermocline indicator), *G. sacculifer* and *G. ruber* (index species for well stratified water column in the tropics and subtropics, respectively). Subsequently, calibration between the species investigated would reveal an ultrastructure dissolution index applicable to the global ocean.

# Part IV *Appendix*

## Taxonomy

Following the convention of Murray (1897) we distinguish spinose and non-spinose species. Parker (1962) was the first who used this criterion for purposes of classification. The categories were refined by incorporating data on shell wall structure obtained by transmission electron microscopy investigations (Bé et al. 1966; Takayanagi et al. 1968). Our determination of planktic foraminifera is attributed to the work by Bé (1967; 1977), Hemleben et. al (1989), Kennett and Srinivasan (1983), Pflaumann and Krasheninnikov (1978), and van Leeuwen (1989). The taxonomic classification follows Hemleben et al. (1989); different nomenclatur is itemized. All species occurring in our samples are listed below in alphabetical order.

Order **FORAMINIFERIDA** Eichwald 1830
Sub-order **ROTALIINA** Delage and Hérouad 1896

*Spinose planktic foraminifera*

Genus **Globigerina** d'Orbigny 1826

*Globigerina bulloides* d'Orbigny 1826

1989: *Globigerina bulloides* d'Orbigny—Hemleben et al.

*Globigerina falconensis* Blow 1959

1983: *Globigerina (Globigerina) falconensis* Blow—Kennett and Srinivasan
1989: *Globigerina falconensis* Blow—Hemleben et al.

Genus **Globigerinella** Cushman 1927

*Globigerinella aequilateralis* (Brady) 1897

1967: *Globigerinella aequilateralis* (Brady)—Bé
1977: *Globigerinella aequilateralis* (Brady)—Bé
1989: *Globigerinella siphonifera* (d'Orbigny)—Hemleben et al.

*Globigerinella calida* Parker 1962

Other generic assignment (O.G.A.) *Globigerina*

1989: *Globigerinella calida* (Parker)—Hemleben et al.

*Globigerinella digitata* (Brady) 1879

1967: *Globigerina digitata* Brady—Bé
1977: *Globigerina digitata* Brady—Bé
1978: *Globigerina digitata* Brady—Pflaumann and Krasheninnikov
1983: *Beella digitata* (Brady)—Kennett and Srinivasan
1989: *Globigerinella (Beella) digitata* (Brady)—Hemleben et al.

## Genus **Globigerinoides** Cushman 1927

*Globigerinoides conglobatus* (Brady) 1879

1989: *Globigerinoides conglobatus* (Brady)—Hemleben et al.

*Globigerinoides ruber* (d'Orbigny) 1839

1989: *Globigerinoides ruber* (d'Orbigny) *ruber* type—Van Leeuwen
1989: *Globigerinoides ruber* (d'Orbigny) *elongatus* type—Van Leeuwen
1989: *Globigerinoides ruber* (d'Orbigny)—Hemleben et al.

Note: This species occurs as a white and a pink variety. Due to Transfer Function and Modern Analog Technique requirements each variety was distinguished.

*Globigerinoides sacculifer* (Brady) 1877

1978: *Globigerinoides trilobus trilobus* (Reuss)—Pflaumann and Krasheninnikov
1978: *Globigerinoides trilobus sacculifer* (Brady)—Pflaumann and Krasheninnikov
1989: *Globigerinoides trilobus* (Reuss)—Van Leeuwen
1989: *Globigerinoides sacculifer* (Brady)—Hemleben et al.

Note: This species occurs with and without a sac-like final chamber. Due to Transfer Function and Modern Analog Technique requirements each morphotype was distinguished.

## Genus **Globoturborotalita** Hofker 1967

*Globoturborotalita rubescens* Hofker 1967

O.G.A. *Globigerina*

1983: *Globigerina (Zeaglobigerina) rubescens* Hofker—Kennett and Srinivasan
1989: *Globoturborotalita rubescens* Hofker—Hemleben et al.

Note: This species occurs as a white and a pink variety. Since both varieties show different ecological preferences they were distinguished.

*Globoturborotalita tenella* (Parker) 1958

O.G.A. *Globigerinoides*

1977: *Globigerinoides tenellus* Parker—Bé
1978: *Globigerinoides tenellus* Parker—Pflaumann and Krasheninnikov
1983: *Globigerinoides tenellus* Parker—Kennett and Srinivasan
1989: *Globoturborotalita tenella* (Parker)—Hemleben et al.

## Genus **Orbulina** d'Orbigny 1939

*Orbulina universa* (d'Orbigny) 1865

1989: *Orbulina universa* (d'Orbigny)—Hemleben et al.

Note: This species sometimes occurs as biloculate morphotype. Since both varieties show comparable ecological preferences they were not distinguished.

## Genus **Sphaeroidinella** Cushman 1927

*Sphaeroidinella dehiscens* (Parker and Jones) 1865

1989: *Sphaeroidinella dehiscens* (Parker and Jones)—Hemleben et al.

## Genus **Turborotalita** Blow and Banner 1962

*Turborotalita quinqueloba* (Natland) 1938

1977: *Globigerina quinqueloba* Natland—Bé
1978: *Globigerina quinqueloba* Natland—Pflaumann and Krasheninnikov
1983: *Globigerina (Globigerina) quinqueloba* Natland—Kennett and Srinivasan
1989: *Turborotalita quinqueloba* (Natland)—Hemleben et al.

## *Non-spinose planktic foraminifera*

## Genus **Globigerinita** Brönnimann 1951

*Candeina nitida* d'Orbigny 1839

1989: *Candeina nitida* d'Orbigny—Hemleben et al.

*Globigerinita glutinata* (Egger) 1895

O.G.A. *Globigerina, Tinophodella, Globigerinoides*

1989: *Globigerinita glutinata* (Egger)—Hemleben et al.

Note: This species calcifies in the terminal stage an umbilical bulla. Morphotypes with and without bulla were not distinguished.

*Globigerinita bradyi* Wiesner 1931

1967: *Globigerinita bradyi* Wiesner—Bé
1977: *Globigerinita bradyi* Wiesner—Bé
1989: *Globigerinita uvula* (Ehrenberg)—Hemleben et al.

## Genus **Globorotalia** Cushman 1927

*Globorotalia crassaformis* (Galloway and Wissler) 1927

O.G.A. *Globorotalia crotonensis* Conato and Follador 1967; *G. crassula* Cushman, Stewart and Stewart 1930

1977: *Globorotalia crotonensis* Conato and Follador—Bé
1978: *Globorotalia crassaformis crassaformis* (Galloway and Wissler)—Pflaumann and Krasheninnikov
1978: *Globorotalia crassaformis hessi* Bolli and Premoli Silva—Pflaumann and Krasheninnikov
1978: *Globorotalia crassaformis ronda* Blow—Pflaumann and Krasheninnikov
1978: *Globorotalia crassaformis viola* Blow—Pflaumann and Krasheninnikov
1978: *Globorotalia crassaformis* spp.—Pflaumann and Krasheninnikov
1989: *Globorotalia crassaformis* (Galloway and Wissler)—Hemleben et al.

Note: This species shows a wide range of morphotypes which were not further distinguished.

*Globorotalia inflata* (d'Orbigny) 1839

O.G.A. *Globigerina, Truncorotalia*

1989: *Globorotalia inflata* (d'Orbigny)—Hemleben et al.

Note: This species consists of left- and right-coiling varieties. Since both varieties show different ecological preferences they were distinguished.

*Globorotalia menardii* (Parker, Jones and Brady) 1865

O.G.A. *Globorotalia cultrata* (d'Orbigny)

1977: *Globorotalia menardii* (d'Orbigny) *menardii* (d'Orbigny)—Bé
1977: *Globorotalia menardii* (d'Orbigny) *gibberula* (d'Orbigny)—Bé
1989: *Globorotalia menardii* (d'Orbigny)—Hemleben et al.

*Globorotalia scitula* (Brady) 1882

O.G.A. *Globorotalia bermudezi* Roegl and Bolli 1973

1989: *Globorotalia scitula* (d'Orbigny)—Hemleben et al.

*Globorotalia theyeri* Fleischer 1974

1989: *Globorotalia theyeri* Fleischer—Hemleben et al.

*Globorotalia truncatulinoides* (d'Orbigny) 1839

O.G.A. *Globorotalia cultrata* (d'Orbigny)

1989: *Globorotalia truncatulinoides* (d'Orbigny) right-coiling variety—Van Leeuwen
1989: *Globorotalia truncatulinoides* (d'Orbigny)—Hemleben et al.

Note: This species consists of left- and right-coiling varieties. Since both varieties show different ecological preferences they were distinguished.

*Globorotalia tumida* (Brady) 1877

1978: *Globorotalia tumida tumida* (Brady)—Pflaumann and Krasheninnikov
1989: *Globorotalia menardii* (Brady) *tumida* type—Van Leeuwen
1989: *Globorotalia tumida* (Brady)—Hemleben et al.

*Globorotalia ungulata* Bermudez 1960

1989: *Globorotalia ungulata* Bermudez—Hemleben et al.

*Globorotaloides hexagonus* (Natland) 1938

O.G.A. *Globoquadrina*

1989: *Globorotaloides hexagonus* Natland—Hemleben et al.

## Genus **Neogloboquadrina** Bandy, Frerichs and Vincent 1967

*Neogloboquadrina dutertrei* (d'Orbigny) 1839

1967: *Globoquadrina dutertrei* (d'Orbigny)—Bé
1977: *Globoquadrina dutertrei* (d'Orbigny)—Bé
1989: *Neogloboquadrina dutertrei* (Brady)—Hemleben et al.

Note: Between the two species *N. dutertrei* and *N. pachyderma* there was an artificial species defined, namely the "species" *N. pachyderma-dutertrei-intergrade* (PDI), which consists of five chambers and a well-developed apertural lip.

*Neogloboquadrina pachyderma* (Ehrenberg) 1861

1967: *Globigerina pachyderma* (Ehrenberg)—Bé
1977: *Globoquadrina pachyderma* (Ehrenberg)—Bé
1978: *Globoquadrina pachyderma* (Ehrenberg)—Pflaumann and Krasheninnikov
1989: *Neogloboquadrina pachyderma* (Ehrenberg)—Hemleben et al.

Note: This species consists of left- and right-coiling varieties. Since both varieties show different ecological preferences they were distinguished.

## Genus **Pulleniatina** Cushman 1927

*Pulleniatina obliquiloculata* (Parker and Jones) 1865

1989: *Pulleniatina obliquiloculata* (Parker and Jones)—Hemleben et al.

## Presentations at international conferences

(TA = Talk; PO = Poster)

**PO** Dittert N, Kinkel H (1997) Coccolithophore and planktonic foraminifera assemblages as a mirror of equatorial paleoceanography. In: The First International Conference "Application of Micropaleontology in Environmental Sciences". Tel Aviv, Israel:50-51

**PO** Henrich R, Baumann K-H, Dittert N, Huber R, Kinkel H, Meggers H (1997) Quaternary pelagic carbonate production and preservation: North-South Atlantic linkages and palaeoceanographic implications. Gaea heidelbergensis 3:160

**TA** Kinkel H, Dittert N, Henrich R (1997) Late Quaternary carbonate sedimentation in the equatorial Atlantic: Productivity and dissolution cycles. Gaea heidelbergensis 3:199

**PO** Dittert N, Kinkel H (1996a) Calcium carbonate sedimentation in the South Atlantic; accumulation versus dissolution. Geological Society of America, 28th annual meeting 7:122

**TA** Dittert N, Kinkel H (1996b) Pelagische Karbonatflüsse im äquatorialen Atlantik: Produktionsschwankungen, Lösungszyklen während der letzten 300,000 Jahre. Schriftenreihe der Deutschen Geologischen Gesellschaft 1:23

**PO** Kinkel H, Dittert N (1996) Carbonate fluxes in the Equatorial Atlantic; 300,000 yrs planktonic record of productivity and dissolution. Geological Society of America, 28th annual meeting 7:122

**PO** Dittert N, Kinkel H, Baumann K-H, Henrich R (1995) Ecology and productivity of calcareous plankton in the equatorial South Atlantic of the last 120 kyrs. In: Mayer L, Piper DJW, Rack F (eds), 5th International conference on paleoceanography. Halifax, Nova Scotia, Canada:188-189

**PO** Kinkel H, Dittert N, Baumann K-H (1995) A 300 kyrs calcareous plankton record of the Equatorial South Atlantic; reconstructions of surface water productivity and bottom water dissolution cycles. Journal of Nannoplankton Research 17(2):69

## Danksagung

*Bei Herrn Prof. Dr. Rüdiger Henrich möchte ich mich für die Anregung zu dieser Arbeit und deren Betreuung bedanken.*

*Mein besonderer Dank geht an Hanno Kinkel, der als Freund und Kollege nicht nur durch fachliche Diskussionen, sondern auch bei der ein und anderen Flasche Trollinger zum besonderen Gelingen der gemeinsamen Zeit in Bremen beigetragen hat. Alles Gute auf Texel!*

*Allen KollegInnen der Arbeitsgruppe 'Sedimentologie/Paläozeanographie', des SFB 261, des Fachbereichs Geowissenschaften und von außerhalb möchte ich für die ausgezeichnete Zusammenarbeit im Hause und auf Expeditionen danken: Barbara Donner und Bernhard Diekmann für die Abb. I-2 und I-6; Götz Ruhland für die geduldige Hilfe bei EDV- und Zollfragen; Andreas Mackensen für die spontane Bereitschaft, Isotopenmessungen durchzuführen; Helge Meggers für Pizza Gyros und andere Delikatessen; Peter J. Müller für die Überlassung von Messdaten; Helga Heilmann und Renate Henning für jeden nur erdenklichen nichttechnischen und technischen Support; Michael Matthies und Rainer Schlotte für know-how aus der Welt der Modellierer; Jan Bauer und Claudia Wienberg für flinke Hände und zuverlässige Zuarbeit, etc.*

*Gutes Arbeitsklima, fortwährende Diskussionsbereitschaft und fachliche Unterstützung sind keine Selbstverständlichkeit. Allen noch nicht Genannten sei hiermit herzlich gedankt.*

*Kathrin, Deine Hilfe und Dein Beitrag zum Erfolg dieser Arbeit lassen sich nicht in noch so schöne Worte fassen - Danke!!! Nicht zuletzt möchte ich mich bei meinem Freundes- und Bekanntenkreis sowie meiner Familie für die Unterstützung und den menschlichen Zuspruch bedanken.*

*Abschließend sei Herrn Prof. Dr. Helmut Willems für die freundliche Übernahme des Zweit-Gutachtens gedankt.*